THE ROLE OF AQUAPORINS IN THE DEVELOPING OVARIAN FOLLICLE

By

Leanne Williams (BSc Hons)

Thesis submitted to The University of Nottingham

for the degree of Doctor of Philosophy

May 2012

School of Biosciences

Sutton Bonington Campus

Loughborough

Leicester

LE12 5RD

Declaration

I hereby declare that this thesis is my own work and had not been previously submitted for any other degree or award. Sources of information have been referenced. Any help or advice given by other people or collaboration during the execution of experiments has been duly acknowledged.

Leanne Williams

Abstract

The growth of ovarian follicles is well documented in terms of hormonal control, however the fluid dynamics of antral follicle growth is less well understood. Aquaporins (AQP) are transmembrane water channels which facilitate the passive movement of water. In mammals 13 AQPs have been identified in a vast range of tissue types. In terms of ovarian AQPs there is currently a paucity of information. Recent studies in rat, pig and human have revealed the presence of ovarian AQPs, but in doing so have also highlighted a lack of consensus on AQP-type and location.

The main aim of this study was to investigate the potential role of AQP in antral follicle growth. The first objective was to identify tissue expression and localisation of AQP proteins in the bovine ovary. This required the characterisation of a panel of polyclonal serum antibodies. Immunohistochemistry (IHC) was then used to identify AQPs and to detect changes in protein expression during follicular growth. Aquaporin 1 was found in most vascular endothelium; it was plentiful in capillaries surrounding antral follicles and increased in abundance as vasculature increased with follicle development. Aquaporin 2 was not found in bovine ovarian tissue and the remaining antibodies were deemed too non-specific to permit reliable conclusions.

The second objective was to investigate, via RT-qPCR, mRNA levels of AQPs in granulosa and theca cells isolated from preantral, through to large preovulatory follicles. Transcripts of *AQP1, -3, -4, -5, -7* and *-9* were detected in both the granulosa and theca of antral follicles with expression levels generally higher in theca. The expression of *AQP1, -5, -7* and *-9* was initiated in the theca cells of early antral follicles. Finally, swelling assays using bovine and porcine granulosa cells demonstrated the ability of granulosa to swell. This was inhibited by $HgCl_2$ which is characteristic of AQP function. Porcine granulosa cells incubated with androgen swelled by 27%, this effect was inhibited by hydroxyflutamide. Protein analysis of AQP5 via IHC and Western blotting showed possible up-regulation in porcine follicles. RT-qPCR did not reveal AQP5 transcript, the reasons for this currently remain unclear.

In conclusion, this study has revealed for the first time the involvement of AQPs in bovine ovarian follicle development, with AQP1, -5, -7 and -9 potentially playing a pivotal role in antrum formation. The AQP system in porcine granulosa cells is androgen sensitive however identification of the AQP/s responsible needs further investigation. The evidence from this investigation suggests a role for AQPs in facilitating follicle growth. The stage-dependent expression of certain AQPs and the androgen sensitive porcine granulosa cells reveals the possibility that AQPs may be modulated by follicle-regulating hormones.

Acknowledgments

This thesis is dedicated to my family, past and present... thank you for everything!

First and foremost I would like to thank my supervisor Dr Martin Luck for giving me this opportunity. I could not have wished for a better mentor. Thank you for all your support, encouragement and patience, I have thoroughly enjoyed working with you and thanks for being a great travelling companion too.

I would like to thank all the support staff who helped me with the day to day stresses and strains. Especially, Ralph Hoard, with whom I spent many an interesting day at the abattoir! I'd like to thank Scott Hulme and Ceri Allen in the Vet School for your help with my IHC 'issues'; Pat Fisher and Lydia Kwong in South Lab for all their technical advice and much needed words of support. I would like to acknowledge Dr Andrew Green for the use of the laser capture equipment and Sarkawt for your help.

Huge thanks go to my Mam and Dad, Joanne, Kirk, Leah and Sam, for their continued support and encouragement, just knowing you were at the end of the phone made all the difference. I'm sorry that I've been so busy for so long, you were always in my thoughts...'think seat'! To my friend Lisa who stuck by me even when I dropped off the radar; Louise, Sarah S, Ismail...we can do it! Thanks to Jules for keeping me sane and Katherine for being there from start to finish. To all the friends I've made at the Vet school, thanks for everything, especially the laughs this will undoubtedly be an experience I will never forget!

And finally but by no means least, if it was not for you; your love and support, understanding, patience and sheer technical brilliance, I would never have made it through to the end. Star gazing and red wine... that's all I'm going to say. Thank you so much Jaime, I will be forever indebted to you.

This project was funded by BBSRC, School of Bioscience, School of Veterinary Medicine and Science and the SRF.

List of Contents

List of Figures

List of Tables

List of Abbreviations

Å	Ångström
A	antrum
ACTB	Beta actin
ANOVA	Analysis of variance
APM	Apical plasma membrane
AQP	Aquaporin
AQP0	Aquaporin 0
AQP1	Aquaporin 1
AQP2	Aquaporin 2
AQP3	Aquaporin 3
AQP4	Aquaporin 4
AQP5	Aquaporin 5
AQP6	Aquaporin 6
AQP7	Aquaporin 7
AQP8	Aquaporin 8
AQP9	Aquaporin 9
AQP10	Aquaporin 10
AQP11	Aquaporin 11
AQP12	Aquaporin 12
AR	Androgen receptor
AtR	Antigen retrieval
ar/R	Aromatic/arginine
ARE	Androgen response element
Arg	Arginine
$As(OH)_3$	Arsenite
Asp	Asparagine
At	Arteriole
Bax	Bcl-2–associated X protein
Bcl-2	B-cell lymphoma 2
BCP	1-bromo-3-chloropropane
bFGF	Basic fibroblast growth factor
BL	Broad ligament

BLAST	Basic Local Alignment Tool
BM	Basement membrane
BMP15	Bone morphogenetic protein 15
bp	Base pair
BPM	Basolateral plasma membrane
BSA	Bovine serum albumin
CA	Corpus albicans
Ca^{2+}	Calcium
cAMP	Cyclic adenosine monophosphate
CD	Cluster of differentiation
CDE	Collecting duct epithelium
cDNA	Copy deoxyribonucleic acid
CHIP28	Channel-like integral membrane protein of 28 kDa
CL	Corpus luteum
cm	Centimetre
CO_2	Carbon dioxide
COC	Cumulous-oocyte-complex
COP	Colloid osmotic pressure
CT	Collecting tubules
CV	Central vein
Cxs	Connexions
CYP11A1	P450 side chain cleavage
CYP17A1	17α-hydroxylase
CYP19A1	Aromatase
Cys	Cysteine
Cys	Cystine
DAB+	3,3' diaminobenzidine
DARC	Duffy antigen receptor for chemokines
DCT	Distal convoluted tubules
DHT	Dihydrotestosterone
DMEM	Dulbecco's Modified Eagles Medium
DNA	Deoxyribonucleic acid
DTLE	Descending thin limb epithelium

DVRE	Descending vasa recta endothelium
E_2	Oestradiol
E_a	Arrhenius activation energy
EC	Endothelial cell
ECM	Extracellular matrix
EDTA	Ethylenediaminetetraacetic acid
EGF	Epidermal growth factor
EGFR	Epidermal growth factor receptor
EO	Early ovulatory phase
ERE	Oestrogen response element
ESR1	Oestrogen receptor-α
ESR2	Oestrogen receptor-β
F	Forward primer
F.V.	Final volume
FAI	Free androgen index
FcR	Fragment crystallisable receptor
FF	Follicular fluid
FGF	Fibroblast growth factor
FIGα	Factor in the germline α
FSH	Follicle stimulating hormone
FSHr	Follicle stimulating hormone receptor
G	Granulosa
g	G force
g	Gram
GAG	Glycosaminoglycan
GAPDH	Glyceraldehyde 3-phosphate dehydrogenase
GDF9	Growth differentiation factor 9
GL	Glomerulus
GnRH	Gonadotrophin releasing hormone
h	Hour
H&E	Haematoxylin and eosin
H_2O_2	Hydrogen peroxide
HCl	Hydrochloric acid

HF	Hydroxyflutamide
$HgCl_2$	Mercury chloride
His	Histidine
HK	House keeping
Hp	hepatocytes
HSD3B1	3β-hydroxysteroid dehydrogenase
hSGLT1	Human sodium-glucose transporter 1
HYPO	Hypotonic
Ig	Immunoglobulin
IGF	Insulin-like growth factor
IGFBP	Insulin-like growth factor binding protein
IHC	Immunohistochemistry
ISO	Isotonic
IV	Intracellular vesicles
Kc	Kidney cortex
KCC	Potassium chloride cotransporter
kDa	Kilodalton
kg	Kilogram
KHL	Keyhole limpet hemocyanin
Km	Kidney medulla
L	Liver
L_1	Large (10-15 mm follicle)
L_2	Large (18-22 mm follicle)
LAS	Leica Application Suite
LCM	Laser capture micro-dissection
LH	Luteinising hormone
LHr	LH receptor
LLC	Large luteal cells
LMPC	Laser Microdissection and Pressure Catapulting
LO	Late ovulatory phase
Log	Logarithm
LoH	Loop of Henle
LYVE-1	Lymphatic vessel endothelial hyaluronal receptor 1

M	Medium (6-9 mm follicle)
MD	Molecular dynamic
min	Minute
MIP	Major intrinsic protein
ml	Millilitre
mm	Millimetre
mM	Millimolar
mmol	Millimoles
MMP	Matrix metalloproteinase
mOsm	Milliosmoles
mRNA	Messenger ribonucleic acid
MW	Molecular weight
NBF	Neutral buffered formalin
NDI	Nephrogenic diabetes insipidus
ng	Nanogram
NGS	Normal goat serum
nm	Nanometer
NO	Nitric oxide
NPA	Asparagine-proline-alanine
O	Oocyte
OCT	Optimum cutting temperature
OSC	Oocyte stem cells
P_4	Progesterone
PAGE	Polyacrylamide gel electrophoresis
PAPP-A	Pregnancy-associated plasma protein A
PBS	Phosphate buffered saline
PBS+T	Phosphate buffered saline + Tween 20
PCOS	Polycystic ovary syndrome
PCT	Proximal convoluted tubules
PDGF	Platelet derived growth factor
P_f	Permeability coefficient
$PGF_2\alpha$	Prostaglandin F2α
pH	Potential hydrogen

Phe	Phenylalanine
P_{if}	Interstitial pressure
PKA	Protein kinase A
PM	Plasma membrane
PNT	Peripheral nerve tissue
PO	Preovulatory phase
PPIL1	Cyclophilin
PSO	Postovulatory phase
PTE	Proximal tubule epithelium
PV	Portal vein
R	Reverse primer
RBCs	Red blood cells
RCL	Regressing corpus luteum
RNA	Ribonuleic acid
ROD	Relative optical density
RT-qPCR	Real Time quantitative Polymerase Chain Reaction
S	Small (2-5 mm follicle)
SD	Striated ducts
SEM	Scanning electron microscopy
SEM	Standard error of the mean
SG	Salivary gland
SHBG	Sex hormone-binding globulin
Sin	Sinusoids
SLC	Small luteinised cells
SMC-MHC	Myosin heavy chain of smooth muscle cell
StAR	Steroid acute regulatory protein
Str	Stroma
T	Testosterone
T+HF	Testosterone plus hydroxyflutamide
TA	Tunica adventitia
TB	Toluidine blue
TE	Theca externa
TGF-α	Transforming growth factor polypeptide-α

TGF-β	Transforming growth factor-β
TI	Theca interna
TIMP	Tissue inhibitors of metalloproteinase
TIP	Plant tonoplast AQP
Tm	Annealing temperature
TM	Tunica media
TNF	Tumour necrosis factor
TT	Total testosterone
TuI	Tunica intima
TUNEL	Terminal deoxy-UTP nick end labelling
UT-B	Urea uniporter
UV	Ultraviolet
V	Vasculature
VEC	Vascular endothelial cells
VEGF	Vascular endothelial growth factor
Vn	Venule
VP	Vasopressin
VP2R	VP receptor type 2
vWF	von Willebrand factor
v/w	Volume to weight
WB	Western blotting
ZP	Zona pellucida
α-sma	Alpha smooth muscle actin
%	Percent
°C	Degrees celsius
µg	Microgram
µl	Microlitre

Chapter 1

Literature Review

1.1 Introduction

This investigation is concerned with the mechanisms of ovarian follicle development. In terms of the ovary's role in reproductive efficiency, there are two main areas of interest; the inability to ovulate viable oocytes; and the growth of ovarian cysts (Garverick 1997). It is accepted that endocrine, paracrine and autocrine feedback systems regulate the complexities of follicle development, including the initiation of follicle growth; the formation of a fluid filled antrum providing the necessary environment for oocyte maturation, successful ovulation and conception. The literature surrounding these events is vast and well understood in terms of the hormonal control of the reproductive cycles. However the physical mechanism of antrum expansion is less well understood. This study aims to extend this knowledge. The evidence presented could also further our understanding of abnormal follicular development, including cystic follicles in cattle and the polycystic ovary syndrome (PCOS) which afflicts one in 15 women worldwide (Norman *et al.* 2007)

This study will consider the mechanism of follicle growth in terms of antrum formation and expansion, and the role of aquaporins (AQPs) in this pivotal stage of follicle development. The protein and mRNA expression of AQPs throughout the stages of follicle development will be determined through immunohistochemistry (IHC) and real time quantitative polymerase chain reaction (RT-qPCR) respectively. Potential modulation of AQP expression and therefore fluid transport, by androgen will be investigated via granulosa swelling assay.

1.2 Bovine reproductive physiology and cyclicity

1.2.1 Bovine abdominal physiology.

The broad ligament is an extension of the abdominal peritoneum, it supports and houses the vasculature, lymphatic and nervous supply to most of the reproductive tract. It is separated into three distinct domains (Senger 2003). The mesovarium is the anterior fraction of the broad ligament which attaches to and supports the ovary; lateral to this is the mesosalpinx which supports the oviducts. Caudal to the mesosalpinx is the mesometrium, which sustains the uterine horns and body, it is continuous with the

abdominal peritoneum, thus suspends the reproductive tract in the abdominal cavity (Senger 2003; Budras and Habel 2003).

1.2.2 Structure of the bovine ovary

The bovine ovary is a dense ovoid structure measuring approximately 4 x 2.5 cm and is separated into two main compartments; the outer cortex or zona parenchymatosa and the inner medulla or zona vasculosa (Plendl 2000). Figure 1.1 shows the major structures of a generalized mammalian ovary; the surface is covered in a layer of non-vascular cuboidal epithelial cells known as the surface epithelium, previously and erroneously called the 'germinal epithelium'. Directly below this is the tunica albuginea which is a layer of dense connective tissue. The cortex of the ovary lies immediately beneath the tunica albuginea and is the site of folliculogenesis. Follicles at every stage from microscopic primordial follicles, to preovulatory Graafian follicles will be found in random locations within this area (van Wezel and Rodgers 1996). A follicle is an oocyte surrounded by specialised granulosa cells encompassed by a basal lamina or basement membrane; granulosa cells increase in number and alter in function as the follicle develops (Plendl 2000). The basal lamina or basement membrane is the boundary between the granulosa cells and recruited stroma cells which will further differentiate into theca cells. Theca cells lying closest to the basement membrane immediately surrounding the follicle are theca interna cells. Theca externa cells develop beyond the theca interna as a distinct layer. The ovulated follicle undergoes radical morphological changes becoming the corpus luteum (CL) and further the corpus albicans. The granulosa cells of an antral follicle laying closest to the basement membrane are mural, basal or membrana granulosa cells.

Membrana granulosa cells can demonstrate varying morphology from columnar to rounded, columnar tend to be more associated with early antral follicles (Marion *et al.* 1968; Rodgers and Irving-Rodgers 2010c). Beyond the mural cells are layers of stratum or antral granulosa cells. Projecting from the stratum granulosa cells is a stalk like structure called the cumulus oophorus. At the end of this is a mass of granulosa cells which encompass the oocyte called the corona radiata (Marion *et al.* 1968; Fig 1.1). The combined structure is termed the cumulous-oocyte-complex (COC) and is expelled from the follicle upon ovulation. The mural granulosa cells, however remain *in situ* and contribute to the formation of the CL (Hunter, 2003).

Corpora lutea are contained in the cortex of the ovary but are present at different developmental stages depending on the stage of the oestrous cycle. Toward the center of the ovary is the medulla (Fig. 1.1), which is composed of dense connective tissue or stroma and houses the major vasculature, lymphatic and nerve supply. Just before the ovarian artery enters the ovary via the hilus, it divides into smaller arteries that penetrate the central medulla; this region is highly vascularised and dense with connective tissue (Plendl 2000).

1.2.3 The oestrous cycle

Reproductive cyclicity is a series of physiological events that offer the female the opportunity to conceive and become pregnant. Each event is referred to as an oestrous cycle; one cycle is the time from the beginning of 'heat' or oestrus, when the female is sexually receptive, to the onset of the next 'heat' or oestrus. The bovine is a polyestrous breeder, meaning that the cow will cycle throughout the year (Senger 2003).

The bovine oestrous cycle is approximately 21-22 days and is divided into two main phases. The follicular phase accounts for 20% of the overall cycle and is the period of corpus luteum regression from the previous cycle, to ovulation. This phase is dominated by oestradiol (E_2) production and sexual receptivity or oestrus. The remaining 80% of the cycle is the luteal phase and is the period from ovulation to CL regression. The main events during the luteal phase include the development and maturation of the corpus luteum and the secretion of progesterone (P_4; Adams 1999).

The two main phases can be further divided into four distinct stages; proestrus and oestrus (the follicular phase); metestrus and diestrus (the luteal phase).

Proestrus (2-5d) – P_4 levels fall as a result of luteolysis, the degeneration of the corpus luteum. As P_4 inhibits gonadotrophin releasing hormone (GnRH) release from the hypothalamus, the drop in P_4 releases its inhibitory hold over GnRH secretion. Gonadotrophin releasing hormone stimulates the release of follicle stimulating hormone (FSH) and luteinising hormone (LH) from the anterior lobe of the pituitary and targets the ovary. There is a transition from P_4 to E_2 dominance, resulting from follicle development and maturation (Ball and Peters 2004; Adams 1999; Senger 2003).

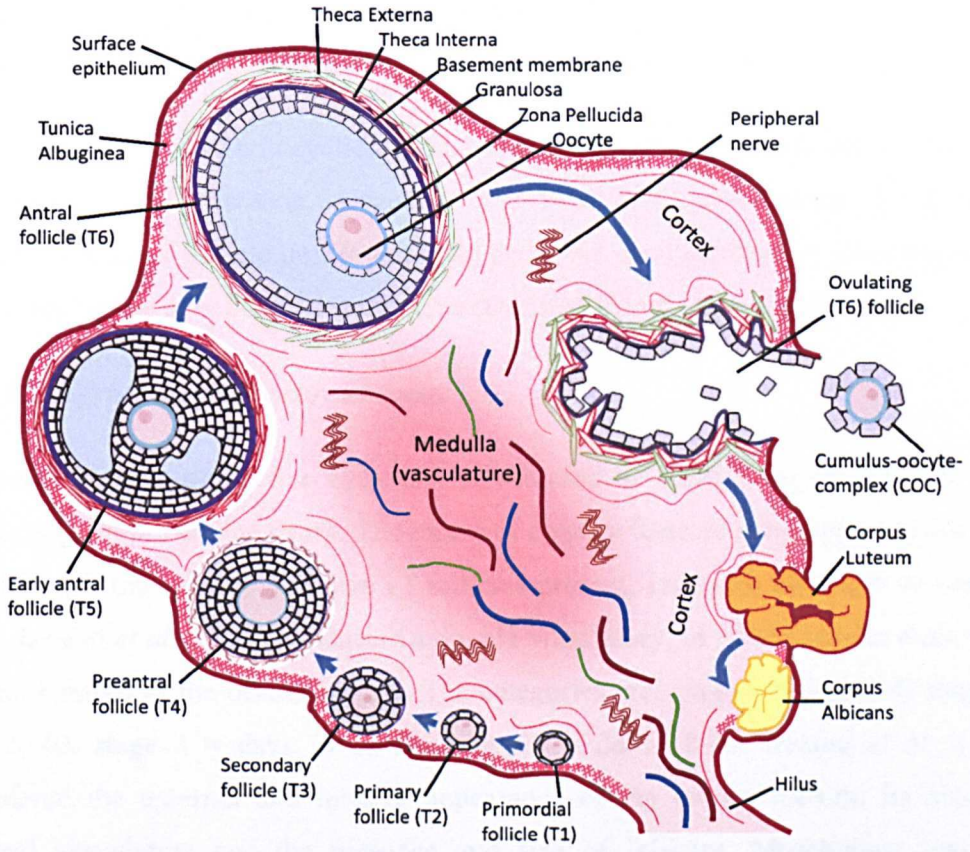

Figure 1.1 A generalised mammalian ovary showing the location of follicles from primordial to ovulatory follicle, corpus luteum formation and regression in the outer cortex of the ovary. The medulla houses the major blood and lymph vessels and nervous tissue. Illustration by author based on and adapted from Senger (2005).

Oestrus (6-24 hr) – The increasing concentration of E_2 from proestrus induces sexual behaviour and receptivity to the bull and results in ovulation 24 – 32 hr after the onset of oestrus. Cattle are mono-ovulatory; only one follicle becomes dominant and ovulates thus they are monotocous and predominantly give birth to single young (Ball and Peters 2004; Adams 1999; Senger 2005).

Metestrus (~5d) – This is the duration between ovulation, immediately after oestrus, and the formation of the mature CL. During early metestrus both P_4 and E_2 are low. The ovulated follicle differentiates into a CL and secretes P_4 increasingly as it matures (Ball and Peters 2004; Adams 1999; Senger 2005).

Diestrus (10 – 14d) – P_4 levels remain high throughout diestrus preparing the uterus for implantation if fertilisation occurred following ovulation. If fertilisation has not occurred, the CL will deteriorate around day 17 of the cycle. This is luteolysis and

results in a significant drop in P_4 levels marking the end of diestrus and prompting the onset of proestrus (Ball and Peters 2004; Adams 1999; Senger 2005).

Anestrus is a period of non cyclicity which can be caused by many situations, including time of the year or season, pregnancy and lactation, environmental stressors and diseases. Waves of follicle development do occur but standing oestrus and ovulation do not, rendering the cow infertile at this time (Ball and Peters 2004; Senger 2005).

1.2.4 Identifying stage of oestrous cycle.

The stage of the reproductive cycle can be assessed by considering the external gross morphology of the bovine ovary. The extent of corpora lutea development, considered in parallel with the number and size of follicles present, indicates the stage of oestrous cycle. Ireland *et al.* (1980) conducted a double blind study, in which ovaries were sorted into four stages of the oestrous cycle. The categories are; stage 1 = days 1-4, stage 2 = days 5–10, stage 3 = days 11-17 and stage 4 = days 18-20. Ireland *et al.*, (1980) considered the external and internal appearance of the corpus luteum, its diameter, external vasculature and the presence and size of follicles. Morphology was then compared with actual days of the oestrous cycle as determined by observation of oestrous behaviour and concentrations of progestins in peripheral plasma (Fig. 1.2). This was the first study to provide the connection between the external anatomy of the ovary and cycle stage. The significance of this is the ability of the researcher to accurately recognise stage of cycle without prior knowledge of the animal. This is particularly useful when collecting abattoir derived material.

1.3 Folliculogenesis

The maximum number of primordial germ cells in the developing prenatal bovine ovary is estimated to be 2100000. Postnatally this number drops due to atresia, to approximately 133000 viable primordial follicles. This number remains stable from birth until four to six years of age, declining to about 3000 by 15 – 20 years of age (Erickson 1966a, 1966b; Hunter 2003). Throughout the reproductive life span of the cow there are cyclical patterns of follicle growth. The growth rate of one of the follicles will exceed that of the others, resulting in one dominant ovulatory sized follicle and regression of the subordinate follicles. The dominant follicle will ovulate or undergo atresia depending on the timing of the developing follicle within the oestrous cycle and its hormonal milieu.

The central dogma for the last 60 years has been that mammals are born with a finite number of oocytes. This stock of potential egg cells decline prenatally and throughout the reproductive life span of the animal. It is considered therefore that once this stock is depleted the animal is no longer able to reproduce and in the case of humans, females undergo the menopause. However, in 2004 Johnson *et al.* presented evidence to suggest there must be some form of oocyte renewal, as oocyte depletion was occurring at a much faster rate than originally calculated. Further work has since identified rare oocyte germ cells (OGC) which when isolated and cultured result in viable mature oocytes (Brinster *et al.* 2007; Tilly *et al.* 2009). The OCS were initially identified in mice and in 2012 was also identified in human ovaries (White *et al.* 2012). The significance of this work not only has the potential to alter our understanding of female reproductive biology as well as alter the treatment for ovarian dysfunction, IVF and reproduction research via the distinct possibility of an unlimited egg supply.

1.3.1 The primordial germ cell and its activation

Primordial germ cells are the embryonic precursors to gametes and are identified in the epiblast of early embryonic life (Buher 1997). The germ cells will proliferate during a migratory journey from the extra-gonadal region to the genital ridge (Picton and Gosden 1999). In the case of the cow the germ cells migrate to the cortex of the ovary and commence meiotic divisions up to late diplotene stage of the first meiotic prophase. They become oogonia and differentiate into primary oocytes as they are surrounded by somatic cells. These are now called primordial follicles and are embedded in a matrix of fibroblasts, collagen and elastin fibres of the ovarian cortex. As a result of meiotic divisions a significant amount of the germinal population has been lost as mentioned above (Hunter 1995). Miyamura *et al.* (1996) used Japanese black cattle to identify the proportion of primordial follicles in the ovary; whilst their sample number was small, they concluded that 94.3% of follicles were indeed arrested at the primordial stage. During each oestrous cycle approximately 500 – 1000 follicles will become activated and begin the journey toward the Graafian follicle stage; few will become antral follicles and only 0.1% of primordial follicles will ultimately ovulate (Ireland 1987).

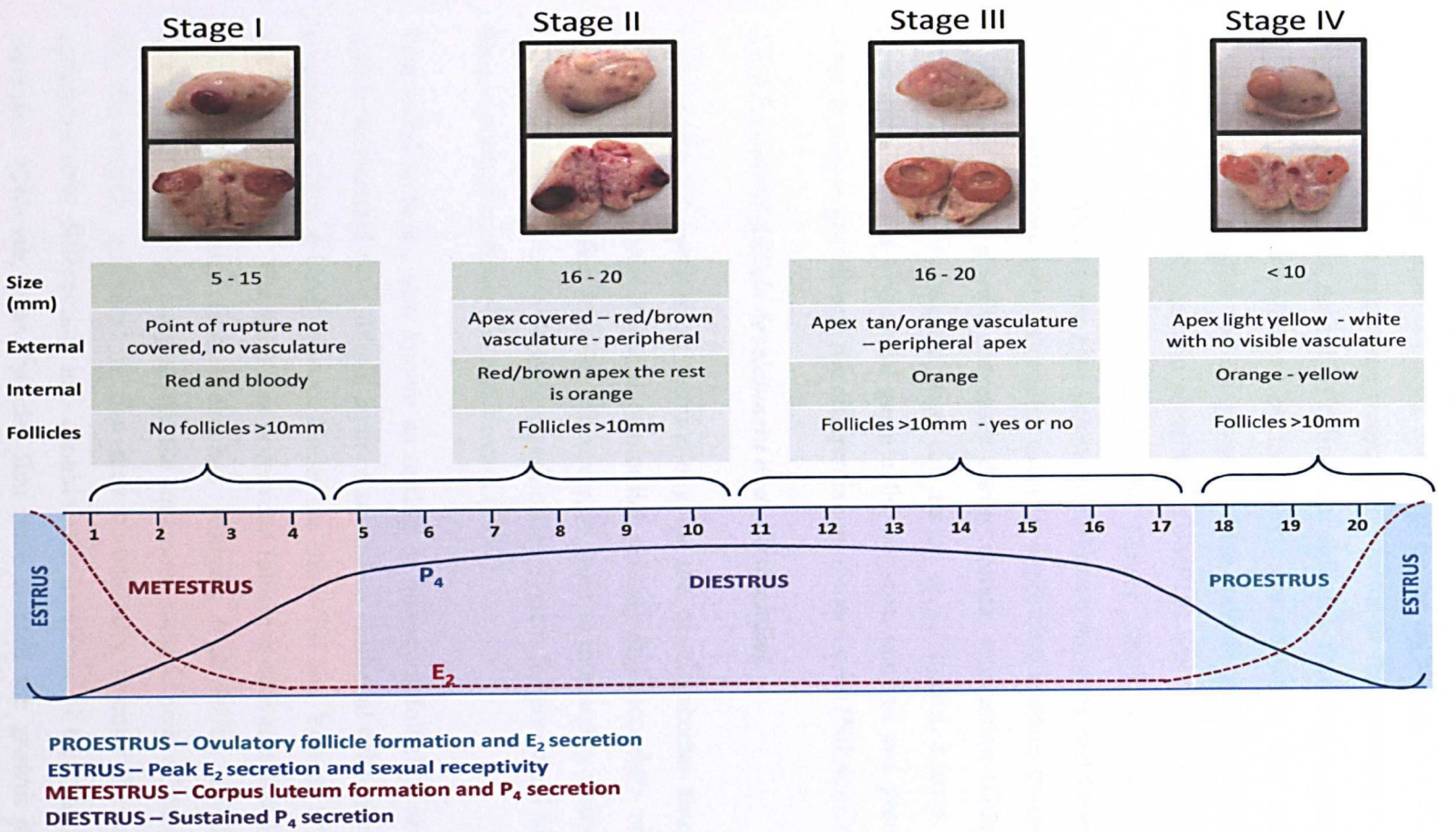

Figure 1.2 External and internal appearance of bovine ovaries at each stage of the oestrous cycle, detailing the main structures of the ovary at each stage parallel with P_4 and E_2 levels. The number and size of surface antral follicles and the size and appearance of corpora lutea accurately indicates the phase of cycle. Based on Ireland *et al.* (1980)

The precise mechanism involved in primordial follicle activation remains unclear (Braw-Tal 2002; Oktem and Oktay 2008; Aerts and Bol 2010a). Whilst granulosa cells have been implicated in oocyte growth regulation (Senbon *et al.* 2003), there is ample evidence to suggest that the oocyte itself may be the regulating factor in folliculogenesis. For example, oocyte expressed transcription factor in the germline α (FIGα) knockout mice develop ovaries devoid of primordial follicles, resulting in sterility (Soyal *et al.* 2000). Other factors produced by the oocyte are known to play crucial roles in the induction of primordial follicle growth. These include growth differentiation factor 9 (GDF9); bone morphogenetic protein 15 (BMP15) and basic fibroblast growth factor (FGF2; Elvin *et al.* 2000; Knight and Glister 2001; Nilsson and Skinner 2001, respectively). Oocytes are also known to influence the gene expression of LH receptor (LHr) on granulosa cells. Cumulus cell LHr expression remains constant, however LHr expression in mural cells increases during follicle maturation (Goudet *et al.* 1999). Granulosa cells also secrete stem cell factor or kit ligand, known to exert an anti-apoptotic effect on primordial germ cells, oogonia, oocytes and pre-antral follicles; it controls oocyte growth and the differentiation of theca cells (Nilsson and Skinner 2001).

1.3.2 Pre-antral follicle development and classification.

Historically the commonest terminology for the developmental stages of the follicle refers to the pre-antral stages as primordial, primary and secondary, and to antral stages as tertiary or Graafian follicles. However, in order to thoroughly study and describe this dynamic process a more detailed classification system for pre-antral bovine follicles has been described by Braw-Tal and Yossefi (1997).

Primordial follicles, also known as resting or quiescent follicles, are identified as an oocyte surrounded by a simple layer of squamous epithelial cells or pre-granulosa cells contained within a basal lamina. Under the Braw-Tal and Yossefi (1997) system these are type-1 follicles. The quiescent primordial follicle is activated and differentiates to the primary follicle stage (van Wezel and Rodgers *et al.* 1996). Hirshfield (1991) and Meredith *et al.* (2000) suggest that the squamous somatic cells of the primordial follicle are not entirely quiescent in that they occasionally re-enter the cell cycle. As the squamous cells differentiate into cuboidal, the incidence of entering into the cell cycle increases. However, even follicles that have entered the growth phase with a high percentage of active granulosa cells may still stop growing or become atretic at any consecutive stage. As the granulosa cells proliferate and differentiate, the oocyte itself

remains relatively inactive and unaltered in size (Aerts and Bols 2010). Braw-Tal, (2002) also demonstrated that when there are seven cells in the largest cross-section of the follicle the number of squamous cells declines and the number of cuboidal cells increases.

At the 18 cell stage complete transformation to cuboidal and thus primary or type-2 follicle stage has occurred. The fourth generation of follicle cells develop, resulting in ~ 40 granulosa cells in the largest cross section. Oocyte diameter also increases in positive correlation with the number of granulosa cells (Braw-Tal 2002).

When there are two or more layers of cuboidal granulosa cells the follicle is now termed a secondary follicle or according to the classifications of Braw-Tal and Yossefi (1997) a small preantral type-3; at this stage theca cells are becoming defined. The secretion of zona pellucida is initiated between the stages of type-2 and -3 follicles; the oocyte itself noticeably increases in diameter whilst developing a more organised ultra structure (Hunter 2003).

By the time the follicle becomes a large preantral or type-4 follicle the zona pellucida has fully encircled the oocyte. The number of granulosa cell layers exceeds six, with over 250 granulosa cells in the largest cross section of the follicle, areas of fluid become noticeable within the granulosa cell intercellular spaces and a clearly defined theca layer is apparent. This is now termed a small antral or type-5 follicle (Braw-Tal and Yossefi 1997; Aerts and Bol, 2010). When these pools of fluid coalesce and a clear antrum is formed the follicle is now referred to as a tertiary, Graffian or antral follicle. See Table 1.1 for a summary of this classification system.

Follicles are compartmentalised from the surrounding stromal tissue by the basal lamina (Braw-Tal and Yossefi 1997) and are therefore avascular. Thus, characteristic changes to the granulosa and oocyte throughout follicle development are induced by autocrine, paracrine and two-way communication between the oocyte and somatic granulosa cells. This communication results in the coordinated development of both oocyte and its surrounding granulosa cells from primordial to antral follicle stages, and is done so via gap junctions (Eppig 1991; Oktem and Oktay 2008). Gap junctions connect the granulosa cells with each other. Those surrounding the oocyte extend cytoplasmic processes through the zona pellucida to connect with the oolema (oocyte plasma membrane; Laurincik *et al.* 1992). A gap junction is effectively a communication channel between two adjoining cells which allows the rapid transfer of low molecular

weight (<1 kDa) substrates between cells. It is composed of two symmetrical units or connexions (Cxs); each cell offers one half of the unit which together form a functional intercellular pore (Meşe *et al.* 2007; Gershon *et al.* 2008). At least 20 Cxs have been identified so far and their distribution is species-, cell type- and developmental stage-specific (Gershon *et al.* 2008). In the bovine ovary Cx26, Cx32, Cx37 and Cx43 are expressed (Johnson *et al.* 1999; 2002). Connexin 26 is located in early stage oocytes and granulosa of antral follicles (Johnson *et al.* 1999). Oocytes and granulosa cells of preantral follicles express Cx37 (Nuttinck *et al.* 2000) and Cx43 is localised to the granulosa cells of primary follicles. As the follicle develops, Cx43 expression increases and is abundant in healthy antral follicles (Johnson *et al.* 1999; 2002). Connexin 32 however, is expressed in the oocyte and granulosa cells of atretic follicles (Nuttinck *et al.* 2000).

1.3.3 Antral follicle classification

The introduction of non-invasive ultrasonography (Rajakoski 1960; Savio *et al.* 1988; Sirois and Fortune 1988; Ginther *et al.* 1989) allowed antral follicles of ≥2 mm to be tracked on a daily basis and the patterns of antral follicle development to be described. Lucy *et al.* (1991) present a classification system for antral follicles based on size, function and biochemical characteristics (Table 1.2).

1.3.4 A Time line for folliculogenesis

In the bovine ovary the process of folliculogenesis from primordial follicle activation through to pre-ovulatory status takes approximately 180 days. The largest proportion of time is dedicated to non-gonadotropin dependent follicle development which takes approximately 138 days (Lussier *et al.* 1987; Hunter *et al.* 2004). From type-2 follicles onwards FSH receptors (FSHr) are present in granulosa cells (Bao and Garverick 1998). Luteinising hormone receptor and steroidogenic enzymes are expressed in theca cells from type-4 follicle stage as the theca cells begin to differentiate (Bao *et al.* 1997). As the antrum forms (type-5), follicular fluid plays a role in growth as the antrum expands, and granulosa cells begin to express steroidogenic enzymes and demonstrate steroidogenic capacity. From this point onward follicle growth is gonadotropin dependent. As growth progresses toward 10 mm, LHr are expressed in granulosa cells and one follicle asserts dominance becoming the pre-ovulatory follicle (Aerts and Bols 2010) see Fig 1.3.

1.3.5 Antral follicular dynamics

Follicular dynamics is the process of continued growth and regression of antral follicles resulting in the one ovulatory follicle per oestrous cycle. In cattle the development of antral follicles in preparation for ovulation occurs sequentially in two (Rajakoski 1960; Pierson and Ginther 1987), or three waves (Fortune 1993; Ireland *et al.* 2000) throughout each oestrous cycle (Fig. 1.4). Animals which exhibit two waves usually have shorter cycles with a much shorter luteal phase than animals who display three waves of follicle grow (Fortune and Sirois 1989; Ginther *et al.* 1989). Each wave is divided into three main events; recruitment, selection and dominance (Hodgen 1982; Ireland 1987; Lucy *et al.* 1992)

Table 1.1 Classification of bovine preantral follicles based on histological investigation, absent (–), present (+) and clearly defined (++), adapted from Braw-Tal and Yossefi (1997).

Follicle	Granulosa layer #	Follicle diameter µm	Oocyte diameter µm	Zona pellucida	Defined theca interna
Primordial = Type 1	1	< 40	29 .74 ± 0.30	–	–
Primary = Type 2	1 – 1.5	40 – 80	31.12 ± 0.42	–	–
Small preantral = Type 3	2 – 3	81 – 130	49.48 ± 2.43	–	–
Large preantral = Type 4	4 – 6	131 – 250	68.61 ± 2.78	+	+
Early antral = Type 5	> 6	250 – 500	92.90 ± 4.50	++	++

Table 1.2. Classification of bovine antral follicles based on biochemical, physiological and functional characteristics (Lucy *et al.* 1991;1992).

Diameter	Function within follicular wave	Physiology and biochemistry
2 – 5 mm = Class 1	Recruited pool of small follicles	Below minimum size for ovulation at luteolysis
6 – 9 mm = Class 2	Recruited follicles and selected follicles	Potential ovulatory follicle at luteolysis. Granulosa cells are devoid of LH receptors.
10 – 15 mm = Class 3	Dominant follicle	Granulosa cells have LH receptors. Follicle has ovulatory capacity.
>15 mm = Class 4	Large dominant follicle	Mature dominant or ovulatory follicle

Recruitment signifies the stimulation of three to six follicles from a cohort of small ≤ 5 mm antral follicles (Fortune *et al.* 1991, Mihm and Evans 2008) to mature in response to hormonal stimuli and grow beyond 5 mm in diameter. Of this recruited group one follicle is selected and asserts dominance over the remaining (subordinate) follicles (Ireland *et al.* 2000; Beg *et al.* 2002; Beg and Ginther 2006). This is signified by a clear difference in growth rate between the largest and second largest follicles and is called diameter deviation (Fortune *et al.* 1991; Ginther *et al.* 1996; Beg and Ginther 2006). The diameter of the dominant follicle at the time of selection is approximately 8.5 mm (Ginther *et al.* 1997). If the wave of follicle growth coincides with the secretion of endogenous prostaglandin $F_2\alpha$ ($PGF_2\alpha$), regression of the CL and decline of P_4, the dominant follicle will mature and ovulate (Lucy *et al.* 1992: Ireland *et al.* 2000). Thus the dominant follicle will only ovulate if produced by the last wave of the cycle, maturing at the time of luteolysis (Fortune *et al.* 1991; Lucy *et al.* 1992, Lucy 2007; Ireland *et al.* 2000). Loss of dominance marks the end of a follicle wave and occurs at the same time as emergence of the next wave.

1.3.6 Hormonal control of the oestrus cycle

The hypothalamic nuclei of the tonic center are responsible for basal secretion of GnRH by releasing small pulses of the hormone over a prolonged period of time. These pulses can alter in frequency and amplitude depending on the rate of firing from the hypothalamic nuclei which in turn stimulate the pituitary to release FSH and LH

(Donadeu and Pedersen 2008). The action of pituitary gonadotrophins FSH and LH on the ovary coupled with negative inhibitory feedback to the hypothalamo-pituitary unit provides the regulatory mechanisms that control recruitment, selection and dominance. In terms of initiating early follicular growth, gonadotropins are probably not involved (Webb *et al.* 2003) as bovine follicles can grow up to 4 mm in diameter in the absence of FSH (Garverick *et al.* 2002). In terms of antral follicle growth, the coordination of follicular waves is dependent on complex inter-relations of the hypothalamus-pituitary-ovarian axis.

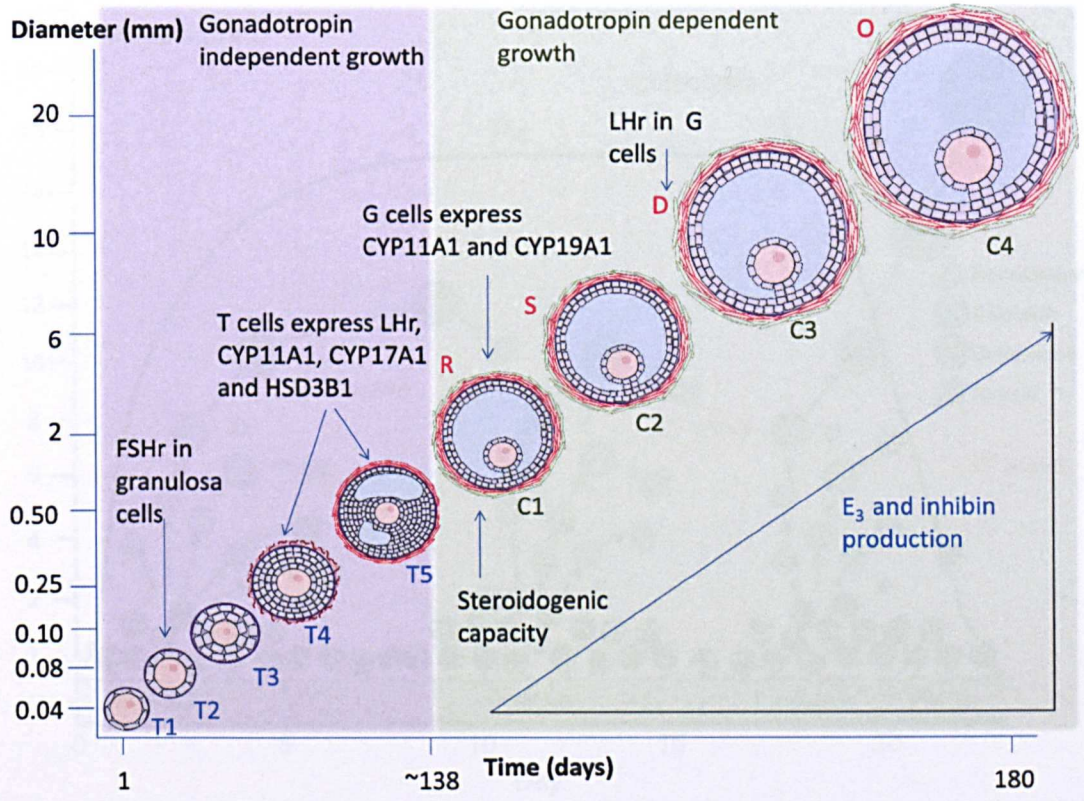

Figure 1.3 A schematic representation of folliculogenesis includes the stages at which granulosa and theca cells express follicle stimulating hormone receptor (FSHr), luteinizing hormone receptors (LHr), steroidogenic enzyme activity such as P450 side chain cleavage (CYP11A1), 17α-hydroxylase (CYP17A1), 3β-hydroxysteroid dehydrogenase (HSD3B1) and aromatase (CYP19A1). The graph is split into gonadotropin dependent growth stages; type-1 (T1) to type-5 (T5), and gonadotropin independent follicle growth stages; class 1 (C1) to class 4 (C4), which also demonstrate increased oestradiol (E_2) production in parallel with follicle maturation. (Hunter *et al.* 2004; Aerts and Bols 2010; Lucy *et al.* 1992; Bao and Garverick 1998; Bao *et al.* 1997; Lussier *et al.* 1987).

It is now well documented that a transient rise in serum FSH concentration precedes the emergence of a new wave of follicle growth (Adams *et al.* 1992; Lucy 2007). Further FSH release is regulated by the products of the developing follicles, namely E_2 and inhibin as a negative feedback loop (Ginther *et al.* 2003). Recruitment is stimulated by FSH and follicles begin to demonstrate steroidogenic capability with increased CYP11A1 cytochrome (P450 side chain cleavage), CYP19A1 (Aromatase) and CYP17A1 (17 α-hydroxylase) activity (Fig 1.3; Garverick 2002; Manikkam *et al.* 2001). Depending on the intrafollicular ratio of E_2 to P_4 or androgens, follicles ≥6 mm can be classified as E_2-active

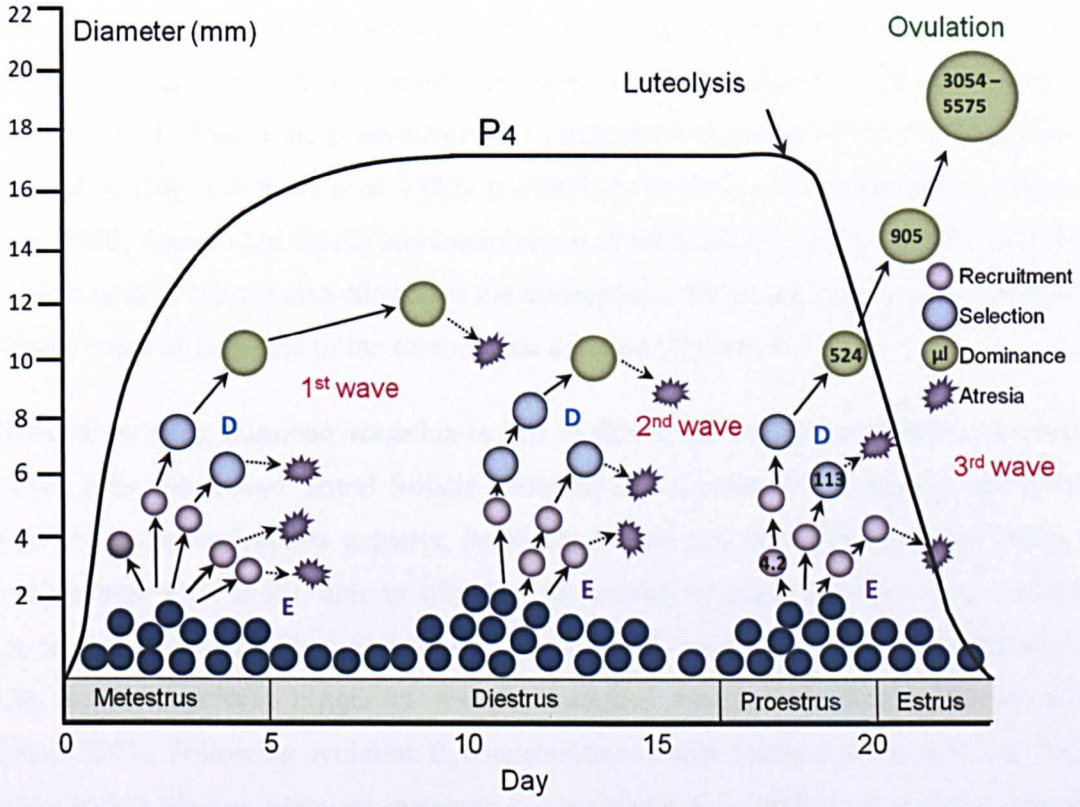

Figure 1.4 Bovine follicle size and volume in relation to the stage of follicular wave, and progesterone level. Adapted from Lucy *et al.* (1992) and Ireland *et al.* (2000).

(E_2 > P_4 and androgens) or E_2-inactive. Healthy growing follicles secrete E_2 and inhibin proportional to growth, inhibiting FSH release; a decline of FSH halts further recruitment of new follicles (P_4 or androgens > E_2; Ireland and Roche 1982; 1983; Nimz *et al.* 2009). Following diameter deviation the commencement of dominance is indicated by the increase in LHr on granulosa cells of the selected follicle, marking the end of FSH dependency and the start of LH dependence (Gong *et al.* 1996; Webb *et al.* 2003). The initiators of deviation include the gonadotrophins, local/intrafollicular factors such as insulin-like growth factor 1 (IGF-1), E_2 and LHr (Beg *et al.* 2002; Beg and Ginther 2006).

During the mid luteal phase (high P_4 levels) LH pulses are high in amplitude but low in frequency, whereas during the follicular phase (low P_4 levels) the amplitude decreases but frequency increases. During the post ovulatory period the amplitude is greatly diminished yet the frequency is at its highest (Fig. 1.5; Rahe *et al.* 1980). Linking the variation in pulsatile secretion of LH with loss or continuation of the dominant follicle suggests that a high frequency of LH pulses results in the maintenance of the dominant follicle. Low frequency LH pulses initiate the loss of the dominant follicle, such as first and second wave non-ovulatory dominant follicles (Lucy *et al.* 1990; Sirois and Fortune 1990; Savio *et al.* 1993; Stock *et al.* 1993; Evans *et al.* 1997). Following luteolysis, the surge center or preovulatory centre of the hypothalamus releases a large amount of GnRH in response to increased E_2 secretion from the developing dominant follicle and low P_4 levels from the deteriorating CL. This is the preovulatory LH surge and is the summation of rapid pulses of LH secretion (Fig. 1.3; Rahe *et al.* 1980). It stimulates ovulation, the inflammatory response (Espey 1980; Assidi *et al.* 2010) and luteinisation of the follicle's granulosa and theca cells (Richards *et al.* 1998). It also stimulates the resumption of meiosis in the oocyte arrested at diplotene stage of prophase of the first meiotic division (Hyttel 1997).

Follicle stimulating hormone secretion is low at this stage as it is suppressed by inhibin released from the mature antral follicle (Bergfelt and Ginther 1985; Knight and Glister 2001). Progesterone imparts negative feedback on LH but not FSH, therefore when P_4 levels are high FSH is still able to stimulate the growth of small follicles. The ovulatory surge in gonadotropins (Fig 1.5) has been shown to rely on increasing E_2 and declining P_4 levels, as an important trigger of the physiological mechanisms leading to ovulation (Zalányi 2001). Following ovulation E_2 concentrations reach baseline levels within a couple of days and in the non-pregnant mammal, prostaglandin $F_2\alpha$ ($PGF_2\alpha$) is released from the uterus and is the main luteolytic mediator promoting the degeneration of the CL (Knickerbocker *et al.* 1988).

1.3.7 Local, intra-ovarian and intra-follicular regulators of growth

It is well established that folliculogenesis is regulated by gonadotrophins; locally produced steroid hormones, peptides and growth factors are also considered important contributors to follicle development and ovarian function (Fortune 1994). Secretions of E_2 and inhibin A and -B from growing follicles inhibit FSH; the dominant follicle is less reliant on FSH and so continues to grow and develop, while the subordinate follicles regress due to a lack of FSH stimulation and so effectively cause their own demise (Ginther *et al.* 2001).

Changes in ratio of intrafollicular growth factors and binding proteins may also play a fundamental role in determining which follicle in a wave achieves dominance. For example inhibin, activin, follistatin, insulin-like growth factor I and II (IGF-I and –II), their binding proteins (IGFBPs) and their proteases, are all thought to have endocrine, paracrine and autocrine actions (Spicer 2004). Differing ratios of intrafollicular IGF-I:IGFBP between dominant and subordinate follicles may explain why the dominant follicle is capable of producing more E_2 and outgrowing its competitors (Mihm *et al.* 2000). Insulin-like growth factors have been reported to stimulate granulosa cell proliferation, differentiation and E_2 secretion (Glister *et al.* 2001). They also increase the secretion of inhibin, activin and

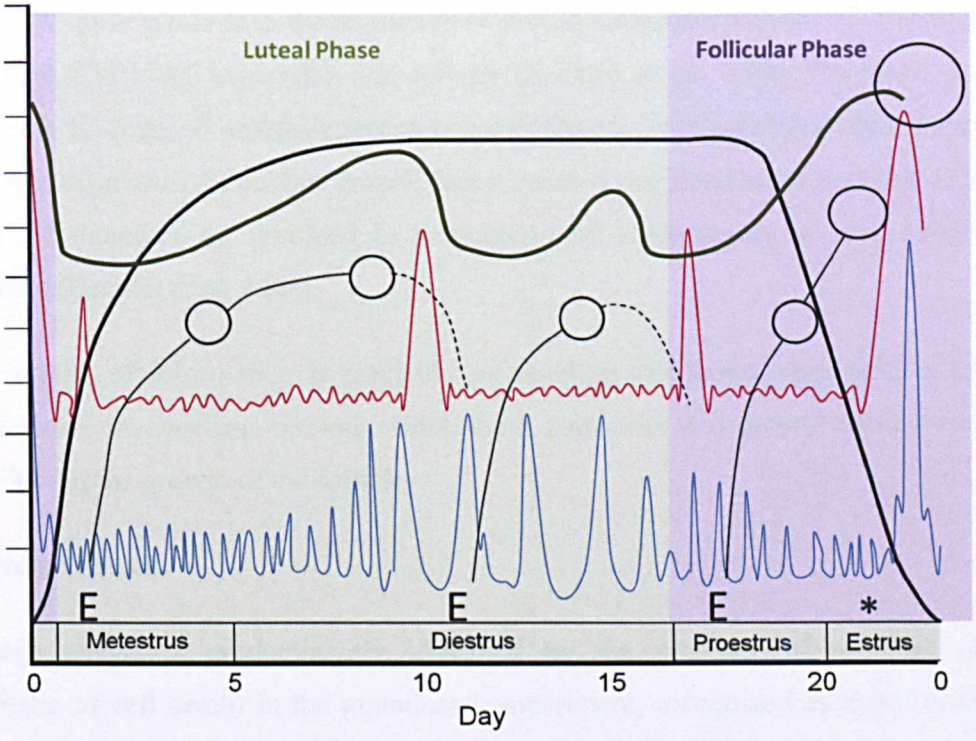

Figure 1.5 This diagram illustrates the hormonal milieu of the dominant follicle throughout the oestrous cycle. Shortly before the emergence (E) of a wave of follicle development there is a transient surge in FSH (red line). The dominant follicles from the first and second wave are under high P_4 levels (black line), decreased frequency and increased amplitude of LH (blue line). These parameters signal loss of dominance and a move to atresia. The increasing levels of E_2 (green line) and inhibin from the growing dominant follicle suppresses FSH and the emergence of a new cohort. When E_2 is high and P_4 is declining at the time of high frequency of LH, GnRH release (*) stimulates a pre-ovulatory surge of FSH and LH. This initiates luteinisation of theca and granulosa cells, maturation of the oocyte and ovulation. (Bergfelt and Ginther 1985; Lucy *et al.* 1990; Sirois and Fortune 1990; Savio *et al.* 1993; Stock *et al.* 1993; Evans *et al.* 1997; Hyttel 1997).

follistatin by granulosa cells and increased androgen synthesis from theca cells (Glister *et al.* 2001). Activins, follistatin and inhibin are considered important autocrine-paracrine modulators of follicular growth, LH and FSH responsiveness, steroidogenesis, oocyte maturation and ovulation (Knight and Glister 2001).

Epidermal growth factor (EGF) and its receptor (EGFR) are expressed in the granulosa cells of several species; it stimulates granulosa cell proliferation, cellular morphological changes, DNA synthesis and protein phosphorylation (Hunter 2003). Transforming growth factor polypeptide-α (TGF-α) can bind to and activate EGF-R (Derynck 1988) and may be involved in granulosa and theca cell proliferation as well as EGF. Transforming growth factor-β (TGF-β) is involved in the regulation of steroid hormone synthesis as it upregulates FSH-induced CYP19A1 expression and activity (Zachow *et al.* 1999). Fibroblast growth factor (FGF) -1, -2 and -7 and their receptors are differentially expressed at different stages of antral follicle growth. Fibroblast growth factor 1 and -7 are localised to preantral follicles and may be therefore be involved in stimulation of angiogenesis at early stages of development (Berisha *et al.* 2004).

Whilst a wealth of information is available surrounding the above, very little is known about the tissue mechanisms through which these hormones and growth factors actually facilitate/inhibit the growth of the follicle

1.4 Follicular atresia

Early stage atresia is predominantly identified by the presence of pyknotic nuclei (symptomatic of cell death) in the granulosa compartment, recognized as hyperchromatic shrunken nuclei. As atresia progresses the incidence of pyknotic nuclei increases and the granulosa cells degenerate (van Wesel *et al.* 1999a; Irving-Rodgers *et al.* 2001), also the number of mitotic nuclei decreases (Kruip and Dieleman 1982). Cell death occurs by several mechanisms, apoptosis, necrosis and terminal differentiation. In apoptotic cells nuclear chromatin condense and bud forming crescent shaped apoptotic bodies phagocytosed by macrophages and/or neighbouring cells (Kerr *et al.* 1995). The DNA is fragmented by endonucleases which can be detected by polyacrylamide gel electrophoresis (PAGE). Terminal deoxy-UTP nick end labelling (TUNEL) is often used as a tissue marker of apoptosis; however there is evidence of inconsistent results using this approach (Funyama *et al.* 1996: D'Herde *et al.* 1994) as it often labels necrotic cells too (Grasl-Kraupp *et al.* 1995).

A family of proteins called B-cell lymphoma 2 (Bcl-2) are known to promote, Bcl-2–associated X protein (Bax) or inhibit (Bcl-2, Bcl-xL) apoptosis by variation in their ratio. In the promotion of apoptosis they activate caspases leading to the irrevocable sequence of the apoptosis cascade (Mignotte and Vayssiere 1998). Necrosis usually involves more than one cell, the nuclei shrink, do not form buds nor is its DNA degraded as in apoptosis, instead it is nicked which again can be detected by PAGE. Cell debris is phagocytosed by macrophages (van Wesel *et al.* 1999). Terminal differentiation involves obliteration or exclusion of the nucleus leading to cell death and is associated with cell exfoliation characteristic of most epithelial tissues (Loktionov 2008).Van Wesel *et al.* (1999a) assessed the modes of cell death in healthy and early atretic bovine follicles. They concluded that the location of the cells within the granulosa compartment determined the mechanism of cell death. Those in the middle proliferative layers undergo apoptosis and are phagocytised by neighbouring cells, possibly destroying the endonuclease activity and potentially explaining why TUNEL results show much inconsistency. Cells in the antral layers or those sloughed off into the antrum result from terminal differentiation and necrosis seems to be associated with advanced atresia (van Wesel *et al.* 1999a). The predominant mechanism responsible for cell death in follicular atresia is apoptosis, the trigger for this mechanism is however not well understood (Tilly 1997; van Wesel *et al.* 1999a; Valdez *et al.* 2005).

The ovulatory follicle is therefore that which evades atresia throughout all stages of follicle development and so atresia is a very significant process. Atresia in bovine follicles, its origin and types, has been described since the early 1900's (Simon 1904). In the 1960's two landmark papers were published by Rajakoski (1960) and Marion *et al.* (1968). However there are many discrepancies between these papers and both offer different classification systems. Marion *et al.* (1968) described three categories of atresia, 1) early, 2) definite and 3) late atresia with four further subdivisions of group 2. Rajakoski (1960) described two main categories, 1) atresia with primary oocyte degeneration and 2) atresia with primary follicular wall degeneration both further divided into at least two subdivisions.

In 2001 Irving-Rodgers *et al.* reconsidered these complex patterns of atresia in bovine antral follicles and concluded that there were in fact only two types of atresia, basal and antral, both with similar degrees of incidence. They concluded that previous studies miss-identified cell types or inaccurately described the origins of one of the forms of atresia. Irving-Rodgers *et al.* (2001) appreciably simplified the morphological identification and therefore investigation of atresia by reducing the types to basal or antral. Basal atresia occurred in follicles <5 mm in diameter only. In these follicles the mural granulosa cells die first,

demonstrating classic apoptotic budding of the nucleus, forming apoptotic bodies which are then phagocytosed by neighbouring cells. They also become separated from the basal lamina as well as each other. In early basal atresia antral cells remain intact and in close association with each other; the outermost cells are very often flattened in shape. There is little evidence of pyknosis, with only a small number of pyknotic nuclei in the antrum. As basal atresia develops, cell death progresses toward the antral layers until the entire granulosa compartment has diminished, often leaving one layer of flattened granulosa cells. Capillaries breach the basal lamina allowing the infiltration of macrophages; as the basal lamina alters, it becomes less organised, convoluted and enlarged in width and more collagenous.

Antral atresia occurred in all sizes of follicles and was associated with the initial degeneration of antral granulosa cells, demonstrating numerous pyknotic nuclei with many of them evident in the antrum (Irving-Rodgers *et al.* 2001). As antral atresia continues, cell death progresses toward the basal layers, with the basal cells maintaining structure and integrity until very advanced stages. Similarly, the basal lamina appears singular with few convolutions, lies in close association with the basal granulosa cells and is not breached by capillaries or macrophages.

In healthy and antral atretic follicles the vasculature and thecal cells were in parallel with the basal lamina. In basal atresia, endothelial cells were randomly orientated and radiated toward the antrum. There was also increased cell debris within the vasculature which was associated with a reduced blood flow. TUNEL staining demonstrated a higher incidence of cell death in theca cells of basal atresia, particularly of the endothelial and thecal steroidogenic cells (CYP11A1 positive; Clark *et al.* 2004). This supported findings by Irving-Rodgers *et al.* (2003) where steroidogenic capacity and steroid hormone production in antral atretic follicles was similar to that of healthy follicles. Basal atretic follicles however, had up regulated steroidogenic enzymes and an increased capacity to synthesise P_4.

1.5 Steroidogenesis

Gonadotropins increase steroidogenesis activity in thecal and granulosa cells via the activation of cAMP-dependent processes. Gonadotrophin receptors are transmembrane G protein-coupled receptors and as gonadotropins bind to these receptors they activate adenylate cyclase, increasing cyclic 3', 5'-adenosine monophosphate as a second messenger (Hillier *et al.* 1994; Hunter 2003). High density and low density lipids are taken up by both

theca interna and granulosa cells; they are converted into cholesterol which is presented to the CYP11A1 (side-chain cleavage) enzyme on the inner mitochondrial membrane by steroid acute regulatory protein (StAR; Stocco 2000b). Cholesterol is cleaved at the C-20, 22 bond to give pregnenolone (C_{21}) by CYP11A1. Pregnenolone is converted to P_4 (C_{21}) by HSD3B1 (Erickson and Danforth 1985; Hillier *et al.* 1994). Whilst both cells follow these conversion pathways, it is the thecal cell which does so to a greater degree. CYP17A1 and HSD3B1 convert P_4 to androgen (androsteredione or testosterone) which diffuse across into the granulosa cell where the subsequent conversion into estrone and E_2 occurs by CYP19A1 action. The capacity for aromatization of C_{19} steroids is greater in granulosa cells than in the theca interna cells (Erickson and Danforth 1985; Fortune 1986; Hillier *et al.* 1994). See Fig. 1.6 for a summary of this process. As the granulosa cells are avascular E_2 has to pass back across the basement membrane and enter into the circulatory system through the theca cells.

The rate limiting step of steroidogenesis is the translocation of the substrate cholesterol from the outer to the inner mitochondrial membrane and its presentation to CYP11A1. Steroid production up-regulation goes hand in hand with increased expression of StAR protein. In several species including bovine and porcine, LH (Juengel *et al.* 1998; Zhang *et al.* 2000) has been shown to up-regulate StAR expression. Protein kinase A is activated when LH binds to its receptor which increases the synthesis of StAR (Stocco 2000a). Follicle stimulating hormone has also been shown to up-regulate StAR expression (Pescador *et al.* 1997).

1.6 Luteinisation and luteolysis.

Whilst this investigation is primarily concerned with the process of fluid accumulation and follicle growth it is important to briefly discuss the events which occur following ovulation. Up until this point steroidogenesis has primarily been concerned with the aromatization of testosterone to E_2 to provide the correct hormonal milieu for follicle maturation and initiation of the pre-ovulatory LH surge followed by ovulation. The process of ovulation involves the loss of follicular basal lamina integrity; as a result the theca and granulosa are no longer discrete compartments. This allows thecal cells and capillaries to penetrate the membrana granulosa mixing with the granulosa cells (Irving-Rodgers *et al.* 2006a). The rupture of thecal vasculature also subjects the granulosa cells to blood as the follicle collapses and blood fills the antral void and a corpus hemorrhagicum is formed. The theca, granulosa cells and connective tissue are transformed into luteal tissue and ultimately into the corpus luteum.

Both thecal and granulosa cells become luteinised under the influence of LH which is now freely accessible. Both are clearly distinguishable histologically with luteinised granulosa cells being larger than luteinised theca cells. In terms of steroidogenesis, small luteinised cells (SLC) are responsible for increased P_4 secretion under the influence of LH. Large luteal cells (LLC) secrete oxytocin, relaxin and contribute to basal P_4 levels independently of LH (Miyamoto and Shirasuna 2009). Progesterone targets the hypothalamus, uterus and mammary gland all in preparation for implantation and pregnancy (Niswender *et al.* 1985). Therefore a dysfunctional CL can clearly lead to reproductive dysfunction. In cattle the structural and functional degradation of the CL, or luteolysis, is triggered by pulsatile secretion of $PGF_2\alpha$ from the endometrium. As the structure diminishes it becomes a corpus albicans (Acosta *et al.* 2002).

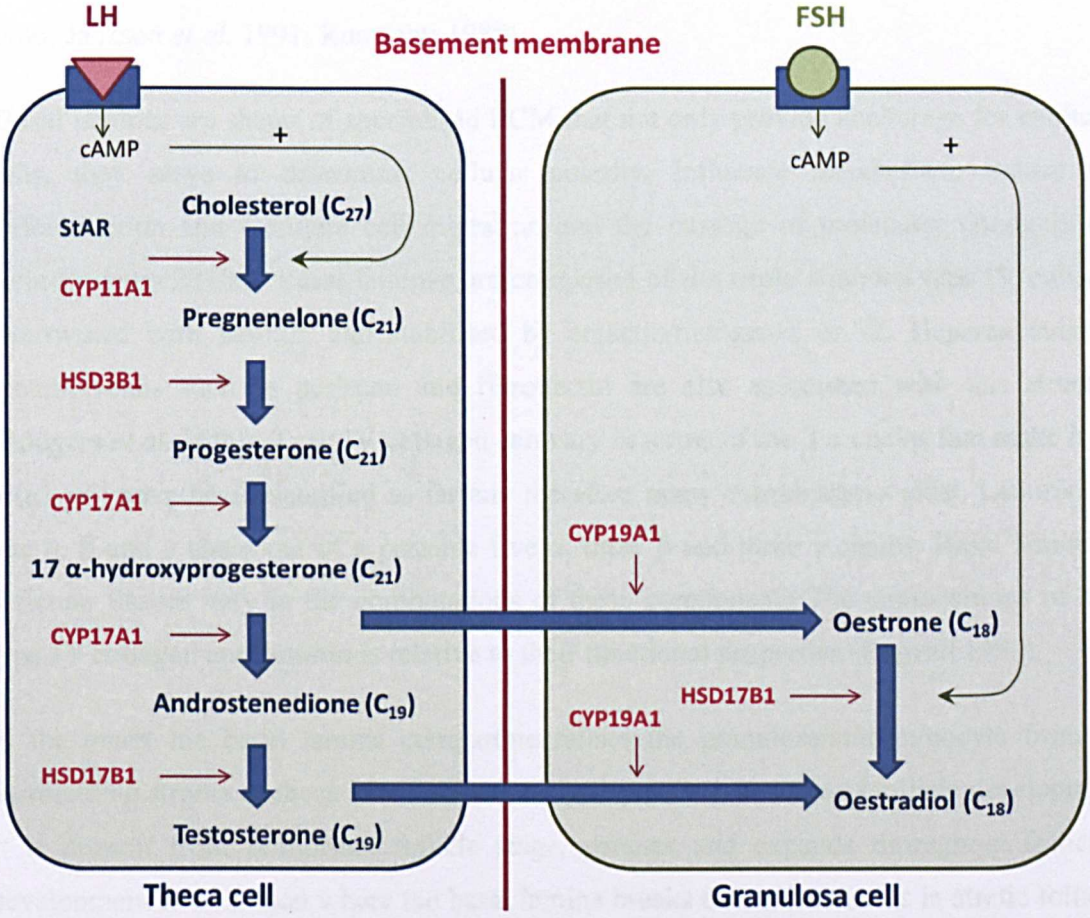

Figure 1.6 Schematic illustration of E_2 synthesis via the two-cell, two gonadotropin model. Cholesterol is converted into androgen predominantly by the theca cell and by a lesser extent by the granulosa cell. Androgens are passed into the granulosa to be aromatised into oestradiol. The major intermediate products and steroidogenic enzymes are shown. (Illustration by author, based on Leung and Armstrong 1980; Hillier *et al.* 1994; Knobil and Neill 1994; Senthilkumaran *et al.* 2004; Payne and Hales 2004).

1.7 Ovarian extracellular matrix

1.7.1 Production, composition and function

Epithelial cells in mammalian tissues are structurally organised by extracellular matrix (ECM) and cell-cell interaction. The cellular sheet or epithelium is anchored to the ECM or basal lamina (cell-matrix attachment) and specialised inter-cell junctions (cell-cell attachment). The ECM is usually produced by the epithelial cells themselves or by other local cells and plays an important role by influencing the development, proliferation, migration, shape, function and fluid dynamics of a tissue. The ECM also has the ability to bind growth factors (Rodgers *et al.* 2000). The most abundant macromolecules that make up the ECM are glycosaminoglycans (GAGs) and proteoglycans, adhesive proteins, fibronectin, laminin and structural proteins including collagen and elastin (Ekblom *et al.* 1986; Jackson *et al.* 1991; Ruoslahti 1988).

Basal laminas are sheets of specialised ECM that not only provide anchorage for epithelial cells, they serve to determine; cellular polarity, influence metabolism, induce cell differentiation and facilitate cell migration and the passage of molecules (Rodgers and Irvin-Rodgers 2010a). Basal laminae are composed of the triple stranded type IV collagen intertwined with laminin and stabilised by entactin/nidogen-1 or -2. Heparan sulphate proteoglycans such as perlecan and fibronectin are also associated with this structure (Rodgers *et al.* 2000). Type IV collagen can vary in terms of the 3 α chains that make it up; 6 (α1-α6) have been identified so far and therefore many combinations exist. Laminin has one α, β and γ chain out of a possible five α, three β and three γ chains. Basal lamina of different tissues vary in the combinations of these components The compositions of both type IV collagen and laminin is relative to their functional properties (Engvall 1993).

In the ovary the basal lamina compartmentalises the granulosa/antrum/oocyte from the surrounding stroma or theca externa and interna depending on stage of follicle development. It is present from primordial follicle stage, persists and expands throughout follicular development to ovulation where the basal lamina breaks down; it remains in atretic follicles to an advanced stage of atresia (Irvin-Rodgers and Rodgers 2000; Irvin-Rodgers *et al.* 2006a and Irvin-Rodgers *et al.* 2002 respectively). Although the basal lamina persists throughout follicle development its composition changes and is summarised in Table 1.3.

Recent studies identified a novel basal lamina-type matrix called focal intra-epithelial matrix (focimatrix). It appeared in between the granulosa cells of follicles >5 mm and

increased in abundance as the follicle developed. It is composed of type IV collagen α1 and α2, laminin chains α1, β2, γ1, perlecan and nidogen 1 and 2 (Irving-Rodgers *et al.* 2006b). Focimatrix appears before deviation and persists beyond this stage. Irving-Rodgers *et al.* (2006b) therefore consider it to be developmentally regulated and of potential importance in the development of dominance. Further investigation found that focimatrix expression was significantly elevated in dominant follicles highly correlating with CYP11A1 expression. Focimatrix could therefore be a potential modulator of CYP11A1 expression and play a role in follicular dominance (Irving-Rodgers *et al.* 2009).

Literature concerned with the cellular origin of basal lamina concludes that granulosa cells are capable of secreting the majority of basal lamina components (Zhao and Luck 1996; van Wezel *et al.* 1999b, 1998; Rodgers *et al.* 1995, 1996). Less is known about the origin of thecal basal laminae.

Table 1.3 Composition of follicular and thecal basal laminae in relation to stage of follicle development (adapted from Rodgers *et al.* 2003).

Matrix	Developmental stage	Laminins	Collagens	Other components
Follicular basal lamina	Primordial (T1)	α1, β2, γ1	Type IV α1 α2 α3 α4 α5 α6	
	Preantral (T3/4)	α1, β2, γ1	Type IV α1 α2 α3 α4 α5 α6	Nidogen, perlecan
	Antral	α1, β2, γ1	Type IV α1 α2	Nidogen, perlecan
	Atretic,antral	α1, β2, γ1, +/- α2	Type IV α1 α2	Nidogen, perlecan
Thecal sub-endothelial basal lamina	Antral	B1, β2	Type IV α1 α2	
Thecal arteriole smooth muscle basal lamina	Antral	β2	Type IV α1 α2	

According to van Wezel and Rodgers (1996) the surface area of a follicle grown from primordial to 18mm preovulatory, on average, doubles 19 times. Irving-Rogers and Rodgers (2000) investigated the ultrastructure of bovine follicular basal laminas and found significant variation between follicles. Basal laminas were either conventional, single layered and in alignment with the membrana granulosa, or made up of many layers and loops. Conventional basal lamina was associated with healthy follicles with rounded granulosa cells. 'Loopy' basal lamina was found in follicles with columnar granulosa cells. Irving-Rodgers and Rodgers (2000) and van Wezel *et al.* (1999a) related granulosa morphology to the speed with which the follicle grows. Thus follicles that had conventional laminae with rounded granulosa cells grow more rapid than follicles with columnar cells and loopy lamina. It appears therefore that the basal lamina is remodelled during follicular development and its resulting morphology is related to the rate of follicle growth. Whether the granulosa cell (columnar or rounded) influences the morphology of the basal lamina (conventional or loop) or vice versa remains to be determined.

Extracellular matrix remodelling is fundamental to the reorganisation of tissue during the processes of follicular development, atresia, ovulation, corpus luteum formation and regression. Remodelling of the ECM occurs by matrix metalloproteinases (MMPs). These are zinc- and calcium-dependent enzymes such as; collagenases, gelatinases, stromelysins, and membrane-type MMPs (Nagase 1997). When activated they cleave components of the ECM and are themselves inhibited by tissue inhibitors of metalloproteinases (TIMPS; Smith *et al.* 1999). As mentioned previously ECM binds a number of growth factors, therefore the proteolytic effect of MMPs can liberate growth factors from the ECM, such as that for IGFs. As follicle development progresses, binding proteins for the IGFs diminish due to the actin of MMPs, effectively releasing IGFs and increasing its availability (Fowlkes *et al.* 1994). It is postulated that MMPs must play a role in follicular atresia however evidence provided by Irving-Rodgers *et al.* (2002) illustrate the persistence of the basal lamina until advanced stages of atresia and so the exact action of MMPs in this instance remains undetermined (Smith *et al.* 1999).

1.7.2 Ovulation and the basal lamina

As a preovulatory follicle nears ovulation it protrudes significantly from the surface of the ovary, at the apex of the follicle a small thinning or papilla (stigma) forms (Murdoch 1998). This is the site of rupture and requires the proteolytic degradation of the ECM of the surface epithelium, tunica albuginea, thecal externa and interna, the basal lamina and loosening of

granulosa cells (Murdoch 1998). It has been established by Leonardsson *et al.* (1995) that the plasminogen activator-plasmin enzyme family contributes to the proteolysis involved in the mechanism of ovulation. They are also recognised as being involved in the increase in activation of interstitial collagenase proenzyme (Leonardsson *et al.* 1995). Collagenases may be responsible for the denaturing of the collagen triple helix at the point of the papilla (Reich *et al.*1991; Balbin *et al.*1996). Gelatinases A and B then cleave the unwound gelatin collagen and collagen type IV, they may therefore play a role in basal lamina breakdown (Smith *et al.* 1999) of ovulation. Matrix metalloproteinases are zinc dependent proteases capable of breaking down ECM proteins and have been associated with connective tissue remodelling during ovulation (Curry *et al.* 1988; Tadukuma *et al.* 1993). Therefore the ratio of MMPs and TIMPS regulate net proteolysis during ovulation (Smith *et al.* 1999). Irving-Rodgers *et al.* (2006a) investigated the remodelling of ECM at the time of ovulation in bovine follicles and concluded that both basal laminae and focimatrix were degraded at ovulation however following the LH surge the individual ECM components were degraded at different times.

1.8 The ovarian circulatory system

The ovarian and uterine artery both originate directly from the abdominal aorta. In the cow the ovarian artery traverses the length of the broad ligament and divides into the ovarian branch and uterine branch. The former divides into smaller primary vessels supplying the infundibulum, the oviduct, and the ovary, entering via the hilus and branching to form a plexus within the medulla. Spiral arterioles branch from the medullary vessels, supplying the cortex and forming dense networks of capillaries in the theca interna of growing follicles (Lammond and Drost 1974).

1.8.1 Follicular vasculature

Corrosion casts reveal extensive capillary networks of crowns or wreaths within the theca layers, as the follicle progresses to dominance a double wreath of capillaries form. The outer wreath is of the theca externa and the inner wreath of the theca interna which supplies the avascular granulosa cells (Kanzaki *et al.* 1982; Macchiarelli *et al.* 1993; Yamada *et al.* 1995). Jiang *et al.* (2003) used scanning electron microscopy (SEM) on bovine ovarian corrosion casts to study microvascular changes during follicle development and atresia. They found that small healthy follicles had the smallest number of capillaries in the inner thecal layer, whilst medium follicles had more capillaries with active angiogenesis in the apical part of the inner layer. Large dominant follicles with high E_2 to P_4 ratio demonstrated

highly developed capillaries with active spatial-dependant angiogenesis in the middle or basal part of the inner thecal layer. Capillary degeneration was found to initiate in the outer vascular layers and was closely linked with atresia (Jiang *et al.* 2003).

Venous networks are closely associated with the arterial coils and form many arterio-venous connections creating a counter current feedback system. This could be important in the establishment of local communication between different ovarian compartments (Bendz *et al.* 1982; Einer-Jensen and Hunter 2005). This could also modulate follicular dominance as dominant follicles display increased vascularisation (Macchiarelli *et al.* 1993; Plendl 2000; Jiang *et al.* 2003; Acosta 2007).

1.8.2 Blood vessel cell types.

Blood vessels are composed of three distinct layers. The lumen of the vessel is formed by the tunica intima, it is composed of a single layer of endothelial cells surrounded by an underlying basal lamina and subendothelial connective tissue. The tunic media is primarily circular smooth muscle and the adventitia is longitudinal fibroelastic connective tissue separated from the intima by an elastic lamina. These layers are common to all vessels with the exception of capillaries which are simply endothelial cells anchored to a basal lamina. Endothelial progenitor cells are angioblasts and themselves differentiate from the mesoderm during gastrulation (Risau 1995); when fully differentiated they demonstrate heterogeneity in function, structure and gene expression. Primary functions include barrier function and angiogenesis, vasomotor tone, cell and nutrient trafficking and control of haemostasis (Middleton *et al.* 2005). Whilst endothelial cells make up the inner lining of capillary vessel walls pericytes shroud the surface of the vessel (Bergers and Song 2005). Otherwise known as Rouget cells, mural cells or vascular smooth muscle cells (vSMC) due to the expression of contractile smooth muscle actin, pericytes are localized around capillaries, precapillary arterioles, post capillary venules and collecting venules (Xueyong *et al.* 2008). Morphologically the pericyte cell possesses a cell body with numerous long cytoplasmic projections which connect with the endothelial cell abluminal surface via gap junctions (Armulik *et al.* 2005). Anchored into the basement membrane one pericyte may make direct physical contact with many endothelial cells along the length of the same capillary but may also connect with other capillaries, allowing direct exchange of information and contractile forces (Bergers and Song 2005; Hirschi and D'Amore 1996).

Historically pericytes have been associated with supportive and stabilising functions, however recent evidence suggests they can sense angiogenic stimuli, educe endothelial

survival functions, direct sprouting tubes and demonstrate macrophage characteristics (Bergers and Song, 2005). Bergers and Song (2005) report that when vessels lose pericytes they become hemorrhagic and hyper-dilated; pericytes have therefore been associated with the ability to affect blood flow and the process of angiogenesis. As pericytes are in such close association with vascular endothelial cells (VEC) it can be difficult to ensure the specific isolation and identification of either cell type. The identification of specific molecular markers is therefore paramount in the ability to identify, localize and conduct functional investigations of blood vessel cells types.

Less is known about the lymphatic pathways of the ovary. Evidence in rabbit ovaries suggests that lymph vessels follow a similar pattern of development to that of capillaries. As the follicles progress from a type-3 or secondary follicle increasing proliferation of lymph vessels become apparent in the theca layers (Hunter 2003).

1.8.3 Molecular markers of endothelium

The literature indicates a considerable variety of markers for endothelial cells. The expression of these markers is dependent on numerous factors including tissue and organ specificity as well as endothelial location of the vascular tree. Middleton *et al.* (2005) carried out a comparative study of endothelial cell markers to identify specificity and to see if the expression altered between rheumatoid arthritis and non rheumatoid arthritis tissue. They used; von Willebrand factor (vWF), MECA-79, Duffy antigen receptor for chemokines (DARC), cluster of differentiation 31 (CD31), CD34, CD105 and CD146. Their results showed that vWF was widely distributed and localized to venules, capillaries and arterioles, MECA-79 was restricted to venules at sites of inflammation and leukocyte infiltration, and DARC was found in venules of inflamed and non-inflamed tissue. The remaining markers were identified in all endothelial cells of the microvascular bed but they also labelled other cell types including pericytes, smooth muscle cells, macrophages and lymphocytic infiltrate (Middleton *et al.* 2005).

Distinguishing blood vessel endothelia from lymphatic endothelia is also problematic. However, Xu *et al.* (2004) identified lymphatic vessel endothelial hyaluronan receptor 1 (LYVE-1) expression in lymphatic endothelial cells but not blood vessel endothelia. Molecular markers for pericytes include desmin, NG2 proteoglycan, smooth muscle actin alpha (ACTA), myosin heavy chain of smooth muscle cell (SMC-MHC), caldesmon and calponin (Xueyong *et al.* 2008). There are, however, no markers specific to just pericytes

and the markers listed above are not expressed by all pericytes (Xueyong *et al.* 2008; Armulik *et al.* 2005.

1.8.4 Angiogenesis and the ovary

Angiogenesis is the differentiation, development and growth of new capillaries from pre-existing vessels by endothelial cell proliferation (Schams, 2005). First the basal lamina of existing vessels break down, the endothelial cells (EC) migrate into the interstitial space in response to an angiogenic stimulus. Following this, endothelial cells proliferate, the lumen develops and maturation follows as the vessel is stabilised by pericyte recruitment (Risau 1997; Gerhardt and Betsholtz 2003). Antral follicle growth, dominance and achievement of preovulatory status is dependent on neovascularisation potentially providing greater hormonal and nutrient support (Fraser and Duncan 2009). There is evidence to suggest that E_2 active dominant follicles display greater vascularisation and therefore blood flow than subordinate follicles (Grazul-Bilska *et al.* 2007; Acosta *et al.* 2004; 2005). Cellular differentiation, growth and regression are closely dependent on the supply of blood. As a follicle matures from a type-3 (secondary) follicle to a mature corpus luteum the rate of vascularisation is rapid, rivalled only in the aggressive growth of some tumours (Plendl, 2000).

Pro- and anti-angiogenic factors have been identified. Important promoters include vascular endothelial growth factor (VEGF; Ferrara *et al.* 2003), platelet derived growth factor (PDGF; Fredriksson *et al.* 2004), FGF2 (Presta *et al.* 2005), TGFs, angiopoietins (Maisonpierre *et al.* 199 7), EGF, IGF, tumor necrosis factor (TNF) angiotensin-2 and endothelins (Harris 2003). Follicle stimulating hormone, LH, E_2, P_4 and $PGF_2\alpha$, could also be very important in the regulation, promotion and inhibition of angiogenesis (Plendl, 2000). Oestradiol is well documented to influence proliferation of capillaries in a variety of tissues as well as the female reproductive tract (Greenwald and Roy 1994; Taylor *et al.* 2001; Torry and Rongish 1992). Anti-angiogenic factors are less well studied, such as thrombospondin (Armstrong and Bornstein 2003) and angiostatin (Wahl *et al.* 2005), although as discussed previously MMPs breakdown basal laminae and are inhibited by TIMPS. Therefore any protease inhibitor could effectively be an anti-angiogenic factor (Auerbach and Auerbach 1994).

1.9 Follicular fluid

As described in section 1.3.2 the type-5 (early antral) follicle demonstrates small foci of fluid which eventually coalesce forming a fluid filled antrum. As it develops into a fully antral follicle and grows in size, the antrum expands and following the LH surge follicular fluid (FF) accumulation markedly increases. The FF provides the oocyte with a nutritional milieu conducive to maturation (McNatty 1978), as well as physical extrusion of the follicle, contributing to the mechanism of ovulation (Espey and Lipner 1994).

1.9.1 Antrum formation

Granulosa cells are a type of epithelial cells devoid of tight junctions and are therefore unlikely to establish osmotic gradients of small molecules such as sodium across the follicle wall. Gap junctions, as previously discussed, have been shown to play a functional role in intercellular communication and the maintenance of healthy follicle development (Johnson *et al.* 2002; Gittens *et al.* 2003). Connexin 32 has been identified in the cytoplasm of granulosa cells of atretic follicles only (Johnson *et al.* 2002) with decreased expression at the onset of antral cavity formation (Nuttinck *et al.* 2000). At this stage of development (type-5/early antral follicle) the follicle accumulates fluid and expands as follicle development progresses. The precise m echanism of this process, however, is not well understood. The initial foci of fluid may develop in regions where cell-cell junctions are less abundant so fluid seeps in between the cells. Alternatively, cells may undergo apoptosis freeing up space, possibly in parallel with the expression of apoptotic-specific gap junctions such as Cx32. If these mechanisms do play a part in antrum formation it would only be during the initial stages where the movement of very small amounts of fluid are concerned. A fully antral follicle of ~2ml with an avascular antrum of ~4.2 µl in volume has to create an osmotic differential great enough to allow progression to a 22 mm follicle with a volume of ~5575 µl. Osmotically active molecules would need to be directionally secreted into the forming foci of fluid and increasingly the expanding antrum.

1.9.2 Follicular fluid composition.

Follicular fluid initially originates from secretions of the granulosa cells and the COC as well as transudate from the thecal capillaries (Andersen 1976; Gosden 1988; McConnell *et al.* 2002; Hunter 2003; Clarke *et al.* 2006). Its composition therefore shares some similarity with that of plasma (Shalgi *et al.* 1972). Andersen *et al.* (1976) looked at the protein composition of bovine FF and found that the mean protein concentration was 86.4% that of

serum whereby large molecules > 100 kDa were only present in the FF at low concentrations. This is partly determined by the selective nature of the basal lamina which the transudate and its solutes traverse in contributing to the forming antrum. This also suggests that transport across the basal lamina may be size dependent.

Therefore FF differs from plasma in terms of, high molecular weight (MW) plasma proteins and by the addition of local secretions (Leroy *et al.* 2004). These secretions include electrolytes, metabolites and nutrients such as ions, glucose, lactate, pyruvate, and amino acids; steroid hormones, peptides and GAGs. The presence of macromolecules was investigated by Clarke *et al.* (2006). They identified large MW molecules such as versican and inter-alpha trypsin inhibitor and hyaluronan, in follicular fluid. Gèrard *et al.* (1998) conducted an electrophoretic comparison of high molecular mass proteins from equine FF and granulosa cell lysates. They also found the presence of a high MW protein of 200 kDa (yet to be identified), its presence was stage related and found in preovulatory follicles rather than in earlier stage or subordinate follicles. Table 1.4 lists some of the main components of FF.

1.9.3 Cyclical variation of follicular fluid composition

Many studies have provided evidence to suggest that the biochemical composition of FF changes throughout the oestrous cycle and from small to large follicles, via local mediation and metabolic changes in serum. Certain alterations may have profound effects on the quality of the developing follicle and ultimately the oocyte (Leroy *et al.* 2004). Understanding the local and systemic contributions to FF change may increase understanding of the optimum microenvironment needed for follicular development leading to ovulation. Much literature is therefore concerned with changes in FF and its correlation with follicle selection and dominance.

Orsi *et al.* (2005) characterised the pyruvate, glucose, lactate and amino acid profile of bovine FF in comparison to plasma concentrations and pertaining to oestrous stage. Their findings showed no significant changes in pyruvate between plasma and FF of dominant follicles. Follicular fluid glucose content was lower than plasma at all developmental stages whereas lactate was higher and more so in non-dominant follicles. Amino acid concentrations in dominant follicles did fluctuate dependent on oestrous stage. Whilst some amino acids were found at lower concentration in FF than in plasma, valine was consistently and significantly higher in FF than plasma.

Dominant follicles have a higher concentration of E_2 (Kruip and Dieleman 1985; Fortune *et al.* 2004; Beg *et al.* 2002; Watson *et al.* 2002). This has been attributed to lower concentrations of IGFBPs and higher IGFBP-4/-5 protease activity via pregnancy-associated plasma protein A (PAPP-A). Increased PAPP-A results in increase free IGF which interacts with FSH to promote rapid E_2 production (Fortune *et al.* 2004). This finding also supports those by Beg *et al.* (2002).

Gerard *et al.* (2002) studied follicular fluid variation during follicular growth and maturation in mares. Intrafollicular E_2 and P_4 were related to intrafollicular glycoconjugates, lipoproteins, glucose metabolites and amino acids. Intrafollicular sugar content decreased up to preovulatory stage development and was associated with changing metabolic activity of the follicle towards ovulation. Whilst alanine was significantly higher in FF than serum both alanine and lipoproteins (CH_3) decreased from early to late dominant stage.

Table 1.4 Major components of follicular fluid (adapted from Baker 1982; Sinosich 1987; Lenton *et al.* 1988; Clarke *et al.* 2006).

Major Proteins	Enzymes	Steroid Hormones	Peptide Hormones
Complement factors	Proteinase	Androstenedione	Luteinizing Hormone
Immunoglobulins (Ig)	Plasmin	Testosterone	Follicle stimulating Hormone
Albumin	Alkaline Phosphatase	Estradiol	Inhibin
α_2-macroglobulin	Acid Phosphatase	Progesterone	Prolactin
PAPP-A	Lactate dehydrogenase		
Placental protein 5	Aspartate/Alanine aminotransferase		
α-follicular fluid antigen	Hyaluronoglucosidase		
IGF, IGFBP-2,-4 and -5			
Hyaluronan			
Versican			
Inter-alpha trypsin			

Progesterone and E_2 concentration increased from early to late dominance, following this E_2 levels dropped in preovulatory follicles whereas P_4 levels increased. Trimethylamine and acetate decreased between late dominant and preovulatory stage. Similar results were found in cows by Brantmeier *et al.* (1987).

1.9.4 Follicular fluid and osmotic potential

Microvascular fluid exchange depends on the net imbalance of colloid osmotic pressure (COP) and capillary hydraulic pressure (Levick and Michel 2010). Control of interstitial fluid volume through microcirculation filtration – reabsorption balance, is heavily dependent on lymphatic drainage of capillary filtrate. Interstitial pressure (P_{if}) therefore plays an important role in transcapillary exchange as lowered P_{if} increases capillary filtration (Reed and Rubin 2010). The degree of permselectivity of the membrane and/or the reflection coefficient of differing solutes exerts a strong influence on the overall osmotic potential of that solution. Some small solutes can pass through the cell membrane more readily than others and ions may move by passi ve and facilitated diffusion via ion channels. Na^+ and K^+ are also moved across the membrane by active transport through the Na^+K^+ATPase pump (Loo *et al.* 2002).

To create an osmotic differential between the antrum and that beyond the basement membrane, directional secretion of osmolites must be secreted from the granulosa and/or oocyte. As follicles proceed to dominance and beyond, thecal vasculature becomes more developed. Factors which increase blood flow and vascular permeability will affect the amount of interstitial fluid seen by the theca cells; increased thecal oedema is known to occur following the pre-ovulatory LH surge (Espey 1980; Cavender and Murdoch 1988). As a consequence of increased filtration pressure and vascular permeability, fluid crosses the endothelium, sub-endothelium basal lamina, thecal interstitium, follicular basal lamina and granulosa cells accumulating within the antrum. However, there has to be a driving force to allow the directional movement of this fluid (Rodgers and Irvin-Rodgers 2010b).

In their investigation of macromolecules, Clarke *et al.* (2006) used a range of MW cut off membranes to consider the effect of differing MW molecules on osmotic pressure in healthy and atretic bovine follicles. They found that dialysis against a 500 MW cut off membrane significantly reduced osmotic pressure of both healthy and atretic follicles by 60% and 80% respectively. The large osmotically active molecules identified in equine and bovine FF by Gèrard *et al.* (1998) and Clarke *et al.* (2006) could be drivers of

osmotic potential in follicles. Evidence from these studies suggests that the basement membrane serves as a selective blood-follicle barrier at sizes >100 kDa between the thecal blood supply and the granulosa cells and antral fluid. If these molecules identified in the above studies are too big to diffuse out of the follicle then similarly large MW molecules cannot move into the follicle. Glycosaminoglycans such as hyaluronan become hydrated and swell even under isotonic conditions (Mayer *et al.* 1983) and in doing so reduce P_{if}. Therefore, alterations in the oncotic pressure (π) and the action of GAGs in FF may influence ovarian P_{if}. These factors may contribute to an osmotic gradient capable of driving fluid into the ovarian antrum.

The physical mechanism of how fluid responds to such osmotic differentials however remains elusive. McConnell *et al.* (2002) compared the movement into antral follicles of $^{3}H_2O$ which diffuses freely through the cell membrane and ^{14}C-Inulin which is restricted to pericellular transport. The rate of movement of $^{3}H_2O$ was significantly greater than that of ^{14}C-Inulin. The results lead McConnell *et al.* to conclude that total water permeability of an antral follicle is 70% transcellular and 30% pericellular. Whilst there are questions surrounding some aspects of the methodology and assumptions made in McConnell *et al's* study, it does provide evidence for transcellular movement of water across granulosa cells. Not only did they identify a possible transcellular route of water permeability through granulosa cells but they also identified the presence of water channels called aquaporins (AQPs). It is possible that these channels mediated the water transport across granulosa cells into the antral cavity, McConnell *et al.* (2002) also provided the first evidence of AQP expression in ovarian tissue.

Considering their potential importance in membrane permeability and water transport, the following section will address AQPs in terms of their function, selectivity/inhibition and where possible function and modulation in both non- and reproductive tissues.

1.10 Membrane permeability

Since the 1950's the field of membrane permeability has defined osmosis as mass flow of solvent through the 'pores' of the membrane (barrier) and understood that the permeability and osmotic effect of the solvent molecule are dependent on the nature of the barrier (Mauro 1957). Based on investigations of erythrocyte and kidney tubule permeation in the 1950's, membrane proteins were thought to create these 'pores' allowing a rapid movement of water (Preston *et al.* 1993). However, the functional protein remained elusive until the recent discovery of aquaporins and altered the way

that membrane permeability is considered. As a result, it is now understood that water movement can be modulated independently of solute transport.

1.10.1 The discovery of aquaporin 1

In 1988 Peter Agre's team isolated and purified a novel 28 kDa integral membrane protein, fully associated with the membrane skeleton, from erythrocytes and renal proximal tubules (Denker *et al.* 1988). It was initially thought to be involved in linking the cytoskeleton to the lipid bilayer. Interestingly its NH_2 amino acid sequence shared 37% identity with 26 kDa major intrinsic protein (MIP) of the lens, originally thought to be a specialised component of gap junctions (Gorin *et al* 1984). Membrane localisation of MIP in lens fibres demonstrated a 'checkerboard' arrangement and was not actually found at the junctions connecting cell membranes (Zampighi *et al* 1989). Amino acid sequence identities were identified between the 28 kDa protein and other members of the MIP channel family from divergent species (Pao *et al* 1991; Smith and Agre 1991). Smith and Agre (1991) confirmed the existence of 28 kDa protein, as a homo-tetrameric complex, including one glycosylated monomer which was anchored to a large polylactosaminoglycan called gly28 kDa and three unglycosylated 28 kDa monomers.

Preston and Agre (1991) isolated cDNA, deduced the amino acid sequence of 269 amino acid residues and proposed a structure of 28 kDa now called CHIP28 (channel-like integral membrane protein of 28 kDa). They identified six transmembrane α-helical domains, composed of a tandem repeat orientated at 180° with respects to each other. There are three extracellular loops (A, C and E) and two intracellular loops (B and D) with cytosolic NH_2 and COOH termini. Loops B and E are generally hydrophobic and associated with the bilayer. They both also contain a highly conserved NPA (asparagine-proline-alanine) motif at residues 76-78 in loop B and 192-194 in loop E (see Fig. 1.7). A search for homologues in the GenBank DNA data base revealed a 42% identity with MIP26; CHIP28 is therefore related to all members of the MIP family now known to facilitate the transport of water or small neutral solutes like glycerol (Pao *et al* 1991).

Functional analysis of CHIP28 was conducted by expressing CHIP28 mRNA in *Xenopus laevis* oocytes and measuring water permeability in response to hypotonic conditions. By expressing the protein in *Xenopus laevis* oocytes and placing it in distilled water Preston *et al.* (1992) witnessed the oocytes rapidly swell and burst. This revealed high membrane permeability (p_f) to water of 11.7 x 10^{-14} ml/s (Zeidel *et al.*

1992). The swelling response was reversibly inhibited by mercury chloride ($HgCl_2$), a known inhibitor of hydrophilic water channels (Macey 1984 and Zhang *et al* 1991).

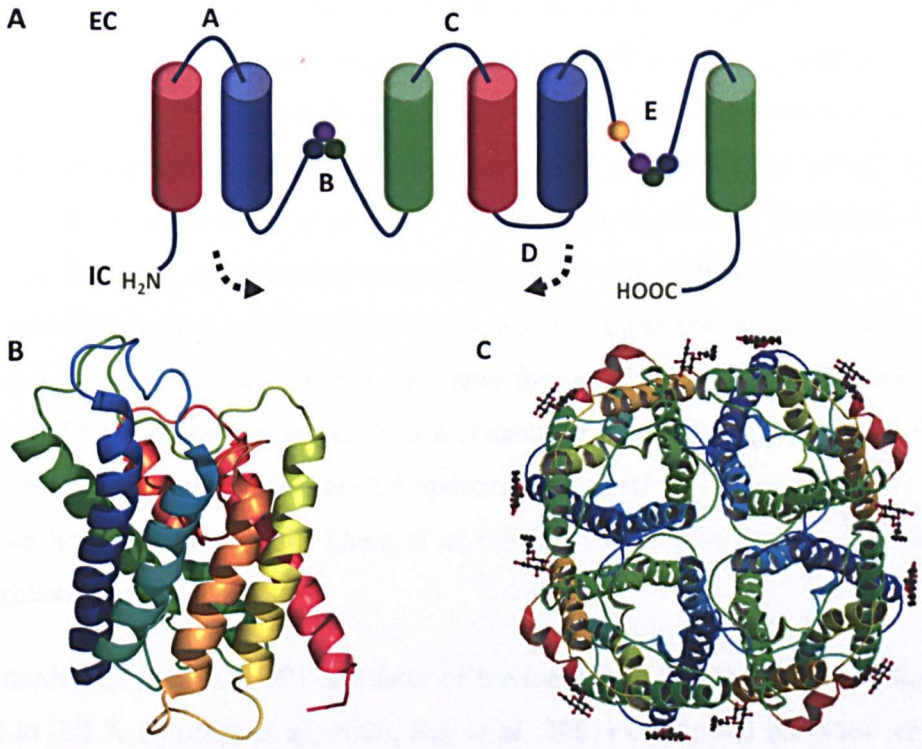

Figure 1.7 **(A)** Topology of Human AQP1 demonstrating the tandem repeats of three transmembrane domains each with a conserved loop harbouring an NPA motif (blue/purple and green spheres); the orange sphere represents the mercurial sensitive cystine residue. Illustration by author. **(B)** The tertiary structure of AQP1 displaying the interaction of loops of B and E and their corresponding motifs creating the 'hourglass' pore. **(C)** AQP1 tetramer created by four monomers (B and C de Groot 2003).

The researchers came to the conclusion that CHIP28, along with other members of the MIP family, may facilitate water permeation (Preston *et al.* 1992). This was confirmed by reconstituting CHIP28 into proteoliposomes exposed to an osmotic gradient and comparing the membrane permeability coefficient (P_f) with that of intact red blood cells (RBCs). Corresponding P_f values, the exhibition of very low Arrhenius activation energy (E_a) of <5 kcal/mol and permeability for a single CHIP28 molecule of $3x10^9$ per second, strongly points to CHIP28 being the principle water channel of RBCs and proximal kidney tubules. Zeidel *et al.* (1992) also showed that in comparison with control proteoliposomes a reduction in extravesicular pH did not alter proton movement; thus CHIP28 is freely permeable to water but impermeable to protons.

1.10.2 Aquaporin 1 selectivity

Other non-identical gene products from other mammalian and diverse plant tissues functioning as water selective channels have been identified, this group of functionally similar proteins are now termed 'Aquaporins', and CHIP's genome symbol is AQP1 (Agre *et al* 1993a; 1993b). At this point there is a good understanding of AQP1 membrane topology but less well understood is the mechanism of selective water permeation. Work by Preston *et al.* (1994) points to a significant functional role for loops B and E. Using site directed mutagenesis Jung *et al.* (1994b) identified a single aqueous pathway created by the physical association of these two loops. As loop B and E dip into the lipid bilayer from the extracellular face and intracellular face respectively, the conserved NPA motifs associate. Over a distance of one residue (192 of loop E) they form an aperture or constriction site ~3Å approximately half way down the pore (~20Å), creating an hour glass like shape (Jung *et al* 1994b). This is now widely referred to as the 'hourglass model'.

Atomic models of human AQP1 and later of bovine AQP1 by electron crystallography resolved to 2.2 Å (Murata *et al.* 2000, Sui *et al.* 2001) confirmed previous structural findings and further detailed individual residue interactions. This included: helix-helix interactions, monomer-monomer interactions, tetramer formation and anchorage to the lipid bi-layer, and the formation of the individual predominantly hydrophobic 'pores' conferring the 'hour glass' profile. It also confirmed the orientation of the α-helices as right handed and tilted at 30° with respects to the membrane (Fig 1.7 B). An electrostatic barrier created by dipole moments of the interacting asparagines (Asp) of the NPA motifs form H-bonds with the water oxygen, isolating the passing molecule and restricting its movements and rotational capacity, thereby hindering its ability to rearrange electrostatic distribution (Fig 1.8). This stops the movement of protons which usually happens via 'proton wires' or strings of H-bonded water molecules (Sui *et al.* 2001; Beitz *et al.* 2006b).

Another energy barrier, a narrower aromatic/arginine (ar/R) constriction formed by Phe^{58}, His^{182} Cys^{191} and Arg^{197} (bov AQP1) was confirmed and located below the mouth of the extracellular aspect of the pore, ~10 Å above the NPA constriction (Fig 1.8). Whilst the arginine repels positive charges the constriction size determines the nature of this selectivity filter. In predominantly water selective AQPs the ar/R constriction ~2.8 Å allows the passage of a single file of water molecules. In glycerol transporting

aquaporins this filter region is larger and less polar. Point mutations in the ar/R region of rat AQP1 (permeable to water) allowed movement of glycerol, urea and ammonia. The positive charge of ar/Rs was also removed resulting in movement of protons (Beitz *et al.* 2006b). Thus proton expulsion is conducted by both the NPA constriction and the ar/R selectivity filter, whilst determination of permeability based on size is primarily due to the steric limitation of the ar/R region.

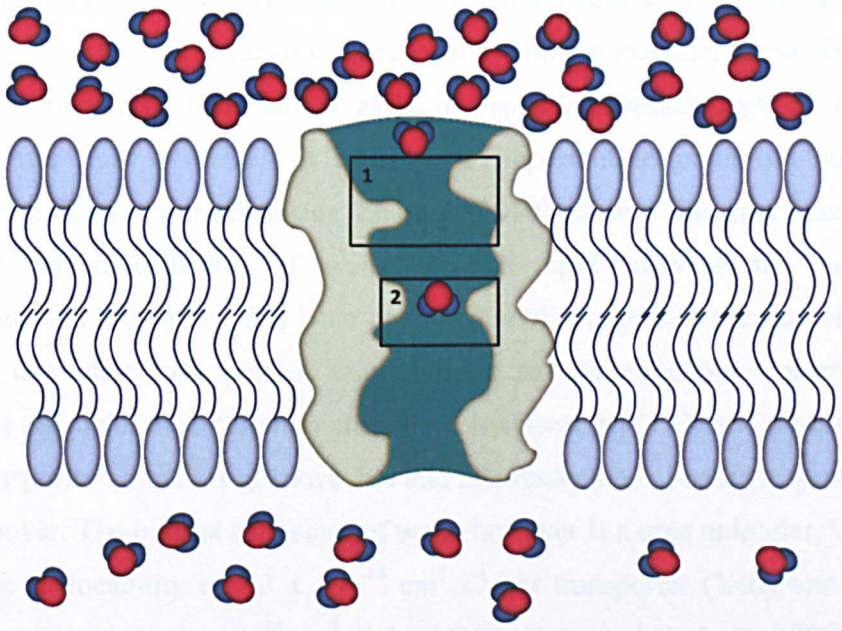

Figure 1.8 Schematic representation of a cross section of the transmembrane AQP1 channel demonstrating selective regions 1 and 2. These give the pore its classic 'hour glass' shape, with one vestibule open to the extracellular and the other the intracellular compartments. Osmotic differential stimulates the movement of single file water molecules. **1**= ar/R selectivity filter ~2.8 Å (size exclusion and repulsion of cations) **2** = NPA constriction region (predominant in exclusion of protons). Illustration by author.

1.10.3 Aquaporin inhibition

Preston *et al.* (1993) identified four cysteine residues (Cys^{87}, ^{102}, ^{152} and ^{189}) as the potential binding site of Hg^{2+} resulting in mercurial inhibition. Each cysteine residue was systematically replaced by serine via site-directed mutagenesis and incubated with $HgCl_2$. All except the substituted $Cys^{189}S$ were still inhibited by $HgCl_2$ indicating that Cys^{189} is the mercurial sensitive residue (Preston *et al.* 1993). Molecular dynamic simulation of mercurial inhibition of water permeation suggests the binding of mercury to the Cys^{189} Human (Cys^{191}Bovine), forming covalent bond between the sulphur atoms of the ar/R Cys molecule. This causes significant conformational change altering the

orientation of the residues of the ar/R region and ultimately constriction size. However simple blockage of the pore by a mercury molecule cannot be completely ruled out (Hirano *et al.* 2010).

1.10.4 Other water transporters

Aquaporins have been identified as a large family of integral membrane proteins, shown to selectively and rapidly transport water and other small neutral solutes across epithelial cell membranes of a diverse range of species and with far reaching tissue distribution. These discoveries have been hailed as a fundamental breakthrough in membrane physiology and fluid dynamics. It is however important to point out other water transporting proteins and mechanisms. Zeuthen (2010) reviews this area describing the osmotically driven diffusion of water through lipid bilayers and aquaporins; cotransporters and uniporters. The latter operate directly coupled to the flux of substrate specific to that membrane protein and in doing so can effectively transport water 'uphill'. For example, the potassium chloride cotransporter (KCC) and human sodium-glucose transporter 1 (hSGLT1), move 500 and 235 molecules of water respectively, per protein turnover. The biggest conductor of water however is a urea uniporter, UT-B with a membrane permeability of 7.3×10^{-14} cm^3 s^{-1} per transporter (Yang and Verkman 2002) compared with 47.3×10^{-14} cm^3 s^{-1} for AQP1 (Yang and Verkman 1997).

So whilst AQPs appear to be a fundamental family of water channels of ancient origin, other transmembrane mechanisms have evolved to modulate the flux of large quantities of water. Some epithelial transport mechanisms contend with small osmotic differences almost iso-osmotic diffusion, whilst others are exposed to variable hyperosmotic extracellular conditions. In this instance the presence of AQPs could result in the undesired movement of water. Certain AQP-null mice (Agre and Nielsen 1996) and humans (Colton-null; King *et al.* 2001) appear to function normally unless under extreme conditions. So, why is there need for AQPs? It appears that water flux across compartments which have small osmotic differences can still achieve rapid flux by utilising AQPs. Tissues such as the small intestine with less AQP expression than say the kidney, rely on the ability of the epithelial cells to transport water in conjunction with cotransporters and uniporters as previously discussed.

1.11. The aquaporins

Since the serendipitous discovery of a 28kDa protein over 20 years ago aquaporins have been isolated from archebacteria, eubacteria, plants, invertebrates and vertebrates. In mammals 13 aquaporins have been discovered. Figure 1.9 represents the phylogenic tree of human aquaporins, (Verkman and Mitra 2000), showing the homology between *E.Coli* aquaporins AQPZ and GlpF and *Arabidopsis* tonoplast aquaporin TIP (Ishibashi *et al.* 2009).

1.11.1 Aquaporins in mammals

Based on hydropathy plots and primary sequences there are three classes of aquaporins. Class one includes the orthodox aquaporins AQP0, -1, -2, -4, -5, -6 and -8; these are predominantly water selective with the exception of AQP6 which is a gated chloride ion channel (Yasui *et al.* 1999) and AQP8 which also transports H_2O_2 (Ishibashi *et al.* 2009; King *et al.* 2004; Agre *et al.* 2002).

Class two includes AQP3, -7, -9 and -10; these are called aquaglyceroporins, permeable to neutral solutes such as urea, glycerol and even arsenite as well as water (Ishibashi *et al.* 2009; King *et al.* 2004; Agre *et al.* 2002). AQP11 and -12 are class three aquaporins; they are the newest to be discovered and thus less well understood. They have deviating NPA motifs, are called 'superaquaporins' and are in a different subgroup to the others as illustrated by Fig. 1.9 (Ishibashi *et al.* 2009).

As can be seen in Table 1.5 characterisation of the 13 mammalian aquaporins is quite comprehensive. Table 1.6 illustrates tissue distribution of aquaporins but this is still in its infancy with regards to cross species variation.

1.11.2 Class 1 aquaporins - Non-reproductive tract tissue distribution and function.

1.11.2.1 AQP0

Aquaporin 0 constitutes 60% of lens membrane protein and serves to maintain transparency and has a water permeability 40% less than AQP1. Defects in its functional ability or trafficking can result in cataracts (Mulders *et al.* 1995). It has also been identified in the retina (Farjo *et al.* 2008). Aquaporin 0, null mice develop cataracts

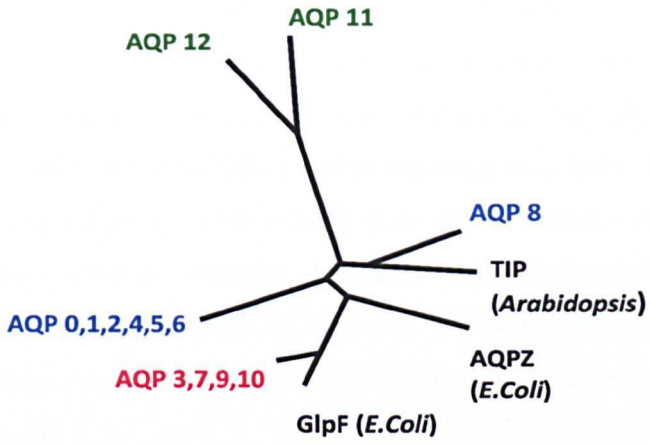

Figure 1.9 Human aquaporin phylogenic tree; Class 1 - blue, Class 2 - red, Class 3 - green. Adapted from Ishibashi *et al.* (2009).

suggesting that AQP0 may have a structural role as cell-cell adhesion molecule (Engel *et al.* 2008). Liu *et al.* (2011) determined the physiological role of AQP0 as a regulator of gap junction channels. Connexin 50 directly interacted with AQP0 and increased the intercellular coupling of Cx50 gap junctions through the cell adhesive function of AQP0 (Liu *et al.* 2011).

1.11.2.2 Aquaporin 1

Aquaporin 1 is predominantly an endothelial AQP, although it is not expressed in all endothelium. In humans and rodents it has been identified in capillary, venular and lymphatic EC but absent in small arteries (Devuyst *et al.* 1998). Aquaporin 1 tissue distribution as a vascular component is vast (see Table 1.6). There are other cell types which express AQP1; however its function in many of these remains unclear. As previously described AQP1 is expressed in erythrocytes, the apical and basolateral plasma membranes in the proximal convoluted tubules (PCT) and thin descending limb of Henle, and is present in the vascular endothelium of the kidney (Fig 2.1; Preston *et al.* 1992). It is also found in the choroid plexus of the brain (Gunnarson *et al.* 2004). It is expressed in the apical membrane of bile ducts (Tietz *et al.* 2003) and has recently been proposed to permeate nitric oxide (NO; Herrera and Garvin 2007) and carbon dioxide (CO_2 Nakhoul *et al.* 1998; Cooper and Boron 1998) as well as water. Aquaporin 1 has been implicated in the stimulation of cell migration in angiogenesis (Monzani *et al.* 2009). It is strongly expressed in proliferating tumour microvessels in several species (Endo *et al.* 1999; Saadoun *et al.* 2002).

Tumour growth and metastasis in AQP1 null mice was markedly reduced as a result of poor tumour microvascular development (Verkman *et al.* 2008). Aquaporin 1 null mice are unable to concentrate urine under extreme conditions; they also have decreased water permeability of the proximal tubule and descending vasa recta. (Agre and Nielsen 1996). Aquaporin 1 null humans (Colton-null) there are no obvious clinical side effects until under extreme conditions whereby decreased water permeability occurs in the descending thin limp and/or vasa recta (King *et al.* 2001). Huebert *et al.* (2011) found that AQP1 is over expressed in cirrhosis of the liver and promotes angiogenesis, fibrosis and portal hypertension.

1.11.2.3 Aquaporin 2

Aquaporin 2 is predominantly expressed in the apical membrane and intracellular vesicles of principal cells of the kidney collecting ducts which are relatively impermeable to water. Regulated by vasopressin (VP), it plays a significant regulatory role in concentrated urine production. Increased collecting duct permeability in response to VP is achieved by the trafficking of intracellular AQP2 via vesicles, followed by insertion into the apical membrane of the principal cell. Vasopressin binds to its basal receptor, activating adenylate cyclase and cAMP stimulating protein kinase A (PKA) which initiates the mechanism of vesicular translocation to the apical membrane. Aquaporin 2 is then fused in to the membrane, increasing its permeability to water (Fig 1.10; Deen *et al.* 1994). Aquaporin 2 null mice die of dehydration within two weeks of birth; humans however can compensate by increased oral hydration (Dibas *et al.* 1998, Noda and Sasaki 2006). The inherited disorder nephrogenic diabetes insipidus (NDI) can be caused by a mutation in the VP receptor type 2 (VP2R) or the AQP2 gene (Deen *et al.* 1995). Recent studies have identified calcitonin has a VP-like effect on AQP2 trafficking and could be a potential therapeutic target for NDI (Bouley *et al.* 2011). Symptoms of NDI are severe dehydration and thirst which if left untreated can be fatal.

1.11.2.4 Aquaporin 4

Aquaporin 4 is largely mercurial insensitive or inhibited according to isoform (Yang and Verkman 1997; Yukutake *et al.* 2008). It is expressed in the basolateral membrane of collecting duct cells (Agre and Nielsen 1996), in glial cells (Badaut *et al.* 2002) and endothelial cells of the brain (Nielson *et al.* 1997; Yang *et al.* 2008), skeletal myocytes (Frigeri *et al.* 1998) and gastric parietal cells (Fugita *et al.* 1999). It also plays a part in fluid movement in the upper respiratory tract and being found in the basolateral

membrane of ciliated columnar cells (Kreda *et al.* 2001). Aquaporin 4 null mice have mildly impaired urine concentrating abilities, decreased olfaction, vision and hearing (Lu *et al.* 2008). More interestingly and of great clinical relevance, is that they suffer far less brain oedema initiated by ischemia (Papadopoulos and Verkman 2007).

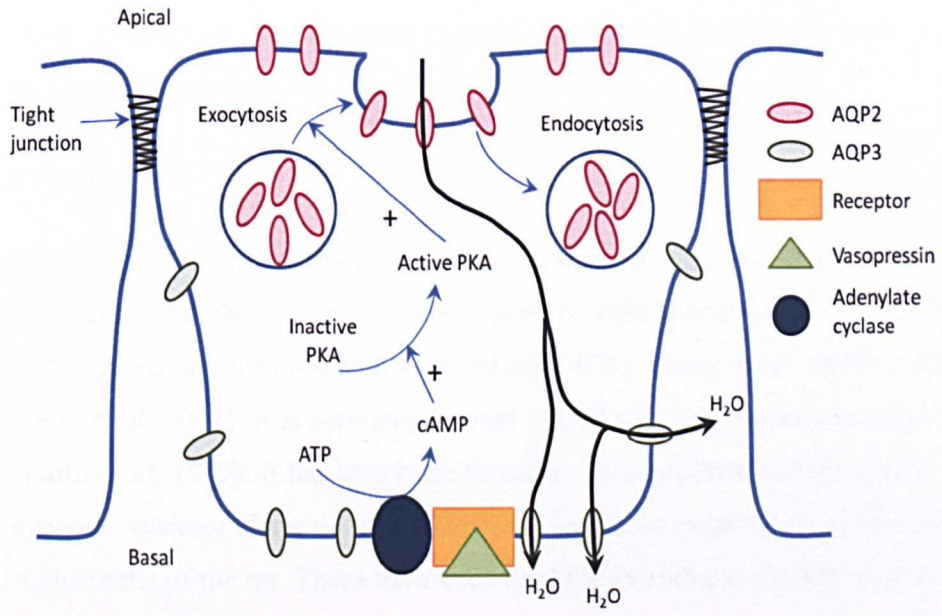

Figure 1.10 Principle cells of the collecting duct displaying the directional movement of water, facilitated by the vasopressin induced translocation of AQP2 to the apical surface. Basolateral localisation of AQP3 allows complete transcellular movement of water. This is known as 'AQP2 shuttling'. Illustration by author based on Deen *et al.* (1995); Brown (2003); Bouley *et al.* 2011).

1.11.2.5 Aquaporin 5

Aquaporin 5 is expressed in the cornea of the eye, apical membranes of acinar cells of the lacrimal gland (Hamann *et al.* 1998) and serous salivary gland (Krane *et al.* 2001). Aquaporin 5 is found in the apical membrane of ciliated columnar cells of the upper respiratory tract and in the apical membrane of type 1 pulmonary epithelial cells (Funaki *et al.* 1998) and in submucosal glands (Nielsen *et al.* 1997). In culture AQP5 expression was decreased with tumour necrosis factor-α (TNFα; Towne *et al.* 2001), and increased with hypertonicity (Hoffert *et al.* 2000) and cAMP through the PKA pathway (Yang *et al.* 2003). Aquaporin 5 null mice have significantly decreased water permeability across alveolar epithelium (Ma *et al.* 2000); and lung endothelium (Bai *et al.* 1999).

Null mice have thickened corneas that are less able to respond to changes in osmotic gradients (Hamann *et al.* 1998), and permeability of salivary gland secretory cells is reduced (Krane *et al.* 2001). Over expression of AQP5 has been associated with human ovarian and lung cancer (Moon *et al.* 2003; Yang *et al.* 2006b). Recently AQP5 has been identified as being over expressed in cervical cancer and linked with lymph node involvement. Correlation between over expression of AQP5 and Ki-67 was associated with poor prognosis and survival (Zang *et al.* 2011).

1.11.2.6 Aquaporin 6

Aquaporin 6 is almost exclusively localized to intracellular vesicles of the acid secreting intercalated cells of the collecting duct and is colocalised with H^+-ATPase. It demonstrates gated anion permeability of chloride (Cl^-; Yasui *et al.* 1999) and nitrate (NO_3^-; Ikeda *et al.* 2002). It is activated by low pH, nitrate and contrary to other AQPs, $HgCl_2$ (Yasui *et al.* 1999). It has also been found in the cerebellum (Nagase *et al.* 2007) and in synaptic vesicles (Jeremic *et al.* 2005). It has more recently been discovered in parotid acinar cells of the rat. There have been no AQP6 knockout studies to date.

1.11.2.7 Aquaporin 8

Whilst AQP8 is considered a class one AQP, its primary sequence is closer to that of plant tonoplast AQP (TIP); it has six exons as opposed to four and it transports hydrogen peroxide (H_2O_2; Bienert *et al.* 2007). It is expressed in the apical membrane of pancreatic acinar cells and may be colocalised with the cystic fibrosis transmembrane-conductance regulator (along with AQP1 and -5). Therefore AQP8 may play a role in the regulation of pancreatic exocrine secretions (Burghardt *et al.* 2003). As with AQP6 there could be a mechanism of trafficking AQP8 to the apical plasma membrane (Hurley *et al.* 2001). It is found at low levels in rat proximal tubules and collecting duct of the kidney and is cell type dependent in liver, testis, gastrointestinal tract and airways. There also appears to be quite distinct variation in permeability and tissue localisation amongst species (Elkjaer *et al.* 2001). Aquaporin 8 knockout mice do not demonstrate any obvious clinical defects (Ishibashi *et al.* 2009).

Table 1.5 AQP characteristics. Permeability, +<++<+++<++++; Hg inhibition; + inhibited by Hg, - not inhibited by HG. Subcellular distribution; **PM** – Plasma membrane apical and basolateral, **APM** – Apical plasma membrane, **BPM** – Basolateral plasma membrane, **IV** – Intracellular vesicles (Ishibashi *et al.* 2009, King *et al.* 2004).

	AQP0	AQP 1	AQP2	AQP3	AQP4	AQP5	AQP6	AQP7	AQP8	AQP9	AQP10	AQP11	AQP12
Water transport	+	+++	+++	++	++++	+++	++	++	+++	++	++	+++	?
Glycerol transport	-	-	-	++	-	-	-	++	-	++	++	?	?
Other solutes		CO_2 NO		Urea			Anions (NO_3^-> Cl^-)	Urea Arsenite	H_2O_2	Urea Arsenite	Urea		
Hg inhibition	+	+	+	+	-	+	Induced	-	+	+	+	?	?
Exon numbers	4	4	4	6	4	4	4	6	6	6	6	3	3
Chromosome locus	12q13	7p14	12q13	9p13	18q22	12q13	12q13	9p13	16p12	15q22	1q21	11q13	2q37
Subcellular distribution	**PM**	**PM**	**APM IV**	**BPM**	**BPM**	**ABM**	**IV**	**PM**	**PM IV**	**PM**	**IV**	-	-

Table 1.6 Simplified tissue distribution of mammalian aquaporins; present +<++; absent - (Ishibashi *et al.* 2009; Thoroddsen *et al.* 2011)

Tissue	AQP0	AQP1	AQP2	AQP3	AQP4	AQP5	AQP6	AQP7	AQP8	AQP9	AQP10	AQP11	AQP12
Brain	-	+	-	+	++	-	+	-	-	-	-	+	-
Eye	+	+	-	+	+	+	-	-	-	-	-	-	-
Salivary gland	-	+	-	+	+	+	-	-	+	-	-	-	-
Trachea	-	+	-	+	+	+	-	+	+	-	-	-	-
Lung	-	+	-	-	-	+	-	-	-	-	-	-	-
Heart	-	+	-	+	+	-	-	+	-	-	-	+	-
Liver	-	+	-	+	-	-	-	-	+	+	-	+	-
Pancreas	-	+	-	-	-	-	-	-	+	-	-	-	+
Spleen	-	+	-	+	-	-	-	-	-	+	-	+	-
GI tract	-	+	-	+	+	+	-	+	+	-	+	+	-
Kidney	-	+	+	+	+	-	+	+	-	-	-	+	-
Testis	-	-	-	-	-	-	-	++	++	++	-	++	-
Ovary	-	+	+	+	+	+	-	+	+	+	-	+	-
Muscle	-	+	-	-	+	-	-	-	-	-	-	+	-
Leukocyte	-	-	-	-	-	-	-	-	-	+	-	+	-
Erythrocyte	-	+	-	+	-	-	-	-	-	-	-	-	-

1.11.3 Class 2 Aquaglyceroporins - Non-reproductive tract tissue distribution and function.

1.11.3.1 Aquaporin 3

Aquaporin 3 is expressed at the basolateral membrane of principal cells of the kidney collecting duct (King *et al.* 2004) and epithelia of gastrointestinal cells (Laforenza *et al.* 2005). It is present apically and basolaterally in upper respiratory tract basal cells and type II pneumocytes of the alveolae (Kreda *et al.* 2001). It is also expressed in erythrocytes (Roudier *et al.* 2002). One of the major areas of interest pertaining to AQP3 is its role in the regulation of skin moisture; it is located in the basal layers of keratinocytes and has been shown to influence skin regeneration and tumour development (Hara-Chikuma and Verkman 2008). It facilitates water and glycerol transport, but in most of the above locations its facilitation of glycerol flux is of great clinical importance. Aquaporin 3 null mice develop very dry skin which is revitalised via the stimulation of cell proliferation with oral glucose. However, overexposure to glycerol and/or increased AQP3 expression stimulates basal skin cancer cells. Skin tumours of AQP3 null mice were significantly inhibited, providing supporting evidence for the hypothesis that glycerol and therefore any up regulation of glycerol facilitation can promote keratinocarcinoma (Hara-Chikuma and Verkman 2008). Increased glycerol transport has also been linked with colon cancer and pulmonary cancer (Ishibasi *et al.* 2009). In culture, magnesium was reported to increase AQP3 expression; this is potentially concerning as magnesium containing medicines such as antacids, laxatives, treatment for diabetes and so on, could potentially predispose tumour growth (Okahira *et al.* 2008).

1.11.3.2 Aquaporin 7

Amongst non-reproductive tissues, AQP7 is highly expressed in adipose tissue and the brush border of the proximal tubules of the kidney (King *et al.* 2004). As with AQP3, it is the facilitation of glycerol which is of most functional importance and interest. During the prolonged fasting of *Aqp7* null mice they became profoundly hypoglycaemic as a result of deficient mobilisation of glycerol from adipose tissue to the liver. Adipocyte size increased and so too did the amount of intra-abdominal fat (Hara-Chikuma *et al.* 2005). Null mice also demonstrate the inability to reabsorb glycerol at the proximal tubule and so glycerol is detected in the urine. However there appears to be no disruption of glucose and glycerol metabolism (Sohara *et al.* 2006). Mercurial

inhibition of AQP7 transport function is dependent on isoform. Rat or mouse *Aqp7* expressed in *Xenopus* oocytes is not inhibited by $HgCl_2$ (Ishibashi *et al.* 1997), however oocytes expressing human AQP7 demonstrate a complete inhibition of function (Kuriyama *et al.* 1997).

1.11.3.3 Aquaporin 9

Aquaporin 9 has been cloned from leukocytes (Ishibashi *et al.* 2009) and osteoclasts which increased in expression during osteoclast differentiation (Aharon and Bar-Shavit 2006). It is abundantly expressed in the basolateral membrane of hepatocytes of the liver where it has been identified as a urea transporter and also involved in the mechanism of glycerol uptake. There is a sex difference in the expression of *Aqp9* in the liver with male rats showing a more uniform expression than females (Nicchia *et al.* 2001). During prolonged fasting AQP9 is increased at the mRNA and protein level and is countered by re-feeding. Aquaporin 9 levels in rat liver increase with induced diabetes mellitus and are normalised with insulin (Kuriyama *et al.* 2002; Carbrey *et al.* 2003). Despite high levels of insulin, in obese insulin-resistant leptin receptor mutant mice ($lepr^{db}/lepr^{db}$), *Aqp9* levels are greatly increased. Aquaporin 9 null mice do not demonstrate abnormal glycerol and glucose metabolism. Even though there was a marked increase in plasma levels of glycerol, urea and glucose levels were normal (Rojek *et al.* 2007). Both AQP7 and -9 are also permeated by arsenite ($As(OH)_3$; Liu *et al.* 2002).

1.12 Aquaporins in the reproductive tract

Fluid flux within the reproductive tract has been well reported and is generally agreed to be influenced by steroid hormones. The physiological significance of AQP expression in relation to fluid movement within the male and female reproductive tracts is becoming increasingly studied. Aquaporins have been identified in many reproductive processes such as, spermatogenesis, secretion and reabsorption of fluids in the male tract. Furthermore, uterine fluid absorption, secretion of oviductal fluid and facilitation of ovum movement; blastocyst formation and embryo amniotic fluid reabsorption; antral follicle and oocyte development and maturation, are all associated with AQP expression. Significant evidence is presented for the modulation of AQP expression by steroid hormones which points to the direct coupling of AQP expression and function with cyclicity, indicating their potential importance. This also highlights their potential therapeutic possibilities pertaining to hormonal imbalance and reproductive dysfunction, improvements in cryopreservation of sperm and oocytes, not to mention the commercial

impact of potentially improved reproduction in domestic species. Table 1.7 identifies AQP tissue distribution in both male and female systems.

Table 1.7 Reproductive tissue distribution of AQPs -1 to -9 (based on and adapted from McConnell *et al.* 2002 (rat); Hermo *et al.* 2004 (rat); Brañes *et al.* 2005 (rat); Huang *et al.* 2006 (rat and mouse); He e*t al.* 2006 (human); Ishibashi *et al.* 2009 (human, rat and mouse); Skowronski 2010 (pig); Otterbach *et al.* 2010 (human); Hermo and Smith 2011(rat); Thoroddsen *et al.* 2011 (human)).

Aquaporin	Major tissue distribution
0	Testis, placenta, efferent ducts, epididymis
1	Vagina, uterus, oviduct, **ovary**, placenta, fetal membrane, embryo, testis, epididymis, vas deferens, seminal vesicles, prostate, breast, cervix, efferent ductules
2	Uterus, testis, epididymis, vas deference, prostate, **ovary**
3	Uterus, cervix, **ovary**, oocyte, placenta, fetal membrane, embryo, epididymis, prostate, breast, testis, efferent ductules, epididymis
4	Uterus, cervix, **ovary**
5	Uterus, cervix, oviduct, **ovary**, embryo, epididymis
6	Embryo
7	**Ovary**, oocyte, embryo, testis, spermatozoa
8	Uterus, cervix, **ovary**, placenta, fetal membrane, embryo, testis, epididymis, spermatozoa
9	**Ovary**, oocyte, oviduct, placenta, fetal membrane, embryo, testis, epididymis, vas deferens, prostate, coagulating gland, spermatozoa

1.12.1 Aquaporins in the ovary.

McConnell *et al* (2002) provided evidence of rapid transcellular flux of fluid in rat granulosa cells as previously discussed (section 1.9.4). To elucidate the mechanism of fluid transfer they conducted a granulosa swelling assay subjecting cells to hypotonic insult with or without of $HgCl_2$, whereby the inhibition of swelling suggested a mercurial sensitive mechanism. Further to this and using flow cytometry they tested for the presence of AQP1 to -9, and detected AQP8, -7 and -9 in rat granulosa cells. They concluded therefore, that transcellular fluid movement was potentially facilitated by

AQPs. However there are limitations to this study pertaining to the absence of certain controls in the swelling assay.

Messenger RNA of *Aqp3* and *-7* has been isolated from mouse oocytes (Edashige *et al.* 2000). Meng *et al.* (2008) confirmed A*qp*3 mRNA in mouse oocytes. Ford *et al.* (2000) investigated the expression of *Aqp9* at different stages of rat oocyte maturation. They report that as maturation proceeds, water osmotic permeability (P_{osm}) decreases as do *Aqp9* transcript. Jo *et al.* (2010) also looked at the effect of maturation in mouse oocytes pertaining to the expression of A*qp*3. They revealed that A*qp*3 mRNA expression increased during development of the immature oocyte, followed by decreased transcript levels during maturation.

Skowronski *et al.* (2009) investigated the localisation of AQP1, -2, -3, -4, -5, -7, -8, -9 and -11 in pig via IHC and western blotting (WB). They presented evidence of AQP1 expression in the endothelium of ovarian capillaries, AQP5 in granulosa cells of type one follicles and AQP5 and -9 in mural cells of developing follicles. Whilst this supports the notion that AQPs are potential modulators of follicular fluid accumulation in antral follicles, the term 'developing' is imprecise and is therefore difficult to relate the presence of AQP5 and -9 directly to developmental stage.

In the human ovary AQP1 expression was identified in healthy ovarian endothelium and compared with endothelium of ovarian tumours where AQP1 expression was slightly elevated (Mobasheri *et al.* 2005). More recently Thoroddsen *et al.* (2011) investigated the expression of AQP1-4 in granulosa and theca cells of preovulatory follicles. They used IHC and mRNA analysis from follicles of preovulatory (PO), early ovulatory (EO), late ovulatory (LO) and postovulatory (PSO) phase follicles. They found that AQP1 mRNA increased in LO and PO phase follicles, and there were similar changes in AQP2 and -3 with a significant increase in EO phase. Aquaporin 4 levels decreased from PO to EO phase. Their IHC analysis of AQP1-4 does show staining in the described cell types, however the staining is very cytoplasmic with a high background and the pattern of staining is common to all antibodies. Aquaporin 1 was found in high abundance in both theca and granulosa cells. There was no significant indication of endothelial localisation, which is contrary to much of the AQP1 literature. Furthermore, given that AQP2 is predominantly a renal AQP regulated by vasopressin it is somewhat surprising to find this AQP in both theca and granulosa.

Qu *et al.* (2010) investigated whether the alteration of AQP9 expression in granulosa cells of women with PCOS was related to the high androgen levels in FF. They found that granulosa cells from the follicles of women with PCOS had significantly lower levels of AQP9 mRNA than those of control women. This was also strongly correlated with total testosterone (TT), sex hormone-binding globulin (SHBG) and free androgen index (FAI) levels. They suggest that hyperandrogenism results in reduced AQP9 expression, impaired granulosa cell function and altered follicle development.

Yang *et al.* (2006a) identified increased expression of AQP1 in the microvasculature of ovarian tumours and suggests a role in ovarian carcinogenesis and its progression, particularly in terms of angiogenesis and ascites formation. Yang *et al.* (2006b) detected weak or no expression of AQP5 in normal ovarian epithelium, but did find it in the basolateral membrane of benign tumour cells, the apical and basolateral membrane of borderline cells and randomly in the membrane of malignant cells. They found that expression of AQP5 in malignant and borderline tumours was significantly higher than in benign tumours and normal epithelium. They concluded that over expression of AQP5 in tumour cells in parallel with increased expression of AQP1 in the vasculature is linked with tumorigenesis of epithelial ovarian tumours. In 2011, Yang *et al.* extended this investigation to consider the localisation AQPs -1 to -9 in healthy ovary and in benign and malignant ovarian tumours. Aquaporin 1 was again found in the vasculature with evidence of the other AQPs (-2 to -9) in the ovarian tumour cells. Expression of AQP1, -5 and -9 was significantly higher in malignant and borderline tumours compared with benign tumour and healthy ovarian tissue. Aquaporin 6 was less expressed in malignant and borderline tumours and AQP2, -3 and -4 were very weakly expressed and not considered to be of functional relevance. In conclusion it appears that AQP1 facilitates the increase in fluid transudate from the circulatory system and that AQP5, -6, -7, -8 and -9 play functional roles in water and glycerol flux in epithelia tumours (Yang *et al.* 2011). This may provide vital clues to understanding tumour growth and metabolism.

Whilst AQPs have been identified in the ovary of mouse, rat, and humans (particularly with reference to human pathological abnormality), AQPs in domestic species is still in its infancy. The only available literature is limited to the localisation of aquaporins in the porcine ovary. The importance of this investigation is therefore paramount in furthering our understanding of reproductive physiology in domestic species. Considering the differences in preovulatory follicles size and FF volume between the domestic species

(1.5ml to 45 ml in sheep and horse respectively), it seems logical to expect variation in AQP expression and function. Understanding the potential role of AQPs in fluid flux regulation and follicle growth could further our understanding of follicle selection, maturation and atresia.

1.13 Regulation of Aquaporins.

Regulation of AQPs, including gating and insertion into the membrane has been attributed to phosphorylation, as seen in the shuttling of AQP2 from vesicles to the apical membrane (Deen *et al.* 1995; Brown 2003; Bouley *et al.* 2011). Osmolality (Hoffert *et al.* 2000), pH, $HgCl_2$ (AQP6; Yasui *et al.* 1999), hypoxia (Gunnarson *et al.* 2004) and osmotically sensitive microRNAs, are also known to modulate the expression, permeability and activity of certain AQPs. However, the most reported contributor to AQP regulation is that of steroid hormones which are evidenced to elicit both genomic and non-genomic effects. Genomic effects involve modulation of transcriptional processes, activating or inhibiting RNA and protein synthesis, whilst non-genomic or non-transcriptional actions mediate more rapid effects. Both E_2 and androgen have been shown to effect the regulation of AQP1, -4, -5, and -9 in both non-reproductive (Gu *et al.* 2003; Gunnarson *et al.* 2004) and reproductive tissues. In reproductive tissues, for example, AQP1 was modulated by E_2 in rat and marmoset efferent ducts (Fisher *et al.* 1998). In rat epididymis AQP9 expression was up-regulated by androgens (Pastor-Soler *et al.* 2002; 2010). However, increased androgen in women with PCOS lowered the expression of AQP9 in granulosa cells (Qu *et al.* (2010). Aquaporin 5 was induced in E_2 treated, progesterone primed uteri and AQP1 was up-regulated in uterine stromal vasculature by E_2 and progesterone (Richard *et al.* 2003; Lindsay and Murphy 2006).

1.14 Study aims

This investigation aims to identify tissue expression and cellular/subcellular localisation of AQPs in the bovine ovary and to determine if AQPs are differentially expressed in specific tissue/cell types. These include capillary endothelium, stroma, internal/external theca, and granulosa. The objective is to establish whether the expression of AQPs in these tissue/cell types change as follicular development progresses. This will aid future understanding of what drives the growth of the ovarian follicle in terms of, osmotic gradients, fluid dynamics and hormonal influence during specific stages of follicle development.

Chapter 2

Characterisation of aquaporin -1, -2, -3, -4, -5, -6, -7, and -9 and their localisation in the bovine ovary.

2.1 Introduction

2.1.1 Antibodies

Immunohistochemistry (IHC) is an important biochemical technique used in both disease diagnosis and research, where antibodies are developed to target a specific antigen of interest. Labelled antibodies allow the visualisation of antibody-antigen interaction and permit the identification of biomarkers of disease and differentially expressed proteins across different tissue types (Rhodes and Trimmer 2006). To create antibodies certain laboratory animals such as the New Zealand White rabbit are inoculated with a particular antigen of interest. Antigens are complex molecules and therefore present many epitopes (Lipman *et al.* 2005). This stimulates B-lymphocytes to differentiate into a variety of plasma cells, each producing antibodies to the varying epitopes of the antigen. The antisera containing polyclonal antibodies is harvested and used for experimentation or diagnostic procedures. Monoclonal antibodies are produced from a single clonally propagated plasma cell and only recognise one specific epitope (Lipman *et al.* (2005). Monoclonal antibodies therefore demonstrate high specificity and affinity with the antigen under investigation. However structural variation in the epitope to which the antibody has affinity, would limit its application. As polyclonal antibodies are heterogenous, variation in epitope structure is less likely to limit their overall antigen specificity (Lipman *et al.* 2005).

2.1.2 Antibody characterisation and specificity

When using an antibody for the first time it is essential to thoroughly characterise and validate its reactivity and determine appropriate methodology/procedure. Antibodies used on tissue derived from a species different from that which the antibody was raised against, may not recognise the epitope if the protein structure is not conserved amongst species. The species cross reactivity of the antibody should therefore be investigated and this can be done using the on-line Basic Local Alignment Tool (BLAST)

(http://www.ncbi.nlm.nih.gov/BLAST/) database. This provides the percentage identity of the antigen and anti-antigen antibody protein sequences, indicating potential cross reactivity. Working concentrations of antibodies should be validated using serial dilutions, in order to identify the dilution which provides an optimum signal to noise ratio.

The nature of polyclonal serum antibodies means they are a mixture of antibodies to different epitopes on the immunogen. Some of these antibodies may cross react with other molecules resulting in non-specific background staining (Rhodes and Trimmer 2006; Bussolati and Leonardo 2008). If the host animal has been subjected to previous antigen challenge the serum may contain a wide spectrum of non-specific antibodies; there may also be antibodies raised against impurities in the immunogen (Lipman *et al.* 2005). Affinity column purification rids the serum of non-specific elements, resulting in a pure and very specific antibody. The polyclonal serum is passed though a column containing immobilised antigen, the antibody binds to the antigen ligand and the non specific proteins are removed. The antigen-antibody complex is dissociated and the antibody eluted resulting in a purified antibody solution (Zou *et al.* 2001). If the serum antibody is not purified, pre-immunized rabbit serum can be used as a negative control to indicate a base line degree of non-specific staining. Similarly an absorption control assay can help to clarify the quality/specificity of antibodies as any staining that occurs after absorption of the antibody with antigen, would be a result of non-specific or contaminating antibody. To further test the specificity of the antibody, its use on positive control tissue known to express the target antigen should be carried out (Hladik and White 2008).

2.1.3 Aquaporin antibodies and the ovary

Investigations concerning the localisation of AQP proteins in ovarian tissue, using IHC are limited to just two. Skowronski *et al.* (2009) acquired affinity purified commercial rabbit polyclonal serum antibodies, raised against rat AQP1, -2, -3, -4, -5 -8 -9 and -11. They localised AQP1 to capillary endothelium and AQP5 to the granulosa of primary follicles and both AQP5 and -9 to the mural granulosa cells of growing follicles. Thoroddsen *et al.* (2011) used commercial mouse monoclonal anti-AQP1 and -4 and affinity purified rabbit polyclonal serum anti-AQP2 and -3. They localised all four AQPs

on both theca and granulosa cells in preovulatory through to post ovulatory follicles at varying levels of protein expression (see section 1.12.1 for a more detailed description). Whilst McConnell *et al.* (2002) did not use IHC to localise AQP protein expression, they did use a panel of anti-AQP antibodies for flow cytometry of rat granulosa cells. Anti-AQP antibodies to AQP1,-2,-3,-4,-5, -6 and -7 were commercial, affinity purified anti-rat, rabbit polyclonal serum antibodies. Anti-AQP -8 and -9 anti-rat, rabbit polyclonal serum antibodies were raised and affinity purified in their laboratory. Of nine AQPs investigated they detected the presence of AQP7, -8 and -9 in rat granulosa cells. This present investigation used a panel of non-commercial, rabbit polyclonal serum antibodies raised against rat AQP1,-2,-3,-4,-5,-6,-7,-8,-9. These were previously developed in collaboration with Sigma-Genosys (Poole, Dorset, UK). Anti-AQP1 and -2 were further affinity purified (see section 2.2.6).

2.1.4 AQP positive control tissue and membrane localisation.

Since the discovery of aquaporins, their roles in tissues that regulate fluid flux have been greatly debated, not least the role they play in the functional unit of the kidney. Of the 13 mammalian AQPs discovered, eight have been identified in the nephron, all of which are localised to specific cell types and positions in the membrane (King *et al.* 2004). For example, AQP1 and -7 are located in the apical surfaces of proximal convoluted tubule (PCT) epithelial cells. Aquaporin 1 is also located in the basal membrane of PCT and is completely membranous in descending thin limb epithelial cells where it facilitates transcellular reabsorption of filtrate. Vasopressin-mediated up regulation of AQP2 in the apical membrane of collecting duct cells increases collecting duct permeability and works in conjunction with basolateral AQP3. The presence of a range of AQP isoforms with specific cellular localisation is also true of other fluid regulating tissues such as the upper respiratory tract epithelium, cells of the lung alveolus (Nielsen *et al.* 1997; King and Agre 2001) and the eye (Hamann *et al.* 1998).

The kidney is therefore considered to be a useful positive tissue control for many of the AQPs, however, it does not express AQP5 or -9. Aquaporin 5 protein is known to be expressed in the apical membrane of the acinar cells of the lacrimal gland and serous salivary gland (Hamann *et al.* 1998; Krane *et al.* 2001). It is also localised to the apical membrane of ciliated columnar and type I pulmonary cells. Whilst there is a variety of

positive control tissue expressing AQP5 it is clearly an apical protein and should be considered as such when identifying its protein expression in test tissue. The AQP9 protein is abundantly expressed in the basolateral membrane of liver hepatocytes (Elkjaer *et al.* 2000; Nicchia *et al.* 2001). Liver is therefore considered a reliable positive control tissue for AQP9, as for AQP5, membranous position should be considered when localising AQP9 in test tissue.

2.1.5 Aquaporins in the bovine ovary

The repeating nature of the oestrous cycle and thus the continued growth and regression of follicles means that the fluid dynamics of the bovine ovary must be regulated. As follicles develop they expand at different rates dependent on the stage of development. Preantral to early antral (type-1 to type-5; Braw-tal and Yossefi 1997) follicle development takes approximately 4-5 months. Early antral to preovulatory (class-1 to class-5; Lucy *et al.* 1992) follicle development, takes approximately 1.5 months (see section 1.32 -1.34 for a more detailed description of follicle development and classification). Similarly, atretic follicles will regress at different stages of development. This suggests a coordinated control of fluid flux both into and out of the follicle and a close association between this process and the on-going development of the follicle. It would therefore not be unreasonable to postulate differential expression and participation of AQPs in the fluid modulation of follicles, at different stages of growth.

2.1.6 Aim and strategy

The first objective of this investigation was to characterise the available anti-AQP1, -2, -3, -4, -5, -6, -7 and -9 antibodies and the IHC methodology. The second objective was to determine the cellular localisation of AQP1, -2, -3, -4, -5, -6, -7 and -9 in the bovine ovary. A third objective was to ascertain whether the presence of AQPs is cell-type and follicle stage-dependent. To achieve this, a bank of fixed, paraffin embedded bovine ovary and positive control tissue was created from abattoir derived material. Initial haematoxylin and eosin (H&E) staining allowed for morphological assessment and identification of healthy and atretic follicles at all stages of development. Tissue sections encompassing primordial (type-1) through to pre-ovulatory follicles were collected and investigated using IHC.

2.2 Materials and Methods

2.2.1 Tissue collection and fixation.

Bovine ovaries and positive control tissue (kidney, liver and salivary gland) were collected at a local abattoir; tissues were selected, prepared and immersed in fixative within 10 min of animal slaughter.

Ovaries were removed and inspected in pairs to determine general health, the presence of cysts and stage of reproductive cycle. Stage of oestrous cycle was determined by assessing the gross morphology of the ovaries as described by Ireland *et al.* (1980). Upon determination of cycle stage the ovaries were immediately cut into three or four longitudinal sections approximately 5mm thick. These were rinsed in 10% neutral buffered formalin (NBF) solution (Surgipath Europe Limited, UK) to minimise the diluting effect of any fluid and blood released from the tissue as it was sectioned. Specimen pots were filled with fresh 10% NBF at approximately 20 times the volume of the tissue; this was replaced approximately one hour later and samples remained in 10% NBF for no longer than 24h before processing. Positive control tissue known to express target AQPs was collected at the same time, under the same conditions, and included kidney, liver and salivary gland. Specimen collection pots were labelled with date, tissue type and cycle stage where appropriate; on return to the laboratory ovary specimens were ordered into cycle stage from early follicular phase through to late luteal phase.

2.2.2 Tissue Processing and embedding

Tissues were processed using a Leica TP 1020 automated processor (Leica Microsystems, Germany) and a 17h overnight programme (see Table 2.1). Tissue was embedded in moulds using molten Paraplast paraffin (Sigma-Aldrich Dorset, UK) at 58°C and cooled slowly until set.

2.2.3 Tissue sectioning.

Blocks were sectioned using a Leica RM 2255 microtome (Leica Microsystems Ltd, Bucks, UK). Excess wax was trimmed using 30 µm sections until the tissue was sufficiently presented. Serial sections were then cut at 5 µm in ribbons of no more than 10, placed on a glass plate where 30% ethanol was pipetted under each section to aid the removal of any major creases and/or folds by delicately teasing the creases apart with

two fine paint brushes. Sections were floated in a Leica H11210 water bath filled with distilled water at 39°C and left for between 10 – 45 min to flatten. The time required for sections to completely flatten was entirely dependent on the structures within the tissue. Structures of a spherical nature, for example follicles, required the longest time to flatten and in some instances remained a little creased even after 45 min. The ribbon of sections was gently teased apart into pairs with paint brushes and picked up with a pre-labelled Menzel-Gläser Polysine® slide (Thermo scientific, Brunswick, Germany). Slides were then placed on a 40°C heat block for a least an hour to ensure maximum bonding of the tissue to the slide before being placed into a 53°C oven over night for dehydration.

Table 2.1 Protocol for tissue processing prior to paraffin embedding

Bucket #	Solution	Duration	Process
1	70% Ethanol	01:00:00	Progressive dehydration
2	80% Ethanol	01:30:00	
3	95% Ethanol	01:30:00	
4	100% Ethanol	01:00:00	
5	100% Ethanol	01:00:00	
6	100% Ethanol	01:30:00	
7	100% Ethanol	01:30:00	
8	Histoclear	01:00:00	Preparation for paraffin
9	Histoclear	01:30:00	
10	Histoclear	00:30:00	
11	Paraffin	02:00:00	Liquid paraffin saturation
12	Paraffin	03:00:00	

2.2.4 Morphological identification of bovine ovarian and positive control tissue

The first two sections from each block were stained with Harris Haematoxylin (Raymond A Lamb Ltd, Sussex, UK), and Eosin yellowish (Merck, Nottingham, UK). These were used to assess positive control and ovarian tissue integrity, identification of ovarian follicle stages and follicular atresia (Marion *et al.*1968; van Wezel and Rodgers 1996; Braw-Tal and Yossefi 1997; van Wezel *et al.* 1999a; Rodgers and Irving-Rodgers 2010c). The Braw-Tal and Yossefi (1997) follicle classification system was adopted and extended to include fully antral Graafian follicles. The above system provides criteria for the identification of primordial (type-1) through to small antral (type-5) follicles. For the purposes of this investigation a further category was included: these follicles were named type-6 follicles. The range of follicle diameters was ~1 mm – ~22 mm to

encompass fully antral follicles irrespective of the number of granulosa layers or the morphology of granulosa cells (e.g. columnar or rounded). Identification of the types and stages of atresia was also essential (Grimes *et al.* 1987; van Wezel *et al.* 1999a; Irving-Rodgers *et al.* 2001; Irvin-Rodgers *et al.* 2002; Clark *et al.* 2004) to help in the differentiation between stages of atresia and fixation/processing artefacts. Haematoxylin and eosin sections were also used to confirm non-follicular structures such as vasculature and nerve tissue and to corroborate the quality and morphological integrity of the tissue. AQPs have very specific localisation in known positive control tissue types as reported in the literature (Terris *et al.* 1995; Funaki *et al.* 1998; King *et al.* 2004; Ishibashi *et al.* 2009). Therefore H&E sections were used to identify all major structures and cell types (where possible) in kidney (AQP1, -2, -3, -4, -6, -7 and -8) salivary gland (AQP5) and liver tissue (AQP9).

2.2.5 Haematoxylin and Eosin staining procedure

Slides were de-waxed in xylene (Fisher Scientific UK Ltd, Leicestershire, UK) for 2 x 10 min and rehydrated through a graded series of ethanol (Fisher Scientific) baths (100%, 100%, 95%, 70%; 2 min each) and 5 min in a distilled water bath. Slides were immersed into Harris Haematoxylin for 2 min and rinsed with running tap water until it ran clear of stain. The slides were then dipped for 10s into 1% HCl^- in 70% ethanol to removes excess stain, rinsed with tap water, blued in ammoniated water for 10s and again rinsed with tap water. The slides were then placed in 1.5% eosin for 2 min and rinsed with tap water until it ran clear of stain (about 2 min), and dehydrated using the above series of alcohol baths in ascending order (70% ,95%, 100%, 100% 2 min each) followed by two 10 min xylene baths. Slides were removed from the xylene bath individually, mounted with DPX (Fluka Scientific, Sigma-Aldrich, UK) on 22 mm x 50 mm coverslips (BHD, UK) and left to air dry overnight. Sections were examined using an Olympus BH-2 microscope; the structures present were noted and assessed regarding possible value to this investigation.

2.2.6 Antibodies

Antibodies used were polyclonal antibodies which had been raised against rat AQP1-9 previously developed in collaboration with Sigma-Genosys (Poole, Dorset, UK). Aquaporin 1 and -2 were further affinity purified in Dr Marples' lab (Mobasheri *et al.* 2004a; Mobasheri and Marples 2004; Floyd *et al.* 2005; Mobasheri *et al.* 2009). The

polyclonal antibodies were raised against unique epitopes (Table 2.2) at the c-terminus of rat AQP1 to -9 peptides conjugated to keyhole limpet hemocyanin (KHL). The antigen peptide sequences were checked using Basic Local Alignment Tool (BLAST) (http://www.ncbi.nlm.nih.gov/BLAST/) to ensure that they corresponded to the correct protein and were homologous with bovine AQP protein sequence. Each peptide was introduced into two different rabbits resulting in two bleeds and therefore two batches of serum with slightly different specificity to the epitopes (Table 2.2). Only those demonstrating 100% bovine compatibility were further characterised in bovine positive control tissue and ovary (AQP1,-2,-3,-4,-5, and -6 SGAQP6B).

Each antibody was characterised using relevant positive control tissue at antibody dilutions of 1:50, 1:100, 1:200, 1:500, 1:1000 and 1:2000. Based on initial investigations and previous publications (Floyd *et al.* 2007; Mobasheri *et al.* 2009) the following sera were chosen for further characterisation AQP3 - SG2635, AQP4 - SG2641, AQP5 - SG2643. Anti-α-smooth muscle actin (α-sma; A5691 Sigma-Aldrich Ltd, Dorset, UK) antibody raised in mouse against N-terminal synthetic decapeptide of α-smooth muscle actin was diluted 1:100.

2.2.7 Immunohistochemistry staining procedure

Immunohistochemistry (IHC) was carried out using DakoCytomation EnVision+ Dual Link System – HRP (DAB+) kit (Dako UK Limited, Ely, UK). Each antibody was characterised using relevant positive control tissue and antibody dilutions of 1:50, 1:100, 1:200, 1:500, 1:1000 and 1:2000. Following the procedure described in previous publications using these antibodies (Floyd *et al.* 2007; Mobasheri *et al.* 2009), slides were de-waxed in xylene for 2 x 10 min and rehydrated through a graded series of ethanol baths (100%, 100%, 95%, 70%; 2 min each) and 5 min in distilled water. Slides were removed individually from the water bath, carefully dried and the tissue sections encircled with an ImmEdge hydrophobic barrier pen (Vector laboratories Ltd, Peterborough, UK), covered in water to prevent dehydration and placed in a humidity chamber. Slides were incubated for 15 min at room temperature with 3% hydrogen peroxide (H_2O_2) in absolute methanol to extinguish endogenous peroxidise activity, rinsed in water then treated with 1X phosphate buffered saline (PBS; GIBCO Invitrogen Corporation, UK) + 0.05% Tween 20 (PBS+T, Sigma Aldrich, Dorset, UK) for 5 min. The blocking step included 30 min incubation at room temperature with 1% protease free

Table 2.2 All antibodies used were produced in collaboration with Sigma Genosys prior to this investigation (Mobasheri *et al.* 2009). The table shows target protein and peptide codes pertaining to the antigen peptide sequence inoculums and host rabbit identity codes. The polyclonal serums that shared 100% compatibility (red) in terms of antigen sequence identity with bovine, were used for further characterisation. Serum antibodies to AQP7 and -9 (red) were used as negative controls.

Protein	Peptide code	Rat antigen peptide sequence	Host Rabbit ID	Compatibility with Bovine
AQP1	-	NH_2-(C)LDADDINSRVEMKPK-COOH	-	100%
AQP2	-	NH_2-(C)VELHSPQSLPRGSKA-COOH	-	100%
AQP3	SGAQP3A	NH_2-(C)ENVKLAHMKHKEQI-COOH	SG-2635	100%
			SG-2636	
	SGAQP3B	NH_2-(C)LHIRYRLLRQALAEC-COOH	SG-2637	100%
			SG-2638	
AQP4	SGAQP4A	NH_2-(C)DNRSQVETDDLILK-COOH	SG-2639	100%
			SG-2640	
	SGAQP4B	NH_2-(C)RSQVETEDLILKPG–COOH	SG-2641	100%
			SG-2642	
AQP5	SGAQP5	NH_2-(C)WEDHREERKKTIEL –COOH	SG-2643	100%
			SG-2644	
AQP6	SGAQP6A	NH_2-(C)LEPQKKESQTNSED–COOH	SG-2645	92%
			SG-2646	
	SGAQP6B	NH_2-(C)EPQKKESQTNSEDTE–COOH	SG-2647	100%
			SG-2648	
AQP7	SGAQP7A	NH2-(C)MVQASGHRRSTRGS–COOH	UK-3675	0%
			UK-3676	
	SGAQP7B	NH2-(C)AYEDHGITVLPKMG–COOH	UK-3677	85%
			UK-3678	
	SGAQP7C	NH2-(C)APPLHESMALEHF–COOH	UK-3679	0%
			UK-3680	
AQP8	SGAQP8	NH_2- (C)GDEKTRLILKSR–COOH	SG-2649	0%
			SG-2650	
AQP9	SGAQP9	NH_2- (C)KAEPSENNLEKHEL–COOH	SG-2651	0%
			SG-2652	

bovine serum albumin (BSA, Sigma Aldrich Dorset UK) dissolved in PBS+T to reduce non-specific uptake of antigen. Primary antibodies were appropriately diluted in 1% BSA/PBS+T and incubated overnight at 4°C.

The following day unbound antibody was removed by washing slides twice in 1xPBS for 5 min and once in 1xPBS+T for 5 min combined with gentle agitation. Secondary antibody -horseradish peroxidise labelled polymer, conjugated to goat anti-mouse and anti-rabbit immunoglobulin from DakoCytomation EnVision+ Dual Link System – HRP (DAB+) kit was used. This was diluted one drop in 1 ml of PBS+T and applied to the tissue section and incubated at room temperature for 1h. This was followed by three 5 min washes with agitation: two with 1XPBS and one with 1XPBS+T, to remove unbound secondary antibody in preparation for chromagen development. One millilitre of 3,3' diaminobenzidine (DAB+) substrate was mixed with one drop of DAB+ chromagen. 100 µl was applied/section and developed for between 0.5 – 2 min. When appropriate intensity of stain (dark/brown polymeric oxidation product) was achieved, slides were immersed in tap water, counterstained using haema toxylin as described above (section 2.2.5) and then mounted, cover-slipped and left to air dry overnight. Omission of primary antibody was initially used as the negative control, no antigen retrieval was performed and 10% NBF was the only fixative used in accordance with published information (Floyd *et al.* 2007; Mobasheri *et al.* 2009)

2.2.8 Image capture

A Leica DM4000B microscope with a (c-mount) Q-imaging MicroPublisher 5.0 RTV digital camera with Image Pro Plus v6.3 software (Media Cybernetics MD, USA) was used to capture all images.

2.2.9 Optimisation

The initial aim was to create a bank of ovary tissue demonstrating healthy and atretic follicular structures from type-1 to type-6. This proved very difficult over a short time period as histological classification of early stage atresia without biochemical investigation lead to difficulties in separating signs of early atresia from fixation and processing artefacts. Therefore follicular phase ovaries became the focus of interest, in order to minimise the probability of atretic follicles.

In terms of IHC methodology the serum polyclonal antibodies produced high background staining and what appeared to be heavy non-specific staining. In order to reduce the background attributed to the binding of the secondary enzyme to endogenous peroxidise, treatment with 3% H_2O_2 was increased to 30 min from application to the last slide. To minimise non-specific staining caused by primary antibody binding to charged moieties, 1% BSA was substituted for 5% normal goat serum (NGS, Vector) and blocking duration was increased to 1h.

In addition to the omission of primary antibody, normal rabbit IgG (Vector) was used. This was done to estimate the non-specific binding of target primary antibodies due to fragment crystallisable receptor (FcR) binding or other protein-protein interactions. To offer direct comparison with the polyclonal serum antibodies, non-immune rabbit serum (Sigma Aldrich, Poole, UK. S7523 now replaced by R4505) was used as a negative control at the same dilution range as the polyclonal AQP antibodies (1:50 – 1:2000).

Serum antibodies to AQP7 and -9 (UK-3679 and SG2651 respectively, see Table 2.2) were used as negative controls on ovary and all three positive control tissue types. Based on their 0% compatibility with bovine, any staining as a result of these antibodies would be regarded as non-specific.

A set of experiments was carried out using a Leica BOND-MAX™ automated system and Ready-to-use Bond™ reagents (Leica, Wetzlar, Germany). This experiment compared the labelling of anti-AQP3 and NIRS diluted to 1:200 without antigen retrieval (AtR) and a 1:500 dilution with EDTA and citric acid AtR. EDTA AtR proved more effective than citric acid. The fully automated system de-waxed the tissue sections, performed a 10 min EDTA (pH9) AtR step prior to the peroxidase block and 30 min incubation with primary antibodies at room temperature. The system protocol chosen was Protocol X. This system was able to de-wax, perform AtR and complete IHC over a short time period allowing for a more intense yet highly sensitive and consistent IHC protocol with less damage to the tissue. Anti-AQP3 was chosen as it appeared to specifically label the membrane of kidney collecting duct cell. This was considered the most challenging result to provide evidence to suggest it was non-specific staining and therefore a false positive result.

2.3 Results - Histology

2.3.1 Haematoxylin and eosin morphological observations of preantral follicles

Figure 2.1 shows the stages of follicle development from a primordial or type-1 follicle to late or large preantral type-4 follicle. All follicles are presented at the interface of zones three and four of the ovarian cortex, the thicknesses of which vary considerably between differing sections of the same ovary and between ovaries. The type-1 follicle (Fig. 2.1 (1)) demonstrates a prolate shape formed buy the cuboidal cells at the poles of the follicle; these differentiate into a simple layer of cuboidal cells forming a type-2 follicle (2). From type-2 onwards the increase in follicle size is predominantly dependent on the formation of further granulosa layers, demonstrated by the type-3 follicle, surrounding the now growing oocyte, as shown in Fig. 2.1 (3). In this example not only has the oocyte enlarged but a zona pellucida can clearly be seen. The remaining images represent type-4 follicles with increasing oocyte diameter of ~50 μm and four layers of granulosa cells (4) to an oocyte ~90 μm in diameter surrounded by greater than six layers of cells (6). The main difference between the type-4 follicles in Fig. 2.1 (4), (5) and that in (6) is in the formation and organisation of the thecal compartment; in (6) the cells have become aligned in parallel with the basement membrane. The follicle and oocyte diameter along with the large number of granulosa layers and the distinct theca interna place this follicle within the range of characteristics for a type-5 early antral follicle, however further sectioning did not reveal any obvious evidence of antrum formation.

2.3.2 Haematoxylin and eosin morphological observations of early antral follicle to corpus albicans

Figure 2.2 shows a panel of images representing the stages of follicle development from early antral (type-5) through to the fibrous structure of the corpus albicans. The type-5 follicle measures ~350 μm in diameter and the oocyte ~90 μm; it has a well defined theca layer surrounding the granulosa cells which are beginning to develop a small antral cavity. It also demonstrates a slightly elongated shape which was extremely common amongst the type-5 follicles in this study (Fig. 2.2 (1)). A small fully antral type-6 follicle of 1 mm has in excess of 10 layers of granulosa cells and the mural cells closest to the basement membrane are distinctly columnar in shape; this was also common amongst the small type-6 follicles in this study. The theca is now fully distinct and quite

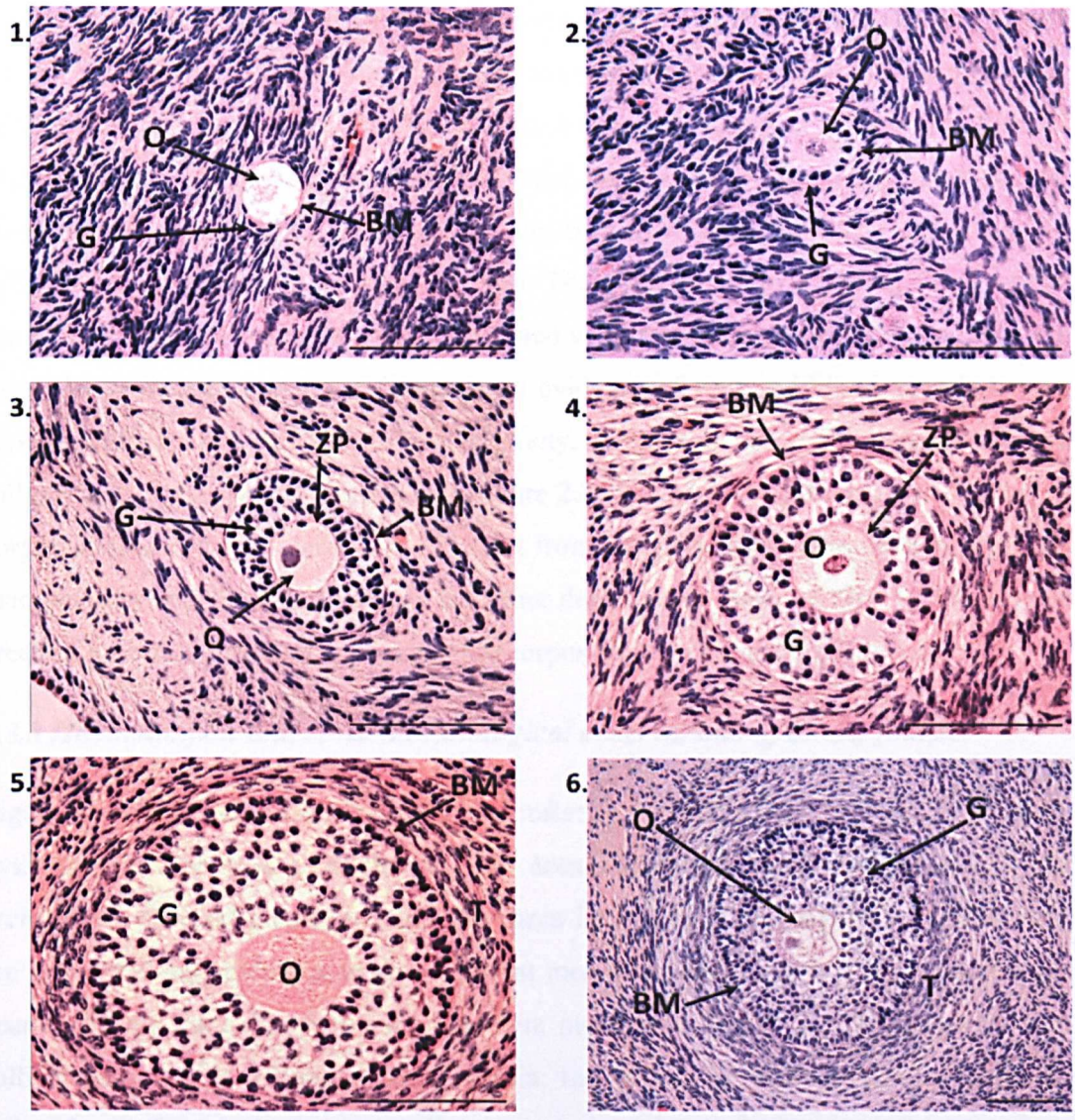

Figure 2.1 Visualisation of 5 µm bovine ovary sections using H&E staining illustrating preantral follicles stages. (**1**) Primordial follicle (type-1) oocyte (**O**) surrounded by flattened granulosa (**G**) cells with cuboidal cells at the poles enclosed by a basement membrane (**BM**). (**2**) A primary (type-2) follicle; the oocyte is surrounded by one layer of cuboidal granulosa cells. (**3**) A small preantral (type-3) follicle; the oocyte commences growth with two to three layers of surrounding granulosa. (**4**) Early stage large preantral (type-4) follicle; four layers of granulosa surrounds the enlarging oocyte with early zona pellucida. (**5**) Large preantral (type-4) follicle; the oocyte has not grown but is surrounded by a clear zona pellucida (**ZP**) and five to six layers of granulosa; the theca (**T**) interna is recognisable but is poorly defined at this stage. (**6**) The oocyte has enlarged and is surrounded by >6 layers of granulosa cells; its diameter is approximately 250µm with a more defined theca layer; its characteristics overlap those of type-4 and type-5 (small antral), with no evidence of antrum formation; this is probably a transitory type-4/-5 follicle. Scale bar = 100 µm.

thick and small blood vessels become apparent (Fig. 2.2 (2)). In a preovulatory type-6 follicle the number of granulosa cell layers has reorganised to four and the morphology of the mural cells is rounded. The theca layer is thin with abundant vasculature (Fig. 2.2 (3)). Figure 2.2 (4) shows a large follicle which appears to be luteinising; the basement membrane is nonexistent and so too any distinction between the theca and granulosa cells, the latter appearing to have enlarged. The vasculature surrounding the structure has proliferated and appears to have penetrated what was the granulosa layer; leucocytes have also infiltrated the tissue. There is no evidence of ruptured blood vessels having leaked erythrocytes into the follicular cavity, suggesting an un-ovulated luteinised follicle in the process of degeneration. Figure 2.2 (5) shows a regressing non-functional corpus luteum still vascularised and distinct from the surrounding stroma, penetrated by macrophages and fibroblast cells as it further degenerates, forming type I collagen and creating a fibrous structure known and the corpus albicans (Fig. 2.2 (6)).

2.3.3 Haematoxylin and eosin morphological observations of atretic follicles

Figure 2.3 illustrates differing forms of atresia: (1) a 5 mm follicle shows significant pyknotic hyperchromatic nuclei in the antral granulosa and destruction of the architecture of basal granulosa cells; the theca interna cells are largely intact but some are orientated perpendicular to the basement membrane and there is a slight increase in space between the cells nearest the basement membrane. Figure 2.3 (2) shows a 4 mm follicle with classic advanced antral atresia; the remaining antral granulosa cells are pyknotic yet the mural granulosa cells remain intact with the basement membrane, theca interna cells and its vasculature remain relatively parallel to the basement membrane. Figure 2.3 (3) shows a follicle approximately 2 mm in diameter with advanced basal atresia, there are few pyknotic nuclei in the antrum with one layer of flattened antral granulosa cells remaining intact and the remaining granulosa cells are devoid of structure and loosely arranged. This is also true of the thecal cells which have a significant amount of collagen between the cells nearest the basal lamina (Fig 2.3 (3) *). The oocyte appears intact and relatively healthy. Figure 2.3 (4) demonstrates very advanced antral atresia of a 6 mm follicle; there are few granulosa cells remaining except one layer of flattened cells next to the basement membrane; theca cells near the basement membrane are still in parallel and appear intact. The remaining theca cells are devoid of structure; the vasculature is also breaking down and has released macrophages into the surrounding tissue.

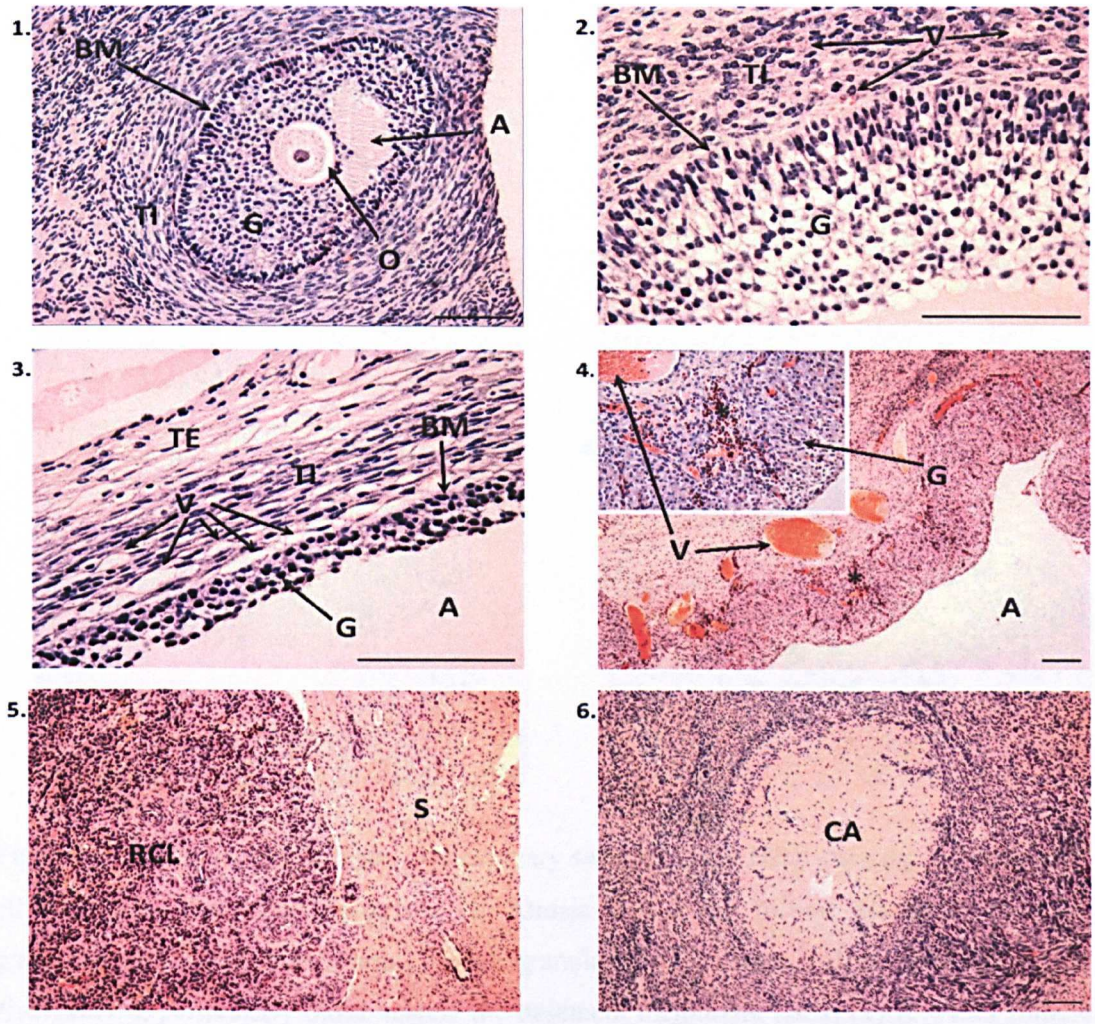

Figure 2.2 Visualisation of 5 µm bovine ovary sections using H&E staining illustrating early antral follicle to corpus albicans. (**1**) shows a small early antral (type-5) follicle demonstrating a slightly elongated shape and early antrum (**A**) formation; the oocyte (**O**) has enlarged to ~90µm and is surrounded by a distinct zona pellucida (**ZP**); there are greater than eight layers of granulosa (**G**) cells surrounded by the basement membrane (**BM**); the theca interna (**TI**) compartment is more organised and distinct. (**2**) Section of a small fully antral (type-6) follicle of 1 mm; the mural granulosa cells are organised and columnar and the theca interna is fully organised and interspersed with small blood vessels (**V**). (**3**) A section of a pre-ovulatory follicle with four layers of rounded granulosa cells and a theca layer abundant with vasculature. (**4**) A luteinised follicle; granulosa cells have increased in size; the basement membrane has broken down and the theca compartment is less well defined; the vasculature from the theca interna and externa has enlarged and penetrated the granulosa layers also infiltrated by leucocytes (Insert *). (**5**) A regressing corpus luteum (**RCL**) distinct from the stroma (**S**) is non functional and will continue to diminish forming the collagenous scar mass that is the corpus albicans (**CA, 6**) Scale bar = 100 µm.

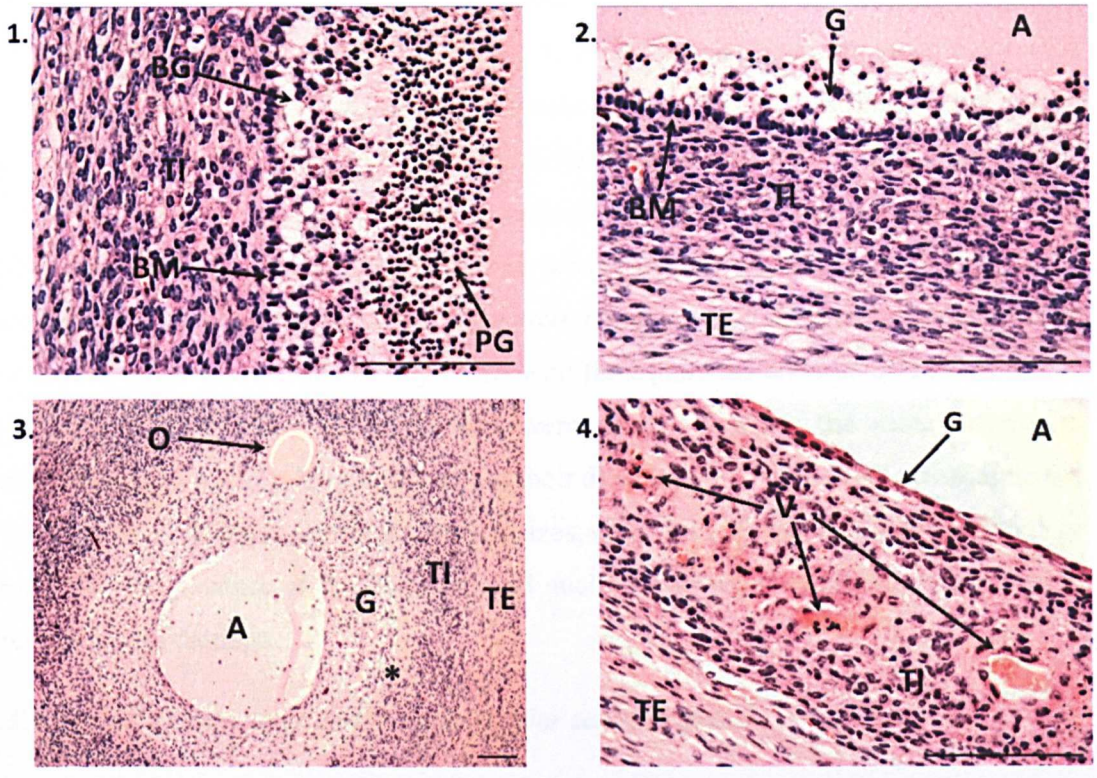

Figure 2.3 Visualisation of 5 µm bovine ovary sections using H&E staining demonstrating different types and stages of atresia. (**1**) Atresia of a 5 mm follicle displaying pyknotic granulosa (**PG**) and deteriorating basal granulosa cells; theca interna (**TI**) cells are disorganised, particularly those nearest the basement membrane (**BM**) (**2**) A 4 mm follicle with advanced antral atresia with pyknotic granulosa (**G**) cells. (**3**) 2 mm follicle with advanced basal atresia; there are few pyknotic cells in the antrum (**A**) and basal granulosa (**G**) cells have significantly deteriorated. Theca interna cells are also atretic and devoid of structure, particularly nearest what was the basement membrane which is now developing into a collagenous glassy membrane (*). The oocyte (**O**) appears relatively healthy. (**4**) Extremely advanced antral atresia of a 6 mm follicle; one layer of flattened granulosa cells remain and the theca layer including the vasculature (**V**) has deteriorated. **TE** = Theca externa. Scale bar = 100 µm.

2.3.4 Haematoxylin and eosin morphological observations of non-follicular structures of the bovine ovary.

Figure 2.4 (1) is the outer zones of the ovarian; cortex zone one = the surface epithelium; zone two = the outer region and zone three = the inner region of the tunica albuginea; both have few cells and contain a high percentage of collagenous tissue. In zone four cells are more abundant, are often arranged in whorls and harbour type-1, -2, -3 and -4

follicles at the interface of zone three and -four. Zone five is not shown (van Wesel and Rodgers 1996). Macrovasculature is abundant in the ovarian medulla particularly near the hilus and Fig 2.4 (2) shows a large muscular artery. This is identified by the simple squamous endothelial lining and sub endothelial connective tissue of the tunic intima, the thicker layer of the tunica media composed of circular smooth, muscle and fibro elastic tissue all surrounded by the tunica adventitia housing collagenous and elastic tissue and the *vasa vasorum.* Large veins were recognised by their large lumen and the few layers of smooth muscle cells parallel with the squamous endothelial cells (Fig. 2.4 (3)). Arterioles, venules and capillaries were identified using the same criteria as described above whilst taking into account their dimensions (Fig. 2.4 (4)). Ovarian tissue was rife with peripheral nerves of varying sizes, (Fig. 2.4 (5)) shows a single fascicle of fibres, the wavy nature of the Schwann cell nuclei reflecting the ability of the axons to stretch without damage.

2.3.5 Bovine kidney, liver and submandibular salivary gland.

Figure 2.5 (1) illustrates a renal corpuscle of which the glomerulus is easily distinguishable from the surrounding proximal (PCT) and distal convoluted tubules (DCT). Proximal convoluted tubules are composed of simple cuboidal epithelium with a prominent microvilli brush border. Distal convoluted tubules have a larger lumen and are absent of microvilli (Fig. 2.5 (1)). Collecting tubules (CT) have cuboidal epithelium similar to that of DCT (Fig. 2.5 (1) and (2)) but elongate towards a columnar appearance as they merge with the collecting ducts (CD) which have larger diameters. Thick descending and ascending limbs of the loop of Henle are difficult to distinguish from collecting ducts with the exception that they are narrower and more regular in shape. Thin limbs of the loop of Henle have squamous epithelial cells and can only be distinguished from the *vasa recta* by the absence of erythrocytes. The portal tract of the hepatic lobule shown in (Fig. 2.5 (3)) and demonstrates the portal vein with its irregular shape, bile duct and lymph vessels; the hepatic artery is not present. At the centre of the hepatic lobule is the central vein which drains the blood channelled through the plates of hepatocytes (polyhedral cells with large round nuclei), by the sinusoids (Fig. 2.5 (4)). Submandibular salivary gland is recognised by the presence of both serous and mucous secreting acini often in the form of mixed seromucous units. Here mucous acini which stain poorly with H&E are capped by serous demilunes; the secretory units are embraced by myoepithelial cells recognised by large flattened nuclei which are difficult to see in

section. Striated ducts are easily recognisable by their columnar cells and large nuclei (Fig. 2.5 (5)).

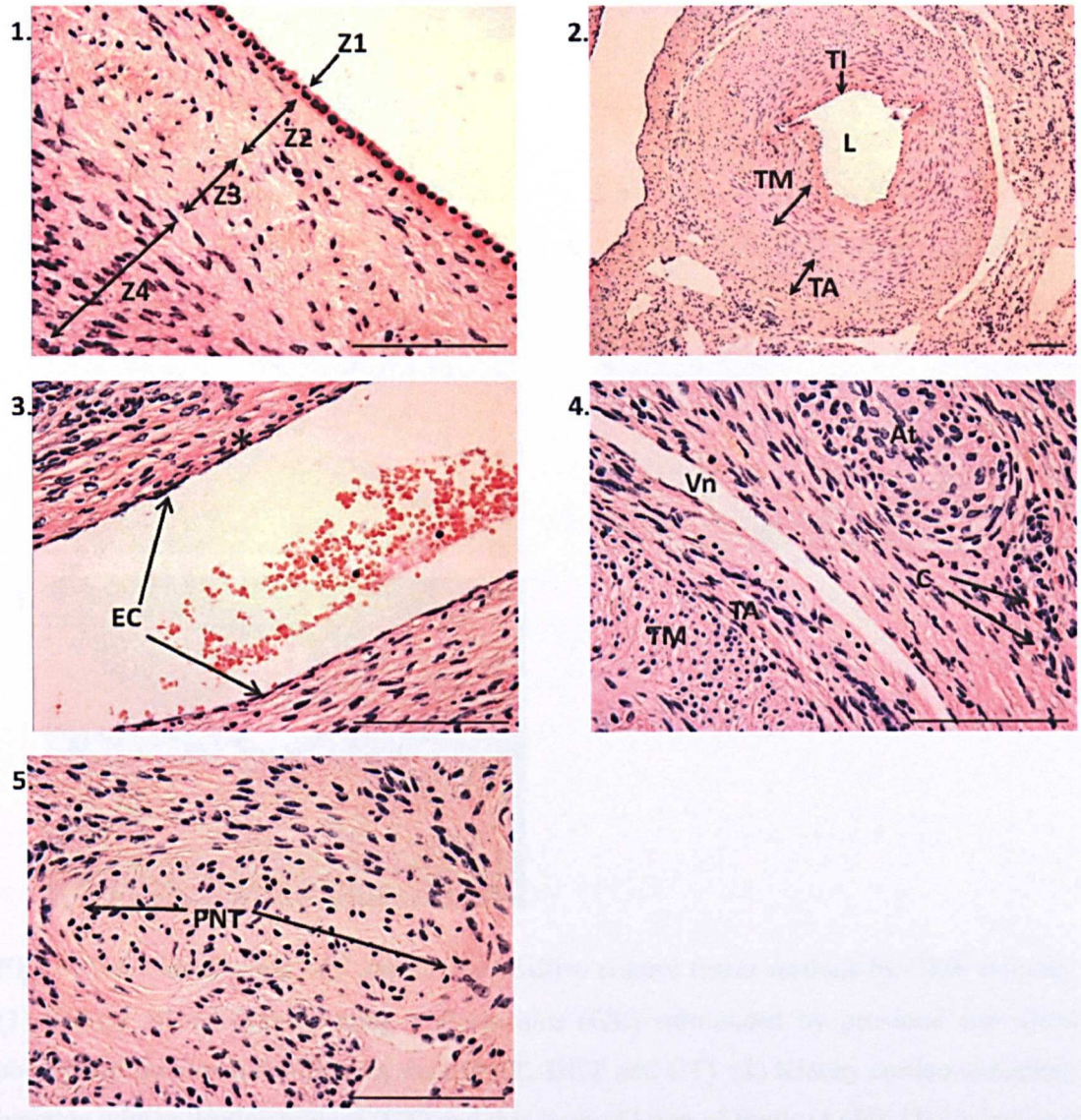

Figure 2.4 Visualisation of 5 µm bovine ovary sections with H&E detailing non-follicular structures. (**1**) Zones 1, 2, 3 and 4 of the ovarian cortex, zone 5 is not shown. (**2**) A larger muscular artery located near the hilus; positioning and orientation of the cells define the three clear bands of the tunica intima (**TI**) surrounding the lumen (**L**), tunica media (**TM**) and tunica adventitia (**TA**). (**3**) A large diameter vein, lined with endothelial cells (**EC**); the thin wall is composed of two to three layers of smooth muscle (*****); the lumen (**L**) still houses a number or erythrocytes and leucocytes. **4**) A venule (**Vn**) situated between a small arteriole (**At**) to the right, under which are some small capillaries (**C**) and to the left a muscular artery, of which the tunica media and adventitia can be seen. **5**) A small peripheral nerve consisting of a single fascicle of fibres with Schwann cell nuclei. Scale bar = 100 µm.

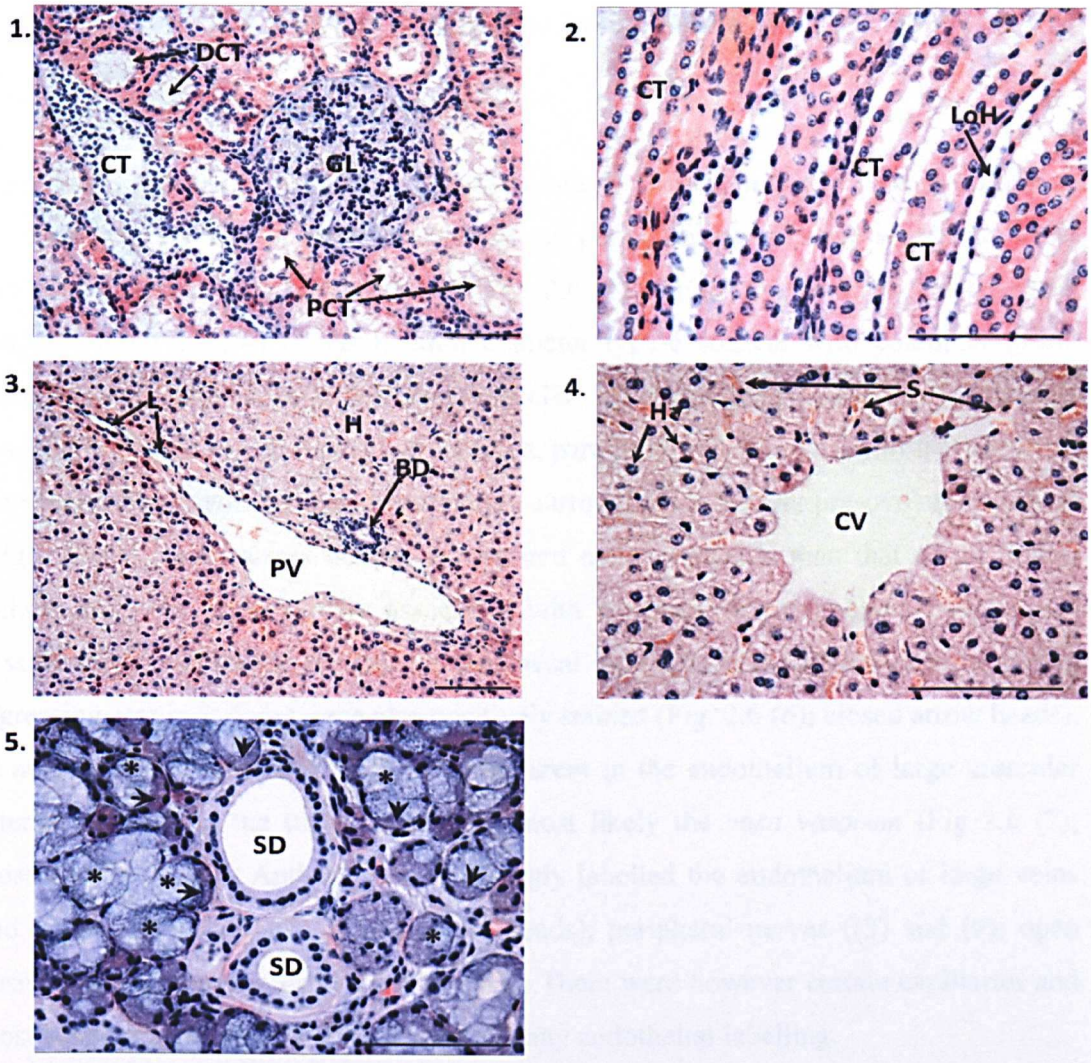

Figure 2.5 Visualisation of 5 µm bovine positive control tissue sections by H&E staining. (**1**) Kidney cortex demonstrating a glomerulus (**GL**) surrounded by proximal and distal convoluted tubules and collecting duct (**PCT**, **DCT** and **CT**). (**2**) Kidney cortico-medullary junction with collecting tubules (**CT**) and thin limb of Loop of Henle (**LoH**). (**3**) Liver tissue showing the portal tract separating hepatic lobules and housing the portal vein (**PV**), bile duct (**BD**) and lymphatic vessels (**L**). (**4**) The hepatic lobules at higher magnification showing the central vein (**CV**) with plates of hepatocytes (**H**) penetrated by sinusoids (**S**). (**5**) Submandibular salivary gland with mucous acini (*) capped by serous demilunes (closed arrows) surrounding striated ducts (**SD**). Scale bar = 100 µm.

Histological identification of non-follicular structures in the ovary and positive control tissues was based on a range of histology textbooks (Young *et al.* 2006; Ross and Pawlina 2006; Gartner and Hiatt 2001) and discussion with veterinary pathologists Dr Peter Brown and anatomist Dr Catrin Rutland (Nottingham University School of Veterinary Medicine and Science).

2.4 Results - Aquaporins in the bovine ovary.

2.4.1 Aquaporin 1 immunohistochemistry

There was no evidence of reactivity in granulosa or oocytes in type-1 to type-6 follicles but there was staining of microvasculature and peripheral nerve tissue within the theca and stroma surrounding these follicles (Fig. 2.6 (1), (2), (3), (4) and (5); closed arrow heads). Figure 2.6 (4) shows a 3mm diameter type-6 follicle with columnar mural granulosa cells and six to seven layers of cells. The vasculature in the theca interna is rounded in appearance and positively stained, particularly that located near the basement membrane. There was increased vasculature surrounding the larger pre-ovulatory follicle (Fig 2.6 (5); closed arrow heads), it appeared more elongated than that of the 3 mm follicle and was again closely associated with the basement membrane. Staining of vessels can be observed throughout the thecal compartment. Capillaries surrounding regressing atretic follicles were also positively stained (Fig. 2.6 (6); closed arrow heads). In non-follicular structures, AQP1 was apparent in the endothelium of large muscular arteries and within the tunica adventitia, most likely the *vasa vasorum* (Fig 2.6 (7); closed arrow heads). Anti-AQP1 also strongly labelled the endothelium of large veins and venules (Fig. 2.6 (8); closed arrow heads), peripheral nerves ((3) and (9); open arrow heads and erythrocytes (9); asterisks). There were however certain capillaries and most small arteries that did not demonstrate any endothelial labelling.

In kidney positive control tissue, anti-AQP1 strongly labelled basolateral and apical membrane of proximal convoluted tubule epithelium. The glomerulus itself was devoid of label but there is some indication of faint stain as a result of positive erythrocytes (see control panel, Fig. 2.10 (1)).

2.4.2 Aquaporin 2 immunohistochemistry

Affinity purified AQP2 (1:200) gave no immunopositivity in bovine ovarian tissue (Fig. 2.6 (10) - (12)). In positive control kidney tissue, AQP2 antibody was localised to the apical membrane and intracellular vesicles within principal cells of the collecting duct (Fig. 2.10 (2)).

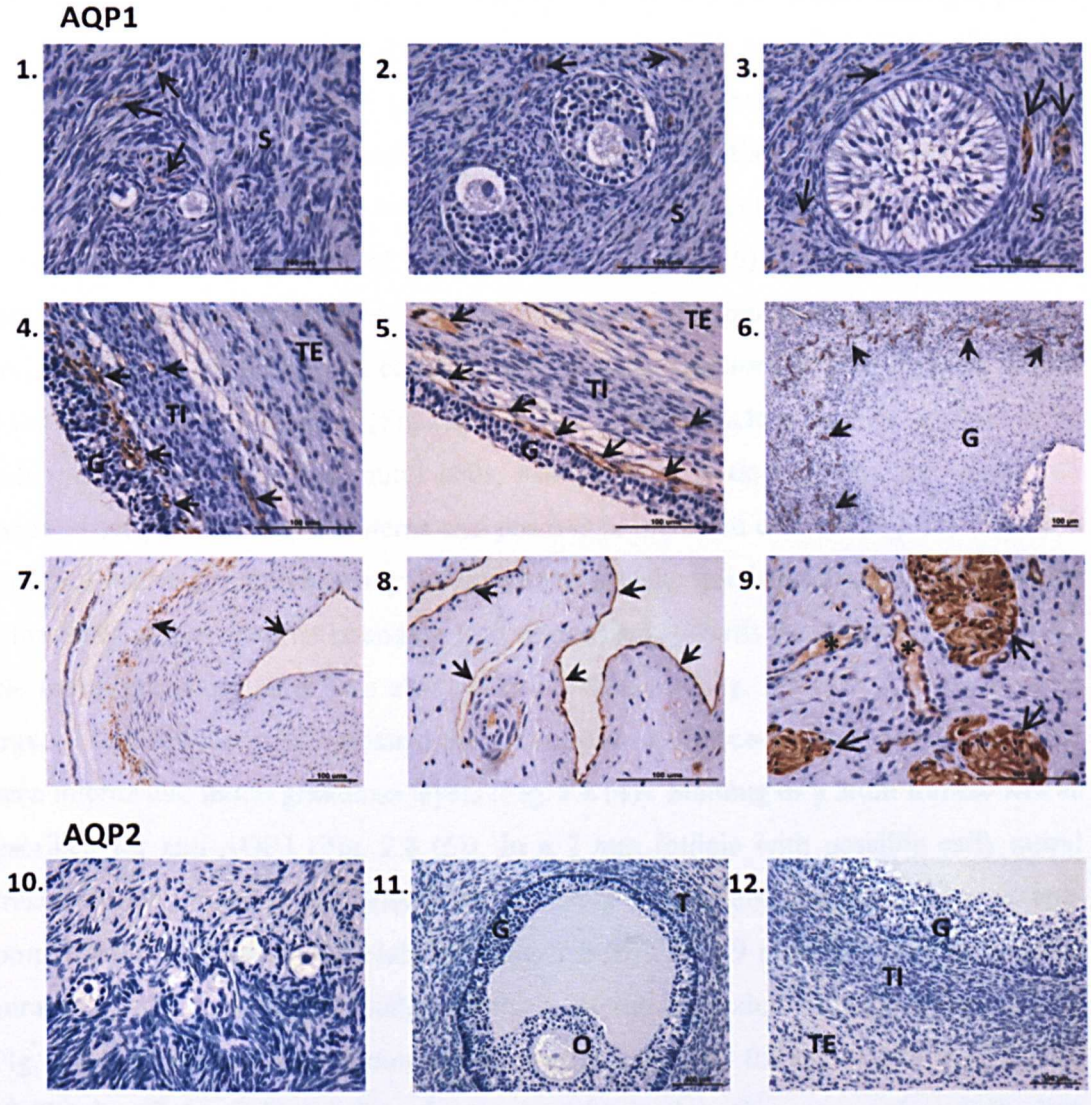

Figure 2.6 IHC staining of anti-AQP1 (**1-9**; 1:200) and AQP2 (**10-13**; 1:200) in paraffin embedded sections of bovine ovary. Anti-AQP1 antibody (brown stain) labels endothelial cells of stromal capillaries (**1**, **2** and **3**; closed arrows); thecal vasculature surrounding healthy type-6 follicles (**4** and **5**; closed arrows) and atretic follicles (**6**; closed arrows). It also labels endothelial cells of muscular arteries and the *vasa vasorum* of the tunica adventitia (**7**; closed arrows). Endothelium of veins and venules (**8**; closed arrows). Peripheral nerves and erythrocytes (**3, 9**; open arrows and **9**; asterisk respectively). Anti-AQP2 did not label any cell type of the bovine ovary (**10**, **11** and **12**). **S** – stroma . **G** – granulosa. **TI** – theca interna. **TE** – theca externa. **O** – oocyte. Scale bar =100 µm.

2.4.3 Aquaporins 3, -4 and -5 immunohistochemistry

Figure 2.7 shows bovine ovary tissue treated with AQP3 (1:100), -4 (1:200) and -5 (1:200) polyclonal serum antibodies which labelled oocytes of all follicle types (Fig. 2.7 (1) – (12); type-6 oocytes not shown) and in the granulosa cells from type-1 to type-4

follicles (Fig 2.7 (1) – (12); open arrow heads). In type-4 follicles the staining appeared to demonstrate basolateral localisation in the mural cells. Type-5 follicles showed a distinct loss of labelling in the granulosa; the oocyte however maintained expression (Fig. 2.7 (13) – (15)). The collagenous rich zones of the tunica albuginea were extensively stained, and so too were the underlying zones, yet there was a great degree of variation within these areas of the cortex (Fig. 2.7 (1) – (6)). There was considerable variation in the labelling of theca interna, externa and the granulosa of type-6 follicles. Anti-AQP3 labelled both theca compartments of a preovulatory follicle and was absent in the rounded granulosa cells (Fig.2.8 (1)). In a 3 mm follicle with what appears to be both rounded and columnar mural cells, staining was predominant in the mural cell layers, absent from the theca interna and positive in the theca externa (Fig. 2.8 (2)). In a 2 mm follicle with predominantly columnar mural cells, staining was particularly heavy in the theca externa/interna boundary then diminished towards the basement membrane. The mural granulosa layer was also positively labelled (Fig. 2.8 (3)). Anti-AQP4 in a large 10 mm follicle lightly labelled the theca extern and became more prominent in the theca interna and mural granulosa layers (Fig. 2.8 (4)). Staining of a 3mm follicle was as described for anti-AQP3 (Fig. 2.8 (5)). In a 2 mm follicle with possible early antral atresia, the columnar mural cells were delicately stained and the large theca interna compartment was prominently labelled (Fig. 2.8 (6)). In a 9 mm follicle with rounded mural granulosa anti AQP5 labelled the theca interna and externa but not the granulosa (Fig. 2.8 (7)). Staining of a 3 mm follicle was as described for anti-AQP3 and -4 (Fig. 2.8 (8)). In a 2 mm follicle with columnar mural granulosa there was a clear distinction between heavy staining of the thick theca interna layer and complete absence of stain in the granulosa (Fig. 2.8 (9).

In non-follicular tissue (Fig. 2.9) all three antibodies again showed the same pattern of staining including the tunica adventitia of microvasculature ((1) – (3)), cells surrounding arterioles and venules ((4) – (6)) and peripheral nerve ((7) – (9)).

The control panel (Fig. 2.10) shows some membranous and cytoplasmic staining of kidney collecting duct by AQP3 antibody (3), labelling of collecting duct, collecting tubules and thin limb of loop of Henle with AQP4 antibody (4). AQP5 antibody intensely staining striated ducts of the salivary gland and demonstrated some stain of cell type surrounding the mucous acini (Fig. 2.10 (5)).

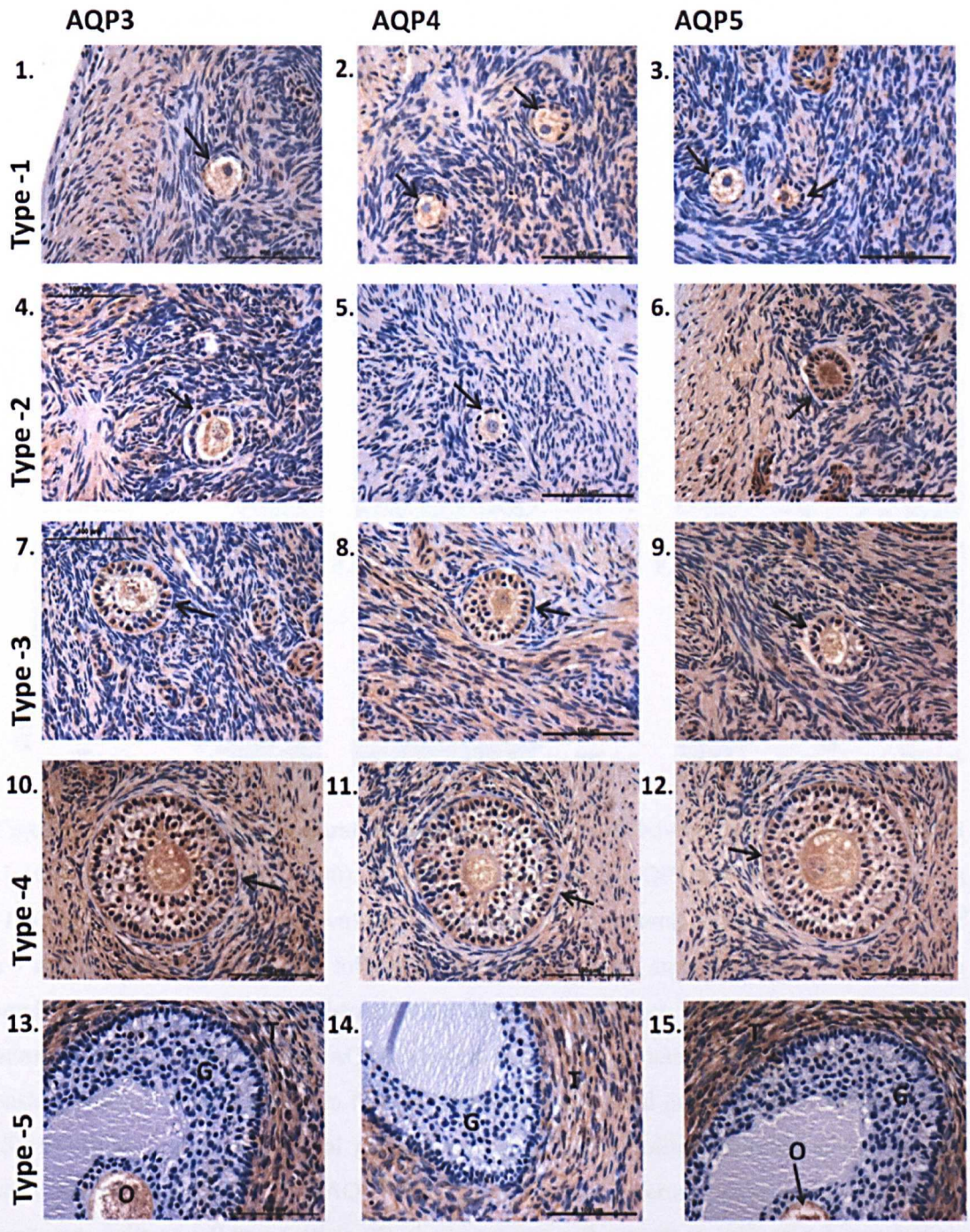

Figure 2.7 IHC staining in paraffin embedded sections of bovine ovary using anti-AQP3 (1:100), -4 (1:200), and -5 (1:200). Type-1 to type-5 follicles. All three antibodies demonstrate the same pattern of staining; they label the granulosa and oocyte of type-1 though to type-4 follicles (open arrow heads **1-12**). The degree of stromal staining appears to be dependent on the location of the follicles within the ovarian cortex. Staining persists in the oocyte (where shown) and is lost in the granulosa of type-5 follicles, in contrast to the heavy staining of the surrounding theca (**13 – 15**). **G** – granulosa, **T** – theca, **O** – oocyte. Scale bar = 100 µm.

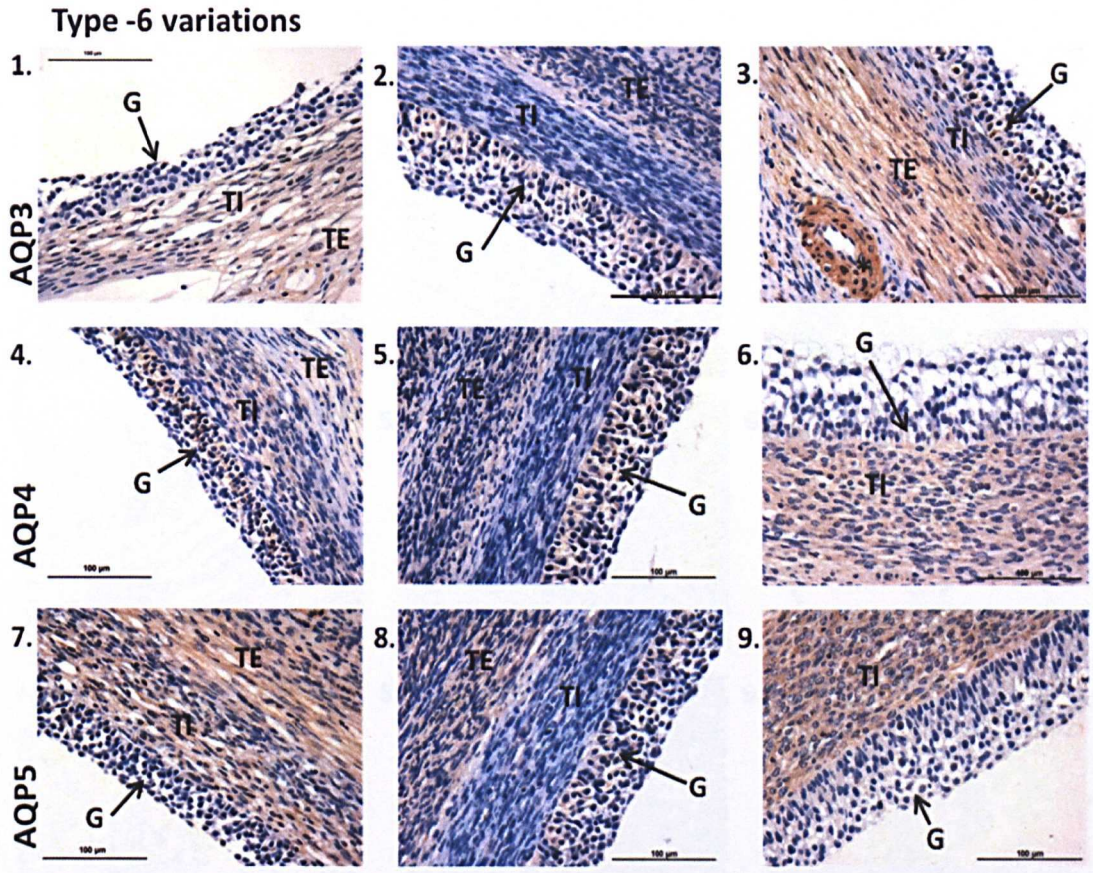

Figure 2.8 IHC labelling in paraffin embedded sections of bovine ovary using anti-AQP3 (1:100), -4 (1:200) and -5 (1:200). Type-6 variations. Anti-AQP3 labelled the theca interna (**TI**) and externa (**TE**) of a preovulatory follicle (**1**), theca externa and granulosa (**G**) cells of a 3 mm follicle (**2**) Of a 2 mm follicle the theca externa and smooth muscle surrounding a small artery (*) demonstrated clear staining, less so in the theca interna but clearly labelled mural granulosa cells (**3**). Anti-AQP4 labelled theca externa, interna and predominantly the basal granulosa cells of a 10 mm follicle (**4**) theca externa and granulosa of a 3 mm follicle (**5**), the theca interna and mural granulosa cells of 2 mm follicle possibly demonstrating early antral atresia (**6**). Anti-AQP5 labelled the theca interna, externa and occasional granulosa cells of a 9 mm follicle (**7**), theca externa and granulosa cells of a 3 mm follicle (**8**) and clear staining of the theca interna with absence in the granulosa of a 2 mm follicle (**9**). Scale bar = 100 μm.

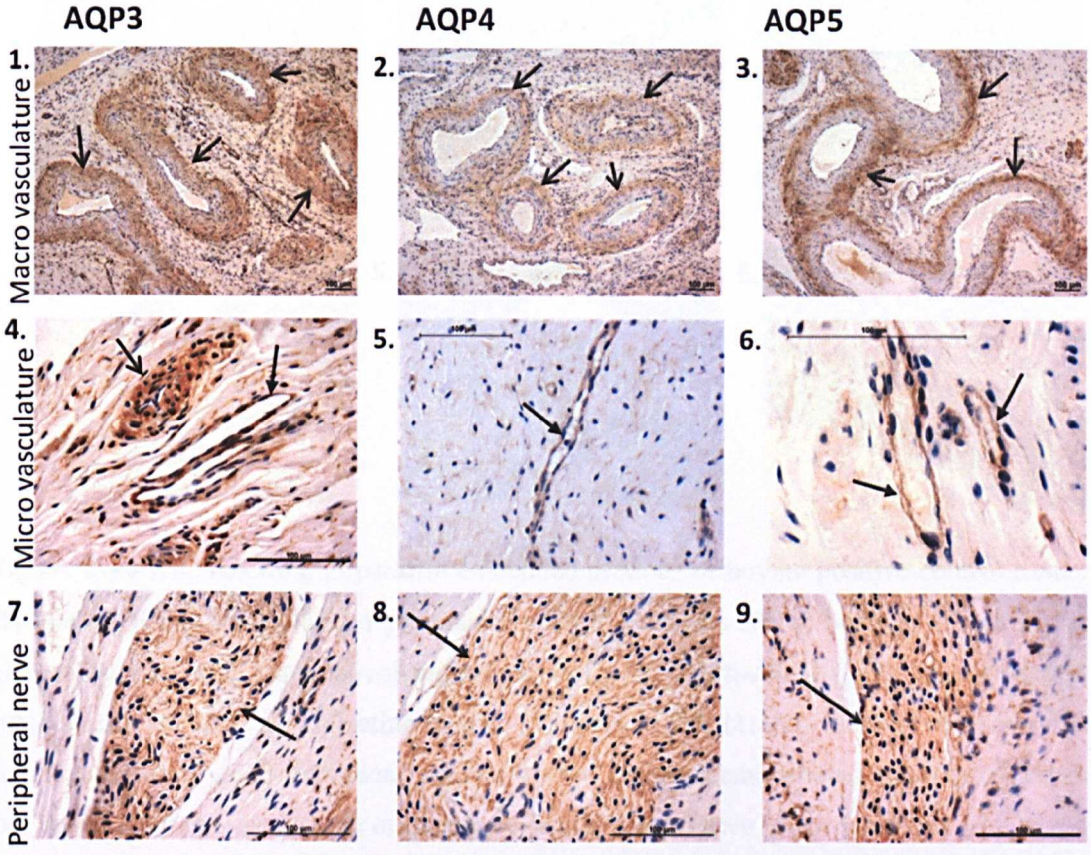

Figure 2.9 IHC labelling in paraffin embedded sections of bovine ovary of anti-AQP3, -4 and -5 in non- follicular structures. All three antibodies label the tunica adventitia of muscular arteries and arterioles (**1**, **2**, **3** and **4** respectively; open arrow heads); the endothelium of venules (**4**, **5**, and **6;** closed arrow heads) and peripheral nerves (**7**, **8**, and **9;** closed arrow heads). Scale bar = 100 μm.

2.4.4 Aquaporins 6 immunohistochemistry

The polyclonal serum antibody for AQP6 revealed no staining whatsoever in kidney positive control tissue at all dilutions described in section 2.2.7, therefore this antibody was not further characterised.

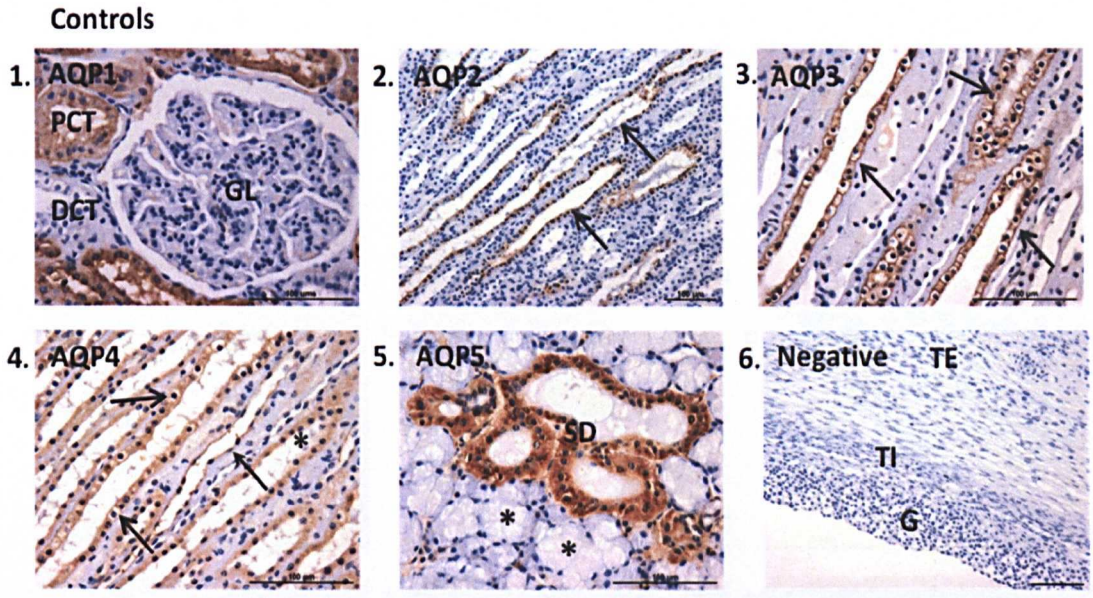

Figure 2.10 IHC labelling in paraffin embedded sections of bovine positive control tissue. (**1**) Anti-AQP1 (1:200) labelled proximal convoluted tubules (PCT) but was absent in the glomerulus (GL) and distal convoluted tubules (DCT). (**2**) Anti-AQP2 (1:200) demonstrated cytoplasmic staining of collecting ducts. (**3**) Anti-AQP3 (1:100) showed membranous staining of kidney collecting ducts. (**4**) Anti-AQP4 (1:200) demonstrated some cytoplasmic and some membranous staining of kidney collecting ducts (open arrow heads) as well as the thin descending limb of the loop of Henle (closed arrow heads) and collecting tubules (*). (**5**) Anti-AQP5 (1:200) intensely labelled striated ducts of sublingual salivary gland and was absent in the mucous acini; faint staining of cell types in between the acini was observed (<), these were possibly myoepithelial cells or underlying ducts. Negative control was done so via omission of primary antibody on bovine ovary sections (**6**). **G** = granulosa, **TI** = theca interna and **TE** = theca externa. Scale bar = 100 µm.

2.4.5 Aquaporin 7 and -9 immunohistochemistry

Figure 2.11 shows IHC images representative of both AQP7 and -9 antibodies. When reacted with bovine ovary tissue they resulted in remarkably similar staining patterns to those produced by anti AQP3, -4, and -5. Ovarian cortex was labelled extensively but staining varied depending on the area of cortex examined and was almost completely absent in the stroma of ovarian medulla (Fig. 2.11 (1), (2), (3) and (9)). Granulosa and oocytes of type-1 to type-4 follicles were labelled, with apparent basolateral staining of mural cells in type-4 follicles (Fig. 2.11 (3)). Type-5 granulosa were devoid of staining but reaction remained in the oocytes (Fig. 2.11 (4)). Theca and granulosa of type-6 follicles showed considerable variation: some follicles demonstrated heavy staining in

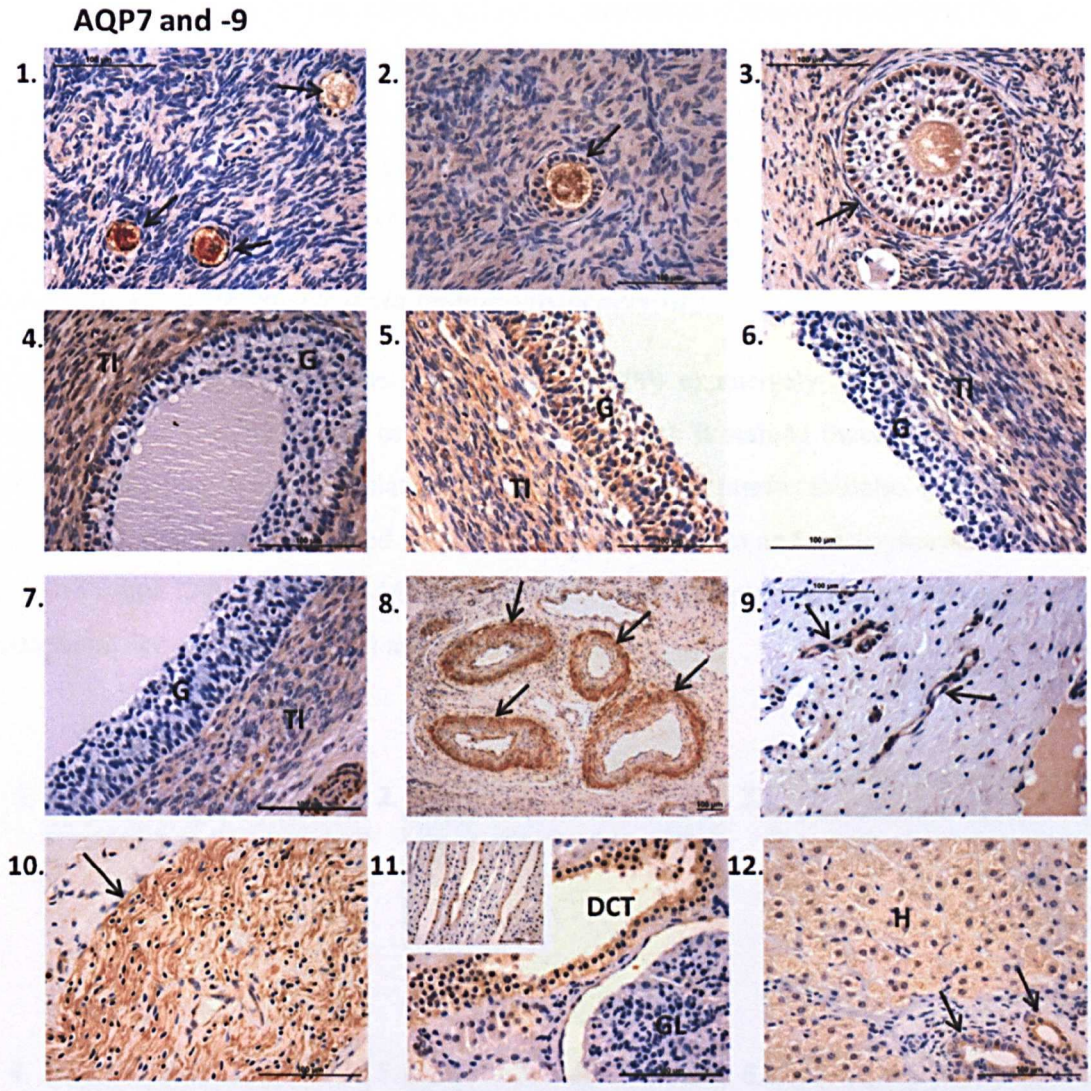

Figure 2.11 IHC labelling in paraffin embedded sections of bovine ovary. Anti AQP7 and -9 diluted 1:200 were non-compatible with bovine AQP7 and 9 peptide sequences and therefore used as an alternative negative control. They both demonstrated staining of oocytes (**O**) and the granulosa (**G**) of type-1, -2, (-3 not shown) and -4 follicles (**1**, **2** and **3**; open arrow heads) with variable staining of theca interna (**TI**) and granulosa of type-6 follicles (**5**, **6** and **7**). There was absence of staining in the granulosa of type-5 follicles (**4**); positive staining of macro- and microvasculature (**8** and **9;** open arrow heads) and peripheral nerve tissue (**10**). (**11**) Kidney positive control tissue for AQP7 shows cytoplasmic and membranous staining of distal convoluted tubules (**DCT**) and collecting duct (**CD**, insert) the glomerulus (**GL**) was devoid of stain. (**12**) Liver positive control tissue shows anti-AQP9 labelling of the hepatocytes (**H**) and bile ducts (open arrow heads). Scale bar = 100 μm.

the thecal interna and/or externa with (Fig. 2.11 (5)) or without ((6) and (7)) staining of the granulosa cells regardless of mural cell morphology. In non-follicular structures both

antibodies showed particular affinity for tunica adventitia of macrovasculature (Fig. 2.11 (8)) the cells surrounding microvasculature (9) and peripheral nerves (10). In control tissue they both heavily stained distal convoluted tubules and collecting ducts of kidney (Fig. 2.11 (11) plus insert) and to a lesser extent PCT and CT (not shown). In liver tissue they both reacted with hepatocytes and bile ducts (Fig. 2.11 (12)).

2.4.6 Alpha smooth muscle actin immunohistochemistry

Figure 2.12 (1) and (6) shows that α-SMA (1:100) extensively labelled the ovarian cortex but not granulosa cells or oocytes ((1) and (2)). It stained theca externa and the cells surrounding thecal vasculature of both healthy and atretic follicles (Fig. 2.12 (2) and (3)). It also heavily labelled the cells surrounding macro and microvasculature (Fig. 2.12 (4) and (5)). Anti α-SMA did not react with stromal tissue of the hilus nor peripheral nerves (Fig. 2.12 (5) and (6) respectively).

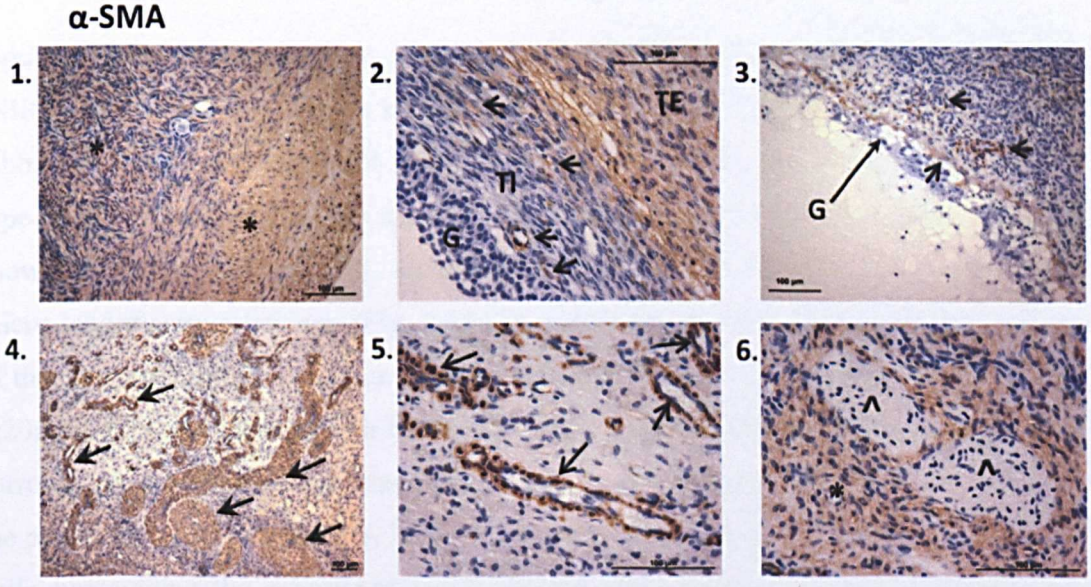

Figure 2.12 IHC labelling of α-SMA (1:100) in paraffin embedded sections of bovine ovary to help identify the specific cell types labelled with AQP antibodies. Labelling by α-SMA occurred uniformly in all zones of the ovarian cortex ((**1**) and (**6**); *) including theca externa (**TE**; (**2**)). The theca interna (**TI**), granulosa (**G**) and oocytes (not shown) of all follicle types remained devoid of stain ((**1**) - healthy and atretic type-1 follicles, healthy and atretic type-6 follicles (**2**) and (**3**) respectively). Smooth muscle cells surrounding micro- (**2**, **3** and **5**; open arrow heads) and macrovasculature (**4**; closed arrow heads) were clearly labelled. Medullary stromal tissue exhibited reduced labelling, particularly that of the hilus. Staining was absent in peripheral nerve tissue (^). Scale bar = 100 μm.

2.4.7 Rabbit IgG immunohistochemistry

Rabbit IgG was used at a range of dilutions. The images shown (Fig. 2.13) are for IgG at a dilution of 1:200. Figure 2.13 shows affinity for pure rabbit IgG in certain cell types of bovine ovary tissue sections. There was intense labelling of the outer and inner zones of the cortex ((1), (2) and (3)). The granulosa and oocytes (Fig. 2.13 (1), (2), and (4); type-6 oocytes not shown) of follicles, with the exception of type-5 granulosa, were positively stained. In type-5 follicles the oocyte remained heavily stained and in the granulosa cells labelling was completely lost (Fig. 2.13 (3)). Cells surrounding macro- and microvasculature including thecal vasculature and peripheral nerve tissue were clearly stained (Fig. 2.13 (5)). In kidney tissue, DCT, CD and CT were positive (Fig. 2.13 (7) and (8)), SD and some cells surrounding mucous acini of sublingual salivary gland were heavily stained (9) and in liver hepatocytes and bile ducts were also labelled (10).

2.4.8 Non-immune rabbit serum with normal goat serum block

Figure 2.14 shows the treatment of bovine ovary sections with non-immune rabbit serum (NIRS) and AQP3 following a normal goat serum (NGS) blocking step. Non-immune rabbit serum at 1:200 labels all zones of the ovarian cortex, granulosa, albeit weak of type-1, -2, -3, and -4 follicles and oocytes of all follicle types (not all follicle types shown, Fig. 2.14 (1) and (3)). Non-immune rabbit serum labelled cells surrounding micro- and macrovasculature (Fig. 2.14 (2); open arrow heads). There was also staining of theca externa, interna and mural granulosa cells of type-6 follicles (Fig. 2.14 (3)). At 1:200 dilution and blocked with NGS, AQP3 demonstrated labelling of the theca interna surrounding a type-5 follicle (open arrowhead), no labelling of the granulosa but some the positivity in the oocyte (Fig. 2.14 (4); closed arrowhead). There was faint staining of cells surrounding the macrovasculature and the theca interna of a type-6 follicle, the granulosa cells appear devoid of any staining (Fig. 2.14 (5) and (6) respectively). Figure 2.14 (7) and (8) display automated BOND IHC of anti-AQP3 in kidney tissue at a 1:500 dilution without antigen retrieval (AtR). Weak staining was observed in the PCT and CT, the CD cells revealed particularly noticeable membranous staining (Fig. 2.14 (8)). However NIRS also displayed the same pattern and intensity of staining in CD (9). Following EDTA AtR background levels were elevated in PCT and CT (Fig. 2.14 (10) and (11)), anti-AQP3 revealed increased basolateral labelling of CD; this was particularly noticeable in ((10) and (11)) compared with ((7) and (8)). Non-immune rabbit serum staining intensity was also greatly increased and the pattern of staining appeared to remain fully membranous (12).

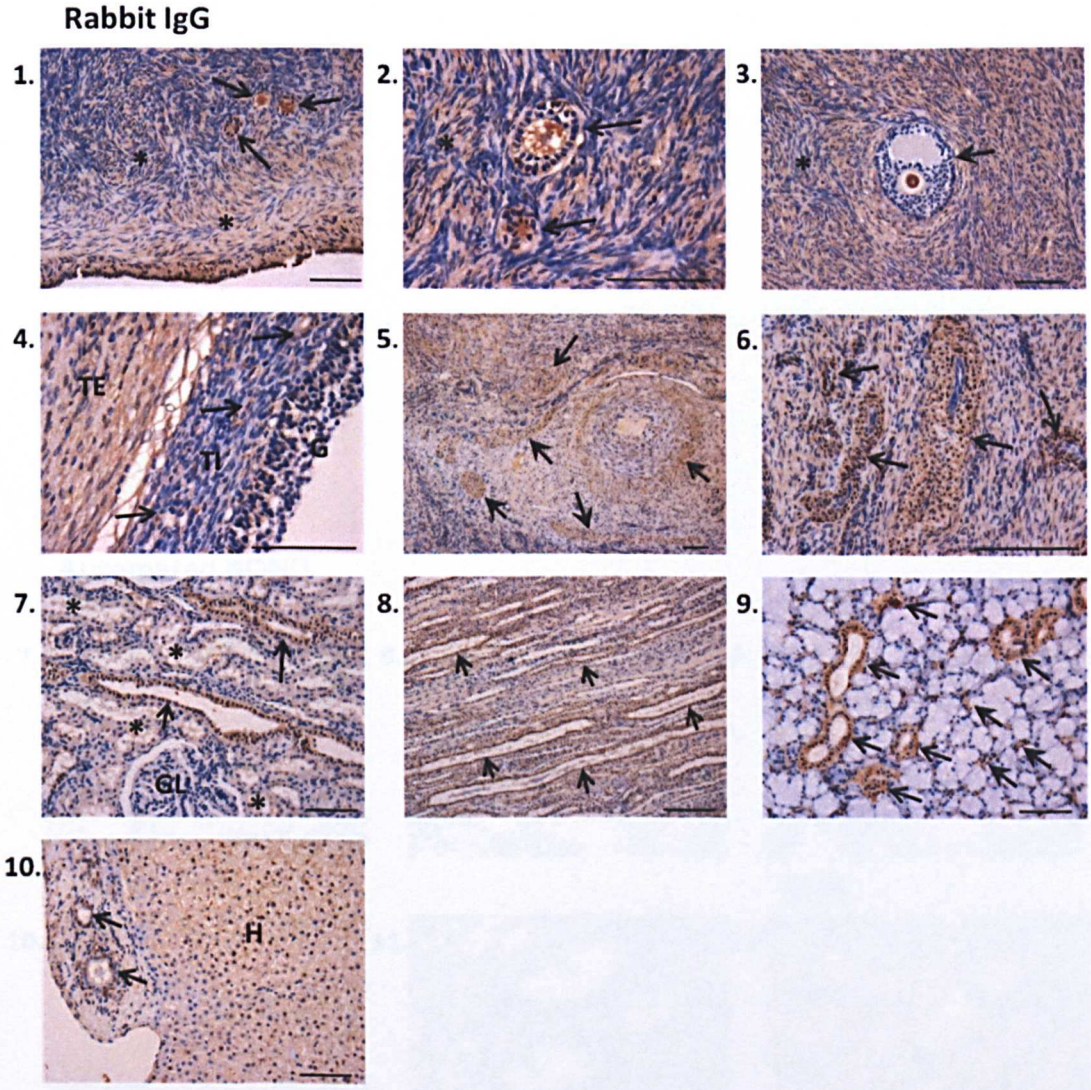

Figure 2.13 Rabbit IgG (1:200) labelling in paraffin embedded sections of bovine ovary. Rabbit IgG binds to and therefore labels, all zones of the ovarian cortex (*) as well as the theca surrounding type-5 follicles (**3**) and theca externa of type-6 follicles (**4**). Staining also occurred in the granulosa and oocytes of follicle types -1, -2, -3, -4 and -6 (Fig 2.13 (**1**), (**2**), and (**4**) respectively; open arrow heads). Granulosa cells were devoid of label (closed arrow head) yet staining persisted in the oocyte (**3**). Cells surrounding microvasculature of the theca interna (**4** and **6**; open arrow heads) and macrovasculature (**5**; open arrow heads) were labelled and so to was peripheral nerve tissue (**5**; closed arrow heads). In kidney cortex (**7**) IgG strongly labelled distal convoluted tubules (open arrow heads); weakly labelled proximal convoluted tubules (*) and was absent in the glomerulus (GL). **8** In kidney medulla labelling was clear in collecting duct, collecting tubule and thin limb of loop of Henle (**9;** open arrow heads). In sublingual salivary gland striated ducts were abundantly labelled. Scale bar = 100 μm.

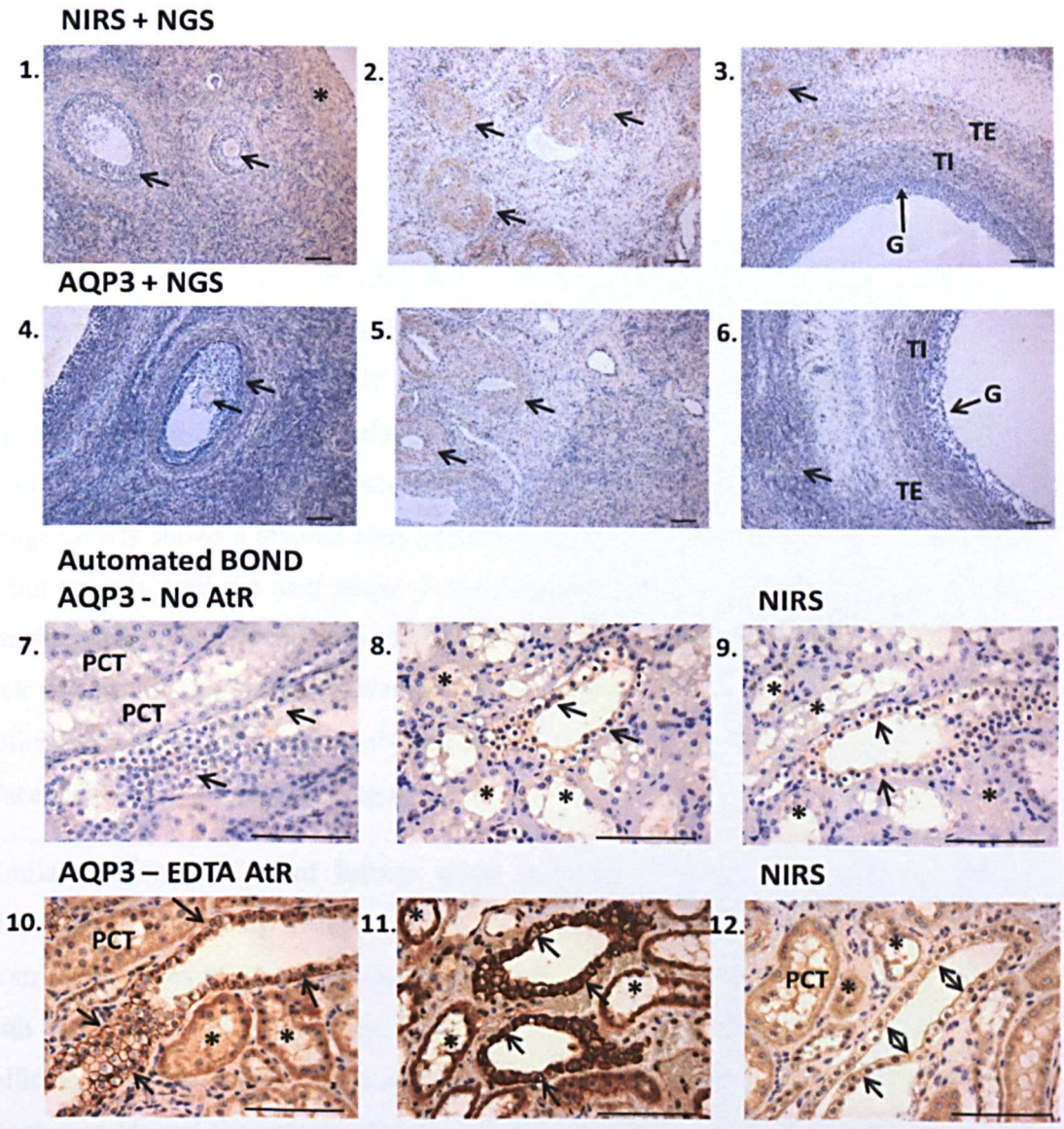

Figure 2.14 IHC labelling in bovine sections blocked with normal goat serum (NGS). (**1**) Non-immune rabbit serum (NIRS at 1:200) labels all zones of the ovarian cortex, granulosa and oocyte of type 1, -2, -3, -4 and -6 follicles (**1** and **3;** not all follicle types shown). (**2**) and (**3**) NIRS labelled cells surrounding vasculature (open arrow heads) also theca externa and faintly in theca interna and mural granulosa cells. (**3**) At 1:200 dilution and blocked with NGS, anti-AQP3 gave weak labelling of theca interna (open arrow head) and stromal cells (**4** and **6** *), oocytes (**4**) and mural granulosa in type-6 follicles (**6**), and surrounding vasculature (**5** and **6**; open arrow heads). (**7**) and (**8**) automated BOND IHC of anti-AQP3 (1:500 minus antigen retrieval (AtR) in kidney, revealed weak staining in the proximal convoluted tubules (**PCT**) collecting tubules (*) and membranous staining of collecting duct cells (open arrow heads). (**9**) NIRS (1:500) demonstrated the same pattern and intensity of staining. (**10**) and (**11**) EDTA AtR gave more intense staining, anti-AQP3 gave a more basolateral pattern of labelling compared with NIRS. Scale bar = 100 μm.

2.5 Discussion

2.5.1 Follicle identification.

In order to thoroughly document processes of folliculogenesis it is essential to base the investigation on a solid and widely recognised frame of reference. Even though the stages of follicle development have been well documented in the literature, there is still variation in the way different follicular stages are described. It remains no easy task to be precise about which follicle type is being examined. For example Fig. 2.1 (3) represents a type-3 follicle consisting of an enlarged oocyte surrounded by two to three layers of granulosa cells as described by Braw-Tal and Yossefi (1997). However, the image clearly shows a distinct zona pellucida which, according to Braw-Tal and Yossefi, is not present until the next stage of development has been achieved. Figure 2.1 (6) is considered by this investigation to be a type-4 follicle because of its spherical shape and lack of antrum formation. However, characteristics pertaining to diameter and thecal definition exceed the range attributed to type-4 follicles by Braw-Tal and Yossefi and place it firmly in the type-5 category.

Similarly, identification of follicle status in terms of health also remains difficult. Fixation and processing of tissue can cause artefacts which are difficult to differentiate from early stages of atresia. Irving-Rodgers *et al* (2001) identified two types of atresia with roughly the same frequency, basal atresia and antral atresia. Basal atresia occurs in follicles less than 5 mm where atresia initiates at the basal/mural granulosa cells and progresses toward the antrum. Antral atresia occurs in follicles of all sizes and initiates at the antral granulosa layers and progresses toward the basal/mural granulosa cells (see section 1.4 for a detailed description). Throughout this investigation antral atresia was by far the most abundant and on the few occasions where basal atresia was identified it was extremely advanced (Fig. 2.3 (3)). However there may have been cases of basal atresia that were overlooked.

This highlights the subjectivity involved in identifying stages of follicle development and atresia. It is possible therefore that one may overlook or fail to include follicles which do not meet the most recently accepted criteria, which could bias results and conclusions.

2.5.2 Aquaporin 1 and -2

Aquaporin 1 was localised to ovarian macro- and microvasculature endothelial cells (Fig. 2.6 (1)-(8)), peripheral nerve tissue and erythrocytes (Fig 2.6 (9)). Whilst it was seen in the endothelial cells of large arteries it seemed more abundant in the majority of capillary endothelial cells, veins and venules. In terms of follicular development, as follicles grew the degree of vascularisation increased and so did the incidence of AQP1. It also persisted in the vasculature of advanced atretic follicles (Fig 2.6 (6)). Aquaporin 2 was not found in bovine ovary tissue, even though it was present in kidney positive control (Fig. 2.6 (10)-(12); Fig. 2.10 (2)).

These results are consistent with AQP1 results in porcine ovary (Skowronski *et al.* 2009) with the exception of peripheral nerve tissue which as yet is unreported in any other species. Skowronski *et al.* (2009) also identified AQP1 in oviduct and uterine capillaries and did not find AQP2 in porcine ovarian tissue. In contrast to this, Thoroddsen *et al.* (2011) localised AQP1 and -2 to human granulosa and theca cells. McConnell *et al.* (2002) investigated granulosa cells of rat but did not identify AQP1 or -2. These results could point to significant species differences, but overall the amount of information is extremely limited. Aquaporin 2 has also been reported in human uterine endometrium and myometrium (He *et al.* 2006: Jablonski *et al.* 2003).

The detection of AQP1 in the bovine ovarian microcirculation is consistent with its reported association with angiogenesis, vascular reactivity (Endo *et al.* 1999; Saadoun *et al.* 2002; Monzani *et al.* 2009; Nico and Ribatti 2010) and transport of NO (Herrera and Garvin 2007). AQP1 is also reportedly up-regulated by E_2 (Fisher *et al.* 1998; Richard *et al.* 2003; Oliveira *et al.* 2005; Lindsay and Murphy 2006) and progesterone (Lindsay and Murphy 2006). Vascular endothelial growth factor is a potent regulator of vascular permeability (Bates 2010) and could therefore be a potential modulator of AQP1. Vasculature endothelial growth factor is abundant in the ovary and is considered to facilitate antral follicle and corpus luteum development (Robinson *et al.* 2009). It mediates vascular permeation, vasodilatation, endothelial cell migration and vascular tube formation (Glass *et al.* 2006; Ferrara and Davis-Smyth 1997; Ku *et al.* 1993). Endothelium-derived factors such as NO and endothelin-1 are also potential regulators of permeability and are both modulated by E_2. Nitric oxide is a vasodilator and increases in parallel with rising E_2 levels whereas endothelin-1 is a potent vasoconstrictor and is reduced by E_2 (Huxley and Wang 2010). Aquaporin 1 transports NO and could facilitate

the increased NO levels seen under the influence of rising E_2. Aquaporin 1 is therefore likely to be involved with a number of factors in controlling follicular vascular permeability.

Taken together, this information suggests that AQP1 is present in the ovarian vasculature and has a role in terms of vascular permeability and fluid flux but also in the development of antral follicles.

2.5.3 Aquaporin 3, -4 and -5

The shared pattern of staining for AQPs -3, -4 and -5 in follicles and non-follicular structures could be due either to ubiquitous expression of AQP proteins across bovine ovarian tissue, or to artefactual signals resulting from non-specific reaction of serum antibodies to certain cells types or cross linking with secondary antibody. Distribution of AQPs in tissue is reported so far to be very cell-type and membrane specific, as discussed in section 2.1.3. Therefore the presence of ubiquitous expression of all three AQPs in the ovary seems unlikely. This conclusion is also encouraged by the detection of a similar pattern of DAB+ staining produced by serum antibodies with 0% compatibility with bovine (anti-AQP7 and -9).

Neither McConnell *et al.* (2002) nor Skowronski *et al.* (2009) identified AQP3, or -4 in rat and pig ovary respectively. Aquaporin 5 was found by Skowronski's group but it was localised to granulosa cells of type-one follicles and the basolateral membrane of mural granulosa cells in growing antral follicles. The antibodies used in their investigation were affinity purified and perhaps demonstrated strong affinity and therefore specificity. Thoroddsen *et al.* (2011) however, identified AQP3 and -4 in both granulosa and theca of pre-post ovulatory follicles at varying levels. These IHC results also seem to display ubiquitous staining, although, there are questions surrounding their methodology and use of appropriate controls (further discussed in section 5.1). Similar to this investigation it is difficult to be sure of the reliability of their results.

Aquaporins 3 and -4 are found in the basolateral membrane of principal cells of the CD epithelium (Ishibashi *et al.* 1994 and Terris *et al.* 1995). The positive control tissue sections in this present investigation do demonstrate positive membranous staining of CD cells with anti-AQP3 and -4 (Fig. 2.10 (3) and (4)). Anti-AQP4 also labelled the thin descending limb of the Loop of Henle and both demonstrated staining in the distal convoluted tubules (images not shown). However, anti-AQP7 and -9 also displayed

membranous staining of CD cells and distal tubules (Fig. 2.11 (11); insert). Salivary gland is known to express AQP5 in the apical membrane of the acini (Funaki *et al.* 1998; Steinfeld *et al.* 2001). In this investigation there was no distinct evidence for apical acini staining; however, heavy staining was localised to the striated ducts of the salivary gland which are known to secret IgG (Korsrud and Brandtzaeg 1981). This pattern was again shared with anti-AQP7 and -9. Due to the lack of consistency in the literature and the questions surrounding the reliability of the antibodies used in this investigation, it is not possible to draw any conclusion on the potential role of AQP-3, -4 and -5 in the ovary.

2.5.4 Antibody evaluation

The anti-AQP1 to -5 antibodies were selected on the basis of two recent publications from our lab. However, the present investigation suggests that these earlier results may be open to alternative interpretation.

Firstly, Mobasheri *et al.* (2009) used the same antibodies as in this investigation (Table 2.1) and describe results for AQP1,-2,-3,-4,-5,-6,-7 and -9 in bovine mammary gland tissue. The AQP1 and -2 antibodies were affinity purified and so can be considered to provide reliable results. The remaining antibodies were not affinity purified. Basic local alignment search tool (BLAST) results for the antigen sequences used to raise the antibodies for this investigation, however, revealed that anti-AQP6 to -9 peptide sequences are not compatible with bovine. Positive control tissue images for AQP3 and -4 did demonstrate some weak, seemingly specific staining but the current investigation also reveals similar staining with both anti-AQP7, -9 antibodies and NIRS. Aquaporin 5 positive control image was absent from Mobasheri *et al.* (2009) and so a comparison with the AQP5 results from this investigation is not possible. Omission of primary antibody was the only negative control to be performed in the Mobasheri *et al.* (2009) study and so some results described could also be due to non-specific staining. This could potentially be resolved by a further negative control with NIRS.

Secondly, Floyd *et al.* (2007) investigated AQP1-4 (Table 2.1) in equine kidney; AQP1 and -2 again appear to show specific and reliable results. The affinity purified antibodies produced vey specific staining with no background. The staining with anti-AQP3 and -4 (both known to be CD AQPs) shows very high background levels and prominent labelling of DCT and CD. Again only the omission of primary antibodies was used as a negative control.

In conclusion, in the absence of a more rigorous negative control, both papers could potentially have misinterpreted non-specific labelling as true protein expression. To investigate the non-specific components of these serum antibodies, rabbit IgG was used as a crude measure of rabbit IgG affinity for bovine ovary and positive control tissue (Fig. 2.13). Alpha-smooth muscle actin was also used to try to ascertain if there was a particular cell type for which the serum antibody had affinity (Fig 2.12). Found in the cortex, theca externa and surrounding vasculature, these results for α-SMA in bovine ovary comply with those in human ovary (Czernobilsky *et al.* 1989), rat and monkey (Osvaldo-Decima 1970). It is suggested that α-SMA plays a role in stromal contractility (Santini *et al.* 1995). The pattern of serum antibody labelling reflects that of α-SMA labelling to some extent: α-SMA did not react with oocytes, PNT or consistent theca interna and granulosa as did the serum antibodies. These results suggest that rabbit IgG showed affinity for cell types that also label with α-SMA, including oocytes and, to a limited degree granulosa cells. In kidney, rabbit IgG labelled DCT, CD, CT and thin limb of loop of Henle (Fig. 2.13 (7) and (8)). In salivary gland, striated ducts and possibly myoepithelium or other underlying ducts were labelled; hepatocytes and bile ducts were also labelled in liver tissue (Fig 2.13 (9) and (10)). This evidence points to non-specific binding of rabbit IgG from these AQP polyclonal serum antibodies to certain cell types.

If the antibody of interest is of a low concentration within the antisera it will be unlikely that the non-specific components can be diluted out. This was pursued by using the Automated BOND machine (for consistency) with and without antigen retrieval (AtR; Fig 2.14). Firstly, anti-AQP3 treatment was blocked with NGS and no AtR. In ovary the degree of background staining was much diminished but the same pattern remained nevertheless (Fig. 2.14 (4)-(6)); this was also reflected in the NIRS incubation results (Fig. 2.14 (1)-(3)). Similarly in kidney tissue, NIRS produced the same labelling effect as with anti-AQP3 (Fig. 2.14 (7)-(9)). The experiment was repeated exactly but this time with AtR; this appeared to reveal basolateral sites of AQP3 localisation in kidney CD not previously seen, but background levels were greatly elevated (Fig 2.14, (10) and (11)). The NIRS again displayed staining localised to the same cell type, but there was a significant difference in membrane localisation and intensity (Fig. 2.14 (12)). It could be that the application of AtR would allow a less concentrated antibody solution to be used, effectively diluting out the non-specific components. This would also have a comparable effect on the NIRS, which at a higher dilution would be a more effective negative

control. A range of rabbit sera could also be purchased to investigate the possibility of varying levels of NIRS affinity for certain cell types.

Certain tissues demonstrate background staining as a result of hydrophobic and ionic interactions. These include, connective tissue elements such as collagen, laminin, elastin, and proteoglycans, as well as epithelia and adipocytes (Boenisch 2007). Aldehyde - containing fixatives such as formalin cause increased cross-linking of amino acids which heightens their hydrophobicity and makes them susceptible to background staining. The ovary has abundant connective tissue and so if these polyclonal antibodies were to be used for further investigations they would require further characterisation, incorporating full investigation of AtR and fixation strategies.

There is also much discussion regarding the proper storage conditions for antibodies. Middleton *et al.* (1988) found no variation in quality of antibody serum stored at -20°C or 4°C over a period of three years. However more recent on-line information provided by the companies such as Dako suggest the storage of working concentrations at -20°C and long term storage at -70°C (Boenisch 2007). The serum antibodies used in the present studies had been stored at 4°C in excess of six years and so protein degradation resulting in low titre cannot be completely ruled out. The prevalence of non-specific components could be masking 'real' antibody labelling as well as giving false positive signals.

2.5.5 Conclusions

The objectives of the studies described in this chapter were to characterise and evaluate the panel of AQP antibodies, and to analyse AQPs in follicles at different stages. Without an extensive battery of techniques (such as biochemical/hormonal analysis, reliable IHC, electron microscopy) to provide supporting evidence of the stage of follicle development, or the use of ultrasound-monitored animals, interpretation of results remains subjective. Follicles are likely to have undetected differences in atresia, extracellular matrix integrity, cellular ultra structure, and steroidogenic activity. This investigation relied solely on morphological assessment of ovarian and positive control tissue from H&E sections and IHC. It was also limited by the quality and specificity of the available antibodies. Nevertheless, this investigation has revealed for the first time that AQP1 is localised to the endothelium of bovine ovarian vasculature and peripheral nerve and could potentially play a significant role in the fluid dynamics of ovarian

follicular development and regression. Aquaporin 2 is not present in bovine ovarian tissue. The results obtained using antibodies against AQP3, -4 and -5 at this stage remain unreliable, and no conclusions can be drawn about the presence or potential role of these AQPs in the bovine ovary. There have been no previous investigations of AQPs in bovine ovarian tissue therefore no comparative analysis can be conducted.

Chapter 3

Aquaporin 1, -2, -3, -4, -5, -7, and -9 transcription levels in granulosa and theca cells of the developing follicle.

3.1 Introduction

As follicle development progresses the transcriptome alters (Ben-Shlomo *et al.* 2002); identifying the point at which gene expression changes can provide a link with important time-dependent events. For example, mRNA for LHr, CYP11A1 and CYP17A1 is detected in theca interna cells of type-4 follicles and increases in abundance in parallel to follicle growth; the mRNA expression of CYP11A1 and CYP19A1 is detected in the granulosa cells at the time of recruitment and steroidogenic capacity (Bao *et al.* 1997). These results support findings via non-genomic techniques and help to further clarify the coordinated interactions of these two cell types.

As development progresses and preovulatory status is achieved the preovulatory LH surge promotes the switch from E_2 to P_4 production. Nimz *et al.* (2010) used real-time reverse-transcription polymerase chain reaction (RT-qPCR) to quantify transcript levels of CYP19A1, CYP17A1 and HSD3B1 in granulosa and theca cell populations, from dominant follicles tracked by ultrasonography before and after an induced LH surge. Following the LH surge the follicle at this stage of development displays a unique gene expression profile in which transcripts of all three steroidogenic enzymes are significantly down regulated, confirming previous findings (Voss and Fortune 1993; Conely *et al.* 1995; Nimz *et al.* 2009). To investigate the relationship between epigenetic mechanisms and the involvement in gene regulation Nimz *et al.* (2010) measured the extent of chromatin condensation by DNase 1 protection assay. The results strongly indicate that chromatin condensation is cell-type, and gene-type dependent and differs markedly before and after the LH surge. They conclude that chromatin condensation may be involved in the preovulatory down regulation of gene expression (Nimz *et al.* 2010).

Skinner *et al.* (2008) investigated granulosa and theca cell transcriptomes during antral follicle development using micro array analysis of 24000 bovine genes. They found that gene sets for both theca and granulosa cells were follicle size-dependent (small = <5 mm; medium = 5-10 mm and large = >10 mm). Transcripts that changed significantly

(regulated genes) throughout antral follicle development involved 446 and 248 genes for granulosa and theca cells respectively, with only 28 genes common to both cell types. These regulated genes were categorised into functionally related gene families. For granulosa cells these included immune regulation, metabolism, signalling, extracellular and cytoskeletal genes. Predominant gene categories specific to theca cells included metabolism, signalling and transcription. Candidate regulatory growth factors expressed by both cell types have been identified, for example cytokines (*Ccl2*, *Ccl3l1*, *Ccl5*, *Ccl8* and *Cxcl16*) which increase with follicle development. The receptors for most of these cytokines were also expressed by granulosa cells and demonstrate the potential role of autocrine actions of these cytokines in follicle development (Skinner *et al.* 2008). Genome microarray analysis can produce vast amount of information; however, in doing so it does provides a platform for the hypothesis-driven investigations required to ascertain functional relevance.

The ability to quantify the transcription levels of particular genes of interest via RT-qPCR provides researchers with a powerful means of assessing gene function (Zamorano *et al.* 1996). Investigating transcript levels of granulosa and theca cells through follicular development requires the isolation of pure cell populations. Efficient cell isolation using the method of granulosa cell aspiration (Skinner and Osteen 1988) and removal of theca sheets (Roberts and Skinner 1990) is limited by follicle size. Current literature therefore tends to focus on the investigation of antral follicle development with particular reference to recruitment, selection and dominance. However the progression of follicles from preantral type-4 to early antral type-5 follicles is a crucially important stage of follicle development. Successful preantral follicle growth and antrum formation are prerequisites for gonadotropin dependence, steroidogenic capacity, potential dominance and ovulation.

Mechanical (Abir *et al.* 1997) and enzymatic (Eppig and Schroede 1998) isolation of preantral follicles have been used to segregate primary through to preantral follicles of many species. However both techniques have limitations and are predominantly used to isolate follicles for culture studies (Demeestere 2002). Laser capture microdissection is a relatively new technique which allows the isolation of specific cell populations from a heterogeneous sample of frozen or paraffin embedded tissue. The technique is sensitive enough to allow the isolation of single cells or whole tissue regions and allows for the extraction of protein, RNA and DNA from the dissected sample (Espina *et al.* 2007). Adopting this technique could allow investigation of transcriptome variation within

clearly identified and isolated cell compartments of follicles at all stages from primordial through to antral formation and the development of steroidogenic capacity. This will extend the knowledge discussed above pertaining to antral follicle development.

3.1.1 Aim and strategy.

The aim of this investigation was to determine the transcript expression of AQP1, -2, -3, -4, -5, -7 and -9 in both cell layers (granulosa and theca) across all stages of follicle development including type-4 (preantral), type-5 (early antral); small (S, 2-5 mm), medium (M, 6-9 mm), large (L_1, 10-15 mm) and pre-ovulatory (L_2, 18-22 mm) antral follicles. This will identify the prevalence and type of AQP expression at specific stages of follicle development, with particular interest in AQP expression at the preantral/early antral juncture.

To achieve this, follicular phase ovaries were collected, prepared and embedded in optimum cutting temperature (OCT) medium for cyosectioning. Granulosa and theca cells from type-4 and type-5 follicles were isolated by laser capture microdissection. Granulosa and theca material was collected from antral follicles (S, M, L_1 and L_2) dissected from whole ovaries. Samples underwent RNA extraction followed by RT-qPCR analysis. Positive control tissue known to express all AQPs under investigation were used to allow preliminary testing of primer efficiency.

3.2 Materials and Methods

3.2.1 Positive control tissue and ovary collection

Positive control tissue; kidney cortex and medulla, liver, salivary gland and whole ovary were collected and prepared on site at a local abattoir. The tissues were cut into 0.5cm^3 pieces placed into a labelled 2 ml Corning® cryogenic vial (Sigma-Aldrich, Poole, UK) and snap frozen in liquid nitrogen for RNA extraction. Approximately 40 unpaired ovaries from animals of unknown reproductive status were collected and transported to the laboratory within 2h of slaughter. Ovaries were transported in a vacuum flask containing PBS at 37°C for antral follicle granulosa and theca cell isolation, RNA extraction and PCR.

3.2.2. Granulosa and theca cell isolation

The ovaries were washed in sterile PBS and sprayed with 70% ethanol, washed again in sterile PBS, and kept in a hot box maintained at 37°C until required. Ovaries were not collected in animal-related pairs and therefore it was difficult to accurately assess cycle stage except by ovary morphology. Proestrus phase ovaries were identified based on gross external morphological features as described by Ireland *et al.* (1980). Ovaries with a regressing, non-vascularised light yellow to white CL with an apex measuring <10mm, an internal orange to yellow appearance and antral follicles >10 mm were chosen (see Fig. 1.2). Initial observations targeted amber coloured follicles, however quality could not be accurately determined until the follicles had been fully dissected and the FF examined. A deepening of FF colour suggested the presence of erythrocytes and therefore basement membrane degradation and atresia. Furthermore, follicles with very pale FF, or which was turbid or not of the expected consistency were also rejected.

Follicles from approximately 20 ovaries were collected to provide ~50 mg of granulosa and theca cells from each developmental stage (Table 3.1); five separate experimental repeats were conducted. Follicles were carefully dissected (Fig. 3.1) removing the stromal tissue without rupturing the follicle to permit accurate measurement of follicle diameter. Follicles were then assigned one of the four groups (Table 3.1) as determined by size.

Table 3.1 Follicle category, size range and total number of follicles collected per experimental repeat.

Group	Diameter (mm)	Number of follicles collected
Small (S)	2 – 5	16
Medium (M)	6 – 9	10
Large$_1$ (L_1)	≥10	6
Large$_2$ (L_2)	18 – 22	3

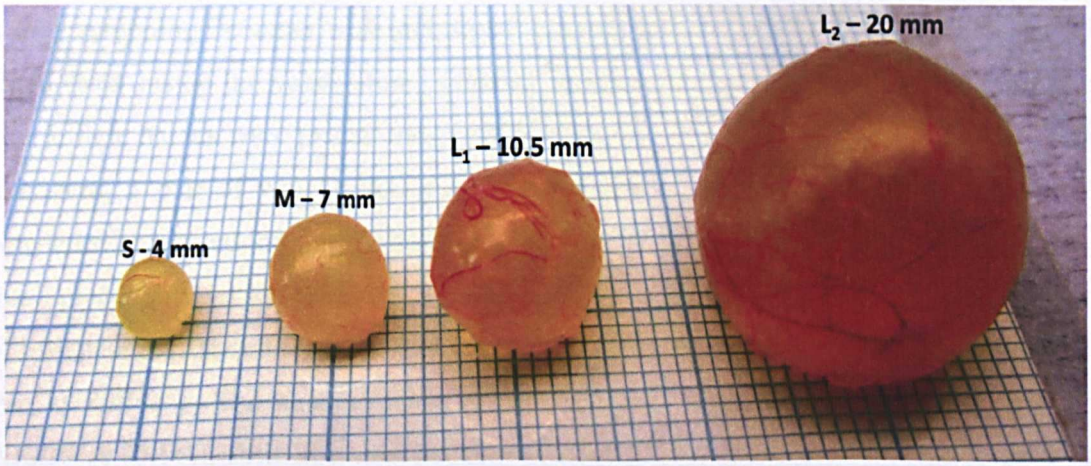

Figure 3.1 Dissected follicles representative of each size category: **(1)** Small **(S)**, **(2)** Medium **(M)**, **(3)** Large$_1$ **(L_1)**, and **(4)** Large$_2$ **(L_2)**, measuring: 4mm, 7mm, 10.5mm and 20mm respectively. Image capture by author.

3.2.2.1 L_1 and L_2 granulosa cell collection

Follicular fluid was extracted using an 18 gauge hypodermic needle and 5ml syringe barrel, assessed for colour and turbidity and then discarded. The flaccid follicle was placed in a petri dish containing sterile filtered PBS/PVA (0.1%; w/v) and a small incision made at the puncture site to allow the entry of a Pasteur pipette. Sterile PBS/PVA (0.1%) was used to flush out the granulosa cells; this was carried out three times. To ensure the collection of attached/mural granulosa cells one edge of the incision

was griped with forceps, the follicle again filled with PBS/PVA (0.1%) and using a disposable sterile loop the inner walls were gently but systematically scraped; this was also carried out three times. The process was repeated for each follicle required for the group and the pooled cell suspension was transferred from the petri dish into a 15 ml falcon tube (BD Biosciences, Oxford, UK) and centrifuged at 800 x *g* for 5 min. The supernatant was discarded and the pellet re-suspended in 1 ml PBS/PVA (0.1%) before being divided into two 1.5 ml labelled Eppendorf tubes (Eppendorf Ltd, Cambridge, UK) and spun at 12000 x *g* for 2 min. The supernatant was removed leaving the pellet in a minimal volume of <2 µl and snap frozen in liquid nitrogen prior to -80°C storage.

3.2.2.2 L_1 and L_2 theca cell collection.

The follicle, now devoid of granulosa cells, was cut in half with a fresh scalpel and placed in a new petri dish containing fresh PBS/PVA (0.1%), and the halves were then gently scrapped again and washed a further time with the aim of removing residual granulosa cells. At this point it was possible to observe the vasculature of the theca layer and by scrapping the inner wall effectively it was possible to expel a large proportion of blood from inside the vasculature, reducing erythrocyte contamination where possible. The follicle halves were placed into a final fresh petri dish containing PBS/PVA (0.1%) and using a pair of watchmaker's forceps to secure the tissue, the theca layer was pinched with curved forceps, peeled away from the outer shell of the follicle and cut into small pieces using a scalpel blade. Theca sheets were removed from the required number of follicles, transferred from the petri dish into a 15ml falcon tube and centrifuged for 5 min at 800 x *g*. The supernatant was removed and the pellet re-suspended in 1 ml PBS/PVA (0.1%), split into two 1.5 ml Eppendorf tubes and spun at 12000 x *g* for 2 min. The supernatant was removed leaving the pellet in a minimal volume of <2 µl which was snap frozen in liquid nitrogen prior to -80°C storage.

3.2.2.3 Small and medium follicle granulosa and theca cell collection.

Follicles were placed into a petri dish with PBS/PVA (0.1%), cut in half with a fresh scalpel and the inner follicle walls gently scraped with a disposable loop dislodging the granulosa cells. Once all the follicles in the group were processed, the cell suspension was collected via Pasture pipette, transferred into a 15 ml falcon tube and treated as described above.

The remaining follicle halves were then transferred into a new petri dish containing fresh PBS/PVA (0.1%), the theca layers were carefully peeled away from the follicle and prepared for storage as described above.

3.2.3 RNA extraction.

RNA was extracted from positive control tissue (kidney medulla, kidney cortex, liver, salivary gland and whole ovary), granulosa and theca cells (approx. 50 mg) and erythrocyte fraction ($5x10^5$ cells) of whole blood using TRI Reagent solution (Applied Biosystems/Ambion, Warrington, UK) as per manufacturer's instructions. The RNA precipitation and wash stage however were conducted using chilled alcohols (-20°C) instead of room temperature and centrifuged at 0-4°C instead of room temperature.

Approximately 50mg of positive control tissue was crushed into a powder using liquid nitrogen and a pestle and mortar, the powder was transferred into a 2ml eppendorf containing 500µl of Tri-reagent. Granulosa, theca and blood samples were homogenised in 2ml centrifuge tubes containing 500µl of Tri-reagent. Samples were crushed using a tube pestle, vortexed and passed through a 21 gauge hypodermic needle; this was repeated until satisfactory homogenisation was achieved.

Tri-reagent volume was made up to 1 ml for each sample, vortexed for 10s and incubated at room temperature for 5 min allowing for the dissociation of nucleotide complexes. Samples were centrifuged at 12000 x *g* for 10 min at 4°C. The pellet composed of un-homogenised tissue, extracellular matrix and high molecular weight DNA was discarded following the transfer of the RNA-containing supernatant to a fresh tube. 100 µl of 1-bromo-3-chloropropane (BCP, Sigma-Aldrich, Dorset, UK) was added per sample, the tubes capped and vigorously shaken, incubated at room temperature for 5 min then centrifuged at 12000 x *g* at 4°C for 15 min. The RNA-containing aqueous layer was carefully removed ensuring no contamination from the underlying DNA interphase and organic phase. 500µl of ice cold isopropanol (-20°C, Sigma-Aldrich, Dorset, UK) was added, vortexed for 10s, incubated at room temperature for 10 min then centrifuged at 12000 x *g* at 0-4°C for 8 min. The supernatant was discarded and 1 ml of ice cold 70% ethanol (stored at -20°C) was added and then centrifuged for 5 min at 7500 x *g* at 0-4°C. The appearance/size of pellets were noted and the ethanol was removed without loss of the pellet which was left to air dry, then re-suspended in 50-200 µl of nuclease free water (Fisher Scientific, Loughborough, UK) as determined by the size of the pellet (100 µl of water per ml of pellet).

3.2.4 RNA quality determination.

The quality of RNA was measured using a NanoDrop Spectrophotometer (ND1000, NanoDrop, Wilmington, USA). 1.5 µl of sample was pipetted onto an optical pedestal; the upper pedestal arm was lowered creating a column of sample and the ultraviolet (UV) absorbance at 260 and 280nm was measured. The ratio of absorbance at these values is indicative of RNA quality and a value of 2.0 is considered as 'pure', however the phenol component of TRI reagent absorbs UV at ~230 and ~270 so any remaining in the sample could result in a lower 260/280 ratio (Thermo scientific technical bulletin). The ratio of all the samples used in this study was in the range of 1.8 - 2. The NanoDrop also measures the amount of nucleotide in the sample as µl/ml (see Fig. 3.2).

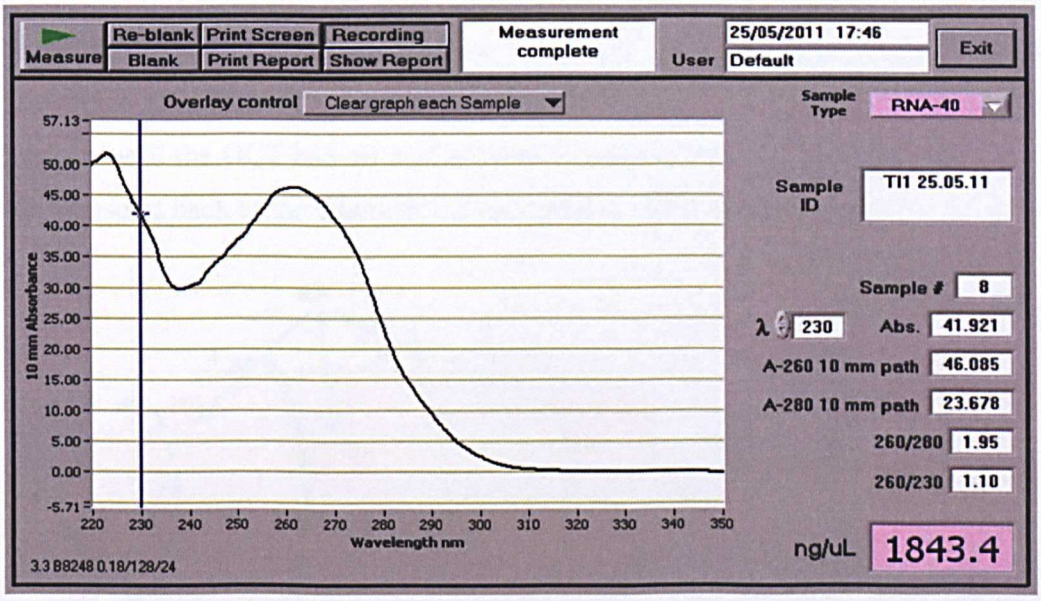

Figure 3.2 Screen shot of the NanoDrop spectrophotometer absorbance graph for RNA extracted from L_1 theca cells indicating a purity of 1.9 via the 260/280 ratio and a nucleotide quantity of 1843 ng/µl

3.2.5. DNase digestion.

During the RNA extraction procedure there is a distinct possibility of genomic DNA contamination and therefore a DNase digestion was carried out to prevent the amplification of genes from genomic DNA during PCR whilst maintaining RNA integrity. 1 µl of RQ1 RNase free DNase (Promega, Southampton, UK) was used per µg of RNA. The quantity of RNA per µl was determined by Nanodrop spectrophotometer. The appropriate volume of RNA sample (to give 2 µg) was added to 2 µl of RQ1 RNase

free DNase, and 2 µl of RNase free DNase 10X reaction buffer. Nuclease free H_2O was added to give a final volume of 20 µl and incubated at 37°C for 30 min. The reaction was stopped with 2 µl of RQ1 DNase stop solution and incubated at 65 °C for 10 min using a Techne TC-512 thermo cycler (Scientific Laboratory Supplies Ltd, Nottingham, UK).

3.2.6 Tissue collection and preparation for Laser Microdissection and Pressure Catapulting (LMPC).

For laser capture micro-dissection (LCM) three animal related pairs of follicular phase ovaries were collected washed in PBS and prepped on site at the local abattoir. The connective tissue of the ovary which attaches to the broad ligament (BL) including the hilus was cut away and the ovary cut into 8 – 10mm sections (Fig. 3.3 A). The three or four mid sections were laid flat into a plastic mould containing a small amount of OCT (Tissue-Tek Sakura). The mould was then filled with OCT ensuring complete coverage of the tissue (Fig. 3.3 B). Moulds were carefully floated on liquid nitrogen-cooled isopentane until the OCT had set and hardened. Samples were temporarily stored in dry ice for transport back to the laboratory, then stored at -80°C until needed.

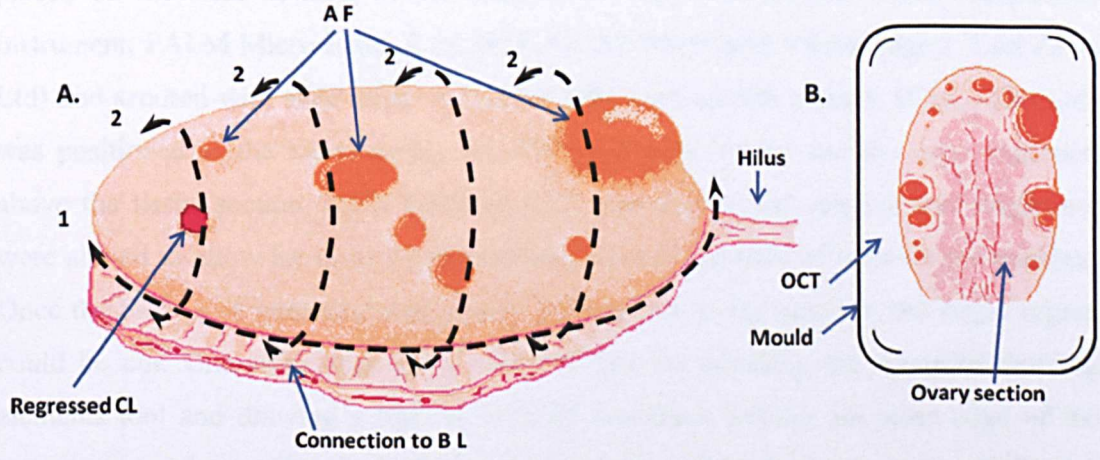

Figure 3.3 A. Ovary dissection guide for LCM. The first incision (**1**) removed the connection to the broad ligament (BL) and the hilus from the remainder of the tissue. Cut **2** sectioned the ovary into 8 – 10 mm thick sections which were laid flat in a mould **B.** then covered with ample OCT embedding medium prior to freezing. Illustration by author.

PAGE
MISSING
IN
ORIGINAL

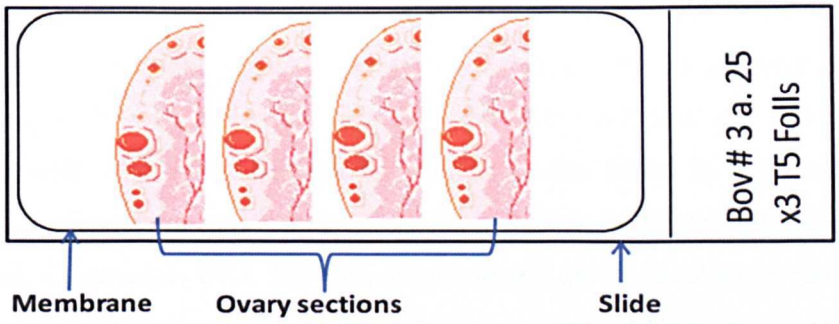

Figure 3.4. Tissue section orientation on a P.A.L.M membrane slide. Illustration by author.

3.2.8 P.A.L.M Microbeam – Laser Microdissection and Pressure Catapulting (LMPC)

Prior to laser capture, slides were stained with 0.025% RNase free aqueous Toluidine blue (TB; Camlab Ltd, Cambridge, UK) for orientation purposes. Slides were immersed for 10s in nuclease free water, the excess removed and 200 µl of TB added to the sections, carefully spread to ensure complete coverage of tissue sections and left for 1 min, dipped twice in nuclease free water then dehydrated in 50%, 75%, 90% and 100% nuclease free ethanol, removing excess fluid between solutions. Each slide was prepared individually and left to air dry for ~5 min. For microdissection, slides were individually placed on the slide housing of the stage of a PALM non-contact Laser catapulsion instrument, PALM Micro Beam 3 LCM (P.A.L.M. Microlaser Technologies, Carl Zeiss Ltd) and secured with slide clips. A PALM AdhesiveCap 500 opaque, (Carl Zeiss Ltd) was positioned in the metal spring assembly and tube holder and the cap positioned above the tissue section. Robo Software v2.2 was started and contrast and brightness were altered to allow for clear visual representation of the field of view on the monitor. Once the follicle of interested was clearly represented on the monitor, the target region could be cut. Granulosa cells were removed first by selecting the freehand drawing elements tool and drawing a line, or element boundary, tracing the outer edge of the basement membrane. The laser followed the element boundary and upon satisfactory dissection a pulse of laser energy catapulted the dissectate into the adhesive cap (Fig. 3.5). All type-4 granulosa cells were collected in one adhesive cap followed by the theca layers in a fresh collection cap and tube. This was then repeated for all type-5 follicles. For follicles which did not have a distinct thecal compartment, six to 10 layers of cells surrounding the granulosa were dissected and captured. The Robo software calculates the on-going area μm^2 of tissue capture, which provides an initial estimation of downstream RNA yield. A minimum of 1000000 μm^2 was collected for both granulosa and thecal cells. Type-5 follicles had varying sized antrums and the theca layers were

dissected as circular bands and so the dissectates were not complete areas. As a result 1-2000000 μm^2 was a rough guideline for type-4 theca and type-5 granulosa and theca. When all targets for one cell type were captured in the adhesive cap 300 µl of RLT buffer (RNeasy® Micro kit, Qiagen, Sussex, UK) was added to the tube. The cap containing the dissectates was carefully closed and secured to the tube with parafilm (Camlab Ltd, Cambridge, UK). The tube was inverted for ~1 hr at room temperature to ensure full lysis of the dissectates in the adhesive cap then stored on ice. On return to the laboratory RLT buffer volume was made up 350 µl, the samples were vortexed for 30s and stored at -80° until RNA extraction.

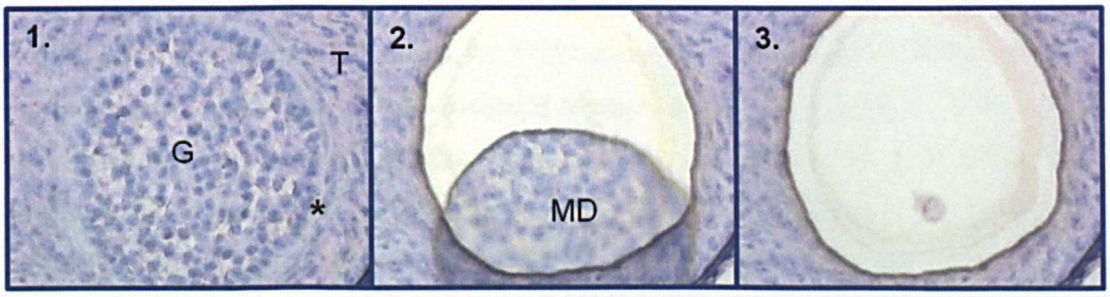

Figure 3.5 Example of a type-4 follicle before (**1**) during (**2**) and after (**3**) micro-dissection. **1. G** - granulosa cells, * denotes the basement membrane segregating the granulosa from the thecal compartment - **T**. The free hand element boundary followed the outside edge of the basement membrane capturing all granulosa cells. **2**. Shows the micro-dissectate before it was catapulted into the adhesive cap - **3**.

3.2.9 Laser capture microdissectate RNA extraction and DNase digestion.

As the nucleic acids had to be purified from very small amounts of starting material, RNeasy® Micro kit (Qiagen, Sussex, UK) was used as per manufacturer's instructions. In brief the P.A.L.M caps containing the dissectates and 350 µl RLT buffer were completely thawed on ice and vortexed for 30s; 350 µl 70% ethanol was added, mixed by gentle aspiration and transferred to an RNeasy MinElute spin column in a 2 ml collection tube. With the lids closed columns were spun for 15s at $\geq$ 8000 x *g* and the flow through discarded, retaining the collection tube for re-use. 350 µl of RW1 buffer was then added to the spin columns and with the lids closed spun at $\geq$ 8000 x *g* for 15s to wash the spin column membrane; the flow through was discarded, again retaining the collection tube for re-use. 10 µl of DNase I stock was added to 70 µl of Buffer RDD per sample and mixed by inversion as DNase is highly sensitive to physical denaturation. The 80 µl of DNase incubation mix was carefully added directly to the spin column

membranes and incubated at room temperature for 15 min. To wash the spin column membranes, 350 µl of RW1 buffer was added, the lids were closed and spun for 15s at ≥ 8000 x *g*; the flow through was discarded along with the collection tube. The spin columns were placed into new collection tubes and 500 µl of RPE buffer was added to wash the column membrane, spun at ≥ 8000 x *g* discarding the flow through. Using the same collection tubes 500 µl of 80% ethanol was added, the lid was closed and centrifuged at ≥ 8000 x *g* for 2 min, the columns were carefully removed from the collection tubes avoiding contact with the flow through to prevent ethanol carryover, the flow through and collection tubes were then discarded. Spin columns were placed into new collection tubes, with the lids open and orientated in the opposite direction of centrifuge rotation, spun at full speed for 5 min removing residual ethanol and to dry the membranes, collection tubes were discarded along with the flow through. New 1.5 ml collection tubes were used for the final RNA elution step whereby 12 µl of RNase-free water was added directly to the centre of the spin column membranes and with the lids closed spun for 1 min at full speed. The dead volume of the spin column is 2 µl; samples were eluted with 12 µl therefore resulting in a 10 µl eluate.

As this procedure results in such a small volume of eluate, it was decided to use all the RNA extracted in the cDNA synthesis step and not to use any in checking quality and quantity with a Nanodrop.

3.2.10 Copy DNA synthesis.

The RNA to cDNA reverse transcription reaction was carried out using the GoScript™ Reverse Transcription System (Promega UK, Southampton, UK) following manufacturer's instructions and using a Techne TC-512 thermo cycler. The reagent component volumes were doubled in the synthesis of cDNA from antral follicle RNA (Fig 3.6) and done in duplicate resulting in 80 µl of cDNA; this remained undiluted to ensure maximal starting copy number. The reagent component volumes for cDNA synthesis of LCM samples were not doubled due to a limited volume of extracted RNA and resulted in 22 µl of cDNA (Fig 3.6). This was diluted 1:2 with nuclease free H_2O to ensure enough template for RT-qPCR. For each cDNA synthesis reaction, samples were stored at 4°C short term if PCR was imminent or long term at -20°C. For each cDNA synthesis reaction a reverse transcriptase negative was run in parallel using the four remaining µl from the DNA digest substituting the enzyme for H_2O. This was however not possible for the LCM cDNA synthesis as the entire sample was used for the conversion.

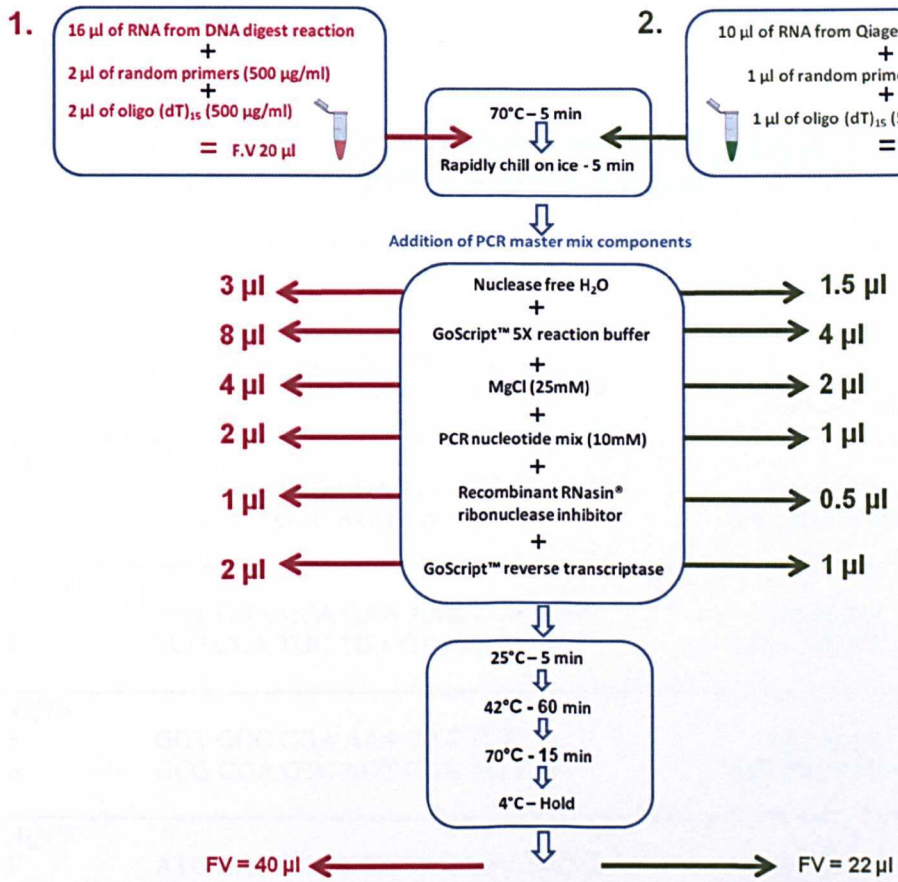

Figure 3.6. cDNA synthesis protocol summary, indicating the component reagent volumes for both antral follicle (1) and LCM (2) RNA and the final volume (F.V) of cDNA for downstream PCR and/or RT-qPCR investigation. Antral follicle cDNA synthesis was done in duplicate and remained undiluted (1:1) whereas LCM cDNA synthesis was not done in duplicate and was diluted 1:2. Diagram by author.

3.2.11 Primer design

Primers were designed using Primer Express 3.0 software (Applied Biosystems, Foster City, CA). Where possible, exon spanning primers were designed to prevent genomic DNA amplification and to have an annealing temperature (Tm) of 60°C. Primers were designed against *Bos Taurus* genomic sequence for *AQP1*,-*2*,-*3*,-*4*,-*5*,-*7*,-*9*, *CYP17A1*, *CYP19A1*, *ACTB*, *GAPDH* (glyceraldehyde 3-phosphate dehydrogenase) and *PPIL1* (Cyclophilin). The primer nucleotide sequences were checked using Basic Local Alignment Tool (BLAST) (http://www.ncbi.nlm.nih.gov/BLAST/) to ensure that they were specific to the correct gene.

Table 3.2 List of primer sequences used for PCR and RT-qPCR analysis, NCBI accession number and primer efficiencies, F = forward primer, R = reverse primer.

Name	Sequence 5' – 3'	NCBI Accession	Primer Efficiency
AQP1			
F	TCC TTC ACT GAG TTG TAG TTG ATC TTT T	*Bos Taurus* NM_174702.3	1.80
R	GGC AAG AGA AAC TGA AGA ACC AA		
AQP2			
F	CGT CAC CGG CAA GTT TGA C	*Bos Taurus* NM_001101199.1	1.89
R	CGG GAA CAG CAC GTA GTT GTA G		
AQP3			
F	TGA CCC TAG GCA TCC TTA TTG CT	*Bos Taurus* NM_001079794.1	1.99
R	TCG CGC GCC AGG AA		
AQP4			
F	GGT GGA GCA GAA AAG CCA CTA	*Bos Taurus* NM_181003.2	1.97
R	TCG CGA TGC TGA GTC CAA		
AQP5			
F	GGT GGC GGA AAT GAT TCT	*Bos Taurus* NM_001191160.1	1.96
R	GCG GGA GTC AGT GGA AGA GA		
AQP7			
F	ATG AAC TCA GGA TAT GCC ATC AAC	*Bos Taurus* NM_001076378.1	1.89
R	GCC AGC GAG GAA GGT GAA G		
AQP9			
F	TGT AGT GGG ACC TTT GGT TGG T	*Bos Taurus* NM_001205833.1	1.99
R	CGG ATC TGG GTG GTG GAT T		
CYP17A1			1.90
F	TGG GTT GCC ATT GCC TTC	*Bos Taurus* NM_174304.1	
R	CGG GCT AGC ATC TCA CCT ACA		
CYP19A1			
F	TCA TCT CGC CAT CGT TAA GCT	*Bos Taurus* NM_174305.1	1.92
R	GGA CAG TAA GGA GCT GGA GTG AG		
ACTB			
F	TGT GCG TGA CAT CAA GGA GAA	*Bos Taurus* AB098974.1	1.99
R	CGC AGT GGC CAT CTC CTG		
GAPDH			
F	TCCGTTGTGGATCTGACCTGT	*Bos Taurus* NM_001034034.1	1.95
R	TGGTTCACCACCTTCTTGATCTC		
PPIL1			
F	CATACAGGTCCTGGCATCTTGTC	*Bos Taurus* NM_001109807.1	1.87
R	TGCCATCCAACCACTCAGTCT		

3.2.12 PCR

To maintain consistency with later RT-qPCR experiments, GoTaq® qPCR mastermix (Promega UK, Southampton, UK) was used for all PCR amplification. Complementary DNA of control tissue and whole ovary was PCR amplified with gene specific primers (Table 3.2) of *AQP1,-2,-3,-4,-5,-7,-9* and *ACTB* to check quality of cDNA synthesis, presence/absence of transcript and therefore specificity, product size and the protocol parameters. 1 µl of cDNA was added to 10 µl of PCR mastermix, 8.2 µl of nuclease free water and 0.4 µl of both forward and reverse primers to equal a 20 µl final volume. Samples were vortexed and centrifuged then incubated at 95°C for 2 min to activate the polymerase enzyme, 45 cycles of 95°C for 15s and 60°C for 1 min followed by 75°C for 5 min. Following this, cDNA of granulosa and theca from S, M, L_1 and L_2 follicles was amplified with the same primer set but to increase intensity of product, 2 µl of cDNA, 10 µl of PCR mastermix, 0.8 µl of both forward and reverse primers was used and made up 20 µl final volume with 6.4 µl of water, cycle number was also increased to 50. PCR products were run on a 3% agarose gel with a low molecular weight ladder (New England BioLabs Ltd, Hertfordshire, UK) and imaged using a ImageQuant™300 (GE Healthcare, Bucks, UK) and ImageQuant™300 V 1.0.3 software.

3.2.13 Quantitative Real Time PCR.

Complementary DNA was quantitatively PCR amplified with gene specific primers as in Table 3.2 using the Roche Lightcycler® 480 amplification system and the Roche Applied Science's E-Method of relative quantification analysis (Roche Diagnostics Ltd., West Sussex, UK). In order to assess primer efficiencies of all AQPs, *ACTB*, *GAPDH* and *PPIL1* primers, a standard curve was created from a 1:5 serial dilution of combined liver, kidney medulla and cortex and salivary gland cDNA. Primer efficiency for *CYP17A1* and *CYP19A1* was assessed using a 1:5 serial dilution of granulosa and theca cDNA see Table 3.2 for primer efficiencies and Fig. 3.7 for an example of a standard curve amplification plot. PCR reaction mix was used as described in section 3.2.12, using GoTaq® qPCR mastermix (Promega, Southampton, UK) for antral follicle cDNA amplification. For LCM cDNA real-time amplification only 1 µl of cDNA was used with 10 µl of PCR mastermix, 0.8 µl of primers and 7.4 µl of nuclease free water, for each primer set cDNA was substituted for H_2O as a negative control. All samples were run in duplicate on a 96 well PCR plate (Lightcycler® 480 multiwell plate, Roche) sealed using sealing foil (Lightcycler® 480 sealing foil, Roche), centrifuged for 2 min at 1500 x g and loaded into a Roche Lightcycler® 480. The cycling conditions and parameters were as in

Table 3.3, Tm calling (melt curve analysis) was carried out for each gene to determine the primer specificity and to check for the presence of primer dimmers (Fig. 3.8). Relative expression of each gene was normalised against the endogenous control gene *ACTB*, which was itself checked for consistent expression relative to two other housekeeping genes, *GAPDH* and *PPIL1*.

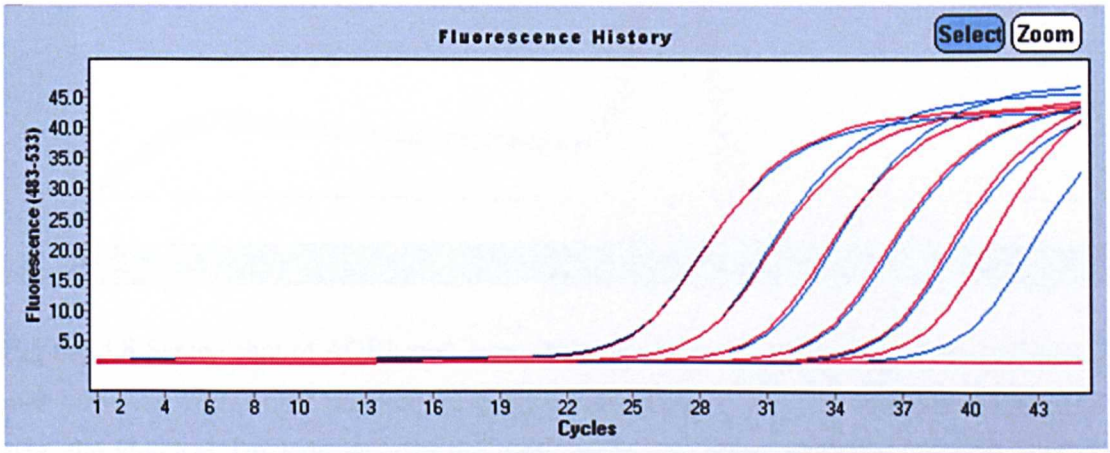

Figure 3.7 Screen shot of *AQP1* 1:5 serial dilution standard curve. Each overlapping red and blue lines represent the amplification plot of one dilution of AQP1 primed positive control sample (duplicated). As the samples become more dilute, more cycles are needed before amplification is detected. This is needed to calculate a primer efficiency (AQP1=1.8).

Table 3.3 Programme and cycling parameters for RT-qPCR analysis.

Programme stage	Cycle number	Target (°C)	Hold (hh:mm:ss)	Ramp rate (°C/s)	Acquisition mode	Acquisitions (/°C)
Denature	1	95	00:02:00	4.4	None	-
Cycling	45	95	00:00:20	4.4	None	-
		60	00:00:15	2.2	None	-
		60	00:01:00	4.4	Single	-
Melt curve	1	90	00:00:20	4.4	None	-
		60	00:01:00	2.2	None	-
		95	-	0.11	Continuous	5
Cooling	1	40	00:00:30	2.2	None	-

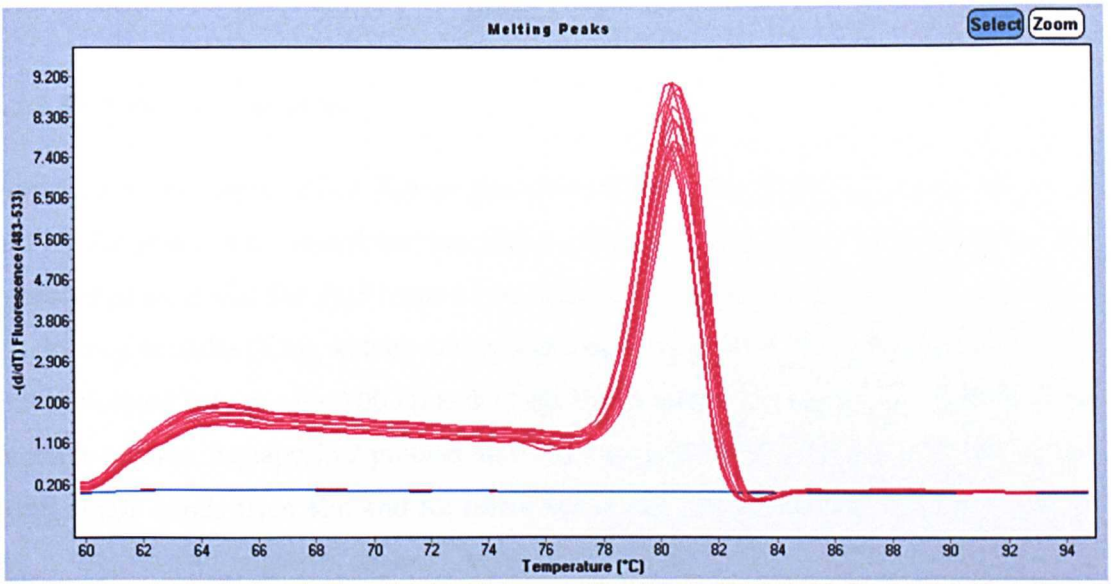

Figure 3.8 Screen shot of AQP1 melt curve analysis. The over-lapping red lines represent a melt curve for each AQP1 product. As melting temperature (Tm) depends predominantly on size, the identical Tm indicates that the same product is being amplified from the various samples, indicating good primer specificity.

3.2.14 Statistical analysis

Transcript abundance of *AQP1,-2,-3,-4,-5,-7, -9, CYP17A1* and *CYP19A1* relative to *ACTB* multiplied by 1000, over five experimental repeats for each follicle type (type-4 and type-5 n=3; S, M, L_1 and L_2 n=5) were amalgamated. Outliers were identified as two times standard deviation away from the median. Outliers were removed from the data set and undetectable transcript was represented as zero. Data is represented as box and whisker plots to provide a summary of the distribution of each data set. The upper and lower horizontal limits of the box represent the 75th and 25th percentiles with the mid line representing the median. This encloses the central 50% of the observations or the interquartile range. The whiskers show the minimum and maximum data points. Non-parametric analysis of variance, inclusive of outliers, was conducted using Kruskal-Wallis one-way ANOVA. This was followed by post hoc Dunn's multiple comparison test, to determine any significant difference in expression of each gene, between all stages of follicle development.

3.3 Results

3.3.1 PCR Primer specificity

Primers designed against *Bos Taurus* genomic sequence for *AQP1, -2, -3, -4, -5, -7 - 9* and *ACTB* genes were tested for specificity using known positive control tissue. The expected product size for *AQP1* was 82 bp. Figure 3.9 (1) shows single bands from liver (L), kidney medulla (Km), kidney cortex (Kc), salivary gland (SG) and whole ovary (O) tissue, situated between the 100 bp and 75 bp ladder bands. No signal was present in the negative control. Aquaporin 2 product size was expected at 97 bp: Fig. 3.9 (1) shows two clear, single bands from Km and Kc tissue below the 100 bp marker, with no signal in the L, SG, O and negative control. Aquaporin 3 product size was 88 bp; Fig. 3.9 (2) demonstrates a single, strong band below the 100 bp marker in Km alone. Aquaporin 3 transcript was not present in L, Kc, SG, O or the negative control. Transcript for *AQP4* was expected at 70 bp; three single bands can be observed (Fig. 3.9 (2)) just below the 75 bp marker in Km, Kc and SG. No evidence of transcript was seen in L, O or the negative control. The only expression demonstrated by *AQP5* (Fig. 3.9 (3)) at the expected product size of 66 bp was in the SG. Liver, Km, Kc, O and the negative control were all absent of transcript. Two single bands demonstrate expression of *AQP7* at 69 bp in Km and Kc but not in L, SG, O or the negative control (Fig. 3.9 (3)). The expected product size for *AQP9* was 79bp; L alone produced a clear single band with no transcript evident for Km, Kc, Sg, O or the negative control (Fig. 3.9 (4). Beta-actin was run on the positive control sample as an indicator of cDNA quality and primer specificity: strong single bands are clearly evident in all positive control tissue types at the expected product size of 72 bp (Fig. 3.9 (4).

3.3.2 Class one and two aquaporin transcripts in small, medium, large $_1$ and large $_2$ follicles

Aquaporin 1 demonstrates clear signals in the granulosa and theca of all S, M, L_1 and L_2 follicle types (Fig. 3.10 (1)). Aquaporin 2 was absent from granulosa and theca of all follicle stages (Fig. 3.10 (2)). Aquaporins -4 and -5 demonstrated varying results over several repeats however there was evidence of *AQP4* and *-5* in both granulosa and theca cells from S, M, L_1 and L_2 follicles (Fig. 3.10 (3) and (4)). A band of *ACTB* was evident in sample one of three erythrocyte cDNA samples however no *AQP1* transcript was present (Fig. 3.10 (5)). Figure 3.11 (1), (2) and (3) respectively shows *AQP 3, -7* and *-9* signals in the granulosa and theca of S, M, L_1 and L_2 follicles. Positive and negative

controls were run for each repeat using appropriate control tissue (Kc - *AQP1*, Km - *AQP3* and -4, SG - *AQP5*, Kc - *AQP7* and L - *AQP9* Fig. 3.11(5)). No signals were present in the negative controls where cDNA was substituted with H_2O.

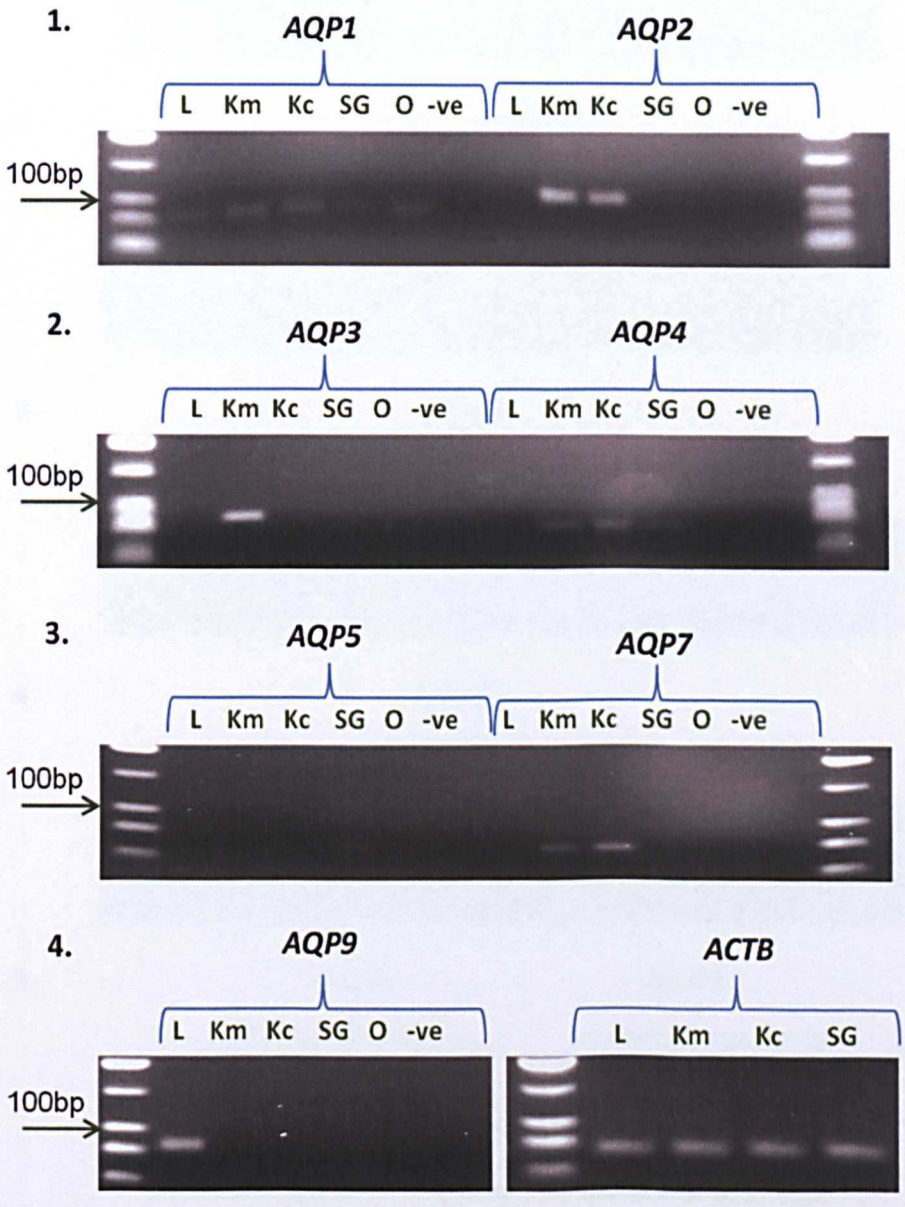

Figure 3.9 Agarose gel electrophoresis of primer check, using known positive control tissue for each AQP. **L** = Liver, **Km** = Kidney medulla, **Kc** = Kidney cortex and salivary gland = **SG**. Whole ovary (**O**) was used as an early indicator of AQP expression, (**-**) denotes the negative control by substitution of cDNA with H_2O. **1.** *AQP1* was found in all tissue types, *AQP2* was expressed in Km and Kc. **2.** *AQP3* was found in Km only, *AQP4* was found in Km, Kc and SG. **3.** *AQP5* was expressed in SG only, *AQP7* was evident in Km and Kc. **4.** *AQP9* was expressed in L only and *ACTB* was found in all four positive control tissue types.

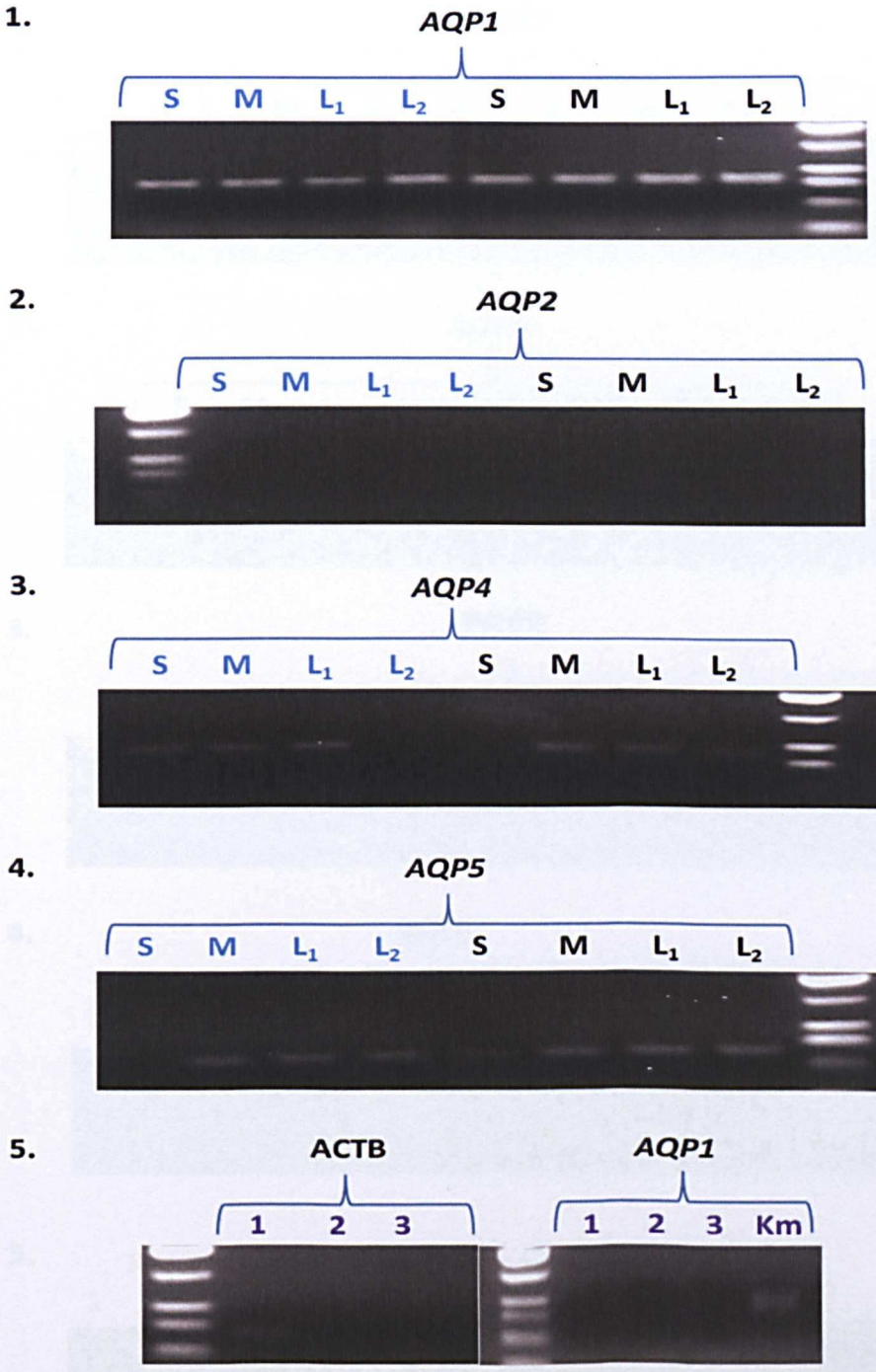

Figure 3.10 Agarose gel electrophoresis of class 1 aquaporin PCR products of isolated granulosa (**G** - blue) and theca cells (**T** - black) from small (**S**), medium (**M**), large$_1$ ($\mathbf{L_1}$), and large$_2$ ($\mathbf{L_2}$) antral follicles. **1.** *AQP1* transcript was evident in **G** and **T** of all follicles types. **2.** *AQP 2* was not expressed. **3.** and **4.** are examples of a *AQP4* and *AQP5* repeat whereby *AQP4* demonstrates expression in **S**, **M**, $\mathbf{L_1}$ **G** and **M**, $\mathbf{L_1}$ and $\mathbf{L_2}$ of **T**, *AQP5* is negative for **S** – **G** but positive for the remaining follicles types in **G** and **T**. **5.** shows *ACTB* expression in 1 of 3 erythrocyte fractions alongside *AQP1* expression in the same samples showing negative expression in erythrocytes compared with positive control Km.

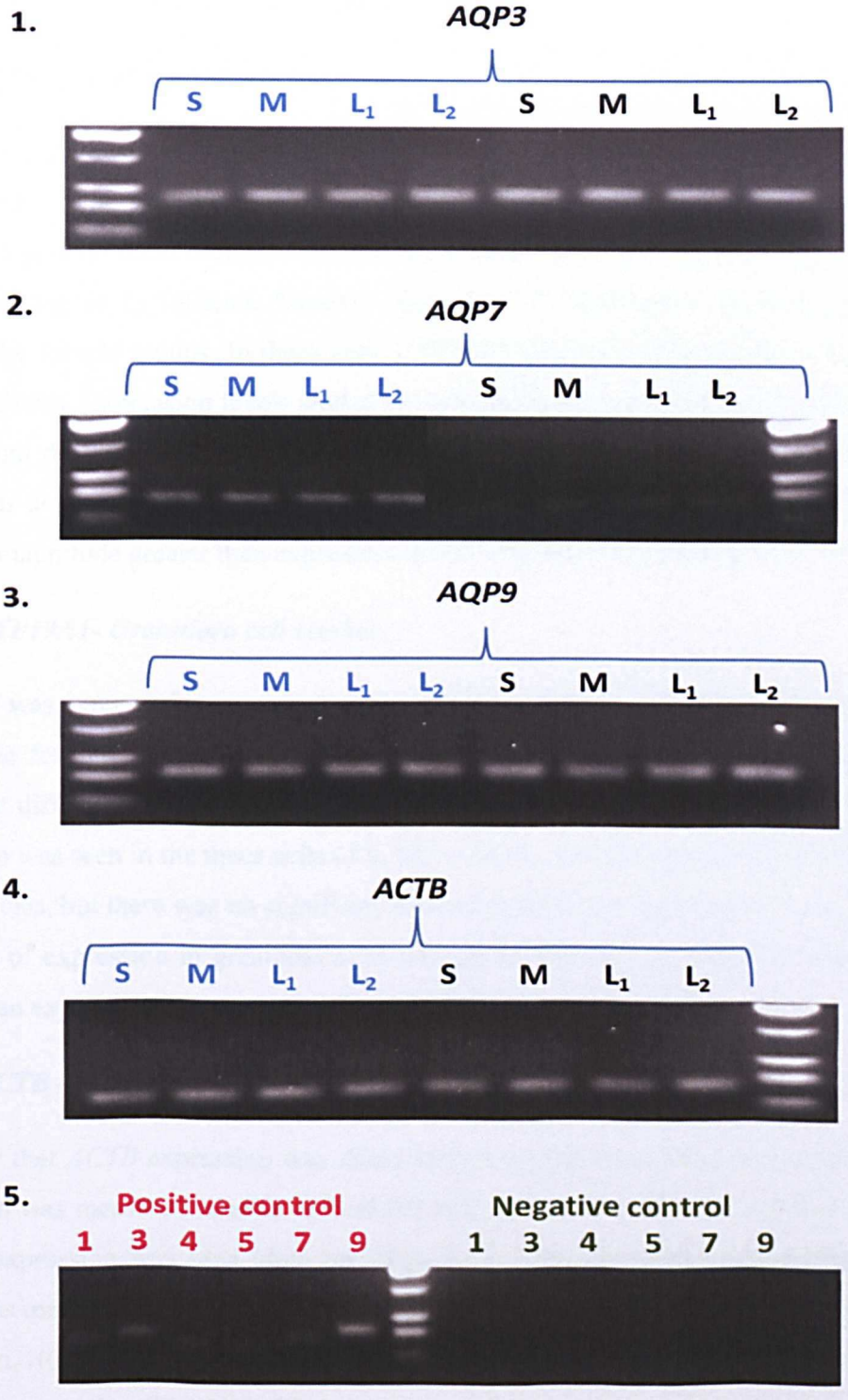

Figure 3.11 Agarose gel electrophoresis of class 2 aquaglyceroporin PCR products of isolated granulosa (**G** - blue) and theca (**T** – black) of **S**, **M**, **L_1** and **L_2** follicles. *AQP3, -7* and *-9* (**1.**, **2.**, and **3.** respectively) were expressed in both cell types in follicles of all stages of development. **4.** Shows β-actin expression in G and T of all follicle stages and positive control tissue. **5.** Shows transcripts for: *AQP1* in Kc, *AQP3* and *AQP4* in Km, *AQP5* in SG, *AQP7* in Kc and *AQP9* in L. Negative controls demonstrate the absence of transcript.

3.3.3 Transcript expression of control genes

3.3.3.1 CYP17A1- Theca cell marker.

There was no transcript expression of *CYP17A1* in the granulosa of type-4 and -5 follicles; trans cript expression was seen in the granulosa cells of S, M, L_1 and L_2 follicles. A general trend indicated an increase in expression up to and including L_1 with levels dropping in L_2 follicles, however there was no significant difference detected between the follicle groups. In theca cells *CYP17A1* was expressed in type-5, S, M, L_1 and L_2 follicles. Expression levels tended to increase from type-5 follicles, peaked in M follicles and declined in L_2 follicles, however, no significant differences between these groups was detected. Transcript expression levels in theca cells were approximately two orders of magnitude greater than expression levels in granulosa cells (Fig 3.12 (1)).

3.3.3.2 CYP19A1- Granulosa cell marker.

CYP19A1 was expressed in type-4, -5, S, M, L_1 and L_2 follicles. Transcript levels tended to increase from S, peaked in L_1 follicles and declined in L_2 follicles. There was a significant difference of $P < 0.01$ between expression levels in S with L_1 follicles. Some expression was seen in the theca cells of S, M, L_1 and L_2 follicles with a higher incidence in L_1 follicles, but there was no significant difference between any of the follicle groups. The level of expression in granulosa cells was approximately two orders of magnitude greater than expression in theca cells (Fig. 3.12 (2)).

3.3.3.3 ACTB – Housekeeping gene.

To ensure that *ACTB* expression was stable and an appropriate endogenous control, its' expression was measured relative to *GAPDH* and Cyclophilin (*PPIL1)*. Against *PPIL1*, variable expression was seen (data not shown). To identify which gene was varying, *PPIL1* was measured in relation to *GAPDH* and this again produced inconsistent relative expression. *ACTB* was then measured in relation to *GAPDH* which resulted in suitably consistent expression (Fig. 3.12 (3)).

3.3.4 Transcript expression of class one aquaporins

3.3.4.1 AQP1

No transcript expression was identified for *AQP1* in the granulosa of type-4 or -5 follicles. It was expressed in the granulosa of S, M, L_1 and L_2 follicles with a varying

pattern of expression, there was no significant difference in expression between the follicle groups. No transcript expression was seen in the theca of type-4 follicles, transcript was identified in the theca of type-5 follicles. It was also expressed in the theca of S, M, L_1 and L_2 follicles with the greatest expression in L_2 follicles. This is illustrated by the significant difference ($P < 0.05$) between the expression in type-5 follicles and that of L_2 follicles. The expression of *AQP1* in theca cells was two orders of magnitude greater than that in granulosa cells (Fig. 3.13 (1))

3.3.4.2 AQP2

No evidence of transcript was found in any of the five experimental repeats; data not shown.

3.3.4.3 AQP4

There was no expression of transcript in the granulosa or theca of type-4 or -5 follicles. Transcripts were detected in both granulosa and theca cells of S, M L_1 and L_2 follicles. In granulosa cells transcript levels tended to increase as follicles increased in size, however not all experimental repeats resulted in the detection of transcript and so expression levels were very variable. There was no significant difference between follicles groups. Again in theca cells, transcript expression was variable in terms of detection in S follicles and general expression levels between follicles groups. There was no significant difference between the levels of expression in theca cells across the antral follicle stages. Expression levels in theca cells were at most twofold higher than granulosa cell expression (Fig. 3.13 (2)).

3.3.4.4 AQP5

There was no evidence of transcript expression in the granulosa of type-4 or -5 follicles. There was expression in the granulosa of S, M, L_1 and L_2 follicles with a general tendency to increase as follicle size increases but there was no significant difference between the groups. In theca cells *AQP5* was expressed in type-5, S, M, L_1, and L_2 follicles. The highest expression of transcript was in type-5 follicles and was one order of magnitude greater than that of antral follicle expression. There was a significant difference ($P<0.05$) between transcript expression levels in type-5 theca and S theca. Levels gradually increased from S to L_2 follicles although there was no significant difference between the antral follicle groups. Theca expression in antral follicles was

approximately one order of magnitude greater that of granulosa cell expression (Fig. 3.13 (3)).

3.3.5 Transcript expression of class two aquaporins

3.3.5.1 AQP3

No *AQP3* transcript expression was found in the granulosa of type-4 or -5 follicles but transcript was found in S, M, L_1 and L_2 antral follicles. Expression levels tended to drop from S to L_1 and increased in L_2 follicles. There was a significant difference in expression of AQP3 between S and L_1 follicles ($P<0.01$). No transcript expression was identified in the theca of type-4 or -5 follicles. Transcripts were expressed in all antral follicles stages with a decrease from S to M follicles and an increase from M to L_2 follicles, but there was no significant difference between the groups. The level of expression in theca cells was approximately five fold higher than granulosa expression (Fig. 3.14 (1)).

3.3.5.2 AQP7

Transcript expression was not found in the granulosa of type-4 or-5 follicles. There was expression in S, M, L_1 and L_2 antral follicles; Expression tended to decrease from S to L_2 but there were no significant differences between the follicle stages. Transcripts were expressed in the theca of type-5 follicles and in S, M, L_1 and L_2 antral follicles. Expression levels were highest in the theca of type-5 follicles, although only by an approximate threefold increase, followed by a gradual decline from type-5 to L_2 follicles. There was no significant difference in expression between any of the follicle sizes, however the level of *AQP7* transcript expression in theca cells was approximately one order of magnitude greater than that in the granulosa cells of antral follicles (Fig. 3.14 (2)).

3.3.5.4 AQP9

Transcript expression of *AQP9* was not found in the granulosa cells of type-4 or -5 follicles. Expression was identified in S, M, L_1 and L_2 follicles but there was no significant difference between the follicle groups. In theca cells transcript expression was absent in type-4 follicles and present in type-5, S, M, L_1 and L_2 follicles. Expression levels were highest in type-5 follicles, levels decrease in S and further in M and L_1 follicles, followed by a slight increase in L_2 follicles. There is a significant difference

(P<0.05) between highest expression in type-5 and that of M and L_1 follicles. Expression levels of *AQP9* in theca cells of type-5 follicles were two orders of magnitude greater than the theca of antral follicle. Expression in the theca of antral follicles was one order of magnitude greater than expression in granulosa cells of antral follicles (Fig. 3.14 (3)).

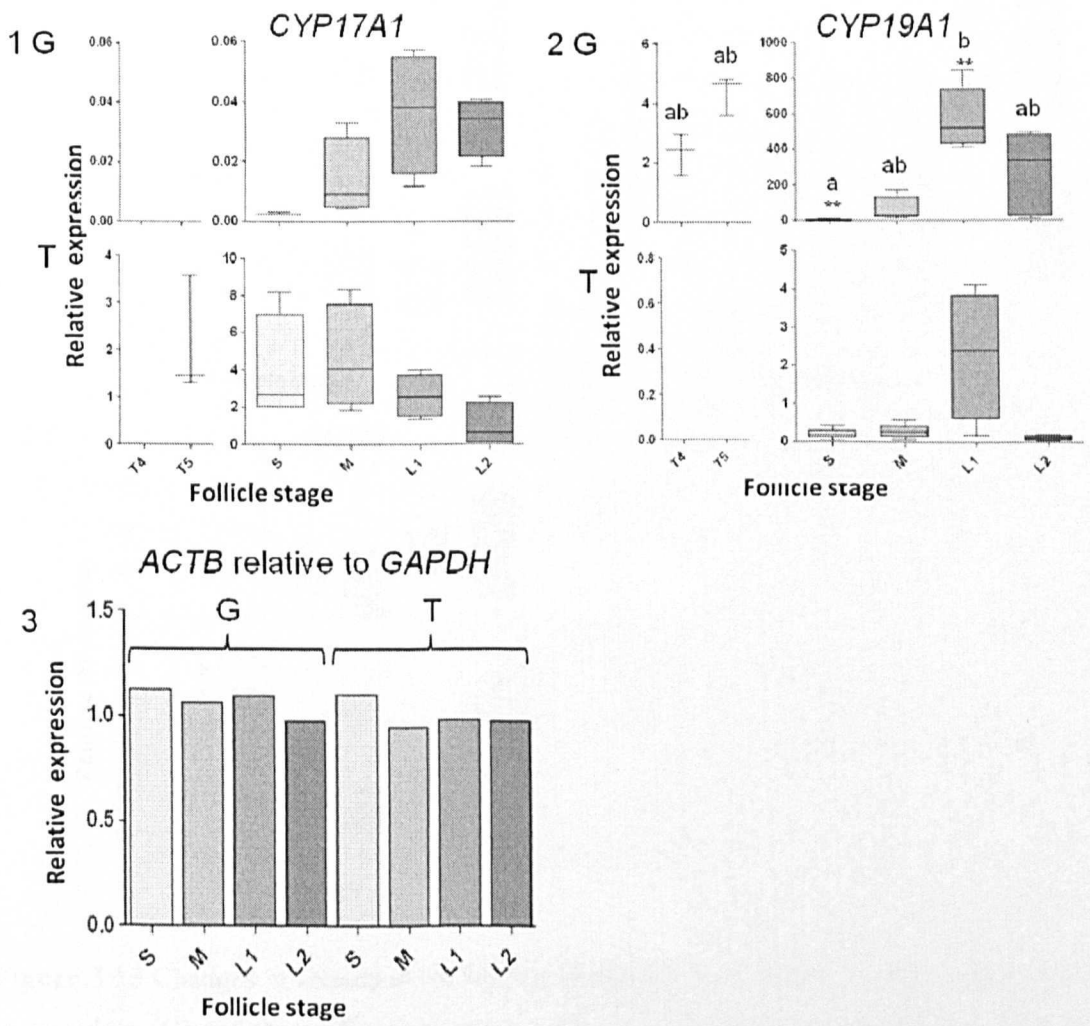

Figure 3.12 Changes in abundance of mRNA transcripts for steroidogenic enzymes **1.** *CYP17A1* and **2.** *CYP19A1* in granulosa (**G**) and theca (**T**) across stages of follicle development from: type-4, -5, S, M, L_1 and L_2 antral follicles, relative to endogenous control gene *ACTB* multiplied by 1000. Where there was no expression for type-4 and -5 follicles the Y-axis scale was set as that for the S, M L_1 and L_2 to allow comparison of data. The box and whisker plots summarise the distribution of each data set exclusive of outliers (identified as 2xSD ± the median). Non-parametric Kruskal-Wallis test was performed on data inclusive of outliers and with the absence of transcript represented as zero. Followed by post hoc Dunn's multiple comparison test. Different superscripts indicate significant difference (**=

P<0.01). **3.** Shows relative expression of *ACTB* across the follicle types for granulosa and theca cells.

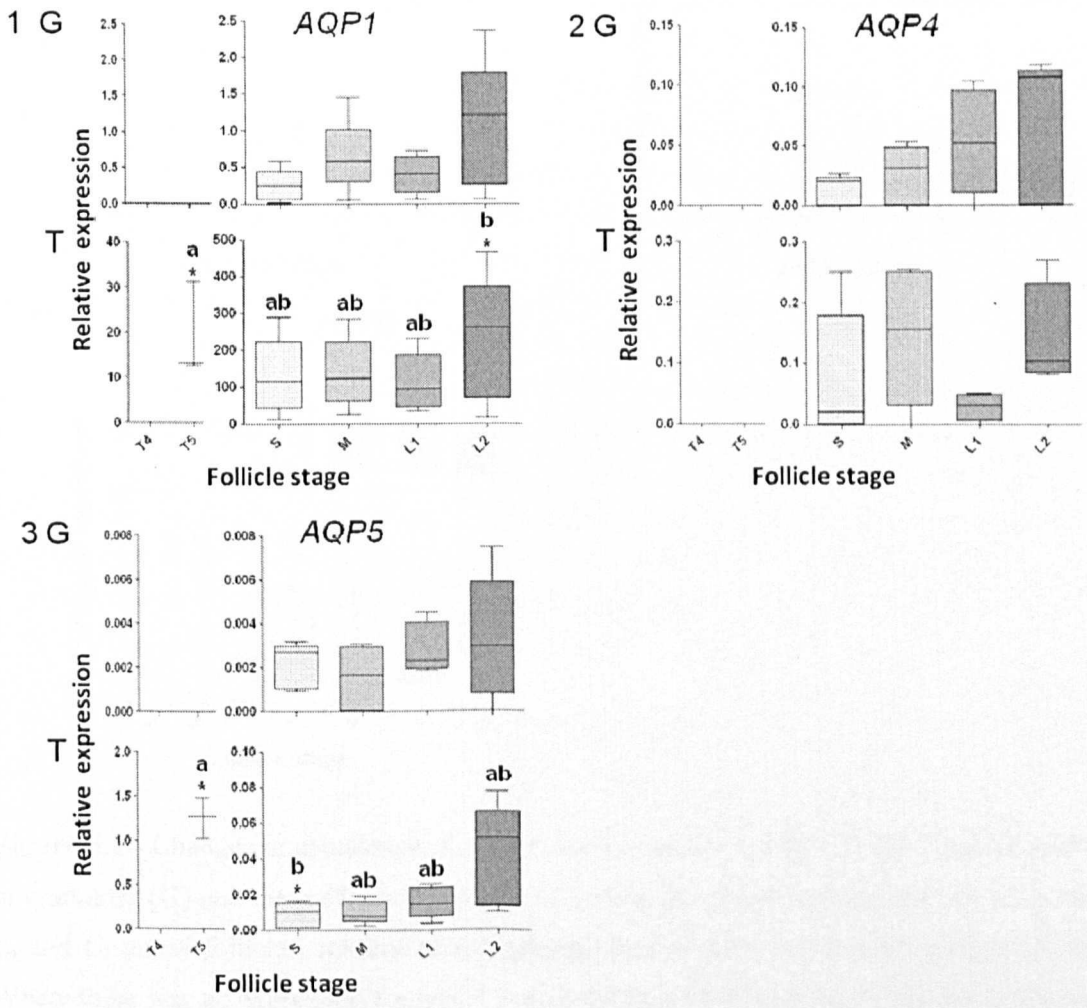

Figure 3.13 Changes in abundance of mRNA transcripts for **1** *AQP1*, **2** *AQP4* and **3** *AQP5* in granulosa (**G**) and theca (**T**) across stages of follicle development from: type-4, -5, S, M, L_1 and L_2 antral follicles, relative to endogenous control gene *ACTB* multiplied by 1000. Where there was no expression for type-4 and -5 follicles the Y-axis scale was set as that for the S, M L_1 and L_2 to allow comparison of data. Non-parametric Kruskal-Wallis test was performed on data inclusive of outliers and with the absence of transcript represented as zero. Followed by post hoc Dunn's multiple comparison test. Different superscripts indicate significant difference (* = P<0.5).

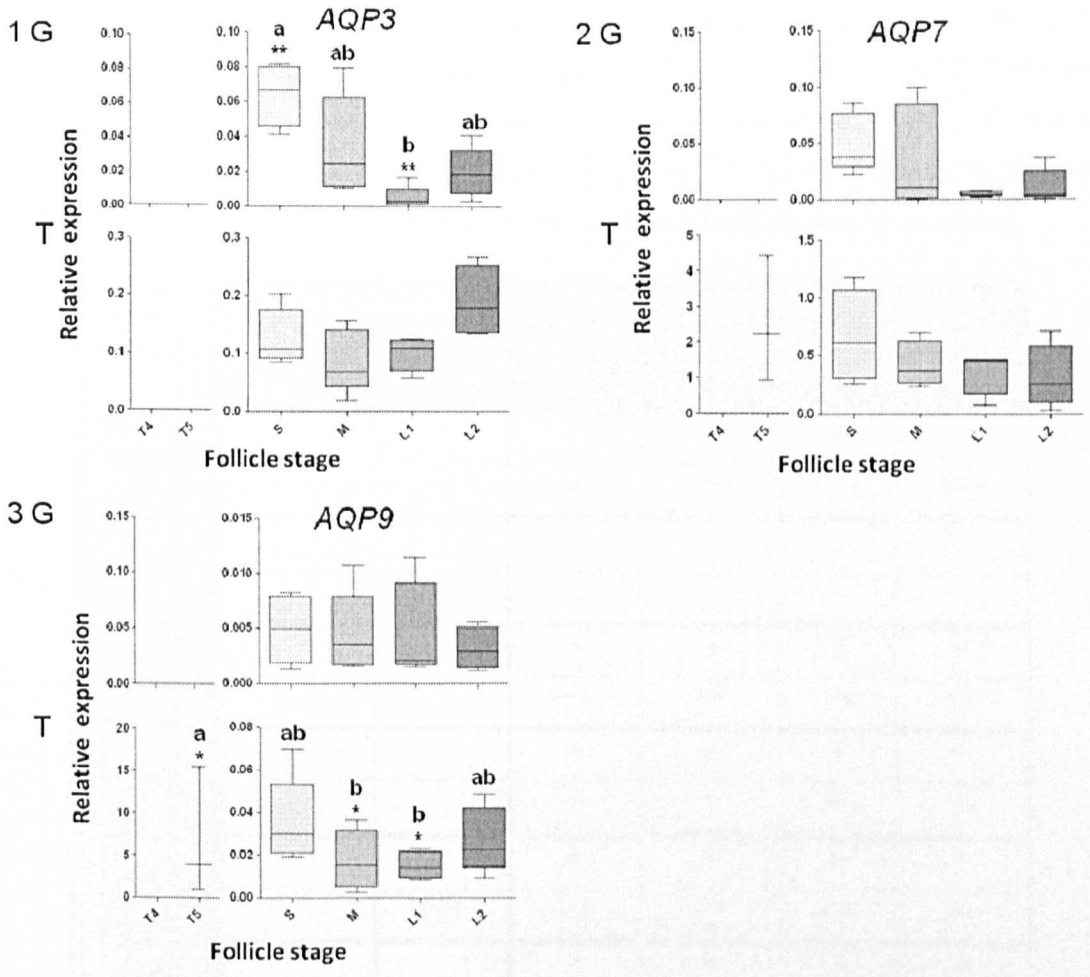

Figure 3.14 Changes in abundance of mRNA transcripts for **1** *AQP3*, **2** *AQP7* and **3** *AQP9* in granulosa (**G**) and theca (**T**) across stages of follicle development from: type-4, -5, S, M, L_1 and L_2 antral follicles, relative to endogenous control gene *ACTB* multiplied by 1000. Where there was no expression for type-4 and -5 follicles the Y-axis scale was set as that for the S, M, L_1 and L_2 to allow comparison of data. Non-parametric Kruskal-Wallis test was performed on data inclusive of outliers and with the absence of transcript represented as zero. Followed by post hoc Dunn's multiple comparison test. Different superscripts indicate significant difference (* = $P<0.5$**= $P<0.01$).

Table 3.4 Summary of expression for each gene in isolation; in granulosa (G) and theca (T) of all follicle stages. The expression level is represented as +<++<+++. All AQPs (with the exception of AQP4) are more highly expressed in theca than granulosa. AQPs -5, -7 and -9 demonstrate their highest level of expression in the theca of type-5 follicles, the time of antrum formation. CYP17A1 is mostly expressed in theca and CYP19A1 in granulosa.

Gene	Type 4 preantral	Type 5 early antral	Small antral	Medium antral	Large 1 antral	Large 2 antral
AQP1 G			+	+	+	+
T		++	+++	+++	+++	+++
AQP2 G						
T						
AQP3 G			+	+	+	+
T			++	++	++	++
AQP4 G			+	+	+	+
T			+	+	+	+
AQP5 G			+	+	+	+
T		+++	++	++	++	++
AQP7 G			+	+	+	+
T		+++	++	++	++	++
AQP9 G			+	+	+	+
T		+++	++	++	++	++
CYP17A1 G			+	+	+	+
T		++	+++	+++	+++	+++
CYP19A1 G	++	++	+++	+++	+++	+++
T			+	+	+	+

3.4 Discussion

3.4.1 Transcript expression of control genes

The gene expression profile of *CYP17A1* in granulosa and theca cells of preantral through to ovulatory follicles shows a clear difference between the two cell types. The data show that *CYP17A1* is primarily theca derived as it is expressed at a level two orders of magnitudes greater than in granulosa cells (Fig. 3.12 (1)). Secondly the appearance of *CYP17A1* in the theca of type-5 follicles coincides with development of a distinct theca interna and the beginnings of steroidogenic capacity (Bao and Garverick 1998). Using a similar approach, *CYP19A1* is seen to be being predominantly of granulosa origin with the level of transcript expression again two orders of magnitude greater in granulosa cells than theca. Transcript expression was seen as early as type-4 preantral follicle stage and increased by approximately two orders of magnitude up to L_1 stage (Fig. 3.12 2) coinciding with the time of increase in E_2 synthesis during follicle development (Fortune *et al.* 2001). Even though there were no significant differences between the expression levels in antral follicles, both *CYP17A1* and *CYP19A1*, indicate a drop in expression in L_2 preovulatory follicles. This agrees with previous findings that the preovulatory LH surge is involved in gene down-regulation (Voss and Fortune 1993; Conely *et al.* 1995; Nimz *et al.* 2009; 2010).

Expression of *CYP17A1* transcript was also noted in the granulosa albeit at a very low level. Similarly *CYP19A1* was also detected in the theca cells of antral follicles with what appears to be an elevation in L_1 follicles. These expressions could either be due to a small amount of cross contamination during the cell isolation procedure, which is considered unlikely given the precautions given, or reflects actual expression. Nimz *et al.* (2010) also noted a small amount of expression of *CYP17A1* and *CYP19A1* in granulosa and theca cells respectively. Skinner *et al.* (2008) too identified a surprisingly large amount of *CYP19A1* in large follicles, although a previous report did not (Roberts and Skinner 1990). The findings of Skinner *et al.* (2008), Nimz *et al.* (2010) and those of this investigation suggest that the unexpected expression of CYP19A1 in the theca of large follicles, is not an artefact of cross contamination between the two cell types.

Common housekeeping (HK) genes such as *ACTB*, *PPIL1*, *GAPDH*, and *28S* have all been shown to vary across certain tissue types, and/or under certain test conditions (Zhong and Simons 1999; Selvey *et al.* 2001; Barber *et al.* 2005). Therefore, in order to check the consistency of *ACTB* expression in both cell types it was measured against

GAPDH and *PPIL1*. Against *PPIL1* there appeared to be some variation (data not shown), against *GAPDH*, ACTB expression was suitably consistent (Fig. 3.12 (3)). PPIL1 was also checked against GAPDH (data not shown). This resulted in significant variation suggesting that PPIL1 is differentially expressed in granulosa and theca cells at different follicle stages. Any variation of HK gene expression will have direct impact on the reliability of expression data. Whilst ACTB is considered to demonstrate consistent expression in the tissue types used for this investigation, the use of a panel of HK genes would strengthen the validity of expression analysis.

3.4.2 Expression profile of class one aquaporins

In the ovary, *AQP1* has been identified in the capillary endothelium only of porcine ovaries via IHC and western blotting (Skowronski *et al.* 2009). The present study localised AQP1 protein expression in both micro- and macrovasculature of the bovine ovary via IHC (Fig. 2.7). Now in the current chapter *AQP1* transcript was found to be expressed in the theca of type-5 follicles at the exact time of antrum formation. The expression significantly increased up to the point of ovulation, consistent with the known increase in vascularisation through antral follicle development (Plendl 2000; Jiang *et al.* 2003; also reflected in the IHC for AQP1 in this study: Fig. 2.7). Transcripts were noted in the granulosa of all antral follicles, but these were at a much reduced level. As no evidence of AQP1 protein could be detected in the granulosa, it may be that *AQP1* gene expression is very low and does not result in a significant level of translation into protein. Using flow cytometry, McConnell *et al.* (2002) also failed to detect AQP1 in rat granulosa cells. Thus any protein present may be below the dynamic range of IHC, western blotting and flow cytometry. In contrast to Skowronski *et al.* (2009), McConnell *et al.* (2002) and the present study; Thoroddsen *et al.* (2011) detected AQP1 protein and mRNA in both granulosa and theca cells, with only minor protein detection in the vasculature of human ovaries. However, as in the present study, the RT-qPCR expression was greater in theca cells compared with granulosa. Thoroddsen *et al.* (2011) additionally showed that *AQP1* expression in granulosa increases during ovulation.

Given the limited studies available, an interpretation of *AQP1* in the general ovary is not yet possible and there may well be important species differences. The present study allows us to conclude that in the bovine, *AQP1* is most prevalent in the thecal compartment of follicles. Expression is initiated in type-5 follicles and increases in abundance as follicles develop.

Aquaporin 2 is not expressed in bovine ovaries, as determined by IHC (Fig. 2.7) and RT-qPCR in this study, neither was it detected in porcine ovaries nor rat granulosa cells (Skowronski *et al.* 2009; McConnell *et al.* 2002). Thorrodsen *et al.* (2011) however, present evidence of mRNA and protein detection of *AQP2* in both granulosa and theca cells of human ovary. Again, no general conclusion is possible at this time but there may be species specific differences.

The transcript profile for *AQP4* shows variable expression in both granulosa and theca cells of antral follicles, with only a marginally higher expression in theca compared with granulosa (Fig. 3.13 (2)) Skowronski *et al.* (2009) and McConnell *et al.* (2002) did not identify AQP4 in porcine follicles and rat granulosa respectively. Thorrodsen *et al.* (2011) detected AQP4 protein in both cell types albeit weak; mRNA in both cell types was also detected, it was generally low and did not demonstrate any significant change from pre- to post ovulatory follicles. The limited evidence available suggests AQP4 expression in humans and bovine is more variable than the other AQPs detected and therefore its functional role in the ovary may be difficult to decipher.

The transcript profile for *AQP5* showed its highest level of expression in the theca of type-5 follicles; levels then dropped 10 fold in S follicles. The general trend in antral follicle theca cells was for a gradual increase up to the preovulatory follicle stage. Expression in granulosa cells was one order of magnitude lower than theca with no evidence in type-4 or -5 follicles (Fig. 3.13 (3)). These results suggest that *AQP5* is more prevalent in theca cells, particularly during the time of antrum formation. However, the relatively low levels of expression in granulosa cells may not reflex a functional significance. The only other evidence for AQP5 in ovary is in the mural granulosa cells of porcine antral follicles (Skowronski *et al.* 2009). Aquaporin 5 is a classic water channel and the results of the present study suggest that it could play a significant role in ovarian FF flux and potentially antrum formation.

3.4.3 Expression profile of class two aquaporins

Expression of *AQP3* transcript shows a significant ($P < 0.01$) decrease in expression in granulosa cells from S to L_1 follicles, followed by a slight increase in L_2 follicles. In theca cells there were no significant differences between groups but the general trend in expression was the same as that for granulosa. Expression was approximately five fold higher in theca than in granulosa cells of antral follicles. There was no evidence of *AQP3*

transcript in type-4 or -5 follicles (Fig. 3.14 (1)) and therefore it is most likely not involved in antrum formation. Thoroddsen *et al.* (2011) identified *AQP3* transcript and protein expression in both cell types from pre- to postovulatory follicles. Theca transcript expression increased from pre- to early ovulatory phase and so too did granulosa expression albeit a fivefold lower expression level. The absence of detection in pig and rat suggest a species- specific difference. The evidence presented for human (Thoroddsen *et al.* 2011) and bovine (the present study) suggests that AQP3 plays a potential role in antral follicle fluid flux.

Aquaporin 7 expression was initiated in the theca cells of type-5 follicles; at this follicular stage it demonstrated its highest level of expression. Levels dropped approximately four fold in S follicles and further declined as follicles progressed towards the preovulatory stage. Transcript expression was generally one order of magnitude lower in granulosa cells, with no evidence in type-4 or -5 follicles (Fig. 3.14 (2)). These results suggest, as with AQP5, that AQP7 potentially plays a significant role in antrum formation. McConnell *et al.* (2002) identified AQP7 in rat granulosa cells but there is no evidence from other species.

Aquaporin 9 demonstrated a similar pattern of expression to that of *AQP7*. Evidence of *AQP9* transcript began in the theca of type-5 follicles. There was a fall in expression in S follicles of some two orders of magnitude and it continued to decline more gradually in M and L_1 antral follicles, followed by a slight increase in L_2 follicles. Transcript in granulosa was present in antral follicles only, was one order of magnitude lower and followed a similar pattern to that of theca cells (3.14 (3)). These results also suggest a potential role for *AQP9* in antrum formation particularly in light of the 100 times greater expression in type-5 follicles compared with antral follicles. McConnell *et al.* (2002) detected AQP9 in rat granulosa and Skowronski *et al.* (2009) identified AQP9 in the mural cells of porcine antral follicles. Again studies are limited, but even though AQP9 is detected in three different species a general conclusion for AQP9 in the ovary is not possible. A difference in AQP9 distribution amongst species does not allow for speculation on its functional relevance at this time.

3.4.4 General discussion

Based on the general picture revealed in Table 3.4, AQPs *-1*, *-3*, *-4*, *-5*, *-7* and *-9* are expressed in both theca and granulosa cells. With the exception of *AQP4*, the remainder are predominantly expressed in the theca. The expression of *AQP1*, *-5*, *-7* and *-9* is initiated in the theca of type-5 follicles; *AQP1* increases from type-5 to ovulatory follicle stage, whereas *AQP5*, *-7* and *-9* demonstrate their highest level of expression in type-5 theca. One difficulty presented by expression analysis is in the determination of functional relevance and what one would consider as 'real' expression. This is somewhat difficult when there is differential expression, by orders of magnitude, of the same gene in different cell types; or when some isoforms show variation in detectable expression (E.G. *AQP4*).

Therefore, a major drawback with the present investigation is the absence of reliable protein detection for most of the AQPs, as this would facilitate an interpretation of gene expression information in terms of transcribed and translated protein. It is however possible to do this in the case for AQP1. There was 100 fold increase in theca expression which was mirrored in theca endothelium IHC results (Fig. 2.7 (1) – (9)). The lack of immunolabelling in granulosa cells could indicate that the level of transcript expression is not truly expressed as functional protein. *CYP17A1* and *CYP19A1* are considered as theca and granulosa cell markers respectively. The level of expression in these cell types is comparable with that for AQP1 in theca but not with any other AQP gene. This could suggest that such low level of mRNA expression would not be translated into functional protein. Based on this assumption, the conclusion would be that AQP1 is the only functionally relevant AQP in the bovine ovary. However, it should be considered that different cell types modulate protein translation differently (Rodríguez *et al.* 2001). AQPs are not ubiquitous proteins; they are usually located at very specific areas of the cell membranous. If these proteins are also localised to one specific cell type as in AQP5 and -9 in porcine mural granulosa cells (Skworonski *et al.* 2009) then their relative mRNA expression would be low.

In terms of methodology this investigation may have benefited from the transportation of follicles from the abattoir on ice as opposed to in 37°C PBS, to reduce nuclease activity, as done by Skinner *et al.* (2008); and Tabandeh *et al.* (2010), particularly if AQP mRNAs have short half-lives (Rodríguez *et al.* 2001). The box and whisker plots illustrate the large spread of results across the experimental repeats for each AQP, even

with outliers removed. This could be explained by variation in quality of mRNA across experimental repeats. However, given the care taken with sample preparation, it is more likely to reflect variations between individual follicles and ovaries. This would be determined by the general health, nutritional and reproductive status of the source animals. Precise identification of cycle stage is difficult with unpaired ovaries and of course identification of early stage atresia via morphological examination is virtually impossible (Irving-Rodgers *et al.* 2001). Thus there could have been several cell populations, representing a range of developmental phenotypes, amongst the cohorts of cells collected. Aquaporins could be differentially regulated in atretic, subordinate, dominant; pre and post ovulatory follicles as concluded by Thoroddsen *et al.* (2011). Some of these issues could be overcome in a future study by the collection of follicular fluid for the quantification of steroid hormones, especially given that the E_2 status of a follicle is known to affect gene expression profiles (Nimz *et al.* 2009). Therefore these results may not represent a clear picture of AQP expression in bovine follicular growth. These results do however present the first evidence of AQP expression in bovine ovaries and provide a platform for assessing antrum formation in terms of AQP expression, function and regulation.

3.4.5 Conclusions

In conclusion, *AQP1*, *-3*, *-4*, *-5*, *-7* and *-9* are expressed in the bovine ovary, whilst *AQP2* is not. With the exception of *AQP4* these AQPs are predominantly expressed in the theca of S, M, L_1 and L_2 antral follicles. Transcript expression of *AQP1*, *-5*, *-7* and *-9* commence in the theca of type-5 follicles during the time of antrum formation.

AQP1 expression increases by one order of magnitude between type-5 and the antral follicle stages, in parallel with follicle growth, vascularisation and E_2 production. It may therefore play an important role in angiogenesis as well as fluid transduction. Its close association with follicle development suggests that it may be modulated by E_2 and this would be a valuable target for future study. The aquaglyceroporins *AQP7* and *-9* are highly expressed in type-5 theca and decline approximately four fold and two orders of magnitude respectively, as follicle development progresses. This suggests that they could be responsible for transporting glycerol and other small neutral solutes across the theca layer. Aquaporin *5* also demonstrates high type-5 theca expression which decreases by approximately two orders of magnitude in small follicles then increases gradually in

parallel with follicle growth. Therefore *AQP1*, *-5*, *-7* and *-9* are highly likely to play a pivotal role in antrum formation.

Chapter 4

Fluid transport in bovine and porcine granulosa cells and potential modulation by androgen.

This work reported in this chapter was done in collaboration with Dr Malgozata Durlej (Jagielonian University, Krakov, Poland). Dr Durlej brought expertise in porcine ovarian development under the influence of androgen and androgen inhibition. This allowed the design of cell culture and swelling assay experiments using androgen concentrations physiologically relevant to porcine tissue. As previously mentioned, there is limited literature surrounding the role of AQPs in domestic species. Skowronski *et al.* (2009) identified AQP5 and -9 in porcine granulosa; there is limited indication that both of these AQP are potentially modulated by androgen (Moehren 2008; Pastor-Soler *et al.* 2002; 2010). Taken together with the findings reported in earlier chapters of this thesis, it was logical to consider the functional role of AQPs in both bovine and porcine follicular tissue and its possible androgen dependence.

With the exception of Cunningham chamber design, mRNA extraction and RT-qPCR, the experiments described in this chapter were carried out with Dr Malgorzata Durlej (Jagielonian University, Krakov, Poland). Protein extraction and Western Blotting was conducted by Dr Durlej in Krakov.

4.1 Introduction

The porcine oestrous cycle is 18 – 24 days in length; the pig is polytocous and ovulates 15-30 oocytes at each cycle. The follicular phase is four to six days and the largest antral follicles (2-4 mm), developed during late luteal phase, undergo recruitment. As in the bovine, this occurs when LH pulse frequency is high and amplitude is low (Knox 2005). Luteinising hormone receptors appear at 5-6 mm and are associated with follicle selection. At this stage atresia may still occur, however once selected atresia is avoided, follicles enlarge and ovulate at 7-8 mm (Driancort 2000). As in most mammals, follicle formation occurs early in foetal life and so the repository of primordial follicles is fixed before birth, in pigs and it takes approximately four months to progress from primordial to preovulatory sized follicle (Morbek *et al.* 1992). Steroidogenesis in the pig follows the 'two cell' hypothesis, however there are some differences unique to porcine. As well as producing aromatizable androstenedione which is converted to testosterone (T) then E_2

in the granulosa cells, the theca interna also produces E_2 at a level comparable with granulosa (Foxcroft and Hunter 1985).

Folliculogenesis is controlled by intra ovarian factors and steroids through a series of sequentially coordinated actions. Theca and granulosa cells respond to these hormones via signal transduction and nuclear receptors which influence gene transcription (Drummond 2006). Granulosa cells express androgen receptor (AR) which bind androgens and modulate cAMP-responsive gene expression (Fitzpatrick and Richards 1991). In primates AR is most prevalent in preantral-early and antral follicles and declines during preovulatory development. Its paracrine effect is therefore diminished during the later stages of follicle development (Hillier *et al.*1997). Vendola *et al.* (1999) found T significantly increased the number of primary follicles and IGF-1 and IGF-1R mRNA in primate oocytes. Androgen stimulates early stages of follicular growth of type-1 to type-5 follicles in the primate ovary by increasing cell proliferation; granulosa AR gene expression increases with follicular growth and was colocalised with FSHR (Weil *et al.* 1999). Testosterone augments FSHR expression therefore androgens stimulate follicular growth and E_2 synthesis (Weil *et al.* 1999).

There is much evidence to suggest a role for androgens in early follicular and preantral follicles. Granulosa cell AR mRNA and protein are down regulated in rat during FSH-induced preovulatory follicle development therefore the paracrine action of androgen is modulated by FSH and receptor expression (Tesuka and Hillier 1996). Hampton *et al.* (2004) found AR mRNA initially appeared in ~40% of granulosa cells in type-2 bovine follicles followed by 100% expression in granulosa cells of type-3, -4 and -5 follicles with a decrease in late antral follicles. Yang and Fortune (2006) examined the effect of T on early bovine follicle growth and found that T promoted receptor-dependent stimulation of follicle progression from type-2 and -3 follicles in vitro. Słomczynska and Tabarowski (2001) localised AR in the granulosa of preantral and growing antral porcine follicles which also decreased in preovulatory follicles.

Theca cells are constantly exposed to blood borne cholesterol in the form of lipoprotein and are therefore capable of synthesising androgen throughout antral follicle development. Granulosa cell function is modulated by the androgens supplied by LH-induced theca cells (Hillier and de Zwart 1981). Therefore E_2 synthesis by avascular granulosa cells under the influence of FSH is rate limited by the provision of androgen via theca cells (Hillier and Tetsuka 1997). Gonadotrophins regulate the expression of steroidogenic enzymes via G-protein coupled receptors. Autocrine factors also likely to

influence FSH action include IGFs and TGF-β, inhibin/activin; plus GDF-9 (Erickson *et al.* 1994; Matzuk 1995 respectively). Paracrine actions from theca derived growth factors include epidermal growth factor (EGF), TGF-α and –β and androgens (Hillier 1994; Fitzpatrick and Richards 1991 respectively).

During early/intermediate follicle stages androgens amplify cAMP-mediated signalling via AR and therefore potentially modulate granulosa cell function and therefore follicular development. As a result of the LH surge elevated cAMP levels via androgen modulation down regulate genes such as CYP19A1 stimulating luteinisation of the granulosa cells and cessation of follicular growth (Voss and Fortune 1993; Conely *et al.* 1995; Hillier and Tetsuka 1997; Nimz *et al.* 2009). In terms of antral follicle growth, much of the literature considers androgens to be inhibitory. Atretic follicles have a low E_2 to androgen ratio and atresia was exacerbated by the administration of androgen (Carson *et al.* 1981). However, treatment of rhesus monkeys with non aromatizable dihydrotestosterone (DHT) led to an increase in the abundance of late preantral and early antral follicles (Vendola *et al.* 1999). In women suffering PCOS, hyperandrogenism stimulates large numbers of developing small antral follicles (Abbott *et al.* 2002; Ehrmann 2005). Otala *et al.* (2004) looked at the effects of T, DHT and E_2 on ovarian tissue in culture and reported an inhibitory effect of androgens on apoptosis. Homozygous Ar -/- mice have recently been produced successfully and have further supported the evidence of a role for androgen in folliculogenesis including the final stages of follicular development and ovulation (reviewed in Walters *et al.* 2008).

Activated AR recognises palindromic DNA sequences of androgen response elements (AREs), and the binding of androgen-activated AR to AREs leads to up-regulation of target gene transcription. Dihydrotestosterone, a non-aromatizable androgen, is used to distinguish between oestrogenic and androgenic actions of T. However, 3α- and 3β-hydroxysteroid oxidoreductases reduce DHT to 3-alpha-diol (3α-diol), which is biologically inert and can be converted back to DHT; and 3-beta-diol (3β-diol) which has high affinity for oestrogen receptor-β (ESR2; Morani *et al.* 2008; Walters *et al.* 2008). Dihydrotestosterone may therefore potentiate ESR-mediated actions in particular tissue types (Kuiper *et al.* 1997; Omoto *et al.* 2005).

The actions of androgen can therefore be direct, in its effect on transcription via androgen receptor and indirect via aromatisation to E_2 or conversion of DHT to 3β-diol. In addition to this there are many non-genomic actions of androgens, these are rapid and not inhibited by androgen or androgen receptor inhibitors (Foradori *et al.* 2008).

Genomic effects of androgen can be inhibited by non-steroidal anti-androgen hydroxyflutamide (HF). It is a potent competitive inhibitor of androgen as it binds to AR, (Yallampalli *et al.* 1993). As well as the classical genomic effects of androgen there has recently been increasing interest in the non-genomic effects of androgens, rapidly acting via cell membrane receptors and non-genomic signal transduction mechanisms. Such effects include changes in membrane flexibility and activation of intracellular signalling molecules particularly rapid changes in $[Ca^{2+}]_i$ (Foradori *et al.* 2008). As these effects are non-genomic, inhibitors of androgen such as HF have no effect on the non-genomic actions of androgens (Yallampalli *et al.* 1993). The variation of direct and indirect genomic effects as well as the non-genomic effects of androgens, could be a reason for certain conflicting reports of androgen inhibitory/stimulatory effects on follicle development.

Moehren *et al.* (2008) adopted a combination of computational and experimental approaches to identify new androgen response elements in the promoter region of 76 genes known to be responsive to androgen. In doing so they identified an androgen-selective ARE in human AQP5; it is 570 bp down stream of the AQP5 transcription initiation site and is highly conserved between human and mouse with only one base pair difference (Moehren *et al.* 2008). Oestrogens also play a pivotal role in the regulation of folliculogenesis and do so via ESRs of which there are two types ESR, alpha (ESR1) and beta (ESR2; Mosselman *et al.* 1996; Lubahn *et al.* 1993). Kobyashi *et al.* (2006) identified a functional oestrogen response element (ERE) in the promoter region of AQP5 which was a target of and regulated by ESR1. They also identified ERE-like motifs in the promoter region of many AQPs with the exception of AQP4 and -10; however, the only AQP activated by E_2 was AQP5. An earlier study by Richard *et al.* (2003) identified AQP1 as the E_2 responsive gene via northern hybridisation, not AQP5. Kobyashi *et al.* consider this to be due to methodological differences and consider their chromatin precipitation and RT-qPCR strategy to be more sensitive and reliable.

4.1.1 Aim and strategy

The aim of this study was firstly to determine whether bovine and porcine granulosa cells swell under hypotonic conditions and if this action can be diminished/knocked out by the introduction of $HgCl_2$. This would suggest a mercurial sensitive water transportation system in granulosa cells, possibly AQPs. As discussed above, androgens play a role in follicle development however little detail is available in terms of androgens

and antrum formation and expansion. Aquaporin 5 was identified in porcine granulosa cells by Skowronski *et al.* (2009) and to date AQP5 is the only AQP identified which has an ARE in its promoter region. Therefore the second aim of this investigation was to determine if the AQP system present in porcine granulosa cells is modulated by androgen and whether AQP5 is a functional component.

These aims were to be achieved by firstly developing the granulosa swelling assay (McConnell *et al.* 2002) in bovine granulosa cells. Transmembrane fluid transport in bovine and then porcine granulosa cells would be determined by degrees of swelling in isotonic and hypotonic conditions, with and without the addition of $HgCl_2$. To determine the effects of androgen, medium sized (growing) porcine follicles would be treated alone with testosterone (T) and androgen receptor blocker HF separately and in combination. Granulosa cells from these follicles would then be subjected to a swelling assay, indicating the dependence of the swelling response on androgen and whether it can be prevented by a specific inhibitor of androgen action. This protocol will also be carried out on bovine granulosa cells, however, androgen concentration derived from porcine studies may not be physiological relevant to bovine. Anti-AQP5 antibody was also used for WB and IHC on porcine ovaries to evaluate AQP5 protein expression in response to androgen.

4.2 Materials and methods

4.2.1 Tissue collection and preparation

Bovine ovaries were collected from a local abattoir and transported back to the laboratory in a vacuum flask containing warm phosphate buffered saline (PBS 37°C at pH 7.4) within 2h of animal slaughter. Ovaries were washed twice with sterile PBS and sprayed with 70% ethanol. The ovaries were unpaired and therefore chosen based on their external appearance. Amber coloured follicles of approximately 10 mm in diameter with a volume of 0.9 – 1.5 ml were chosen for granulosa cell isolation and swelling assays.

Porcine ovaries from cycling sows were obtained from a local abattoir. Tissues were collected and placed in 37°C sterile PBS (pH 7.4) and transported back to the laboratory within 2h of animal slaughter. Salivary gland positive control tissue was collected at the same time and under the same conditions. On return salivary gland was cut into $0.5cm^3$ pieces placed into a labelled 2 ml Corning® cryogenic vial and snap frozen in liquid nitrogen for RNA extraction. Ovaries were washed twice with sterile PBS (pH 7.4) supplemented with antibiotics (penicillin 100U ml^{-1}, streptomycin 100 $\mu g\ ml^{-1}$ and amphotericin B 2.5 $\mu g\ ml^{-1}$).

Medium amber coloured antral follicles, 4 - 5 mm in diameter, were selected; granulosa cells were isolated and split between two pools. Half were used immediately for a swelling assay and the remainder were incubated in four treatment groups for 6h on a rolling stage at room temperature. The treatments were **1** - medium alone (control); **2** - testosterone (T; 10^{-7} M); **3** - hydroxyflutamide (HF; 50 $\mu g\ ml^{-1}$); and **4** - testosterone plus hydroxyflutamide (T+HF). These were then used in a variation of the initial bovine swelling assay (Section 4.2.5).

Other follicles were completely excised, incubated (37°C; 95% air: 5% CO_2) in media supplemented with antibiotics for 6h in the same treatments groups as the above. They were fixed in 10% NBF for IHC investigation (Section 4.2.7), snap frozen in liquid nitrogen for protein extraction and WB (Section 4.2.9) or used to isolate granulosa and thecal for mRNA extraction and RT-qPCR .

4.2.2 Swelling assay

Swelling assay methodology was based on an investigation by McConnell *et al.* (2002) in which a rat granulosa cell suspension was infused into a Cunningham chamber (Cunningham & Szenberg 1968) and incubated over 1h for cell adherence. Cells were washed and incubated in the presence or absence of mercury chloride ($HgCl_2$) for 15 min. The cells were then washed and a photograph taken prior to being subjected to hypotonic (HYPO) conditions. After 30s in HYPO conditions a second photograph was taken, cell diameters were measured and cell volumes calculated.

This technique was refined through initial studies for the purposes of this investigation. Such that **a)** the time for cell incubation and adherence was reduced from 1h to 30 min, **b)** media with or without $HgCl_2$ was introduced and left for 10 min instead of 15 min, at the end of which the initial photo was taken. And **c)** the time allowed for cells to respond to isotonic (ISO) or HYPO media was extended from 30s to 90s, prior to a second photo being taken and cell diameters measured. In contrast to McConnell *et al's* study an ISO control condition was included in all studies in this investigation. Cells were moved from ISO to ISO media with and without $HgCl_2$ as well as from ISO to HYPO conditions with or without $HgCl_2$. Isotonic medium was Dulbecco's modified Eagle's medium/nutrient mixture Ham's F-12 (DMEM–F12) plus 20 mM HEPES (Sigma-Aldrich, Dorset, UK) adjusted to 319 mOsm. Hypotonic media was 30% ISO plus 70% sterile distilled water adjusted to 90 mOsm. Osmolarities were measured by freezing point depression using an advanced Micro Osmometer (Advanced Instruments, Mass., USA).

4.2.3 Cunningham chamber design

Cunningham chamber (Cunningham and Szenberg, 1968) design was crucial to the success of the assay. Chambers had to consistently allow for the infusion of cell suspension, incubation, cell adherence, withdrawal and re-introduction of media with minimum disruption to the integrity of cell preparation (Fig. 4.1). To achieve this Menzel-Gläser Polysine® slides (Thermo scientific, Brunswick, Germany) were used due to their chemical and electrostatic properties encouraging cell adhesion. Chambers were created by marking an area of 18 mm in length and dividing this into three 6 mm sections or zones on the back of the slide. Two layers of double sided sticky tape strips (2x22 mm) were positioned on the correct side of the slide at either end of the designated zones and flush to the back edge of the slide. A 22x50 mm cover slip (BHD laboratory supplies, Poole, UK) was then secured on top of the strips, again parallel to the back

edge of the slide, creating a chamber deep enough to allow the introduction of ~70µl of cell suspension. Cells were examined across all three zones to provide a fair representation of the cell population.

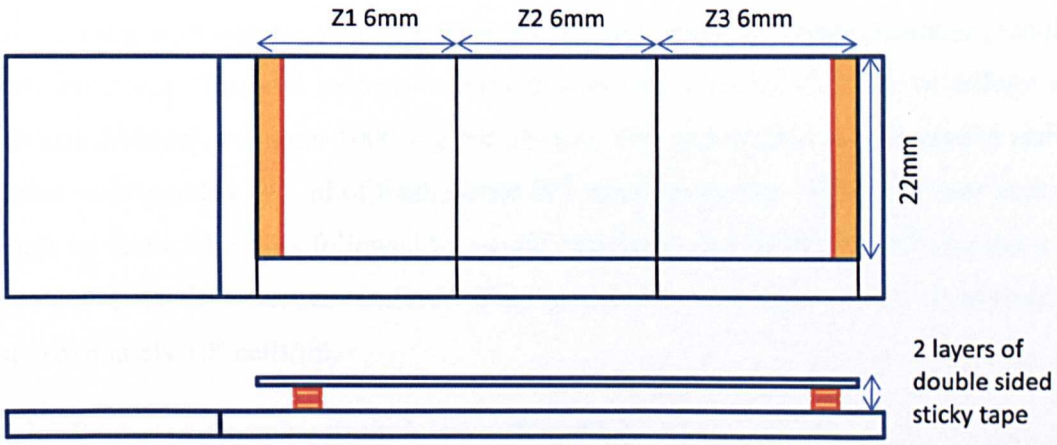

Figure 4.1 Adapted Cunningham chamber design (plan and section). The front edge of the chamber allowed the placing of a pipette at the centre zone and the introduction of 70 µl of cell suspension which completely filled and remained firmly within the chamber due to surface tension. Cells adhered sufficiently to allow the removal of media by holding the slide vertical with the back edge pressed onto absorbent tissue. Capillary action drew the fluid out of the chamber allowing the infusion of isotonic/hypotonic media supplemented with or without $HgCl_2$. One field of view per zone was imaged.

4.2.4 Granulosa cell collection

Ovaries were chosen and prepared in a laminar flow hood. Each ovary was dipped briefly in 70% ethanol and allowed to air dry. Bovine and porcine target follicles (one per ovary) were approximately 10 mm and 4 – 5 mm in diameter respectively. Follicular fluid was removed using a 21 gauge hypodermic needle and 5 ml syringe barrel. This was inserted into the ovary below the follicle and angled so the needle penetrated the follicle from inside the ovary, preventing the follicle from bursting and releasing its FF. The FF was carefully drawn from the follicle until the follicle fully collapsed allowing the volume to be measured and its quality assessed. Follicular health was determined by considering FF colour, clarity and consistency; turbid, reddened or very pale fluid indicated poor health or atresia of the follicle (in this case the fluid was discarded and an alternative follicle was chosen). If the FF was satisfactory, the outer follicle wall was gripped with tissue tweezers, and a small incision made with fine dissection scissors. Whilst holding the follicle wall with tweezers to open up the incision, sterile ISO

medium was introduced with a Pasteur pipette to fill the empty follicle. A sterile loop was then used to gently and systematically scrape the inside of the follicle wall dislodging the granulosa cells into the media. The cell suspension was removed from the follicle using a Pasteur pipette and expelled into a small labelled screw cap bijou pot. The follicle wall was scraped with fresh media twice more to ensure maximal granulosa cell collection. The cell suspension was placed into a 15 ml Corning centrifuge tube (Sigma-Aldrich) and spun 1000 x *g* for 10 min. The supernatant was discarded and the pellet re-suspended in 5 ml of fresh sterile ISO media by gently rolling the tube back and forth by hand. This was followed by gentle aspiration and finally passed through a cell strainer (BD Biosciences Oxford, UK) producing a single celled suspension of approximately 10^6 cells/ml.

4.2.5 Bovine and porcine granulosa swelling assay

Each bovine and porcine granulosa cell suspension was a combination of cells from five and 20 follicles respectively. The separate suspensions were used for four experiments, with each done in duplicate. See Table 4.1 for an outline of the protocol for the four conditions.

See Fig. 4.2 for a schematic representation of the swelling assay protocol and Fig. 4.3 for a screen shot of images from condition **C**-bovine. Conditions **A**, **B**, **C** and **D** were run in parallel and so all eight chambers were prepared at staggered intervals to allow for consistent and accurate timings. For each condition (done in duplicate) at least 30 cells were measured before and after the 90s ISO/HYPO exposure. Four and two experimental repeats were carried out in total for bovine and porcine respectively.

4.2.6 Porcine granulosa swelling in response to androgens

Porcine granulosa cells from approximately 10 follicles were collected and suspended in sterile ISO DMEM-F12 media supplemented with antibiotics, (penicillin 100.0 U ml^{-1}, streptomycin 100.0 µg ml^{-1}, amphotericin B 2.5 µg ml^{-1}) to give 10^6 cells/ml, as described above. This suspension was divided into four groups and pre-incubated for 12h on a rolling stage at room temperature with the following treatments: **1** - medium alone (control); **2** - testosterone (T; 10^{-7} M); **3** - hydroxyflutamide (HF; 50 µg ml^{-1}); and **4** - testosterone plus hydroxyflutamide (T+HF). Following pre-incubation each treatment group was subjected to the same swelling assay as described in section 4.2.5 except the treatments were not subjected to the addition of $HgCl_2$.

Table 4.1 This outlines the four conditions of the granulosa swelling assay. Controls (**A**) and (**B**) measured the response of granulosa cells moved from ISO to ISO conditions in the absence (**A**) and presence (**B**) of $HgCl_2$. (**C**) and (**D**) measured the response of granulosa cells moved from ISO to HYPO conditions in the absence (**C**) and presence (**D**) of $HgCl_2$; they followed the same protocol as above except the 90s bench top incubation was with HYPO media.

Control – A (ISO – ISO) Minus $HgCl_2$	**B – (ISO-ISO) Plus $HgCl_2$**	**C – (ISO-HYPO) Minus $HgCl_2$**	**D – (ISO-HYPO Plus $HgCl_2$**
Cell suspension is infused into two chambers and incubated for 30 min for cell adherence; Bovine - 37°C;95%air:5%CO_2 Porcine – Room Temp.	√	√	√
Media is withdrawn	√	√	√
Fresh ISO media is added - without $HgCl_2$	With $HgCl_2$	Without $HgCl_2$	With $HgCl_2$
10 min incubation (conditions as above)	√	√	√
After 9.5 min – one image per zone is captured with at least 5 cells present per zone.	√	√	√
Media is withdrawn	√	√	√
Fresh ISO is added	ISO	HYPO	HYPO
After 90s bench top incubation – one image per zone is captured with at least 5 cells present per zone.	√	√	√

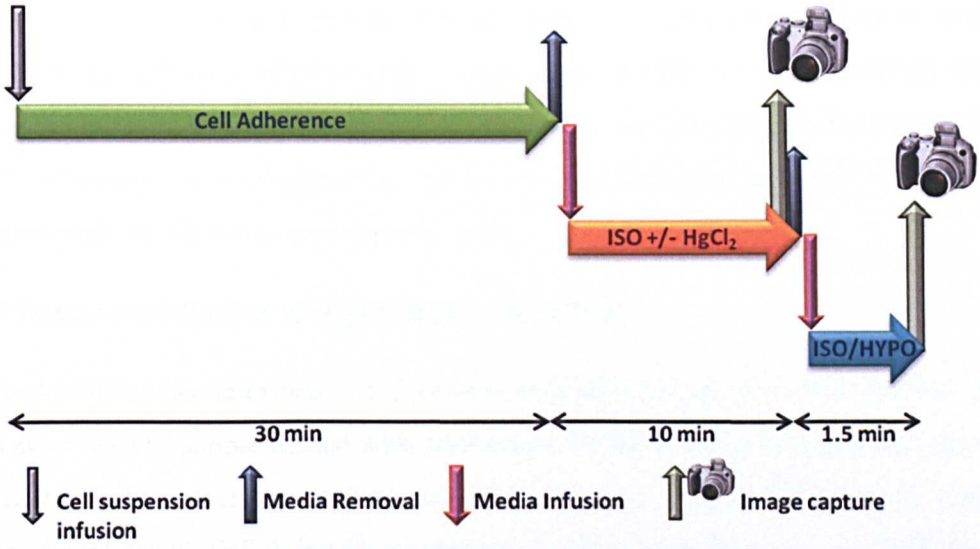

Figure 4.2. This flow diagram represents swelling assay experimental procedure. Cell suspension was introduced and incubated for 30 min for cell adhesion, this was removed and fresh isotonic (ISO) media plus or minus $HgCl_2$ was infused and incubated for 10 min, at the end of this period images were captured. Media was then replaced with ISO or hypotonic (HYPO) for 90 s after which the response images were captured.

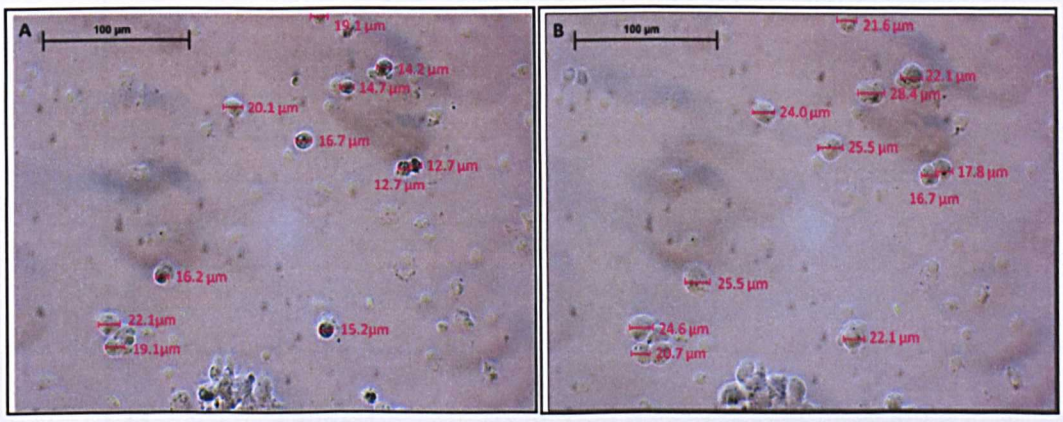

Figure 4.3 Snapshot images of the bovine granulosa swelling assay experiment **C. (A)** This image was captured at the end of the 10 min incubation in ISO media. The cells were then moved into HYPO conditions for 90s after which image **(B)** was captured. Granulosa cells have increased in size in response to the hypotonic conditions. This response was measured by recording all cell diameters in the horizontal plane.

The granulosa cells of developing follicles are normally exposed to a significant androgenic environment, with adult porcine follicular fluid containing concentrations of androgen similar to that used here (Grupen *et al.* 2003).

These two experiments measured the response of porcine granulosa cells pre-treated with androgen and androgen inhibitor (HF) moved from (**A**) ISO to ISO conditions and (**B**) ISO to HYPO conditions. Experiments A and B were run in parallel so the preparation of the 16 chambers was staggered to allow for consistent and accurate timing. Three experimental repeats were carried out in total.

4.2.7 Immunolocalisation of AQP5 in porcine follicles

Excised follicles (as described in 4.2.1) were incubated in 700 µl of ISO medium (37°C; 95% air: 5% CO_2) supplemented with antibiotics, for 6h in the same treatments groups as described for the porcine granulosa cell swelling assay. Three follicles were incubated per treatment group. Following 6h incubation, follicles were fixed in 10% NBF for up to 12h and processed using a Leica TP 1020 automated processor (Leica Microsystems, Germany) and a shortened programme of 10.5h (see Table 4.2).

Table 4.2 Protocol for tissue processing prior to paraffin embedding.

Bucket #	Solution	Duration	Process
1	70% Ethanol	01:00:00	Progressive dehydration
2	80% Ethanol	01:00:00	
3	95% Ethanol	01:00:00	
4	100% Ethanol	00:30:00	
5	100% Ethanol	00:30:00	
6	100% Ethanol	00:30:00	
7	100% Ethanol	00:30:00	
8	Histoclear	01:00:00	Preparation for paraffin
9	Histoclear	01:00:00	
10	Histoclear	01:00:00	
11	Paraffin	01:00:00	Liquid paraffin saturation
12	Paraffin	01:30:00	

Tissue was embedded in moulds using molten Paraplast paraffin and sectioned using a Leica RM 2255 microtome. Five micron sections were cut using a Leica RM 2255 microtome as described in Section 2.2.3 and IHC was performed using the same protocol described in section 2.2.7. Aquaporin 5 polyclonal serum antibody was used diluted 1:200. See Section 2.2.6 for antibodies and Table 2.2 for AQP5 antigen peptide sequence. Negative controls were conducted by omission of primary antibody; two types of non-immune rabbit serum (NIRS) were also used. Anti-AQP5 antibody was tested on porcine salivary gland positive control tissue at a 1:200 dilution.

4.2.8 AQP5 staining quantitative intensity evaluation.

At least four images were captured per follicle, to quantify intensity of immunoreactions and analysed using ImageJ software (National Institute of Health, MD, USA). Aquaporin 5 staining intensity was expressed as relative optical density (ROD), calculated using the following formula:
$ROD=OD_{specimen}/OD_{background}=\log(GL_{blank}/GL_{specimen})/\log(GL_{blank}/GL_{background})$ where *OD*= optical density, *GL*=grey level, *specimen* –stained area, *background*-unstained area and *blank*-grey level was measured after removing the slide from the light path (Smolen 1990).

4.2.9 Protein extraction and Western blot analysis.

Protein extraction, Western blotting and densitometry analysis were performed by Malgorzata Durlej at Jagiellonian University, Krakov , (see Durlej *et al.* 2010 for methods).

4.2.10 Image capture

An Olympus BH-2 microscope and Leica DFC320 digital colour (c-mount) camera was used in conjunction with Leica Application Suite (LAS) software (v2.3.2R1)to capture all images during bovine and porcine granulosa cell swelling assays. Cell diameter was measured horizontally using Image Pro Plus (v6.3) software (Media Cybernetics MD, USA). For AQP5 IHC imaging a Leica DM4000B microscope with a (c-mount) Q-imaging MicroPublisher 5.0 RTV digital camera was used with Image Pro Plus (v6.3) software.

4.2.11 Statistical analysis

For the bovine granulosa swelling experiment, the difference in the $\log_{10}$ of the mean diameter of cells between the ISO and ISO/HYPO medium was calculated for treatment with and without mercury chloride. The log transformation accommodated the effect of variations in initial (isotonic) diameters on the proportionate change occurring in the subsequent isotonic or hypotonic environment. Results shown are the mean of four separate experiments analysed by ANOVA. The difference between pairs of conditions was analyses *post hoc* by Fisher's Least Significant Difference test.

For the porcine granulosa swelling experiment, fractional change from the average diameter of granulosa cells under ISO conditions was calculated for each treatment

group. The results shown are representative of two experiments and are mean values ± SEM and was analysed by ANOVA followed by the Least Significant Difference Test.

The results shown for porcine granulosa swelling in response to androgen are the mean of three separate experiments. Data from three experiments, each with eight treatment conditions (control, T, HF and T+HF; all under isotonic to isotonic or isotonic to hypotonic conditions) was analysed by ANOVA. Differences between pairs of conditions were analysed *post hoc* by Fisher's Least Significant Difference test. For clarity, results in Fig. 4.5 are shown as non-transformed percentage changes in diameter averaged for the three experiments (±SEM) but with significant effects indicated according to the outcome of ANOVA as described.

The quantification of immunostaining intensity and densitometric analysis of AQP5 protein content were examined by one-way ANOVA. Differences between groups were determined using Tukey's test.

4.2.12 Granulosa and theca cell isolation from treated porcine follicles.

Excised follicles (as described in 4.2.1) were incubated in 700 µl of ISO medium (37°C; 95% air: 5% CO_2) supplemented with antibiotics for 6h in the same treatments groups as described in section 4.2.6. Two BD Falcon™ 24 well multi plates (BD Oxford, UK) were prepared, therefore 12 follicles were incubated per treatment. Following incubation, follicles under the same conditions from both plates were dissected in PBS/PVA (0.1%), under a Leica MZ12.5 stereomicroscope (Leica Microsystems Ltd, Milton Keynes, UK). Firstly the follicles were cut in half with a fresh scalpel and the inner walls gently scraped to create a granulosa cell suspension. The remaining shells were placed in a clean petri dish with fresh PBS/PVA (0.1%) and the theca sheets peeled away using a pair of watchmaker's forceps. The granulosa suspension was passed through a BD Falcon 70 µm cell strainer (BD Oxford, UK) to minimise inclusion of theca or larger debris. Similarly theca sheets were washed on top of a nylon filter with the aim of flushing away any residual granulosa cells. Both granulosa cell suspension and theca sheets were placed into separate 15 ml falcon tubes and spun at 800 x g for 5 min. The supernatant was discarded and the pellets resuspended in 1 ml of fresh PBS/PVA (0.1%) and transferred into 1.5 ml eppendorf tubes. These were spun at 12000 x g for 2 min, the supernatant was removed leaving the pellet in a minimal volume of <2 µl and snap frozen in liquid nitrogen prior to -80°C storage. Three separate experimental repeats were carried out. In order to test for any effect on mRNA integrity caused by the 6h

incubation period, granulosa and theca cells from fresh non-incubated follicles were collected and snap frozen.

4.2.13 RNA extraction, cDNA synthesis and RT-qPCR

Ribonucleic acid extraction of incubated and non-incubated granulosa and theca cells as well as and positive control tissue was carried out using Tri-reagent as per manufacturer's instructions, as described in section 3.2.3. The quality and quantity of RNA was measured using a NanoDrop Spectrophotometer as described in section 3.2.4; the quantity was used to determine the correct amounts of reagents needed for efficient DNase digestion (section 3.2.5). Copy DNA synthesis was conducted as described in section 3.2.10, except that the reaction volumes were not doubled due to limited reagent stocks. This resulted in a cDNA final volume of 20 µl, which was diluted 1:3 to ensure enough cDNA for subsequent RT-qPCR.

The RT-qPCR was conducted using primers for AQP5 and ACTB. Both primer sets used were those displayed in Table 3.2 as they demonstrate 100% compatibility with porcine sequence. PCR conditions were the same as in section 3.2.13; 2 µl of cDNA was added to 10 µl of PCR mastermix and 0.8 µl of both forward and reverse primers and made up to a final volume 20 µl with 6.4 µl of water. Samples were loaded on to a Roche Lightcycler® 480; the cycling conditions and parameters were as in Table 3.3. The procedure was conducted three times giving three experimental repeats.

4.3 Results

4.3.1 Granulosa cell swelling

4.3.1.1 Bovine

Figure 4.4 shows the difference between the log values of cell diameters moved from ISO-ISO or from ISO-HYPO conditions in the absence or presence of $HgCl_2$. Bovine granulosa cells moved from ISO-ISO conditions after 90s did not significantly alter in diameter in the absence of $HgCl_2$. Cells moved from ISO-HYPO conditions after 90s in the absence of $HgCl_2$ demonstrated a significant ($P<0.001$) seven fold increase in the mean log value of cell diameter. In the presence of $HgCl_2$ there was no significant difference between the log value diameter of cells moved from ISO-ISO or ISO-HYPO conditions. The only significant response in terms of diameter increase and therefore granulosa swelling was in response to HYPO conditions in the absence of $HgCl_2$. In terms of bovine granulosa swelling in response to androgen, several experiments were carried out however the results were inconsistent and no conclusions could be drawn (data not shown).

4.3.1.2 Porcine

The relative fractional change of cell diameters, under ISO-ISO and ISO-HYPO conditions with and without $HgCl_2$, is represented in Fig 4.5. There was no significant difference between cells moved from ISO-ISO with or without $HgCl_2$. However, cells moved from ISO-HYPO show a significant ($P<0.001$) 3.4 fold increase in cell diameter relative to mean ISO-ISO cell diameter. Cells moved from ISO-HYPO conditions in the presence of $HgCl_2$ only show a 0.06 fold increase in swelling, therefore $HgCl_2$ inhibited the swelling of porcine granulosa cells under HYPO conditions by 82.4% ($P<0.001$).

4.3.2 Porcine granulosa cell swelling in response to androgen

Porcine granulosa cells treated with T and/or HF or neither (control), transferred from ISO to ISO conditions did not significantly alter in cell diameter. When control cells were moved from ISO to HYPO conditions, mean cell diameter increased by an average of 15% showing a significant difference ($P<0.5$) compared with the control group under ISO conditions. Cells pre-treated with T and moved from ISO to HYPO conditions increased in mean diameter by 27%; this was significantly different ($P<0.001$) to T treated cells under ISO conditions. Cells pre-treated with HF and transferred from ISO to

HYPO conditions were not significantly different to other treatments under the same conditions nor to HF treated cells moved from ISO to ISO conditions. Cells pre-incubated with HF+T demonstrated no significant difference in diameter compared with other treatments under the same conditions but showed a significant difference ($P<0.5$) from the parallel treatment group under isotonic conditions. The most significant effect was that of pre-incubation with T on the degree of granulosa cell swelling under HYPO conditions (Fig 4.6).

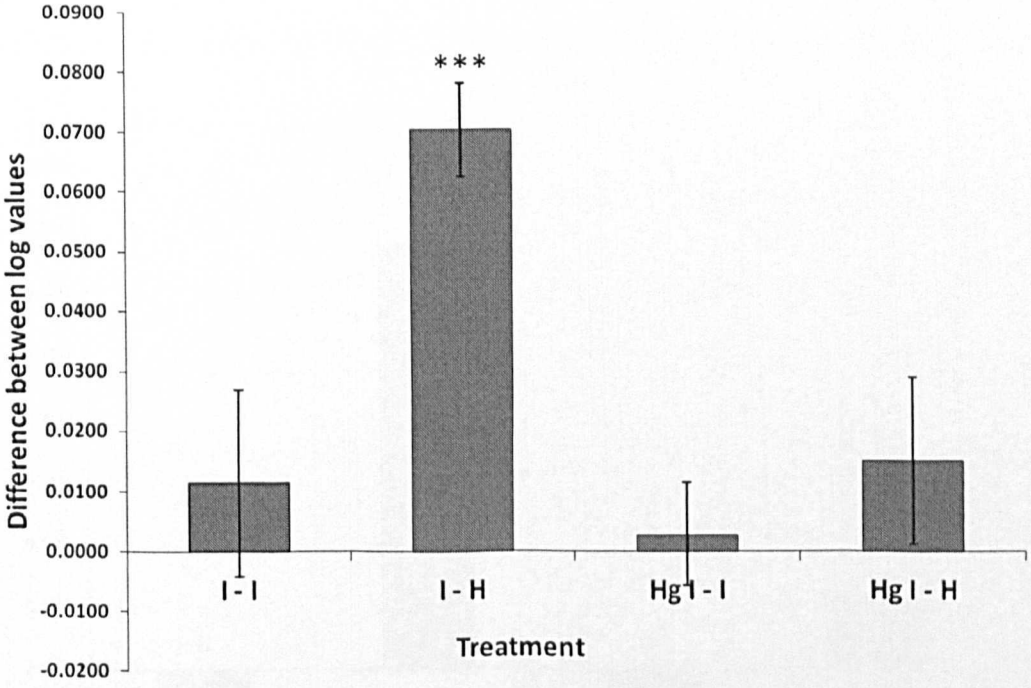

Figure 4.4 Change in the difference between log diameter values of bovine granulosa cells initially incubated in isotonic 319 mOsm/l medium then incubated for a further for 90s in isotonic (I – I), or hypotonic 95 mOsm/l medium (I – H). This was repeated with cells incubated for 90s in isotonic or hypotonic medium supplemented with $HgCl_2$ (Hg I – I and Hg I – H respectively). Results shown are means of four separate experiments, each involving measurements of at least 30 cells under each test condition. Granulosa cells moved from isotonic to hypotonic solution without mercury chloride swelled significantly ($P<0.001$) after 90s. There was no significant difference between the diameters of granulosa cells of the other treatments. Mean values ± SEM. ($^{***}P<0.001$, ANOVA, Fisher's test).

4.3.3 AQP5 immunohistochemistry and Western blot analysis of treated porcine follicles.

Immunological analysis of excised porcine follicles incubated with T and/or HF or neither (control), and then subjected to anti AQP5 antibody IHC revealed a variation in the intensity of labelling. Control follicles showed cytoplasmic staining predominantly of mural granulosa cells as reported by Skowronski *et al.* (2009), however contrary to Skowronski *et al.* this investigation there was staining amongst thecal cells possibly those associated with vasculature (Fig. 4.7 A Control).

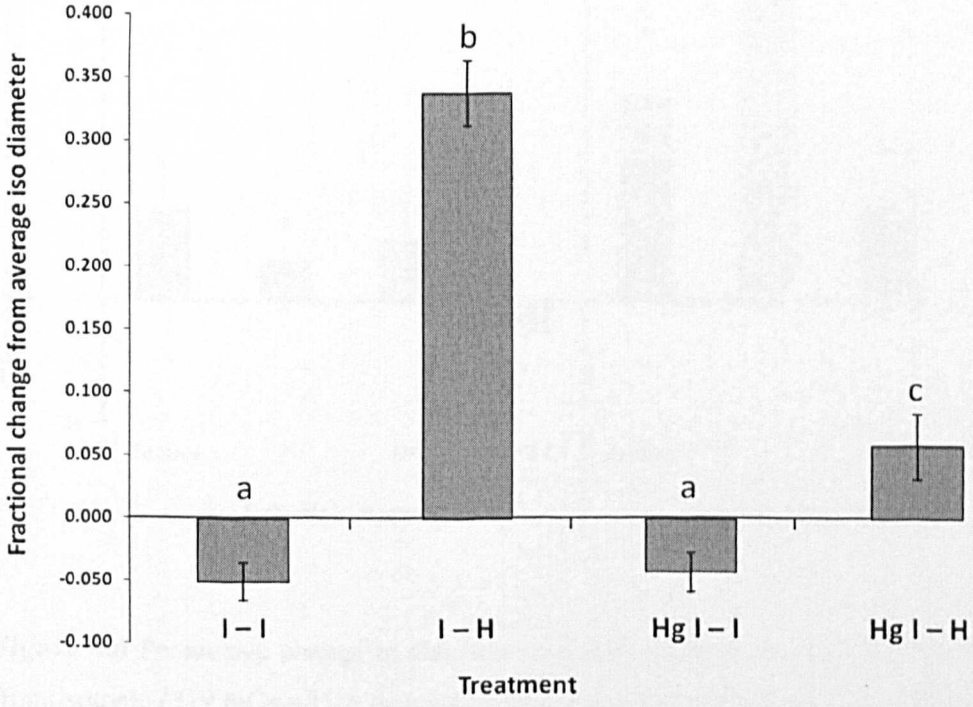

Figure 4.5 Fractional change in the diameter of porcine granulosa cells, relative to the average diameter of cells under isotonic (319 mOsm/l) conditions, in the absence of $HgCl_2$. Cells were initially incubated in isotonic media then incubated for a further for 90s in isotonic (**I – I**), or hypotonic (95 mOsm/l) medium (**I – H**). This was repeated with cells incubated for 90s in isotonic or hypotonic medium supplemented with $HgCl_2$ (**Hg I – I** and **Hg I – H** respectively). Results are representative of two separate experiments, involving the measurement of at least 30 cells from each test condition. Different superscripts denote a significant difference ($P<0.001$ ANOVA, followed by the Least Significant Difference Test). Mean values ± SEM.

Follicles pre-incubated with T demonstrated increased intensity of staining in all granulosa cells. There was also an increase in labelling of certain cell types throughout the theca (Fig. 4.7 T). Hydroxyflutamide treated follicles showed stain throughout the entire granulosa layer but with a much reduced intensity compared with T treated and control follicles. Anti AQP5 labelling of follicles incubated with T+HF showed the least intense staining, with some staining apparent in the mural cells but little throughout the remaining granulosa and theca. These results are quantified in the densitometry

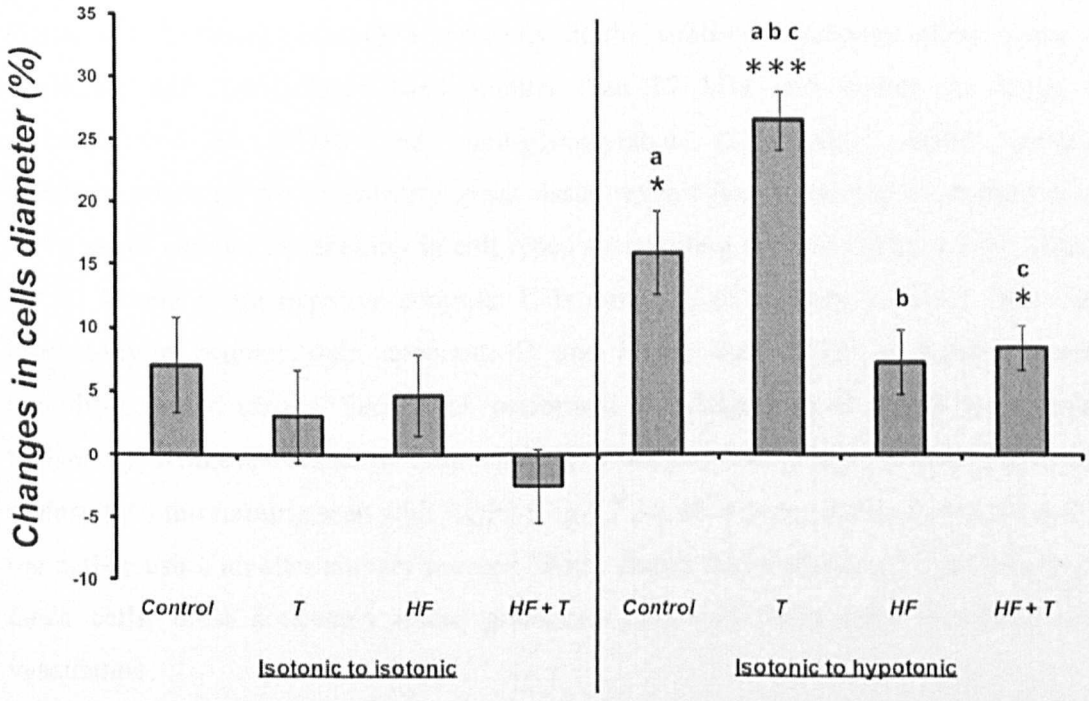

Figure 4.6 Percentage change in diameter of porcine granulosa cells when moved for 90s from isotonic (319 mOsm/l) to isotonic or from isotonic to hypotonic (95 mOsm/l) medium, after preliminary exposure to testosterone (T; 10^{-7}M) and/or hydroxyflutamide (HF; 50 μg ml^{-1}) or neither (Control). Results shown are means of three separate experiments, each involving measurements of at least 10 cells under each test condition. Statistical differences, based on two-way analysis of variance of log_{10}-transformed original values (to accommodate absolute variations in starting cell diameters), are indicated as a comparison of corresponding treatments between isotonic to isotonic and isotonic to hypotonic conditions (* = $P<0.05$, ***= $P<0.001$), and as a comparison of treatments within each condition (common superscript letters indicate $P<0.05$). There were no significant effects of treatment within the isotonic to isotonic group.

calculations. The intensity of staining of T treated follicles was significantly higher than that of control and HF treated follicles ($P<0.05$) and HF+T treated follicles ($P<0.01$). There was no significant difference between control, HF and HF+T treated groups. The same treatment groups of follicles subjected to WB analysis also revealed a similar pattern of effects (Fig. 4.8 A and B): AQP5 was identified as a 28 kDa protein, the expression of which varied according to treatment group. Relative to ACTB, pre-treatment with T had a significant effect on AQP5 expression ($P<0.01$) doubling the level of expression compared with control follicles. Hydroxyflutamide treatment alone and in combination with T was without significant effect.

Figure 4.9 A shows anti-AQP5 reactivity in the sublingual salivary gland (done in duplicate) with an isolated band smaller than 37 kDa and within the range of glycosylated (34 kDa) and non-glycosylated (27 kDa) AQP5 protein. Immunohistochemistry on salivary gland tissue reveals heavy staining of striated ducts and a small amount of labelling in cell types surrounding the acini (Fig. 4.9 B). Figure 4.9 C, D and E are negative controls: C is omission of primary antibody with only haematoxylin counter stain apparent; D and E are both NIRS at 1:200 showing incredibly varied results. Section D, performed by Malgorzata Durlej at Jagiellonian University, Krakov, does show faint staining of oocytes and granulosa cells and is less intense than the staining seen with AQP5 (Fig 4.7 A). However, section E, carried out by the author using an alternatively sourced NIRS, shows dense labelling of granulosa and theca cells, most noticeably mural granulosa cells and theca cells associated with vasculature.

4.3.4 AQP5 mRNA expression in granulosa and theca cells of treated follicles

There was no evidence of AQP5 mRNA transcript in the granulosa or theca of porcine follicles from three separate experimental repeats. Salivary gland positive control was run in parallel as an indicator of primer specificity and demonstrates a significant abundance of AQP5 transcript. Non-incubated granulosa and theca cells also did not demonstrate any AQP5 transcript. Following the unexpected absence of AQP5 mRNA, the RT-qPCR was repeated and revealed the same outcome.

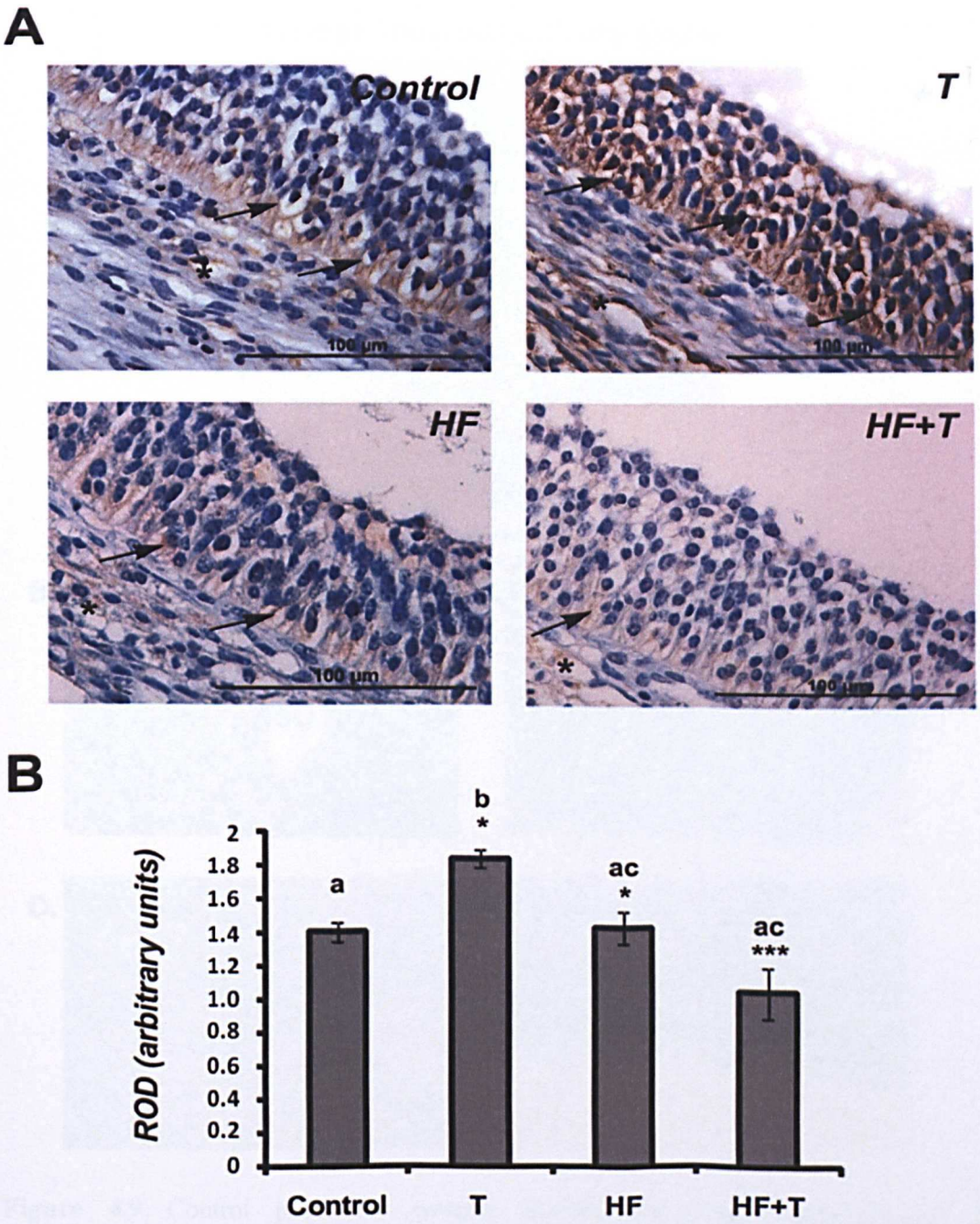

Figure 4.7 (A) Immunohistochemical localization of AQP5 in porcine medium-sized antral follicles following testosterone (10^{-7}M; T) and/or hydroxyflutamide (50 µg ml^{-1}; HF) treatments. Arrows indicate positive staining in granulosa cells; asterisks indicate staining within theca compartments. All slides were counterstained with Harris hematoxylin. **(B)** The intensity of immunohistochemical staining for AQP5 in porcine ovarian follicles from control and testosterone and/or hydroxyflutamide treated groups, expressed as ROD (relative optical density; arbitrary units) of diaminobenzidine reaction products. Mean values ± SEM. Different letter superscripts indicate significant differences; $^{*}P<0.05$, $^{***}P<0.001$ (ANOVA, Tukey's test).

PAGE
MISSING
IN
ORIGINAL

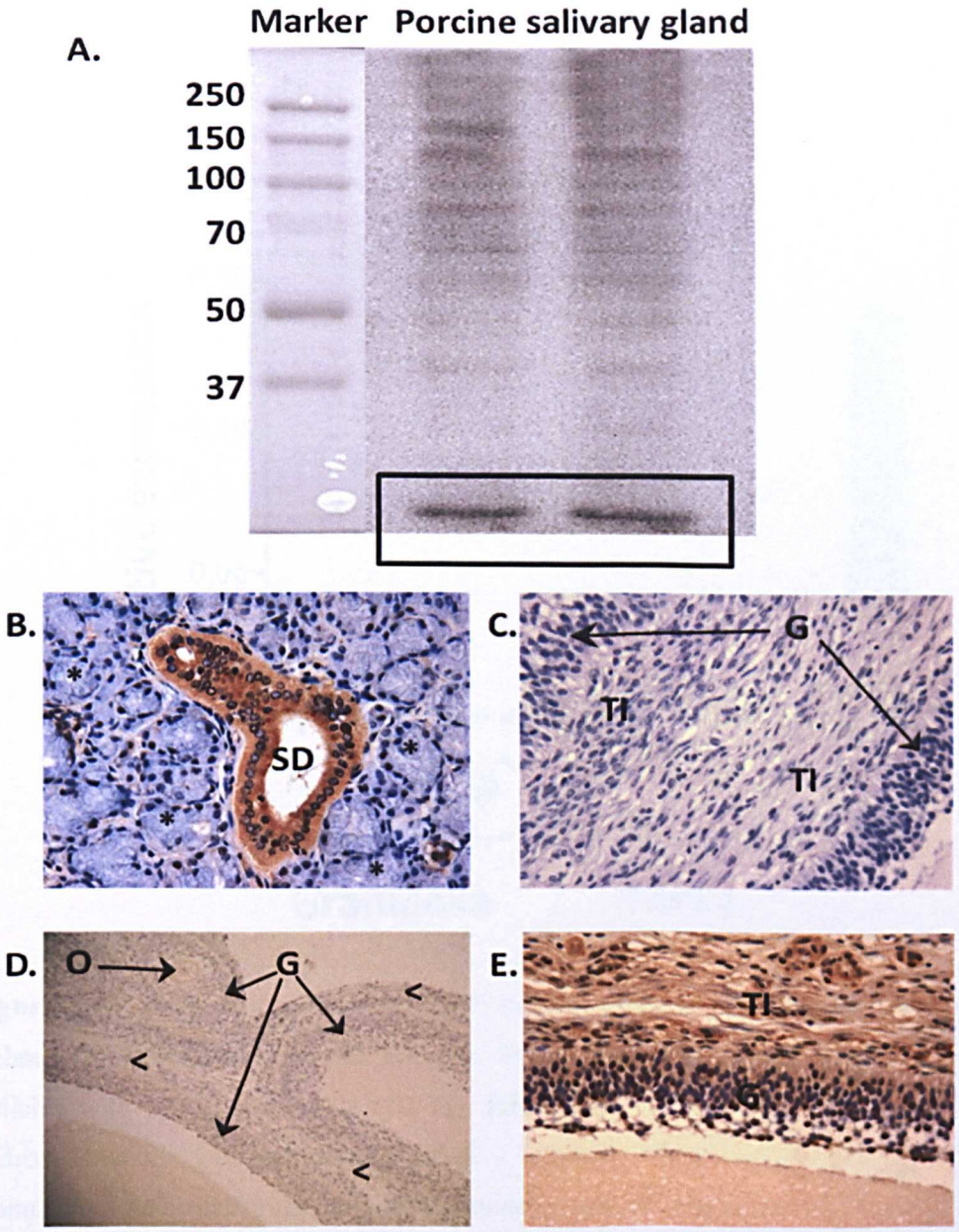

Figure 4.9 Control panel for western blotting and immunohistochemistry. (**A**) Representative blot of AQP5 protein expression in porcine salivary gland. (**B**) IHC staining of anti AQP5 in paraffin embedded tissue sections, the striated ducts (**SD**) are heavily stained with some staining of cell types surrounding the acini (*). (**C**) IHC negative control by omission of primary (anti AQP5) antibody; there is no signal present. (**D**) Non-immune rabbit serum at a 1:200 dilution on porcine ovary tissue. There is some feint staining of certain cell types most noticeably the granulosa and oocyte although this is difficult to see against the background staining [performed by Malgorzata Durlej at Jagiellonian University, Krakov]. (**E**) Alternative non-immune rabbit serum at a 1:200 dilution on porcine ovary tissue resulting in heavy non-specific staining of both granulosa and theca. [(**B**), (**C**) and (**E**) were performed by the author].

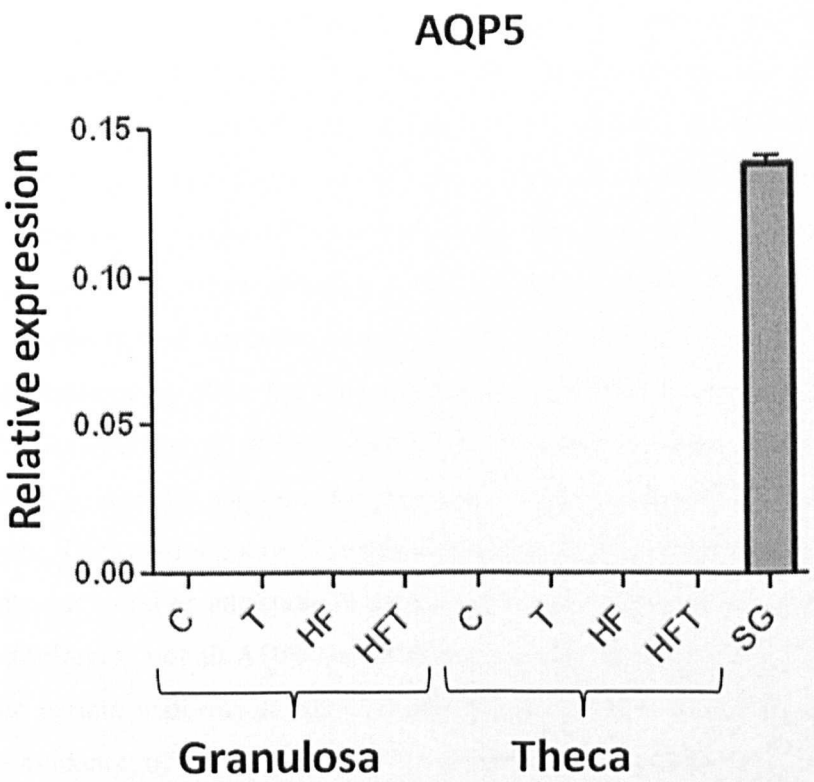

Figure 4.10 Relative abundance of AQP5 mRNA transcript in granulosa and theca cells isolated from pre-treated porcine follicles. Treatments included 6 h incubation of 5-6mm follicles with **T** – Testosterone (10^{-7}M), **HF** – hydroxyflu tamide (50 μg ml^{-1}), **HFT** – hydroxyflutamide and testosterone and **C** – nothing. There was no AQP5 transcript in granulosa or theca cells relative to endogenous control ACTB, however salivary gland (SG) demonstrated an abundance of AQP5 expression. The data are inclusive of three experimental repeats, on which the RT-qPCR was carried out twice.

4.4 Discussion

4.4.1 Granulosa cell swelling

These findings show that bovine and porcine granulosa cells swell in response to tonic stimulation. The rapid nature of the swelling i.e. within 90s of exposure to hypotonic solution, points to the presence of water channels allowing fast transmembrane flux of water. In both bovine and porcine swelling assays, the cells swelled significantly when subjected to hypotonic conditions (Fig. 4.4 and 4.5), consistent with the observations of McConnell *et al.* (2002). When carried out in the presence of $HgCl_2$, both bovine and porcine cells demonstrated mercurial sensitivity which decreased the ability of the cells to swell by approximately 80%. Mercury inhibition is a well documented characteristic of AQP function (Hirano *et al.* 2010) therefore the rapid flux of water, diminished by the addition of $HgCl_2$, strongly suggests the presence of AQPs in both bovine and porcine granulosa cells. The small amount of residual swelling seen in the cells of both species after Hg treatment could be attributed to the slower water permeation via non-facilitated diffusion. Additionally not all AQPs are mercurial sensitive including AQP4 (Jung *et al.* 1994a, b) and certain isoforms of AQP7 (Ishibashi *et al.* 1997; Kuriyama *et al.* 1997). There is no evidence of either AQP4 or -7 in porcine granulosa cells however this investigation has identified mRNA transcript for both in bovine granulosa cells (section 3.3.4.3 and 3.3.5.2). However, evidence of protein has yet to be determined.

In terms of the functional relevance, these findings merely allow for the conclusion that there are mercurial sensitive water channels in granulosa cells. There is no evidence in the literature that granulosa cells swell in vivo and so their ability to do so as reflected in this experiment is unlikely to represent an aspect of normal granulosa cell function. It simply indicates the presence of water channels in their membranes. This methodology creates a false osmotic gradient relative to the inside of the cell and so water will move into or out of the cell in response to the osmotic differential. *In vivo*, water movement is osmotically driven from one side of the granulosa cell layer to the other. This drives transcellular water flux through the cell; the rate of flux may increase but water would not accumulate and therefore nor would its diameter change.

4.4.2 Porcine granulosa cell swelling in response to androgen

Follicles pre-treated with T demonstrated a 27% increase in diameter in response to hypotonic conditions (Fig. 4.6). This effect was counteracted by incubation with HF.

Hydroxyflutamide inhibits the genomic action of T as it competes for the AR site which cannot then bind to the ARE. This stops any gene transcription that would have been triggered by activated AR. Therefore the increased swelling seen with T suggests the increased fluid flux may be due to the up regulation of androgen modulated water channels. The duration of the incubation period was appropriate for changes in gene expression to be manifest. Incubation with HF alone also led to a significant reduction of water movement, possibly suggesting inhibition of endogenous androgen action on water channel function.

These findings suggest androgen mediated regulation of water channel expression in porcine granulosa cells.

4.4.3 Androgen modulated AQP5 protein and mRNA expression

Porcine follicles treated with anti-AQP5 antibody demonstrate clear labelling of the mural granulosa cells as well as some staining of cells within the thecal compartment (Fig. 4.7 A (Control)). Mural granulosa cells are those nearest the basal lamina and are therefore the first layer of avascular granulosa cells across which any transudate has to pass. In the case of rapid movement of fluid, the mural cells would be the optimum site for the localisation of water channels. Skowronski *et al.* (2006) identified both AQP5 and -9 in the mural granulosa of porcine follicles, however no protein was seen in any of the cells types of the theca. In this current investigation follicles pre-incubated with T showed what appears to be a significant up regulation of anti-AQP5 labelling in all granulosa cells and certain theca cells (Fig. 4.7 A (T)). This effect appeared significantly decreased in follicles incubated with HF and T again suggesting a genomic response to T countered by HF (Fig. 4.7 A (HF) and (HF+T)).

To quantify the IHC experiments the intensity of staining was translated into relative optical density (4.7 B). This reflects the changes in staining intensity and allows analysis of variance to be performed. The statistical analysis therefore supports the notion that T up regulates AQP5 protein expression in porcine granulosa cells. This further suggests that the identification of the androgen sensitive water channel, as seen in the swelling assay, as AQP5.

The same antibody used for IHC was used for WB detection of AQP5 protein extracted from pre-incubated whole follicles. The results (Fig. 4.8 A) concur with those of the IHC (Fig. 4.7) in that protein expression of AQP5 is significantly up regulated in follicles pre-

treated with T. The effect of T was again diminished by the concurrent incubation with HF. Densitometric analysis of the protein band intensity, normalised against ACTB (Fig. 4.8 B) quantifies the variation in protein expression. Western blot protein isolation was performed on whole follicles and so the detection of AQP5 cannot be attributed to any particular cell type. However, the pattern of variation clearly corresponded with that for IHC.

The findings of these two investigations taken together strongly point to androgen mediated AQP5 function in antral follicle fluid flux, by a mechanism involving the AR and altered gene expression. However, certain questions arise when considering the quality of the antibody used for both techniques. Figure 4.9 (A) shows a blot of porcine salivary gland treated with AQP5. Whilst there is a clear band below the 37 kDa marker, the exact size of the band is difficult to ascertain due to limited marker bands at the low molecular weight end of the range. The rough size of the band in conjunction with its intensity strongly suggests that it is AQP5, as expected in a positive control tissue. However, there are also numerous faint bands suggesting a certain degree of non-specificity. The labelling of salivary gland with anti-AQP5 is localised to the striated ducts (Fig. 4.9 (B) SD) and not the expected apical membrane of the acini (Fig. 4.9 (B) asterisk; Krane *et al.* 2001). The negative controls included omission of primary antibody and two sources of NIRS. Both NIRS show non-specific staining albeit at very different intensities, when used at the same dilution as anti-AQP5. Concerns surrounding the specificity of the polyclonal serum antibodies used in this investigation are discussed in more detail in section 2.5.4.

Given the uncertainty of these antibodies and results with the evidence supporting non-specific reactivity of these antibodies, it was decided to perform RT-qPCR on granulosa and theca cells isolated from pre-incubated follicles.

The follicles used for RT-qPCR were collected and prepared at a different time from those discussed above and so conditions of source animals, seasonal affected change and possible experimental procedure may have varied slightly. However, it was surprising to find no evidence of AQP5 mRNA transcript whatsoever, in both theca and granulosa cells. Expression in salivary gland was abundant and therefore primer non-specificity could be discounted. It is widely accepted that the presence of transcript does not mean the presence of a functional protein, however to have protein expression without transcript is much more difficult to explain.

It could suggest that either the antibody is picking up something other than AQP5, which is also androgen sensitive, or the expression of AQP5 in porcine is more stage-dependent than had been previously considered. Loss of transcript due to experimental procedure could have occurred, however, one would still expect some evidence of transcript. The same procedure was used as in section 3.2.2.3 for small and medium bovine follicle granulosa and theca cell collection. As discussed in section 3.4.4 the transportation of ovaries on ice, as opposed to 37°C PBS, may have reduced nuclease activity. The main difference compared with the RT-qPCR performed on granulosa and theca cells collected from bovine follicles, was the 6h incubation of follicles prior to cell isolation. However, if transcript levels had deteriorated during the incubation period, some evidence of transcript would be expected in the non-incubated samples.

4.4.4 Conclusions

Taking these results into account, the only completely reliable conclusion that can be drawn from th is investigation is that both bovine and porcine granulosa cells have mercurial sensitive water channels, most likely AQPs. The AQPs present in porcine granulosa cells are androgen sensitive and up regulated by physiological levels of T. Immunohistochemistry and WB analysis provide some evidence to suggest AQP5 as the androgen sensitive AQP, although this does need further investigation. The RT-qPCR results however, do not support this conclusion. Both AQP5 and -9 proteins have previously been identified in porcine granulosa cells by Skowronski *et al.* (2006) using WB and IHC. Aquaporin 5 was initially targeted in the current study because it has as androgen response element in its promoter region (Moehren *et al.* 2008). However, current limited evidence indicates that AQP9 is also very closely associated with androgen modulation (Pastor-Soler *et al.* 2002; 2010). Further AQP5 detection via WB on the samples used for the above RT-qPCR investigation, including AQP9 RT-qPCR, would go part way to clarifying this situation. It seems plausible that the androgen modulated AQP in porcine granulosa could in fact be AQP9. Further investigation may have to wait until a clearer picture of steroid regulation of AQPs, especially AQP9, emerges in the literature.

Chapter 5

General discussion and conclusions

The overall purpose of the investigations described in this thesis was to determine the potential role of aquaporins in the developing ovarian follicle. The first objective was to identify tissue expression and cellular/subcellular localisation of AQPs in the bovine ovary and to determine if AQPs are differentially expressed in specific tissue/cell types. Secondly, this investigation sought to establish whether the expression of AQPs in these tissue/cell types change as follicular development progresses. This was done with the overall aim of strengthening current understanding of what drives the growth of the ovarian follicle in terms of, osmotic gradients, fluid dynamics and hormonal influence during specific stages of antral follicle development.

5.1 Immunohistochemistry

The initial stages of this investigation were dependent on accurately identifying the stages of follicle development, and characterising a panel of polyclonal serum antibodies. Through this investigation it has become clear that a singular diagnostic approach to follicle characterisation is subjective at best. This also highlights the risk of excluding objects of potential interest in order to satisfy the currently accepted criteria. As mentioned in section 2.5.5 a range of techniques is therefore advisable if accurate and reliable conclusions relating to the stages of follicle growth and development are to be drawn.

In terms of antibody characterisation from the available bank of five antibodies, only those for AQP1 and -2 were found to be suitable for application to the bovine ovary. Anti-AQP1 and -2 were affinity purified antibodies. The results from the remaining polyclonal serum antibodies against AQP3, -4 and -5, were deemed unreliable at this stage due to their demonstration of significant non-specificity.

Aquaporin 1 was localised to the endothelial cells of the ovarian vasculature. This is consistent with the findings of Skowronski *et al.* (2009) who identified AQP1 in porcine ovarian endothelial cells. All fluid reaching the follicle originates from the circulatory system and so endothelial AQP1 may play a significant role in modulating the availability of interstitial fluid in the tissues of the ovary. Anti-AQP1 demonstrated abundant staining of endothelial cells which increased in accordance with the developing

vasculature of growing follicles. This can be seen in preovulatory follicles where the AQP1-labelled thecal vasculature is abundant and in very close proximity to the basal lamina (Fig. 2.7 (5)). Vascularisation increases with follicle development in parallel with increased production of E_2 and recent reports have provided strong evidence that AQP1 is an angiogenic factor and modulated by steroid hormones, most notably E_2. It would seem therefore that due to its vascular location and possible modulation by E_2 that AQP1 is potentially the pivotal AQP involved in fluid dynamics of the developing bovine ovarian follicle.

Aquaporins are bi-directional water channels and so AQP1 is likely to facilitate both the outward and inward movement of fluid in capillaries, according to the direction of prevailing osmotic gradient. Aquaporin 1 labelling was still abundant in the vasculature of atretic antral follicles suggesting that AQP1 could play a role in the reabsorption of antral fluid. Usually the lymphatic system is largely responsible for the reintroduction of interstitial fluid back into the circulatory system. Therefore, relationship between AQP1 and lymphatic vasculature would be a valuable area to investigate.

Aquaporin 2 was not detected anywhere in the bovine ovary; it was abundant however in positive control tissue. These results again agree with those of Skowronski *et al.* (2009) who also did not find AQP2 present in the porcine ovary.

Thoroddsen *et al.* (2011), presents the only other investigation alongside Skowronski *et al.* (2009) and this investigation to consider AQPs in the ovarian follicle. The investigation by McConnell *et al.* (2002) looked at rat granulosa cells in isolation. Thoroddsen *et al's* results are rather intriguing as they fundamentally differ from those of other ovarian investigations. Firstly they saw only minimal staining of capillary endothelium with AQP1; this differs markedly from the literature consensus as AQP1 is predominantly a vascular protein and should be expressed in abundance. While AQP1 has been reported in other cell types such as kidney proximal tubules, it is always in parallel with abundant vascular expression in the tissue being investigated. Secondly, Thoroddsen *et al.* found AQP1 in both theca interna and granulosa cells; again this is novel information and whilst the staining does appear to be specific to these two cell types it i s completely cytoplasmic with little evidence of membranous localisation. Aquaporin 2 was located to granulosa, theca interna and externa, which differs from rat granulosa (McConnell *et al.* 2002), porcine (Skowronski *et al.* 2009) and bovine (present study). Aquaporin 2 has been identified in human endometrium and myometroium (He *et al.* 2006; Jablonski *et al.* 2003) and so these results could be highlighting a species

differentiation in AQP2 ovarian expression. Thoroddsen *et al's* result for AQP3 and -4 also demonstrate complete cytoplasmic staining of both theca and granulosa cells. As discussed in section 2.1, AQPs are usually localised to very specific areas of a cell membrane, and so the absence of any clear membranous staining and the ubiquitous localisation of all four AQPs is interesting. Whilst these results may be highlighting species differences it may also be suggestive of potentially questionable antibody quality. Thoroddsen *et al* do not include examples of positive control with any of the four antibodies, which would have helped to clarify some of these issues.

5.2 Aquaporin expression during folliculogenesis

The predominant expression of *CYP17A1* and *CYP19A1* in theca and granulosa cells respectively, suggests that the methodology for cell isolation is rigorous enough to have ensured minimal cross contamination of both cell types. Not only have they allowed the determination of cell population purity and therefore reliability of granulosa and thecal results, but their pattern of expression also helps to confirm the stages of follicle development. *CYP17A1* expression is initiated in theca cells of type-5 (early antral) follicles and increases as follicles develop to dominance size, after which levels tended to decline. Similarly *CYP19A1* expression is also initiated, albeit at low levels, in type-4 (preantral) follicles; this increased as follicles developed to large antral size then also tended to drop at the preovulatory stage. These results are consistent with the literature and provide a reliable reference point for examining changes in the granulosa and theca AQP transcriptome.

Table 3.4 summarises the RT-qPCR results for *AQPs -1, -2, -3, -4, -5, -7* and *-9* in granulosa and theca cells of follicles from type-4 to pre-ovulatory type-6 follicles. It shows that no AQP expression occurs in the theca or granulosa cells of type-4 follicles. The expression of *AQP1, -5, -7* and *-9* begins in the theca of type-5 follicles, the time of antrum formation. Aquaporin -1 is known to transport gases such as CO_2 and NO as well as water. Aquaporin 5 is also a classic water channel but with no evidence to date that it is anything other than a water transporter. Aquaporin 7 and -9 are both aquaglyceroporins and facilitate the flux of small neutral solutes such as glycerol; AQP 9 also allows the passage of urea and they both facilitate the transportation of arsenite (Liu *et al.* 2002). Without full understanding of urea and glycerol transport mechanisms in follicular cell types, it is difficult to speculate on the role of solute transport via AQP7 and 9, in terms of their affect on osmotic pressures. Aquaporin 5 may aide in the

transcellular flux of fluid, altering the general permeability and interstitial pressure within the thecal compartment.

At the type-5 stage changes occur within the granulosa compartment, in that small foci of fluid develop as a result of apoptosis and/or reduced gap junctions (Nuttinck *et al.* 2000). The coalescing fluid must initially originate locally from the surrounding granulosa; as these voids get bigger there would need to be an ever increasing secretion of large osmolites within the forming antral cavity to recruit fluid from the surrounding thecal compartment. This would include materials such as GAGs as described by Clarke *et al.* (2006). Type-5 is also the stage at which follicles express LHr and steroidogenic enzymes in the theca, this could potentially initiate the expression of AQPs which are steroid hormone sensitive, such as AQP5 (Richard *et al.* 2003; Moehren *et al.* 2008) and -9 (Pastor-Soler *et al.* 2002; 2010). Aquaporin 1 expression has been shown to be modulated by E_2 (Fisher *et al.* 1998;) and in this investigation AQP1 becomes increasingly abundant in the theca of antral follicles which could be a result of increased E_2 synthesis as the follicles develop. This is concurrent with the IHC evidence, of AQP1 vasculature labelling, presented in this study (Fig. 2.7 (5)).

Fully antral follicles of 2 mm in diameter now demonstrate AQP1,-3,-4,-5,-7 and-9 expression in both theca and granulosa cells. With the exception of AQP4 the remaining AQPs are more abundant in theca than granulosa cells. It could be suggested therefore that fluid flux in the bovine developing follicles is predominantly regulated by thecal AQPs. The relatively low expression of AQPs in granulosa cells does not necessarily mean they are functionally irrelevant. It could simply be that AQPs are only expressed, for example, in the mural layer only; as seen in Skowronski *et al*'s AQP5 and -9 results from porcine mural granulosa cells. These AQPs could in fact be pivotal in allowing rapid transcellular flux of fluid under the influence of osmotic differential between the thecal compartment and the antral cavity. Although AQP transcripts may be present in both cell types, the regulation of translation will be dependent on the availability of relevant transcription factors. Certain AQPs may be expressed in terms of mRNA in both thecal and granulosa cells but may be successfully translated into functional protein in only one cell type (Rodríguez *et al.* 2001). Therefore mRNA expression and function will not be directly relative to protein expression.

In terms of interpretation of these gene expression results, it is difficult to speculate on the functional relevance of these data without appropriate and reliable protein analysis.

The expression levels for each gene are represented as box and whisker plots (Fig 3.13 and 14) which reveal a large spread of data for each AQP. As mentioned previously, this may be a result of variation between individual follicles, general health, nutrition and reproductive status among the animals from which the ovaries were obtained. It could also be a reflection of differences in the stage of follicle development within these groups. These follicles were chosen on the basis of external gross morphological and FF appearance. Even though grouped in the same category, certain follicles may have been more or less advanced in development and so me may have been atretic. Thus the dynamic nature of follicle development provides a large scope for variation. Five experimental repeats were carried out and so patterns pertaining to individual repeats were looked considered. For example if all results for repeat 1 were outliers, a technical error or difference could have been the reason and the entire results cohort would have been excluded. However, the outliers identified all originated from the sample of different repeats. Increasing the number of experimental repeats could have gone some way to resolving this issue concerning the large spread of data.

Thoroddsen *et al.* (2011) also noted *AQP1* to -4 mRNA expressions in both theca and granulosa cells, of early preovulatory to post-ovulatory phase follicles. A strength of their study was a precise allocation of follicles into four ovulatory phases, having followed the progress of follicle development of each human subject by ultrasound. Despite this, their data also demonstrates a large spread of data for each AQP gene expression. As mentioned above, this variation could reflect a difference between individuals in terms of follicular development as well as differences between individual follicles.

Thoroddsen *et al.* (2011) presented evidence of AQP1 to -4 protein expression via IHC. Their IHC however was not done on sections from each follicle group and so there can be no comparison of gene and protein expression across the stages of ovulation. This would have helped to answer certain questions regarding the validity of the IHC results, as discussed above in section 5.1. Secondly they do not fully describe their cell isolation procedure nor do they present any evidence of specific theca or granulosa cells markers. The purities of their two cell populations are also unclear, making the conclusion drawn from the AQP RT-qPCR data uncertain. The Thoroddsen *et al.* data does however, support the present study in the isolation of mRNA for a range of AQPs in both theca and granulosa cells, that the spread of data for individual genes can be large and that AQP antibodies may need further investigation in terms of validity.

5.3 Granulosa swelling assays.

This investigation provided conclusive evidence of the ability of bovine and porcine granulosa cells to swell when moved from isotonic to hypotonic conditions. The ability of the cells to swell rapidly demonstrated by a 7 and 3.4 fold increase in diameter by bovine and porcine cells respectively. This was followed by significant inhibition of swelling on the addition of $HgCl_2$ strongly suggests the presence of AQPs. This is consistent with the swelling investigation by McConnell *et al.* (2002), which reported a doubling of granulosa cell volume following 90s exposure to hypotonic conditions. This was also inhibited by $HgCl_2$. However, control responses to isotonic conditions were not shown by McConnell *et al.* and neither did they state the osmolarity of their isotonic and hypotonic solutions. Secondly they describe changes in cell volume which assumed a spherical shape to the granulosa cell. For the method to work, cells need to adhere within the Cunningham chamber so as not to be washed away when media is changed, and so the cell is anchored to the slide by a section of membrane. In this situation the entire cell is unable to swell symmetrically, and so assuming a spherical shape could lead to inaccurate measurements. The current investigation does not go as far as to calculate volume from diameter measurements and so eliminates this possible source of error. However, taken together, the two investigations present evidence of mercurial sensitive water channels in the granulosa cells of rat, bovine and porcine. T he present also supports McConnell *et al's* (2002) finding that granulosa cells are capable of rapid transcellular fluid transport.

As discussed in section 4.1, androgens can have a direct or in-direct influence on folliculogenesis. During early antral follicle development theca cells already expressing AR begin to express LHr and certain steroidogenic enzymes (Bao *et al.* 1997). The exact influence of gonadotrophins, steroid hormones and growth factors on the process of antrum formation and growth remain uncertain, as does molecular mechanism by which growth actually occurs. However, the transition from gonadotropin independence to gonadotropin dependence and the acquisition of steroidogenic capacity are initiated at the time of antral formation in type-5 follicles (Aerts and Bols 2010). After having ascertained the presence of AQPs in the granulosa cells of both bovine and porcine, it was logical to consider the potential regulation of AQP expression by steroid hormones.

The pre-incubation of porcine granulosa cells with T displayed a significant increase in their capacity to swell when moved from ISO to HYPO conditions, compared with control cells and those incubated with the anti-androgen HF. This investigation assumed

that the duration of incubation allows time for the genomic effects of T to manifest themselves. Secondly, if the effects of T are countered by HF it would be clear that the effect of T was as a result of AR-mediated genomic effects. Thus this investigation indicates that T up-regulates the water transporting mechanisms of granulosa cells and, establishes a connection between AQPs in granulosa cells and their potential modulation via androgen.

As previously mentioned AQP5 was considered a candidate for androgen modulation due to the ARE in its promoter region. However, AQP5 is also reported to have an ERE in the promoter region allowing a potential explanation of the result in terms of aromatised T. The abolition of the androgen effect by HF appears to exclude this possibility. Intriguingly, HF on its own also resulted in decreased swelling. This could be attributed to the inhibition of endogenous androgen or another effect of HF itself. Hydroxyflutamide is a competitive inhibitor of T by binding to the AR, so whilst it stops T from binding to the receptor and acting upon AREs, free T remains. It seems possible that any T transported into granulosa cells unbound to AR would be aromatised to E_2, there is also the possibility that free androgen could act on non-genomic (cell membrane) receptors. Whilst is seems highly likely that the results of the swelling assay are indicative of genomic effects of T and HF, and not E_2 this experiment would benefit by the substitution of T with non-aromatizable DHT.

These conclusions and possibilities also apply to the IHC and WB results. However whilst the IHC and WB results may parallel those seen in the swelling assay, certain questions do surround the validity of the anti-AQP5 antibody. The non-specificity of this antibody may be masking true AQP protein expression and needs further investigation.

In order to localise AQP5 mRNA to granulosa and theca cells and to determine if its expression is influenced by androgen, RT-qPCR was performed on cells isolated from follicles collected at a different time of the year than from those used for the initial swelling assays and protein investigations. Whilst incubated under the same four conditions as described for the swelling assay, IHC and WB, no AQP5 transcript could be found in the incubated and non-incubated samples. There was AQP5 transcript in abundance in the salivary gland positive control tissue. As discussed in 4.4.3 the reasons for the complete absence of transcript remain unclear and needs further investigation. This is particularly important in light of Skowronski *et al's.* (2009) identification of the protein in porcine mural granulosa cells by WB and IHC. These results are rather convincing and suggest that AQP5 is expressed in porcine granulosa cells.

The fact still remains however, that steroid sensitive water transport is operative in porcine granulosa cells. An alternative target for further investigation would be AQP9. Aquaporin 9 was also identified in porcine granulosa cells by Skowronski *et al.* (2009) and AQP9 transcript had been identified in bovine theca and granulosa cells in this current study. It has also been associated with androgen modulation, particularly in the male reproductive tract (Pastor-Soler *et al.* 2002; 2010). However, information pertaining to the actual presence of an ARE in AQP9 gene is not available as yet. Therefore, our understanding of AQP9 in terms of androgen modulation remains limited until more evidence emerges from the literature.

Whilst the initial IHC study only provided a clear result for AQP1 it would be expected that AQPs would be localised to both basal and apical membranes of cells in order to allow water to transudate the cell. Further investigations with fully validated antibodies, covering the range of remaining AQPs, are needed to resolve this.

It is accepted that FF is derived from thecal capillary vasculature which continue to develop as the follicles grow and expand. Differences in vascular supply could be involved in the attainment of dominance (Acosta 2007; Martelli *et al.* 2009).

However, it could also be that dominance depends on the degree of vascular permeability or the ability to modulate the degree of permeability, not just the amount of vascularisation that surrounds a follicle. This may be particularly so at the early stages of antrum development and recruitment when the follicular vasculature is still developing.

In a review of antrum formation and FF, Rodgers and Irvin-Rodgers (2010b) highlight the importance of increased permeability of the thecal vasculature leading to oedema of the thecal compartment. They discuss the findings of Clarke *et al.* (2006) who identified a 'blood-follicle barrier' at sizes >100 kDa probably existing at the levels of the follicular basal lamina and the thecal vasculature. Clarke *et al.* (2006) also identified locally secreted large osmotically active molecules as discussed in 1.10.2, thought to contribute to an osmotic gradient. Rodgers and Irvin-Rodgers recognise the potential of AQPs in transmembrane fluid transport, as identified by McConnell *et al.* (2002), but question the need for them. If granulosa cells are 'leaky' and if proteins up to 100 kDa can traverse the basal lamina and gain entry into the FF, then surely the movement of such a small molecule as water would be uninhibited and therefore would not need facilitation?

The function of AQPs however, is probably more complex than has been considered to date. There is increasing evidence to suggest that AQPs may serve to function as transporters of many molecules, not just water and glycerol. This study proposes that AQPs are fundamental to the developing follicle, particularly in terms of thecal vascular permeability via AQP1. The abundant localisation of AQP1 to capillary endothelial cells, venules and veins suggests the flux of water across the walls of low-pressure vessels. Thus AQPs may allow for the rapid movement of water in response to shallow osmotic gradients. This investigation supports the notion of rapid transcellular flux via AQPs in granulosa cells in response to hypotonic conditions. The increase in granulosa permeability in response to androgen could allow for a coordinated response to the production of androgen. This would be initiated at the type-4/-5 follicle stage and the beginning of antrum formation. This investigation has provided evidence of AQP5, -7 and -9 in the theca cells of type-5 follicles; whether these are androgen modulated remains to be determined. However, they may be involved in the supply of water, glycerol and other solutes which may act as osmolites and/or nutrients within the thecal compartment. Their appearance at this crucial stage of follicle development strongly suggests an important role for AQP5, -7 and -9 in parallel with AQP1, in antrum formation. The mRNA of all AQPs studied is expressed in the theca and granulosa of small antral follicles and persists throughout follicle development. The relevance of mRNA to functional protein expression however needs further investigation.

5.4 General Conclusions

In conclusion, this study has revealed for the first time the involvement of AQPs across all stages of bovine ovarian follicle development. It has provided evidence to further our knowledge of fluid flux in the bovine and porcine ovary and in doing so has identified AQPs as the potential facilitators and modulators of fluid dynamics. The following conclusions can be stated:

- Rabbit polyclonal serum antibodies raised against rat AQP antigen need to be fully characterised for reliable and valid cross-reactivity in domestic species.
- Aquaporin 1 is a pivotal AQP due to its presence in vascular endothelial cells and increase in abundance as vascularisation develops.
- Transcripts for *AQP1, -3 -4 -5 -7* and *-9* are present in both granulosa and theca cells of bovine antral follicles. Expression of *AQP1, -5, -7* and *-9* is initiated in type-5 theca cells.

- Aquaporin expression is generally higher in theca cells than granulosa cells.
- Granulosa AQP expression, albeit relatively low, may occur in limited locations, for example the mural granulosa cells.
- Granulosa cells are able to swell under hypotonic conditions; th is action is inhibited by $HgCl_2$ and so provides functional evidence for the involvement of AQPs.
- AQPs in granulosa cells demonstrate specific androgen sensitivity; the individual AQPs involved remains to be determined.

5.5 Further investigations

To follow on from this investigation it would be valuable to consider the availability of alternative antibodies to allow for the localisation of AQP protein via IHC and WB in control ovaries and following steroid treatment. It may also prove valuable to substitute non-aromatizable DHT for T in studies of androgen sensitivity. The co-localisation of AQP1 with vasculature and lymphatic vessels would give a better picture of AQP1s involvement in bidirectional fluid flux and would further our understanding of general ovarian fluid dynamics. In situ hybridisation would extend the RT-qPCR studies localising the AQP transcripts to particular cells within the theca and granulosa compartments. Investigation of AQP in connection with granulosa cell morphology would be valuable as columnar granulosa cells are associated with loopy basal lamina and slow follicle expansion. Granulosa and theca cells cultured with range of steroid and gonadotrophins, growth factors and other intrafollicular factors would allow the investigation of the potential modulators of AQP expression and function. Finally, in light of hyperandrogenism in the FF of women with PCOS (Qu *et al.* (2010), studying the role of AQPs in pathological conditions such as bovine cystic follicles and polycystic ovaries in women could highlight a new approach to investigating and/or treating such conditions.

References

Abbott DH, Dumesic DA and Franks S 2002 Developmental origin of polycystic ovary syndrome – a hypothesis. *J Endocrinol.* **174** 1-5.

Abir R, Franks S, Mobberley MA, Moore PA, Margara RA and Winston RML 1997 Mechanical isolation and in vitro growth of preantral and small antral human follicles. *Fertil Steril.* **68** 682-688.

Acosta TJ, Yoshizawa N, Ohtani M and Miyamoto A 2002 Local changes in blood flow within the early and midcycle corpus luteum after prostaglandin F(2 alpha) injection in the cow. *Biol Reprod.* **66** 651-8.

Acosta TJ, Gastal EL, Gastal MO, Beg MA and Ginther OJ 2004 Differential blood flow changes between the future dominant and subordinate follicles precede diameter changes during follicle selection in mares. *Biol Reprod.* **71** 502-507.

Acosta TJ, Hayashi KG, Matsui M and Miyamoto A 2005 Changes in follicular vascularity during first follicular wave in lactating cows. *J Reprod Develop.* **51** 273-280.

Acosta TJ 2007 Studies of follicular vascularity associated with follicle selection and ovulation in cattle. *J Reprod Dev.* **53** 39-44.

Adams GP, Matteri RL, Kastelic JP, Ko JC and Ginther OJ 1992 Association between surges of follicle-stimulating hormone and the emergence of follicular waves in heifers. *J Reprod Fertil.* **94** 177-88.

Adams GP 1999 Comparative patterns of follicle development and selection in ruminants. *J Reprod Fertil Suppl.* **54** 17-32.

Adams GP, Jaiswal R, Singh J and Malhi P 2008 Progress in understanding ovarian follicular dynamics in cattle. *Theriogenology.* **69** 72-80.

Aerts JMJ and Bols PEJ 2010 Ovarian Follicular Dynamics: A Review with Emphasis on the Bovine Species. Part I: Folliculogenesis and Pre-antral Follicle Development. *Reprod Dom Anim.* **45** 171-179.

Agre P, Preston GM, Smith BL, Jung JS, Raina S, Moon C, Guggino WB and Nielsen S. 1993a Aquaporin Chip - the Archetypal Molecular Water Channel. *Am J Physiol.* **265** 463-476.

Agre P, Sasaki S and Chrispeels MJ 1993b Aquaporins - a Family of Water Channel Proteins. *Am J Physiol.* **265** 461-461.

Agre, P. and S. Nielsen 1996 The aquaporin family of water channels in kidney. *Nephrologie.* **17** 409-15.

Agre P, King LS, Yasui M, Guggino WmB, Ottersen OP, Fujiyoshi Y, Engel A and Nielsen S 2002 Aquaporin water channels – from atomic structure to clinical medicine. *J Physiol.* **542** 3-16.

Aharon R and Bar-Shavit Z 2006 Involvement of aquaporin 9 in osteoclasts differentiation. *J. Biol. Chem.* **281** 19305-19309.

Andersen MM, Krøll J, Byskov AG and Faber M 1976. Protein composition in the fluid of individual bovine follicles. *J Reprod Fertil.* **48** 109-18.

Auerbach W and Auerbach R 1994 Angiogenesis inhibition. *Pharmacol Ther.* **63** 265-311.

Armulik A, Abramsson A and Betsholtz C 2005 Endothelial/pericyte interactions. *Circ Res.* **16** 512-23.

Armstrong L and Bornstein P 2003 Thrombospondins 1 and 2 function as inhibitors of angiogenesis. *Matrix Biol.* 22 63-71.

Assidi M, Dieleman SJ and Sirard M 2010 Cumulus cell gene expression following the LH surge in bovine preovulatory follicles: potential early markers of oocyte competence. *Reproduction.* **140** 835-852.

Badaut J, Lasbennes F, Magistretti PJ and Regli L 2002 Aquaporins in brain: distribution, physiology, and pathophysiology. *J Cereb Blood Flow Metab.* **22** 367-78.

Bai C, Fukuda N, Song YL, Ma T, Matthay MA and Verkman AS 1999 Lung fluid transport in aquaporin1 and aquaporin4 knockout mice. *J Clil Invest.* **103** 555-561.

Baker TG 1982 *Oogenesis and ovulation. In Reproduction in mammals*, 2nd Ed, vol. 1, ed Austin CR and Short RV, pp 17-45. Cambridge: Cambridge University Press.

Balbin M, Fueyo A, Lopez JM, Diez-Itza I, Velasco G and Lopez-Otin C 1996 Expression of collagenase-3 in the rat ovary during the ovulatory process. Journal of *Endocrinology* **149** 405-415.

Ball PJH and Peters AR 2004 *In Reproduction in Cattle.* 3rd Ed. Oxford: Blackwell Publishing.

Banerjee SK, Campbell D R, Weston AP and Banerjee DK 1997 Biphasic estrogen response on bovine adrenal medulla capillary endothelial cell adhesion, proliferation and tube formation. *Mol and Cell Biochem.* **177** 97-105.

Bao B, Garverick HA, Smith GW, Smith MF, Salfen BE and Youngquist RS 1997 Changes in messenger RNA encoding LH receptor, cytochrome P450 side chain cleavage, and aromatase are associated with recruitment and selection of bovine ovarian follicles. *Biol Reprod.* **56** 1158-1168.

Bao B and Garverick HA 1998 Expression of steroidogenic enzyme and gonadotropin receptor genes in bovine follicles during ovarian follicular waves. *J Anim Sci.* **39** 360-365.

Barber RD, Harmer DW, Coleman RA and Clark BJ 2005 GAPDH as a housekeeping gene: analysis of GAPDH mRNA expression in a panel of 72 human tissues. *Physiol Genomics.* **21** 389-395.

Bates DO 2010 Vascular endothelial growth factors and vascular permeability. *Cardiovasc Res.* **87** 262-271.

Beg Ma, Bergfelt DR, Kot K and Ginther OJ 2002 Follicle selection in cattle: dynamics of follicular fluid factors during development of follicle dominance. *Biol Reprod.* **66** 120-126.

Beg M A and Ginther OJ 2006 Follicle selection in cattle and horses: role of intrafollicular factors. *Reproduction.* **132** 365-77.

Beitz E, Wu B, Holm LM, Schultz JE and Zeuthen T 2006b Point mutations in the aromatic/arginine region in aquaporin 1 allow passage of urea, glycerol, ammonia, and protons. *Proc Natl Acad Sci U S A.* **103** 269-74.

Bendz A, Hansson HA, Svendsen P and Wiqvist N 1982 On the extensive contact between veins and arteries in the human ovarian pedicle. *Acta Physiol Scand.* **115** 179-182.

Ben-Shlomo I, Vitt UA and Hsueh AJ 2002 Persective: The ovarian kaleidoscope database-II. Functional genomic analysis of an organ-specific database. *Endocrinology.* **143** 2041-2044.

Berisha B, Sinowatz F and Schams D 2004 Expression and localization of fibroblast growth factor (FGF) family members during the final growth of bovine ovarian follicles. *Mol Reprod Devel.* **67** 162-171.

Bergers G and Song S 2005 The role of pericytes in blood-vessel formation and maintenance. *Neuro Oncol.* **7** 452-64.

Bergfelt DR and Ginther OJ 1985 Delayed follicular development and ovulation following inhibition of FSH with equine follicular fluid in the mare. *Theriogenology.* **24** 99-108.

Bienert GP, Moller AL, Kristiansen KA, Schulz A, Møller IM, Schjoerring JK and Jahn TP 2007 Specific aquaporins facilitate the diffusion of hydrogen peroxide across membranes. *J Biol Chem.* **282** 1183-92.

Boenisch T 2007 Pretreatment for immunohistochemical staining simplified. Appl Immunohistochem *Mol Morphol.* **15** 208-12.

Bouley R, Lou H A J, Nunes P, Da Silva N, McLaughlin M, Chen Y and Brown D 2011 Calcitonin has a vasopressin-like effect on AQP2 trafficking and urinary concentration. *J Am Soc Nephrol.* **22** 59-72.

Brañes MC, Morales B, Ríos M and Villaló MJ 2005. Regulation of the immunoexpression of aquaporin 9 by ovarian hormones in the rat oviductal epithelium. *Am J Physiol Cell Physiol.* **288** 1048-1057.

Brantmeier SA, Grummer RR and Ax RL 1987 Concentrations of high density lipoproteins vary among follicular sizes in the bovine. *J Dairy Sci.* **70** 2145-2149.

Braw-Tal, R 2002 The initiation of follicle growth: the oocyte or the somatic cells? Mol *Cell Endocrinol.* **187** 11-8.

Braw-Tal R and Yossefi S 1997 Studies in vivo and in vitro on the initiation of follicle growth in the bovine ovary. *J Reprod Fertil.* **109** 165-71.

Brinster RL 2007 Male germline stem cells:from mice to men. *Science.* **316** 404-405.

Brown D 2003 The inns and outs of aquaporin-2 trafficking. Am. J. Physiol. **284** 893-901.

Budras K and Habel RE (2003) *In Bovine Anatomy.* Germany: Schlutersche.

Buher M 1997 The primordial germ cells of mammals: some current perspectives. Exp *Cell Res.* **232** 194-196.

Burghardt B, Elkaer ML, Kwon TH, Rácz GZ, Varga G, Steward MC and Nielsen S 2003 Distribution of aquaporin water channels AQP1 and AQP5 in the ductal system of the human pancreas. *Gut.* **52** 1008-16.

Burry RW 2000 Specificity controls for immunocytochemistry methods. *J Histochem Cytochem.* **48** 163-165.

Bussolati G and Leonardo E 2008 Technical pitfalls potentially affecting diagnoses in immunohistochemistry. J Clin Path. **61.** 1184-1192.

Carbrey JM, Gorelick-Fwldman DA, Kozono D, Praetorius J, Nielsen S, Agre P 2003 Aquaglyceroporin AQP9; solute permeation and metabolic control of expression in liver. *Proc Natl Acad Sci.* **100** 2945-2950.

Carson RS, Findlay JK, Clarke IJ and Burger HG 1981 Estradiol, testosterone and androstenedione in ovine follicular fluid during growth and atresia of ovarian follicles. *Biol Reprod.* **24** 105-113.

Cavender JL and Murdoch WJ 1988 Morphological studies of the microcirculatory system of periovulatory ovine follicles. *Biol Reprod.* **39** 989-997.

Clark LJ, Irving-Rodgers HF, Dharmarajan AM and Rodgers RJ 2004 Theca interna: The other side of bovine follicular atresia. *Biol Reprod.* **71** 1071-1078.

Clarke HG, Hope SA, Byers S and Rodgers RJ 2006 Formation of ovarian follicular fluid may be due to the osmotic potential of large glycosaminoglycans and proteoglycans. *Reproduction.* **132** 119-31.

Conley AJ, Kaminski MA, Dubowsky SA, Jablonka-Shariff A, Redmer DA and Reynolds LP 1995 Immunohistochemical localization of 3 beta-hydroxysteroid dehydrogenase and P450 17 alpha-hydroxylase during follicular and luteal development in pigs, sheep and cows. *Biol Reprod.* **52** 1081-1094.

Copper GJ and Boron WF 1998 Effect of PCMBS on CO2 permeability of Xenopus oocytes. *Am. J. Physiol.* **275** 1481-1486.

Cunningham AJ, Szenberg A 1968 Further improvements in the plaque technique for detecting single antibody-forming cells. *Immunology.* **14** 599-600.

Curry TE, Sanders SL, Pedigo NG, Estes RS, Wilson EA and Vernon MW 198 8 Identification and characterization of metalloproteinase inhibitor activity in human ovarian follicular fluid. *Endocrinology.* **123** 1611-1618.

Czernobilsky B, Shezen E, Lifschitz-Mercer B, Fogel M, Luzon A, Jacob N, Skalli O and Gabbiani G 1989 Alpha smooth muscle actin (alpha-SM actin) in normal human ovaries, in ovarian stromal hyperplasis and in ovarian neoplasms. *Cell Pathol Incl Mol Pathol.* **57** 55-61.

Deen PM, Croes H, van Aubel RA, Ginsel LA, van Os CH 1995 Water channels encoded by mutant aquaporin-2 genes in nephrogenic diabetes insipidus are impaired in their cellular routing. *J Clin Invest.* **95** 2291-2296.

Deen PM, Verdijk MA, Knoers NV, Wieringa B, Monnens LA, van Os CH and van Oost BA 1994 Requirement of human renal water channel aquaporin-2 for vasopressin-dependent concentration of urine. *Science.* **264** 92-5.

de Groot BL, Frigato T, Helms V and Grubmüller H 2003 The mechanism of proton exclusion in the aquaporin-1 water channel. **J Mol Biol. 333** 279-93.

Demeestere I, Delbaere A, Gervy C, Van den Bergh M, Devreker F and Englert Y 2002 Effect of preantral follicle isolation technique on in-vitro follicular growth, oocyte maturation and embryo development in mice. *Hum Reprod.* **17** 2152-2159.

Denker BM, Smith BL, Kuhajda FP and Agre P 1988 Identification, purification, and partial characterization of a novel Mr 28,000 integral membrane protein from erythrocytes and renal tubules. *J Biol Chem.* **263** 15634-42.

Derynck R 1988 Transforming growth factor α. *Cell.* **54** 593-595.

Devuyst O, Nielsen S, Cosyns J-P, Smith BL, Agre P, Squifflet JP, Pouthier D and Goffin E 1998 Aquaporin-1 and endothelial nitric oxide synthase expression in capillary endothelia of human peritoneum. *Am J Physiol.* **275** 234-242.

D'Herde K, De Pestal G and Roels F 1994 In situ end labelling of fragmented DNA in induced ovarian atresia. *Biochem Cell Biol.* **72** 573-579.

Dibas AI, Mia AJ, and Yorio T 1998 Aquaporins (water channels): role in vasopressin-activated water transport. *Proc Soc Exp Biol Med.* **219** 183-99.

Donadeu FX and Pedersen HG 2008 Follicle development in mares. *Reprod Domest Anim Suppl.* **43** 224-31.

Durlej M, Tabarowski Z and Slomczynska M 2010 Immunohistochemical study on differential distribution of progesterone receptor A and progesterone receptor B within the porcine ovary. Anim Reprod Sci. **121** 167-173.

Driancourt MA 2001 Regulation of ovarian follicular dynamics in farm animals. Implications for manipulation of reproduction. *Theriogenology.* **55** 1211-1239.

Drummond AE 2006 The role of steroids in follicular growth. *Reprod Biol Endocrinol.* **4** 1-11.

Edashige K, Sakamoto M, Kasai M 2000 Expression of mRNAs of the aquaporin family in mouse oocytes and embryos. *Cryobiology.* **40** 171-5.

Ehrmann DA 2005 Polycystic ovary syndrome. *N Engl J Med.* **352** 1223-1236.

Einer-Jensen N and Hunter RF 2005 Counter-current transfer in reproductive biology. *Reproduction.* **129** 9-18.

Ekblom P, Vestweber D and Kemler R 1986 Cell-matrix interactions and cell adhesion during development. *Annu. Rev. Cell Biol.* **2** 27-48

Elkajaer M, Vajda Z, Nejsum LN, Kwon T, Jensen UB, Amiry-Moghaddam M, Frokiaer J, Nielsen S 2000 Immunolocalisation of AQP9 in liver, epididymis, testes, spleen and brain. *Biochem Biophys Res Commun.* **276** 1118-1128.

Elkjaer ML, Nejsum LN, Gresz V, Kwon TH, Jensen UB, Frøkiaer J and Nielsen S 2001 Immunolocalization of aquaporin-8 in rat kidney, gastrointestinal tract, testis, and airways. *Am J Physiol Renal Physiol.* **281** 1047-1057.

Elvin JA, Yan C and Matzuk MM 2000 Growth differentiation factor-9 stimulates progesterone synthesis in granulosa cells via a prostaglandin E2/EP2 receptor pathway. *Proc Natl Acad Sci U S A.* **29** 10288-93.

Endo M, Jain RK, Witwer B and Brown D 1999 Water channel (aquaporin 1) expression and distribution in mammary carcinomas and glioblastomas. *Microvasc Res.* **58** 89-98.

Engel A, Fujiyoshi Y, Gonen T and Walz T 2008 Junction-forming aquaporins. *Curr Opin Struc Biol.* **18** 229-235.

Engvall E 1993 Laminin variants; why, where and when? *Kidney Internat.* **43** 2-6.

Eppig JJ 1991 Intercommunication between mammalian oocytes and companion somatic cells. *Bioessays.* **13** 569-574.

Eppig DG and Schroeder AC 1989 Capacity of mouse oocytes from preantral follicles to undergo embryogenesis and development to live young after growth, maturation, and fertilization in vitro. *Biol Reprod.* **41** 268-76.

Erickson BH 1966a Development and radio response of the prenatal bovine ovary. *J Reprod Fertil.* **11** 91-105

Erickson BH 1966b Development and senescence of the postnatal bovine ovary. *J Anim Sci.* **82** 800-805.

Erickson GF, Nakatani A, Liu EJ, Shimaski S and Ling N 1994 *Role of insulin-like factors (IGF) and IGF binding proteins in folliculogenesis.* In Findlay JK (ed.) Molecular Biology of the female reproductive system, pp 101-151. London: Academic Press.

Erickson GF and Danforth DR 1995 Ovarian control of follicle development. *Am J Obstet Gynecol.* **172** 736-47.

Espey LL 1980 Ovulation as an inflammatory reaction – a hypothesis. *Biol. Reprod.* **22** 73-106.

Espey LL and Lipner H 1994 *Ovulation. In the Physiology of Reproduction*, pp 725-780. Eds Knobil E and Neil JD. New York: Raven Press.

Espina V, Heiby M, Pierobon M, Liotta LA 2007 Laser capture microdissection technology. *Expert Rev Mol Diagn.*7 647-57.

Evans AC, Komar CM, Wandji SA and Fortune JE 1997 Changes in androgen secretion and luteinizing hormone pulse amplitude are associated with the recruitment and growth of ovarian follicles during the luteal phase of the bovine estrous cycle. *Biol Reprod.* **57** 394-401.

Farjo R, Peterson WM and Naash MI 2008 Expression profiling after retinal detachment and reattachment: A possible role for aquaporin-0. *Invest Ophthalmol Vis Sci.* **49** 511-521.

Ferrara N, Gerber HP and LeCouter J 2003 The biology of VEGF and it receptors. *Nat Med.* **9** 669-676.

Ferrara N and Davis-Smyth T 1997 The biology of vascular endothelial growth factor. *Endocr Rev.* 18 4-25.

Fisher JS, Turner KJ, Fraser HM, Saunders PTK, Brown D and Sharpe RM 1998 Immunoexpression of aquaporin-1 in the efferent ducts of the rat and marmoset

monkey during development, its modulation by estrogens, and its possible role in fluid resorption. *Endocrinology.* **139** 3936-3945.

Fitzpatrick SL and Richards JS 1991 Regulation of cytochrome P450 aromatase messenger ribonucleic acid and activity by steroids and gonadotropins in rat granulosa cells. *Endocrinology.* **129** 1452-1462.

Floyd RV, Mason SL, Proudman CJ, German AJ, Marples D and Mobasheri A 2007 Expression and nephron segment-specific distribution of major renal aquaporins (AQP1-) in *Equus caballus*, the domestic horse. *Am J Physiol Regul Integr Comp Physiol.* **293** 492-503.

Foradori CD, Weiser MJ and Handa RJ 2008 Non-genomic actions of androgens. Front *Neuroendocrinol.* **29** 169-181.

Ford P, Merot J, Jawerbaum A, Gimeno MAF, Capurro C and Parisi M 2000 Water permeability in rat oocytes at different maturity stages: Aquaporin-9 expression. J. *Membrane Biol.* **176** 151-158.

Fortune JE 1986 Bovine theca and granulosa cells interact to promote androgen production. *Biol Reprod.* **35** 292-299.

Fortune J E 1993 Follicluar dynamics during the bovine estrous cycle: A limiting factor in improvement of fertility? *Anim Reprod Sci.* **33** 111-125.

Fortune JE 1994 Ovarian follicular growth and development in mammals. *Biol Reprod.* **50** 225-232.

Fortune JE and Sirois J 1989 The use of ultrasonography to study the regulation of follicular development in cattle and horses. *Serono Symp.* Rev. **23** 11-20.

Fortune JE, Sirois J, Turzillo AM and Lavoir M 1991 Follicle selection in domestic ruminants. *J Reprod Fertil Suppl.* **43** 187-98.

Fortune JE, Rivers GM, Evans ACO and Turzillo AM 2001 Differentiation of dominant versus subordinate follicles in cattle. *Biol Reprod.* **65** 648-654.

Fortune JE, Rivera GM and Yang MY 2004 Follicular development: the role of the follicular microenvironment in selection of the dominant follicle. *Anim Reprod.* **82** 109-126.

Fowlkes JL, Enghild JJ, Suzuki K and Nagase H 1994 Matrix metalloproteinases degrade insulin-like growth factor-binding protein-3 in dermal fibroblast culture. *J Biol Chem.* **269** 25742-25746.

Foxcroft GR and Hunter MG 1985 Basic physiology of follicular maturation in the pig. *J Reprod Fert.* **33** 1-19.

Fraser HM and Duncan WC 2009 Regulation and manipulation of angiogenesis in the ovary and endothelium. *Reprod Fert Devel.* **21** 377-392.

Fredriksson L Li H and Eriksson U 2004 The PDGF family: four gene products form five dimeric isoforms. *Cytokine Growth F R.* **15** 197-204.

Frigeri A, Nicchia GP, Verbavatz JM, Valenti G and Svelto M 1998 Expression of aquaporin-4 in fast-twitch fibres of mammalian skeletal muscle. *J Clin Invest.* **102** 695-703

Fujita A, **Horio** Y, **Nielsen** S, **Nagelhus** EA, Hata F, **Ottersen** P **Kurachi Y** 1999 High-resolution immunogold cytochemistry indicates that AQP4 is concentrated along the basal membrane of parietal cell in rat stomach. *FEBS Let.* 459 305-309.

Funaki H, Yamamoto T, Koyama Y, Kondo D, Yaoita E, Kawasaki K, Kobayashi H, Sawaguchi S, Abe H, Kihara I 1998 Localization and expression of AQP5 in cornea, serous salivary glands, and pulmonary epithelial cells. *Am J Physiol.* **275** 1151-1157.

Funayama Y, Sasano H, Suzuki T, Tamura M, Fukaya T and Yajima 1996 Cell turnover in normal cycling human ovary. *J Clin Endocrinol Metab.* **81** 282-834.

Gartner LP and Hiatt JL 2001 *In Colour textbook of Histology.* W.B Saunders Company. PA, USA.

Garverick HA 1997 Ovarian follicular cysts in dairy cows. *J Dairy Sci.* **80** 995-1004.

Garverick HA, Baxter G, Gong J, Amstrong DG, Campbell BK, Gutierrez CG, Webb R 2002 Regulation of expression of ovarian mRNA encoding steroidogenic enzymes

and gonadotrophin receptors by FSN and GH in hypogonadotrophic cattle. *Reproduction.* **123** 651-661.

Gérard N, Duchamp G, Goudet G, Bézard J, Magistrini M and Palmer E 1998 A high-molecular-weight preovulatory stage-related protein in equine follicular fluid and granulosa cells. *Biol Rerod.* **58** 551-557.

Gérard N, Loiseau S, Duchamp G and Seguin F 2 002 Analysis of the variation of follicluar fluid composition during follicular growth and maturation in the mare using proton nuclear magnetic resonance (^{1}H NMR). *Reproduction.* **124** 241-248.

Gerhardt H and Betsholtz C (2003) Endothelial-pericyte interactions in angiogenesis. *Cell Tissue Res.* **314** 15-23.

Gershon E, Plaks V and Dekel N 2008 Gap junctions in the ovary: Expression, localization and function. *Mol Cell Endocrinol.* **282** 18-25.

Ginther OJ, Kastelic jp and Knopf L 1989 Composition and characteristics of follicular waves during the bovine estrous cycle. *Anim Reprod Sci.* **20** 187-200.

Ginther OJ, Wiltbank MC, Fricke PM, Gibbons JR and Knot K 1996 Selection of the dominant follicle in cattle. *Biol Reprod.* **55** 1187 – 1194.

Ginther OJ, Kot K, Kulick LJ and Wiltbank MC 1997 Emergence and deviation of follicles during the development of follicular waves in cattle. *Theriogenology.* **52** 1079-1093.

Ginther OJ, Beg MA, Bergfelt DR, Donadeu FX and Kot K 2001 Follicle selection in monovular species. *Biol Reprod.* **65** 638-47.

Ginther OJ, Beg MA, Donadeu FX and Bergfelt DR 2003 Mechanism of follicle deviation in monovular farm species. *Anim Reprod Sci.* **78** 239-257.

Gittens JEI, Mhawi AA, Lidington D, Ouellette Y and Kidder GM 2003 Functional analysis of gap junctions in ovarian granulosa cells: distinct role for connexin43 in early stages of folliculogenesis. *Am J Physiol Cell Physiol.* **284** 880-887.

Glass CA, Harper SJ Bates DO 1996 The anti-angiogenic VEGF isoform $VEGF_{165}b$ transiently increases hydraulic conductivity, probably through VEGF receptor 1 *in vivo*. J Physiol. **572** 243-257.

Glister C, Tannetta DS, Groome NP and Knight PG 2001 Interaction between follicle-stimulating hormone and growth factors in modulating secretion of steroids and inhibin-related peptides by nonluteinized bovine granulosa cells. *Biol Reprod.* **65** 1020-1127.

Gong JG, Campbell BK, Bramley TA, Gutierrez CG, Peters AR and Webb R 1996 Suppression in the secretion of follicle stimulating hormone and luteinizing hormone and ovarian follicle development in heifers continuously infused with a gonadotropin releasing hormone agonist. *Biol. Reprod.* **55** 68-74.

Gorin MB, Yancey SB, Cline J, Revel JP, Horwitz J 1984. The Major Intrinsic Protein (Mip) of the Bovine Lens Fiber Membrane - Characterization and Structure Based on cDNA Cloning. *Cell.* **39** 49-59.

Gosden RG, Hunter RH, Telfer E, Torrance C, Brown N 1988 Physiological factors underlying the formation of ovarian follicular fluid. *J Reprod Fertil.* **82** 813-825.

Goudet G, Belin F, Bezard J, Gerard N 1999 Intrafollicular content of luteinizing hormone receptor, alpha-inhibin, and aromatase in relation to follicular growth, estrous cycle stage, and oocyte competence for in vitro maturation in the mare. *Biol Reprod.* **60** 1120-1127.

Grasl-Kraupp B, Ruttkay-Nedecky B, Koudelka H, Bukowska K, Bursch W and Schulte-Hermann R 1995 In situ detection of fragmented DNA fails to discriminate among apoptosis, necrosis and sutolytic cell death: a cautionary note. *Hepatology.* **21** 1465-1468.

Grimes RW, Matton P and Ireland JJ 1987 A comparison of histological and non-histological indices of atresia and follicular function. *Biol Reprod.* **37** 82-88.

Grazul-Bilska AT, Navanukraw C, Johnson ML, Vonnahme KA, Ford SP, Reynolds LP and Redmer DA 2007 Vascularity and expression of angiogenic factors in bovine dominant follicles of the first follicular wave. *J Anim Sci.* **85** 1914-1922.

Greenwald GS and Roy SK 1994 *Follicular development and its control. In The Physiology of Reproduction,* ed. Knobil E and Neill J, pp 629-724. New York: Raven press.

Grupen CG, McIlfatrick SM, Ashman RJ, Boquest AC, Armstrong DT and Nottle MB 2003 Relationship between donor animal age, follicular fluid steroid content and oocyte developmental competence in the pig. *Reprod Fertil Dev.* **15** 81-87.

Gu F, Hata R, Toku K, Yang L, Ma Y, Maeda N, Sakanaka M and Tanaka J 2003 Testosterone up-regulates aquaporin-4 expression in cultured astrocytes. *J Neurosci Res.* **72** 709-715.

Gunnarson E, Zelenina M and Aperia A 2004 Regulation of brain aquaporins. *Neuroscience.* **129** 947-955.

Hamann S, Zeuthen T, La Cour M, Nagelhus EA, Ottersen OP, Agre P and Nielsen S 1998 Aquaporins in complex tissues: distribution of aquaporins 1-5 in human and rat eye. *Am J Physiol.* **274** 1332-1345.

Hampton JH, Manikkam M, Lubahn DB, Smith MF and Garverick HA 2004 Androgen receptor mRNA expression in the bovine ovary. *Dom Anim Endocrinol.* **27** 81-88.

Hara-Chikuma M, Sohara E, Rai T, Ikawa M, Sasaki S, Uchida S and Verkman AS 2005 Progressive adipocyte hypertrophy in aquaporin-7-deficient mice: adipocyte glycerol permeability as a novel regulator of fat accumulation. *J. Biol. Chem.* **280** 15493-15496.

Hara-Chikuma M and Verkman AS 2008 Prevention of skin tumorigenesis and impairment of epidermal cell proliferation by targeted aquaporin-3 gene disruption. *Mol. Cell Biol.* **28** 326-332.

Harris AL 2003 Angiogenesis as a new target for cancer control. *Eur J Can Sup.* **2** 1-12.

He RH, Sheng JZ, Luo Q, Jin F, Wang B, Qian YL, Zhou CY, Sheng X and Huang HF 2006 Aquaporin-2 expression in human endometrium correlates with serum ovarian steroid hormones. *Life Sci.* **79** 423–429.

Hermo L, Krzeczunowicz D and Ruz R 2004 Cells specificity of aquaporins 0, 3 and 10 expressed in the testis, efferent ducts and epididymis of adult rats. *J Androl.* **25** 494-505.

Hermo L and Smith CE 2011 Thirsty business: cell, region, and membrane specificity of aquaporins in the testis, efferent ducts, and epididymis and factors regulating their expression. *J Androl.* **32** 565-75.

Herrera M and Garvin JL 2007 Novel role of AQP-1 in NO-dependent vasorelaxation. *Am J Physiol Renal Physiol.* **292** 1443-1451.

Hillier SG 1994 Current concepts of the roles of follicle stimulating hormone and luteinizing hormone in folliculogenesis. *Hum Reprod.* **9** 188-91.

Hillier SG and de Zwart FA 1981 Evidence that granulosa cell aromatase induction/activation by FSH is an androgen receptor regulated process *in vitro*. *Endocrinology.* **109** 1303-1305.

Hillier SG, Whitelaw PF and Smyth CD 1994 Follicular oestrogen synthesis; the'two-cell, two-gonadotrophin' model revisited. *Mol Cell Endocrinol.* **100** 51-54.

Hillier SG and Tetsuka M 1997 Role of androgens in follicle maturation and atresia. *Bailliere Clin Ob Gy.* **11** 249-260.

Hillier SG, Tetsuka M and Fraser HM 1997 Location and developmental regulation of androgen receptor in primate ovary. *Hum Reprod.* **12** 107-111.

Hirano Y, Okimoto N, Kadohira I, Suematsu M, Yasuoka K and Yasui M 2010 Molecular mechanisms of how mercury inhibits water permeation through aquaporin-1: understanding by molecular dynamics simulation. *Biophys J.* **98** 1512-1519.

Hirschi KK and D'Amore PA 1996 Pericytes in the microvasculature. *Cardiovasc Res.* **32** 687-98.

Hirshfield AN 1991 Development of follicles in the mammalian ovary. *Int Rev Cytol.* **124** 43-101.

Hodgen GD 1982 The dominant ovarian follicle. *Fertil Steril.* **38** 281-300.

Hoffert JD, Leitch V, Agre P, King LS 2000 Hypertonic induction of aquaporin-5 expression through an ERK-dependent pathway. *J Biol Chem.* **275** 9070-9077.

Hoffert JD, Pisitkum T, Wang G, Seh R and Knepper M 2006 Quantitative phosphoproteomics of vasopressin-sensitive renal cells: Regulation of aquaporin-2 phosphorylation at two sites. *PNAS.* **18** 7159-7164.

Huang HF, He R H, Sun CC, Zhang Y, Meng QX and Ma YY 2006. Function of aquaporins in female and male reproductive systems. *Hum Reprod Update.* **12** 785-795.

Huebert RC, Jagavelu K, Hendrickson HI, Vasdev MM, Arab JP, Splinter PL, Trussoni CE, LaRusso NF and Shah VH 2011 Aquaporin-1 promotes angiogenesis, fibrosis and portal hypertension through mechanism dependent on osmotically sensitive microRNAs. *Am J Pathol.* 179 1851-1860.

Hunter MG, Robinson RS, Mann GE and Webb R 2004. Endocrine and paracrine control of follicular development and ovulation rate in farm species. *Anim Reprod Sci.* **82-83** 461-77.

Hunter RHF 2003 *In Physiology of the Graafian follicle and ovulation.* Cambridge University press. Cambridge, UK.

Hurley PT, Ferguson CJ, Kwon TH, Andersen MLE, Norman AG, Steward MC, Nielsen S and Case RM 2001 Expression and immunolocalisation of aquaporin water channels in rat exocrine pancreas. *Am J Physiol Gastrointest Liver Physiol.* **28** 701-709.

Huxley VH and Wang J 2010 Cardiovascular sex differences influencing microvascular exchange. *Cardiov res* **87** 230-242.

Hyttel P, Fair T, Callensen H and Greve T 1997 Oocyte growth, capacitation and final maturation in cattle. *Theriogenology.* **47** 23-32.

Ikeda M, Beitz E, Kozono D, Guggion WB, Agre P and Yasui M 2002 Characterization of aquaporin-6 as a nitrate channel in mammalian cells. *J Biol. Chem.* **277** 39873-39879.

Ireland JJ, Murphee RL and Coulson PB 1980 Accuracy of predicting stages of bovine estrous cycle by gross appearance of the corpus luteum. *J Dairy Sci.* **63** 155-160.

Ireland JJ 1987 Control of follicular growth and development. *J Reprod Fert Suppl.* **34** 39-54.

Ireland, JJ and Roche, JF 1982 Development of antral follicles in cattle after prostaglandin-induced luteolysis: changes in serum hormones, steroids in follicular fluid, and gonadotrophin receptors. *Endocrinology.* **111** 2077-2086.

Ireland, JJ and Roche, JF 1983a Development of non-ovulatory antral follicles in heifers: changes in steroids in follicular fluid and receptors for gonadotropins. *Endocrinology.* **112** 150-156.

Ireland, JJ and Roche, JF 1983b Growth and differentiation of large antral follicles after spontaneous luteolysis in heifers: changes in concentration of hormones in follicular fluid and specific binding of gonadotropins to follicles. *J Anim Sci.* **57** 157-167

Ireland JJ, Mihm M, Austin E, Diskin MG and Roche JF 2000 Identification of potential intrafollicular factors involved in selection of dominant follicles in heifers. *Biol Reprod.* **63** 811-819.

Irving-Rodgers HF and Rodgers RJ 2000 Ultrastructure of the basal lamina of bovine ovarian follicles and its relationship to the membrana granulosa. *J Reprod Fertil.* **118** 221-228.

Irvin-Rodgers HF, van Wezel IL, Mussard ML, Kinder JE and Rodgers RJ 2001 Atresia revisited: two basic patterns of atresia of bovine antral follicles. *Reproduction.* **122** 761-775.

Irving-Rodgers HF, Mussard ML, Kinder JE and Rodgers RJ 2002 Composition and morphology of the follicular basal lamina during atresia of bovine antral follicles. *Reproduction.* **123** 97-106.

Irvin-Rodgers HF, Krupa M and Rodgers RJ 2003 Cholesterol side-chain cleavage cytochrome P450 and 3beta-hydroxysteroid dehydrogenase expression and the concentrations of steroid hormones in the follicular fluids of different phenotypes of healthy and atretic bovine ovarian follicles. *Biol Reprod.* **20** 2011-2028.

Irving-Rodgers HF, Cantanzariti KD, Aspden WJ, D'Occhio MJ and Rodgers RJ 2006a Remodelling of extracellular matrix at ovulation of the bovine ovarian follicle. *Mol Reprod Devel.* **73** 1292-1302.

Irving-Rodgers HF, Friden BE, Morris SE, Mason HD, Brannstrom M, Sekiguchi K, Sanzen N, Sorokin LM, Sado Y, Ninomiya Y and Rodgers RJ 2006b Extracellular matrix of the human cyclic corpus luteum. *Mol Hum Reprod.* **12** 525-534.

Irving-Rodgers HF, Harland ML, Sullivan TR and Rodgers RJ 2009 Studies of granulosa cell maturation in dominant and subordinate bovine follicle: novel extracellular focimatrix is co-ordinately regulated with cholesterol side-chain cleavage CYP11A1. *Reproduction.* **137** 825-834.

Ishibashi K, Kuwahara M, Gu Y, Kageyama Y, Tohsaka A, Suzuki F, Marumo F, Sasaki S 1997 Cloning and functional expression of a new water channel abundantly expressed in the testis permeable to water, glycerol and urea. *J Biol Chem.* **272** 20782-20786.

Ishibashi K, Hara S and Kondo S 2009 Aquaporin water channels in mammals. *Clin. Exp. Nephrol.* **13** 107-17.

Jablonski EM, McConnell NA, Hughes FM Jr and Huet-Hudson YM 2003 Estrogen regulation of aquaporins in the mouse uterus: potential roles in uterine water movement. *Biol Reprod.* **69** 1481-1487.

Jackson RL, Busch SJ and Cardin AD 1991 Glycosaminoglycans: molecular properties, protein interactions and role in physiological processes. *Physiol Rev.* **71** 481-539 .

Jeremic, A, Cho WJ and Jena BP 2005 Involvement of water channels in synaptic vesicle swelling. *Exp Biol Med (Maywood).* **230** 674-80.

Jiang JY, Macchiarelli G, Tsang B.K and Sato E 2003 Capillary angiogenesis and degeneration in bovine ovarian antral follicles. *Reproduction.* **125** 211-223.

Jo WJ, Jee BC, Suh CS, Kim SH, Choi YM, Kim JG and Moon SY 2010 Effect of maturation on the expression of aquaporin 3 in mouse oocyte. *Zygote.* **19** 9-14.

Johnson J, Canning J, Kaneko T, Pru JK and Tilly JL 2004 Germline stem cells and follicular renewal in the postnatal mammalian ovary. *Nature*. 428 145-150.

Johnson ML, Redmer, DA, Reynolds LP and Grazul-Bilska AT 1999 Expression of gap junctional proteins connexion 43, 32 and 26 throughout follicular development and atresia in cows. *Endocrine*. **10** 43-51.

Johnson ML, Redmer, DA, Reynolds LP, Bilski JJ and Grazul-Bilska AT 2002 Gap junctional intercellular communication of bovine granulosa and thecal cells from antral follicles: effects of luteinizing hormone and follicle stimulating hormone. Endocrine. *Reproducation*.**18** 261-270.

Juengel JL, Larrick TL, Meberg BM and Niswender GD 1988 Luteal expression of steroidogenic factor-1 mRNA during estrous cycle and in response to luteotropic and luteolytic stimuli in ewes. *Endocrine*. **9** 227-232.

Jung JS, Bhat RV, Preston GM, Guggino WB, Baraban JM and Agre P 1994a Molecular characterization of an aquaporin cDNA from brain: candidate osmoreceptor and regulator of water balance. *Proc Natl Acad Sci USA*. **91** 13952-13056.

Jung JS, Preston GM, Smith BL, Guggino WB and Agre P 1994b Molecular structure of the water channel through aquaporin CHIP. The hourglass model. *J Biol Chem*. **269** 14648-54.

Kanzaki H, Okamura H, Okuda Y, Takenaka A, Morimoto K and Nishimura T 1982 Scanning electron microscopic study of rabbit ovarian follicle microvasculature using resin injection-corrosion casts. *J Anat*. **134** 697-704.

Kerr JFR, Gobe GC, Winterford CM and Harmon BV 1995 Anatomical methods of cell death. *Methods Cell Biol*. **46** 1-27.

King LS and Agre P 2001 Man is not a rodent: aquaporins in the airways. Am J Respir *Cell Mol Biol*. **24** 221-3.

King LS, Choi M, Fernandez PC, Catron JP and Agre P 2001 Defective urinary-concentrating ability due to a complete deficiency of aquaporin-1. *N. Engl. J. Med*. **345** 175-179.

King LS, Kozono D and Agre P 2004 From structure to disease: the evolving tale of aquaporin biology. *Nature rev. Mol. Cell Biol.* **5** 687-698.

Knickerbocker JJ, Wiltbank MC and Niswender GD 1988 Mechanisms of luteolysis in domestic livestock. *Dom Ani Endocrinol.* **5** 91 – 107

Knight PG and Glister C 2001 Potential local regulatory functions of inhibins, activins and follistatin in the ovary. *Reproduction.* **121** 503-512.

Knobil E and Neil JD 1994 In The physiology of reproduction Volume 1. 2nd ed. Raven Press New York. USA.

Knox RV 2005 Recruitment and selection of ovarian follicles for determination of ovulation rate in the pig. *Domest Anim Endocrinol.* **29** 385-97.

Kobayashi ME, Takahashi E, Miyagawa S, Watanabe H and Iguchi T 2006 Chromatin immunoprecipitation-mediated target identification proved aquaporin 5 is regulated directly by estrogen in the uterus. *Genes Cells.* **11** 1133-43.

Korsrud FR and Brandtzaeg P 1982 Characterisation of epithelial elements in human major salivary glands by functional markers: localization of amylase, lactoferrin, lysozyme, secretory component, and secretory immunoglobulins by paired immunofluorescence staining. *J Histochem Cytochem.* **30** 657-666.

Krane CM, Melvin JE, Nguyen HV, Richardson L, Towne JE, Doetschman T, Menon AG 2001 Salivary acinar cells from aquaporin 5-deficient mice have decreased membrane water permeability and altered cell volume regulation. *J Biol Chem.* **276** 23413-23420.

Kreda SM, Gynn MC, Fenstermacher DA, Boucher RC and Gabriel SE 2001 Expression and localisation of epithelial aquaporins in the adult human lung. Am. J. Respir. *Cell Mol. Biol.* **24** 224-234.

Kruip TAM and Dielman SJ 1982 Macroscopic classification of bovine follicles and its validation by micromorphological and steroid biochemical procedures. *Reprod Nutr Dev.* **22** 463-473.

Kruip TAM and Dielman SJ 1985 Steroid hormone concentration in the fluid of bovine follicles relative to size, quality and stage of the oestrus cycle. *Theriogenology.* **24** 395-408.

Ku DD, Zaleski JK, Liu S and Brock TA 1993 Vascular endothelial growth factor induces EDRF-dependent relaxation in coronary arteries. *Am J Physiol.* **265** 586-592.

Kuiper GG, Carlsson B, Grandien K, Enmark E, Haggblad J, Nilsson S and Gustafsson JA 1997 Comparison of the ligand binding specificity and transcript tissue distribution of estrogen receptors alpha and beta. *Endocrinology.* **138** 863-870.

Kuriyama H, Kawamoto S, Ishida N, Ohno I, Mita S, Matsuzawa Y, Matsubara K, Okubo K 1997 Molecular cloning and expression of a novel human aquaporin from adipose tissue with glycerol permeability. *Biochem Biophys Res Commun.* **241** 53-58.

Kuriyama H, Shimomura I, Kishida K,H, Furuyama N, Nishizawa H, Maeda N, Matsuda M, Nagaretani H, Kihara S, Nakamura T, Tochino Y, Funahashi T and Matsuzawa Y 2002 Coordinated regulation of fat-specific and liver-specific glycerol channels, aquaporin adipose and aquaporin 9. *Diabetes.* **51** 2915-2921.

Laforenza U, Gastaldi G, Grazioli M, Cova E, Tritto S, Faelli A, Calamita G and Ventura U 2005 Expression and localisation of aquaporin-7 in rat gastrointestinal tract. *Biol. Cell.* **97** 605-613.

Lammond DR and Drost M 1974 Blood supply to the bovine ovary. *J Anim Sci.* **38** 106-112.

Laurincik J, Kroslak P, Hyttel P, Pivko J and Sirotkin AV 1992 Bovine cumulus expansion and corona-oocyte disconnection during culture in vitro. *Reprod Nutr Dev.* **32** 151-161.

Lenton EA, King H, Thomas EJ, Smith SK, McLachlan RI, MacNeil S and Cooke ID 1988 The endocrine environment of the human oocyte. *J Reprod Fert.* **82** 827-841.

Leonardsson G, Peng XR, Liu K, Nordstrom L, Carmeliet P, Mulligan R, Collen D and Ny T 1995 Ovulation efficiency is reduced in mice that lack plasminogen activator gene function: functional redundancy among physiological plasminogen activators. *PNAS USA.* **92** 12445-12450.

Leung PCK and Armstrong DT 1980 Interactions of steroids and gonadotropins in the control of steroidogenesis in the ovarian follicle. *Ann Rev Physiol.* **42** 71-82

Leroy JLMR, Vanholder T, Delanghe JR, Opsomer G, Van Soom A, Bols PEJ and de Kruif A 2004 Metabolite and ionic composition of follicular fluid from different-sized follicles and their relationship to serum concentrations in dairy cows. *Anim Reprod Sci.* **80** 201-211.

Levick JR and Michel CC 2010 Microvascular fluid exchange and the revised Starling principle. *Cardiovas res.* **87** 198-210.

Lindsay, L. A. and C. R. Murphy 2006 Redistribution of aquaporins 1 and 5 in the rat uterus is dependent on progesterone: a study with light and electron microscopy. *Reproduction.* **131** 369-78.

Lipman NS, Jackson LR, Trudel LJ and Weis-Garcia F 2005 Monoclonal versus polyclonal antibodies:distinguishing characteristics, applications, and information resources. *ILAR Journal.* **46** 258-268.

Liu J, Xu J, Gu S, Nicholson BJ and Jiang JX 2011 Aquaporin 0 enhances gap junction coupling via its cell adhesion function and interaction with connexion 50. *J cell Sci.* **124** 198-206.

Liu Z, Shen J, Carbrey JM, Mukhopadhyay R, Agre P and Rosen B 2002 Arsenite transport by mammalian aquaglyceroporins AQp7 and AQP9. *PNAS USA.* **99** 6053-6058.

Liu Z, Robert S, Youngquist H, Garverick HA and Antoniou E 2009 Molecular mechanisms regulating bovine ovarian follicular selection. *Mol Reprod Dev.* **76** 351-366.

Loo DD, Wright EM and Zeuthen T 2002 Water pumps. *J Physiol.* **542** 53-60.

Lu DC, Zhang H, Zador Z and Verkman AS 2008 Impaired olfaction in mice lacking aquaporin-4 water channels. *FASEB J.* **22** 3216-3223.

Lubahn DB, Moyer JS, Golding TS, Couse JF, Korach KS and Smithies O 1993 Alteration of reproductive function but not prenatal sexual development after

insertional disruption of the mouse estrogen receptor gene. *Proc Natl Acad Sci U S A.* **90** 11162-11166.

Lucy MC 2007 The bovine dominant ovarian follicle. *J Anim Sci.* **85** 89-99.

Lucy MC, Thatcher WW and Macmillan KL 1990 Ultrasonic identification of follicular populations and return to estrus in early postpartum dairy cows given intravaginal progesterone for 15 days. *Theriogenology.* **34** 325-340.

Lucy MC, Staples CR, Michel FM and Thatcher WW 1991 Effect of feeding calcium soaps to early postpartum dairy cows on plasma prostaglanding $F_{2\alpha}$, luteinizing hormone, and follicular growth. *J Dairy Sci.* **74** 483-498.

Lucy MC, Savio JD, Badinga L, De La Sorta RL and Thatcher WW 1992 Factors that affect ovarian follicular dynamics in cattle. *J Anim Sci.* **70** 3615-3626.

Lussier JG, Matton P and Dufour JJ 1987 Growth rates of follicles in the ovary of the cow. *J Reprod Fertil.* **81** 301-7.

Ma T, Fukuda N, Song Y, Matthay MA and Verkman AS 2000 Lung fluid transport in aquaporin-5 knockout mice. J Clin Invest. **105** 93-100.

Macchiarelli G, Nottola SA, Vizza E, Familiari G, Kikuta A, Murakami T and Motta PM 1993 Microvasculature of growing and atretic follicles in the rabbit ovary: a SEM study of corrosion casts. *Arch Histol Cytol.* **56** 1-12.

Maisonpierre PC, Suri C, Jones PF, Bartunkova S, Wiegand S, Radziejewski C, Compton D, McClain J, Aldrich TH, Papadopoulos N, Daly TJ, Davis S, Sato TN and Yancopoulos GD 1997 Angiopoietin-2, a natural antagonist for Tie2 that disrupts *in vivo* angiogenesis. *Science.* **277** 55-60.

Manikkam M, Calder MD, Salfen BE, Youngquist RS, Keisler DH and Garverick HA 2001 *Anim Reprod Sci.* **67** 189-203.

Marion GB, Gier HT and Choudary JB 1968 Micromorphology of the bovine ovarian follicular system. *J Anim Sci.* **27** 451-465.

Martelli A, Bernabò N, Berardinelli P, Russo V, Rinaldi C, Di Giacinto O, Mauro A, and Barboni B 2009 Vascular supply as a discriminating factor for pig preantral follicle selection. *Reproduction.* **137** 45-58.

Matzuk MM 1995 Functional analysis of mammalian members of the transforming growth factor-beta superfamily. *Trends Endocrin Met.* **6** 120-127.

Mauro A 1957 Nature of solvent transfer in osmosis. *Science.* **126** 252-3.

McArthur ME, Irvin-Rodgers HF, Byers S and Rodgers RJ 2000 Identification and immunolocalisation of decorin, versican, perlecan, nidogen and chondroitin sulphate proteoglycans in bovine small ovarian follicles. *Biol Reprod.* **63** 913-924 .

McConnell NA, Yunus RS, Gross SA, Bost KL, Clements MG and Hughes FM 2002. Water permeability of an ovarian antral follicle is predominantly transcellular and mediated by aquaporins. *Endocrinology.* **143** 2905-12.

McNatty KP 1978 *Follicluar fluid. In The Vertebrate Ovary,* pp215-259. Ed Jones RE. Plenum Press. New York.

McNatty KP, Heath DA, Lundy T, Fidler AE, Quirke L, O'Connell A, Smith P, Groome N and Tisdall DJ 1999 Control of early ovarian follicular development. J *Reprod Fertil Suppl.* **54** 3-16.

Meng QX, Gao HJ, Xu CM, Dong MY, Sheng X, Sheng JZ and Huang HF 2008 Reduced expression and function of aquaporin-3 in mouse metaphase-II oocytes induced by controlled ovarian hyperstimulation were associated with subsequent low fertilization rate. *Cell Physiol Biochem.* **21** 123-128

Meredith S, Dudenhoeffer G and Jackson K 20 00 Classification of small type B/C follicles as primordial follicles in mature rats. *J Reprod Fertil.* **119** 43-8.

Meşe G, Richard G and White TW 2007 Gap junctions: basic structure and function.*J Inv Derm.* **127** 2516-2524.

Meyer FA, Laver-Rudich Z and Tanenbaum R 1983 Evidence for a mechanical coupling of glycoprotein microfibrils in Wharton's jelly. *Biochem Biophys Acta.* **755** 376-387.

Middleton J, Americh L, Gayon R, Julien D, Mansat M, Mansat P, Anract P, Cantagrel A, Cattan P, Reimund JM, Aguilar L, Amalric F and Girard JP 2005 A comparative study of endothelial cell markers expressed in chronically inflamed human tissues: MECA-79, Duffy antigen receptor for chemokines, von Willebrand factor, CD31, CD34, CD105 and CD146. *J Pathol.* **206** 260-268.

Mignotte B and Vayssiere JL 1998 Mitochondria and apoptosis. *Eur J Biochem.* **252** 1-1

Mihm M, Austin E, Good TEM, Ireland JLH, Knight P, Roche JF and Ireland JJ 2000 Identification of potential intrafollicular factors involved in selection of dominant follicles in heifers. *Biol. Reprod.* **63** 811-819.

Mihm M and Evans ACO 2008 Mechanisms for dominant follicle selection in monovulatory species: a comparison of morphological, endocrine and intraovarian events in cows, mares and women. *Reprod Dom Anim.* **43** 48-56.

Miyamoto A and Shirasuna K 2009 Luteolysis in the cow: a novel concept of vasoactive molecules. *Anim Reprod.* **6** 47-59.

Miyamura M, Kuwayama M, Hamawaki A and Eguchil Y 1996 Total number of follicles in the ovaries of Japanese Black cattle. *Theriogenology.* **45** 300.

Mobasheri A, Trujillo E, Bell S, Carter SD, Clegg PD, Mart_ın-Vasallo P and Marples D 2004 Aquaporin water channels AQP1 and AQP3, are expressed in equine articular chondrocytes. *Vet J.* **168** 143-150.

Mobasheri A and Marples D 2004 Expression of AQP1 water channel in normal human tissue: a semiquantitative study using tissue micro array technology. *Am J Physiol Cell Physiol.* **286** 529-537.

Mobasheri A, Airley R, Hewitt SM and Marples D 2005 Heterogeneous expression of the aquaporin 1 (AQP1) water channel in tumors of the prostate, breast, ovary, colon and lung: a study using high density multiple human tumor tissue microarrays. *Int J Oncol.* **26** 1149-58.

Mobasheri A, Kendall BH, Maxwell JEJ, Sawran AV, German AJ, Marples D, Luck MR and Royal MD 2009 Cellular localisation of aquaporins along the secretory

pathway of the lactating bovine mammary gland: An immunohistochemical study. *Acta Histochem.* 1-13.

Moehren U, Denayer S, Podvinec M, Verrijdt G and Claessens F 2008 Identification of androgen-selective androgen-response elements in the human aquaporin-5 and Rad9 genes. *Biochem J.* **411** 679-86.

Monzani E, Bazzotti R, Perego C and Porta CAM 2009 AQP1 is not only a water channel: it contributes to cell migration through Lin7/beta-catenin. *PLoS ONE 4* e6167.

Moon C, Soria JC, Jang SJ, Jang SJ, Lee J, Hoque MO, Sibony M, TrinK B, Chang YS, Sidransky D and Mao L 2003 Involvement of aquaporins in colorectal carcinogenesis. *Oncogene.* **22** 6699-6703.

Morani A, Warner M and Gustafsson JA 2008 Biological functions and clinical implications of oestrogen receptors alfa and beta in epithelial tissues. *J Intern Med.* **264** 128-42.

Morbeck DE, Esbenshade KI, Flowers WL and Britt JH 1992 Kinetics of follicle growth in the prepubertal gilt. *Biol Reprod.* **47** 485-491.

Mosselman S, Polman J and Dijkema R 1996 ER beta: identification and characterization of a novel human estrogen receptor. *FEBS Lett.* **392** 49-53.

Mulders SM, Preston GM, Deen PM, Guggino WB, van Os CH, Agre P 1995 Water channel properties of major intrinsic protein of lens. *J Biol Chem.* **270** 9010-9016.

Murata K, Mitsuoka K, Hirai T, Walz T, Agre P, Heymann JB, Engel A and Fujiyoshi Y 2000 Structural determinants of water permeation through aquaporin-1. *Nature.* **407** 599-605.

Murdoch WJ 1998 Regulation of collagenolysis and cell death by plasmin within formative stigma of preovulatory ovine follicles. *J Reprod Fertil.* **113** 331-336.

Nagase H (1997) Activation mechanisms of matrix metalloproteinases. *Biol Chem.* **378** 151-160.

Nagase H, Agren J, Saito A, Liu K, Agre P, Hazama A, and Yasui M 2007. Molecular cloning and characterization of mouse aquaporin 6. *Biochem Bioph Res Co.* **352** 12-16.

Nakhoul NL, Davis BA, Romero MF and Boron WF 1998 Effect of expressing the water channel aquaporin-1 on the CO_2 permeability of *Xenopus* oocytes. *Am J Physiol.* 274 543-548.

Nicchia GP, Frigeri A, Nico B, Ribatti D, Svelto M 2001 Tissue distribution and membrane localization of aquaporin-9 water channel: evidence for sex-linked differences in liver. *J Histochem Cytochem.* **49** 1547-1556.

Nico B and Ribatti D 2010 Aquaporins in tumor growth and angiogenesis. *Cancer Lett.* **294** 135-138.

Nielsen S, Frøkiaer J, Marples D, Kwon TH, Agre P and Knepper MA 2002 Aquaporins in the kidney: from molecules to medicine. *Physiol Rev.* **82** 205-244.

Nielsen S, King LS, Christenson BM and Agre P 1997 Aquaporins in complex tissues. II. Subcellular distribution in respiratory and glandular tissues of rat. *Am J Physiol.* **273** 1549-1561.

Nilsson E and Skinner MK 2001 Cellular interactions that control primordial follicle development and folliculogenesis. *J Soc Gynecol Investig.* **8** 17-20.

Nimz M, Spitschak M, Schneider F, Fürbass and Vanselow J 2009 Down-regulation of genes encoding steroidogenic enzymes and hormone receptors in late preovulatory follicles of the cow coincides with an accumulation of intrafollicular steroids. *Domest Anim Endocrinol.* **37** 45-54.

Nimz M, Spitschak M, Fürbass and Vanselow J 2010 The pre-ovulatory luteinizing hormone surge is followed by down-regulation of CYP19A1, HSD3B1 and CYP17A1 and chromatin condensation of the corresponding promoters in bovine follicles. *Mol Reprod Dev.* **77** 1040-1048.

Niswender GD, Schwall RH, Fitz TA, Farin CE and Sawyer HR 1985 Regulation of luteal function in domestic ruminants: new concepts. *Can J Physiol Pharmacol.* **63** 240-8.

Noda, Y. and S. Sasaki 2006 Regulation of aquaporin-2 trafficking and its binding protein complex. *Biochim Biophys Acta.* **1758** 1117-1125.

Norman RJ, Dewailly D, Legro RS and Hickey TE 2007 Polycystic ovarian syndrome. *Lancet.* **379** 685-697.

Nuttinck F, Peynot N, Humbolt P, Massip A, Dessy F and Flechon E 2000 Comparative immunohistochemical distribution of connexion 37 and connexion 43 throughout folliculogenesis in the bovine ovary. *Mol. Reprod. Dev.* **57** 60-66

Okahira M, Kubota M, Iguchi K, Usui S and Hirano K 2008 Regulation of aquaporin 3 expression by magnesium ion. *Eur J Pharmacol.* **588** 26-32.

Oktem O and Oktay K 2008 The ovary: anatomy and function throughout human life. *Ann N Y Acad Sci.* **1127** 20-26.

Oliveira CA, Carnes K, Franca LR, Hermo L and Hess RA 2005. Aquaporin-1 and -9 are differentially regulated by oestrogen in the efferent ductule epithelium and initial segment of the epididymis. *Biol Cell.* **97** 385-95.

Omoto Y, Lathe R, Warner M and Gustafsson JA 2005 Early onset of puberty and early ovarian failure in CYP7B1 knockout mice. *Proc Natl Acad Sci.* **102** 2814-2819.

Orsi NM, Gopichandran N, Leese HJ, Picton HM and Harris S 2005. Fluctuations in bovine ovarian follicular fluid composition throughout the oestrous cycle. *Reproduction.* **129** 219-28.

Osvaldo-Decima L 1970 Smooth muscle in the ovary of the rat and monkey. *J Ultrastruct Res.* **30** 218-37.

Otala M, Makinen S, Tuuri , Sjoberg J, Pentikainen V, Matikainen T and Dunkel L 2004 Effects of testosterone, Dihydrotestosterone, and 17β-estradiol on human ovarian tissue survival in culture. *Fertil Steril.* **82** 1077-1085.

Otterbach F, Callies R, Adamzik M, Kimmig R, Siffert W, Schmid KW and Bankfalvi A 2010 Aquaporin 1 (AQP1) expression is a novel characteristic feature of a particularly aggressive subgroup of basal-like breast carcinomas. *Breast Cancer Res Tr.* **120** 67-76.

Pao GM, Wu LF, Johnson KD, Höfte H, Chrispeels MJ, Sweet G, Sandal NN and Saier MH Jr 1991 Evolution of the MIP family of integral membrane transport proteins. *Mol Microbiol.* **5** 33-7.

Papadopoulos MC and Verkman AS 2007 Aquaporin-4 and brain edema. *Pediatr Nephrol.* **22** 778-84.

Pastor-Soler NM, Fisher JS, Sharpe R, Hill E, Van Hoek A, Brown D and Breton S 2010 Aquaporin 9 expression in the developing rat epididymis is modulated by steroid hormones. *Reproduction.* **139** 613-621.

Pastor-Soler NM, Isnard-Bagnis C, Herak-Kramberger C, Sabolic I, Van Hoek V, Brown D and Breton S 2002 Expression of aquaporin 9 in the rat epididymal epithelium is modulated by androgens. *Bio Repro.* **66** 1716-1722.

Payne AH and Hales DB 2004. Overview of steroidogenic enzymes in the pathway from cholesterol to active steroid hormones. *Endo Rev.* **25** 947-970.

Pescador N, Houde A and Stocco DM 1997 Follicle-stimulating hormone and intracellular second messengers regulate steroidogenic acute regulatory protein messenger ribonucleic acid in luteinized porcine granulosa cells. *Biol Reprod.* **57** 660-668.

Picton HM and Gosden RG 1999 *Oogenesis in mammals.* In Knobil, E. and Neill, J.D. (eds), *Encyclopedia of Reproduction.* Vol. 3. pp. 488-497.Academic Press, London, UK.

Pierson, RA and Ginther, OJ 1987 Follicular populations during estrous cycle in heifers I. Influence of day. *Anim Reprod Sci.* **14** 165-176.

Plendl J 2000 Angiogenesis and vascular regression in the ovary. *Anat Histol Embryol.* **29** 257-266.

Presta M, Dell'Era P, Mitola S, Moroni E, Ronca R and Rusnati M 2005 Fibroblast groeth factor/fibroblast growth factor receptor system in angiogenesis. *Cytokine* Growth F R. **16** 159-178.

Preston G M and Agre P 1991 Isolation of the cDNA for erythrocyte integral membrane protein of 28 kilodaltons: member of an ancient channel family. *Proc Natl Acad Sci USA* **88** 11110-11114.

Preston GM, Carroll TP, Guggino WB and Agre P 1992 Appearance of water channels in Xenopus oocytes expressing red cell CHIP28 protein. *Science.* **256** 385-387.

Preston GM, Jung JS, Guggino WB and Agre P 1993 The Mercury-Sensitive Residue at Cysteine-189 in the Chip28 Water Channel. *J Biol Chem.* **268** 17-20.

Preston GM, Jung JS, Guggino WB and Agre P 1994 Membrane topology of aquaporin CHIP. Analysis of functional epitope-scanning mutants by vectorial proteolysis. *J Biol Chem.* **269** 1668-1673.

Qu F, Wang F, Lu X, Dong M, Sheng J, Lv P, Ding G, Shi B, Zhang D and Huang H 2010 Altered aquaporin expression in women with polucystic ovary syndrome: hyperandrogenism in the follicular fluid inhibits aquaporin-9 in granulosa cells through the phosphatidylinositol 3-kinase pathway. *Hum Reprod.* **25** 1441-1450.

Rahe CH, Owens RE, Fleeger JL, Newton JH and Harms PG 1980 Pattern of plasma luteinizing hormone in the cyclic cow: dependence upon the period of the cycle. *Endocrinology.* **107** 498-503.

Rajakoski E 1960 The ovarian follicular system in sexually mature heifers with special reference to seasonal, cyclical, end left-right variations. *Acta Endocrinol Suppl (Copenh).* **34** 1-68.

Reed RK and Rubin K 2010 Transcapillary exchange: role and importance of interstitial fluid pressure and the extracellular matrix. *Cardiovas Res.* **87** 211-217.

Reich R, Daphna Iken D, Chun SY, Popliker M, Slager R, Adelmann Grill BC and Tsafriri A 1991 Preovulatory changes in ovarian expression of collagenases and tissue metalloproteinase inhibitor messenger ribonucleic acid: role of eicosanoids. *Endocrinology.* **129** 1869-1875.

Rhodes KJ and Trimmer JS 2006 Antibodies as valuable neuroscience research tools versus reagents of mass distraction. *J of Neurosci.* **31.** 8017-8020.

Richard C, J Gao, Brown N and Reese J 2003. Aquaporin water channel genes are differentially expressed and regulated by ovarian steroids during the periimplantation period in the mouse. *Endocrinology.* **144** 1533-1541.

Richards JS, Russell DL, Robker RL, Dajee M and Alliston T 1998 Molecular mechanisms of ovulation and luteinisation. *Mol Cell Endocrinol.* **145** 47-54.

Risau W 1995 Differentiation of the endothelium. *FASEB J.* **9** 926-933.

Risau W 1997 Mechanisms of angiogenesis. **Nature. 386** 671-4.

Roberts AJ and Skinner MK 1990 Hormonal regulation of thecal cell function during antral follicle development in bovine ovaries. *Endocrinology.* **127** 2907-2917.

Robinson RS, Woad K, Hammond AJ, Laird M, Hunter MG and Mann GE 2009 Focus on vascular function in female reproduction. Angiogenesis and vascular function in the ovary. *Reproduction.* **138** 869-881.

Rodgers RJ and Irving-Rodgers HF 2010a The roles of the ovarian extracellular matrix in fertility. *Reprod in Domest Rum.* 7 215-228.

Rodgers RJ and Irving-Rodgers HF 2010b Formation of the ovarian follicular antrum and follicular fluid. *Reproduction.* **82** 1021-1029.

Rodgers RJ and Irving-Rodgers HF 2010c Morphological classification of bovine ovarian follicles. *Reproduction.* **139** 309-18.

Rodgers HF, Lavranos TC, Vella CA and Rodgers RJ 1995 Basal lamina and other extracellular matrix produced by bovine granulosa cells in anchorage-independent culture. *Cell Tissue Res.* **282** 463-471.

Rodgers HF, Irvine CM, van Wezel IL, Lavranos TC, Luck ML, Sado Y, Ninomiya Y and Rodgers RJ 1998 Distribution of the α1 to α6 chains of type IV collagen in bovine follicles. *Biol Reprod.* **59** 1334-1341.

Rodgers RJ, Vella CA, Rodgers HF, Scott K and Lavranos TC 1996 Production of extracellular matrix, fibronectin and steroidogenic enzymes, and growth of bovine granulosa cells in anchorage-independent culture. *Reprod Fert Dev.* **8** 249-257

Rodgers RJ, Lavranos TC, van Wezel IL and Irving-Rodgers HF 1999 Development of the ovarian follicular epithelium. *Mol Cell Encorinol.* **151** 171-179.

Rodgers RJ, Irving-Rodgers HF and van Wezel IL 2000 Extracellular matrix in ovarian follicles. *Mol and Cell Endocrinol.* **163** 73-79.

Rodgers RJ, Irving-Rodgers HF, van Wezel IL, Krupa M and Lavranos TC 2001. Dynamics of the membrana granulosa during expansion of the ovarian follicular antrum. *Mol Cell Endocrinol.* **171** 41-48.

Rodgers RJ, Irving-Rodgers HF and Russell DL 2003 Extracellular matrix of the developing ovarian follicle. *Reproduction.* **126** 415-424.

Rodríguez CM, Kirby JL and Hinton BT 2001 Regulation of gene transcription in the epididymis. *Reproduction.* **122** 41-48.

Rojek AM, Praetorius J, Frøkiaer J, Nielsen N and Fenton RA 2008 A current view of the mammalian aquaglyceroporins. *Annu Rev Physiol.* **70** 301-327.

Ross MH and Pawlina W 2006 *In Histology a text and atlas.* 5th ed. Lippincott Williams & Wilkins. PA, USA.

Roudier N, Ripoche P, Gane P, Le Pannec PY, Daniels G, Cartron JP and Bailly P 2002 AQP3 deficiency in humans and the molecular basis of a novel blood group system. *J Biol Chem.* **277** 45854-45859.

Ruoslahti E 1988 Structure and biology of proteoglycans. *Annu Rev Cell Biol.* **4** 229-255.

Saddoun S, Papadopoulos MC, Davies DC, Bell BA and Krishna S 2002 Increased aquaporin 1 water channel expression in human brain tumours. *Br J Cancer.* **87** 621-623.

Santini D, Ceccarelli C, Leone O, Pasquinelli G, Piana S, Marabini A and Martinelli GN 1995 Smooth muscle differentiation in normal human ovaries, ovarian stromal hyperplasia and ovarian granulosa-stromal cells tumors. *Mod Pathol.* **8** 25-30.

Savio JD, Keenan L, Boland MP and Roche JF 1988 Pattern of growth of dominant follicles during the oestrous cycle of heifers. *J Reprod Fertil.* **83** 663-671.

Savio JD, Thatcher WW, Badinga L, de la Sota RL and Wolfensen D 1993 Regulation of dominant follicle turnover during the oestrous cycle in cows. *J Reprod Fertil.* **97** 197-203.

Schams D 2005 Ovarian function in ruminants. *Dom Anim Endocrinol.* **29** 305-317.

Selvey S, Thompson EW, Matthaei K, Lea RA , Irving MG and Griffiths LR 2001 β-Actin – an unsuitable internal control for RT-PCR. *Mol Cell Probe.* **15** 307-311.

Senbon S, Hirao Y, Miyano T 2003 Interactions between the oocyte and surrounding somatic cells in follicular development: lessons from in vitro culture. *J Reprod Dev.* **49** 259-69.

Senger P 2003 *In Pathways to Pregnancy and Parturition.* 2nd ed. Current Conceptions, WA, USA.

Senthilkumaran B, Yoshikuni M and Nagahama Y 2004 A shift in steroidogenesis occurring in ovarian follicles prior to oocyte maturation. *Mol Cell Endocrinol.* **215** 11-18.

Shalgi R, Kraicer PF and Soferman N 1972 Human follicular fluid. *J Reprod Fertil.* **31** 515-6.

Sinosich MJ 1987 *Human ovarian follicular antigens. In Future Aspects in Human In Vitro Fertilisation,* ed Feichtinger W and Kemeter P, pp 64-76. Heidelberg & NewYork: Springer-Verlag. Berlin. Germany.

Sirois J and Fortune JE 1988 Ovarian follicular dynamics during the estrous cycle in heifers monitored by real-time ultrasonography. *Biol Reprod.* **39** 308-317.

Sirois J, and Fortune JE 1990 Lengthening the bovine estrous cycle with low levels of exogenous progesterone: A model for studying ovarian follicular dominance. *Endocrinology.* **127** 916-925.

Skinner MK and Osteen KG 1988 Developmental and hormonal regulation of bovine granulosa cell function in the preovulatory follicle. *Endocrinology.* **123** 1668-1675.

Skinner MK, Schmidt M, Savenkova M I, Sadler-Riggleman I and Nilsson EE 2008 Regulation of granulosa and theca cell transcriptomes during ovarian antral follicle development. *Mol Reprod Dev.* **75** 1457-1472.

Skowronski MT, Kwon TH and Nielsen S 2009 Immunolocalization of aquaporin 1, 5, and 9 in the female pig reproductive system. *J Histochem Cytochem.* **57** 61-7.

Skowronski MT 2010 Distribution and quantitative changes in amounts of aquaporin 1, 5 and 9 in the pig uterus during the estrous cycle and early pregnancy. *Reprod Biol Endocrin.* **8** 109-120.

Słomczyñska M and Tabarowski Z 2001 Localization of androgen receptor and cytochrome P450 aromatase in the follicle and corpus luteum of the porcine ovary. *Anim Reprod Sci.* **65** 127-134.

Smith BL and Agre P 1991 Erythrocyte Mr-28,000 Transmembrane Protein Exists as a Multisubunit Oligomer Similar to Channel Proteins. *J of Biol Chem.* **266** 6407-6415.

Smith MF, McIntush EW, Ricke WA, Kojima FN and Smith GW 1999 Regulation of ovarian extracellular matrix remodelling be metalloproteinases and their tissue inhibitors: effects on follicular development, ovulation and luteal function. *J Reprod fertil.* **54** 367-381.

Sohara E, Rai T, Sasaki S and Uchida S 2006 Physiological roles of AQP7 in the kidney:lessons from AQP7 knockout mice. *Biochem Biophys Acta.* **1758** 1106-1110.

Soyal SM, Amleh A and Dean J 2000 FIGalpha, a germ cell-specific transcription factor required for ovarian follicle formation. *Mol Cell Endocrinol.* **127** 4645-4654.

Spicer LJ 2004 Proteolytic degradation of insulin-like growth factor binding proteins by ovarian follicles: a control mechanism for selection of dominant follicles. *Biol Reprod.* **70** 1223-1230.

Steinfeld S, Cogan E, King LS, Agre P, Kiss R and Delporte C 2001 Abnormal distribution of aquaporin-5 water channel protein in salivary glands from Sjögren's syndrome patients. *Lab Invest.* **81**143-8.

Stocco DM 2000a The role of StAR protein in steroidogenesis: challenges for the future. *Endocrinology.* **164** 247-253

Stocco DM 2000b Intramitochondrial cholesterol transfer. *Biochem Biophys Acta.* **13** 489-525.

Stocco DM 2001 StAR protein and the regulation of steroid hormone biosynthesis. Annu *Rev Physiolo.* **63** 193-213.

Stock AE and Fortune JE 1993. Ovarian follicular dominance in cattle: relationship between prolonged growth of the ovulatory follicle and endocrine parameters. *Endocrinology.* **132** 1108-1114.

Sui H, Han BG, Lee JK, Walian P and Jap BK 2001 Structural basis of water-specific transport through the AQP1 water channel. *Nature*, **414** 872-8.

Tabandeh, M. R. Hosseini, A. Saedb, M. Kafi, M. Saeb, S. 2010 Changes in the gene expression of adiponectin and adiponectin receptors (AdipoR1) and AdipoR2) in ovarian follicular cells of dairy cow at different stages of development. *Theriogenology.* **73** 659-669.

Tadakuma H, Okamura H and Kitaoka M 1993 Association of immunolocalization of matrix metalloproteinase-1 with ovulation in hCG treated rabbit ovary. *J Reprod Fertil.* **98** 503–508.

Taylor RN, Lebovic DI, Hornung D and Mueller MD 2001 Endocrine and paracrine regulation of endometrial angiogenesis. *Human Fert and repro.* **943** 109-121

Terris J, Ecelbarger CA, Marples D, Knepper MA and Nielsen S 1995 Distribution of aquaporin-4 water channel expression within rat kidney. *Am J Physiol.* 269 775-785.

Tetsuka M and Hillier SG 1996 Androgen receptor gene expression in rat granulosa cells: the role of follicle-stimulating hormone and steroid hormones. *Endocrinology.* **137** 4392-4397.

Thoroddsen A, Dahm-Kähler P, Lind AK, Weijdegård B, Lindenthal B, Müller J and Brännström M 2011 The water permeability channels aquaporins 1-4 are differentially expressed in granulosa and theca cells of the preovulatory follicle during precise stages of human ovulation. *J Clin Endocrinlo Metab.* **96** 1021-1028

Tietz PS, Marinelli RA, Chen XM , Huang B, Cohn J, Kole J, McNiven MA, Alper S and LaRusso NF 2003 Agonist-induced coordinated trafficking of functionally

related transport proteins for water and ions in cholangiocytes. *J Biol Chem.* **278** 20413-20419.

Tilly JL 1997 Apoptosis and the ovary: a fashionable trend or food for thought? *Fertil Steril.* 67 226-228.

Tilly JL, Niikura Y and Rueda BR 2009 The current status of evidence for and against postnatal oogenesis inmammals: a case of ovarian optimism versus pessimism? *Biol. Reprod.* **80** 2-12

Torry RJ and Rongish BJ 1992 Angiogenesis in uterus: potential regulation and relation to tumor angiogenesis. *Am J Reprod Immunol* . **27** 171-179.

Towne JE, Krane CM, Bachurski CJ and Menon AG 2001 Tumor necrosis factor-alpha inhibits aquaporin 5 expression in mouse lung epithelial cells. *J Biol Chem.* **276** 18657-18664.

Valdez KE, Cuneo SP and Turzillo AM 2005 Regulation of apoptosis in the atresia of dominant bovine follicles of the first follicular wave following ovulation. *Reproduction.* **130** 71-81.

van Wezel IL and Rodgers RJ 1996 Morphological characterization of bovine primordial follicles and their environment in vivo. *Biol Reprod.* **55** 1003-11.

van Wezel IL, Rodger HF and Rodgers RJ 1998 Differential localization of laminin chains in the bovine follicle. *J Reprod Fertil.* **112** 267-278.

van Wezel IL, Dharmarajan AM, Lavranos TC and Rodgers RJ 1999a Evidence for alternative pathways of granulosa cell death in healthy and slightly atretic bovine antral follicles. *Endocrinology.* **140** 2602-2612.

van Wezel IL, Rodger HF, Sado Y, Ninomiya Y and Rodgers RJ 1999b Ultrastructure and composition of Call-Exner bodies in bovine follicles. *Cell Tiss Res.* **296** 385-394.

Vendola KA, Zhou J, Wang J, Famuyiwa OA, Bievre M and Bondy CA 1999 Androgens promote oocyte insulin-like growth factor I expression and initiation of follicle development in the primate ovary. *Biol Reprod.* **61** 353-357.

Verkman AS and Mitra AK 2000 Structure and function of aquaporin water channels. *Am J Physiol.* **278** 13-28

Verkman AS, Hara-Chikuma M and Papadopoulos MC 2008 Aquaporins--new players in cancer biology. *J Mol Med.* **86** 523-529.

Voss AK and Fortune JE 1993 Levels of messenger ribonucleic acid for cytochrome P450 17 alpha-hydroxylase and P450 aromatase in preovulatory bovine follicles decrease after the luteinizing hormone surge. *Endocrinology.* **132** 2239-2245.

Wahl M, Kenan D, Gonzalez-Gronow M and Pizzo S 2005 Angiostatin's molecular mechanism: aspects of specificity and regulation elucidated. *J Cell Biochem.* **96** 242-261.

Walters KA, Allan CM and Handelsman DJ 2008 Androgen actions and the ovary. *Biol Reprod.* **78** 380-389.

Walz T, Hirai T, Murata K, Heymann J B, Mitsuoka K, Fujiyoshi Y, Smith B L, Agre P and Engel A 1997 The three-dimensional structure of aquaporin-1. *Nature.* **387** 624-627.

Watson ED, Thomassen R, Steele M, Heald M, Leask R, Groome NP and Riley SC 2002 Concentrations of inhibin, progesterone and oestradiol in fluid from dominant and subordinate follicles from mares during spring transition and the breeding season. *Anim Reprod Sci.* **74** 55-67.

Webb, R, Nicholas, B, Gong JG, Campbell BK, Gutierrez CG, Garverick, HA, ARmostrong, DG 2003 Mechanisms regulating follicular development and selection of the dominant follicle. *Reproduction* **61** 71 – 90.

Weil S, Vendola K, Zhou J and Bondy CA 1999 Androgen and follicle-stimulating hormone interactions in primate ovarian follicle development. *J Clin Endocr Metab.* **84** 2951-2965.

Weiss J, Bernhardt ML, Laronda MM, Hurley LA, Glidewell-Kenny C, Pillai S, Tong M, Korach KS and Jameson JL 2008 Estrogen actions in the male reproductive system involve estrogen response element-independent pathways. *Reproduction.* **149** 6198-6206.

White YAR, Woods DC, Takai Y, Ishihara O, Seki H and Tilly J 2012 Oocyte formation by mitotically active germ cells purified from ovaries of reproductive-age women. *Nature Med.* **18** 413-21.

Wise T 1987 Biochemical analysis of bovine follicular fluid: albumin, total protein, lysosomal enzymes, ions, steroids and ascorbic acid content in relation to follicular size, rank, atresia classification and day of estrous cycle. *J Anim Sci.* **64** 1153-1169.

Xu H, Edwards RJ, Espinosa O, Banerji S, Jackson G and Athanasou A 2004 Expression of a lymphatic endothelial cell marker in benign and malignant vascular tumors. *Hum Path.* 35 857-861.

Xueyong LMD, Shaozong C, Wangzhou L, Yuejun LMD, Xiaoxing LMS, Jing LMD, Yanli WMS and Jinqing LMD 2008 Differentiation of the pericytes in wound healing: The precursor, the process, and the role of the vascular endothelial cell. *Wound Rep Reg.* **16** 346-355.

Yallampalli C, Osuamkpe C and Nagamani M 1993 Influence of the anti-androgen hydroxyflutamide on *in vitro* development of mouse embryos. *J Reprod Fert.* **99** 467-470.

Yamada O, Abe M, Takehana K, Hiraga T, Iwasa K and Hiratsuka T 1995 Microvascular changes during the development of follicles in bovine ovaries: a study of corrosion casts by scanning electron microscopy. *Arch Histol Cytol.* **58** 567–574.

Yang B and Verkman AS 1997 Water and glycerol permeabilities of aquaporin 1–5 and MIP determined quantitatively by expression of epitope-tagged constructs in Xenopus oocytes. *J Biol Chem.* **272** 14146–16140.

Yang B and Verkman AS 2002 Analysis of double knockout mice lacking aquaporin-1 and urea transporter UT-B. *J Biol Biochem.* **277** 36782–36786

Yang B, Zador Z and Verkman AS 2008 Glial cell aquaporin-4 over expression in transgenic mice accelerates cytotoxic brain swelling. *J Biol Chem.* **283** 15280-15286.

Yang JH, Shi YF, Cheng XD and Qi WJ 2006a The influence of aquaporin-1 and microvessel density on ovarian carcinogenesis and ascites formation. *Int J Gynecol Cancer.* **16** 400-405.

Yang JH, Shi YF, Cheng Q and Deng L 2006b Expression and localization of aquaporin-5 in the epithelial ovarian tumours. *Gyne Onc.* **100** 294-299.

Yang JH, Yu YQ and Yan C 2011 Localisation and expression of aquaporin subtypes in epithelial ovarian tumours. *Histol Histopath.* **26** 1197-1205

Yang MY and Fortune JE 2006 Testosterone stimulates the primary to secondary follicle transition in bovine follicles in vitro. *Biol Reprod.* **75** 924-932.

Yang S, Kawedia JD and Menon NG 2003 Cyclic AMP Regulates Aquaporin 5 Expression at Both Transcriptional and Post-transcriptional Levels through a Protein Kinase A Pathway. *J Biol Chem.* **278** 32173-32180.

Yasui M, Hazama A, Kwon TH, Nielsen S, Guggino WB and Agre P 1999 Rapid gating and anion permeability of an intracellular aquaporin. *Nature.* **402** 184-187.

Young B, Lowe JS, Stevens A and Heath JW 2006 *In Wheater's functional histology a text and coulor atlas.* 5th ed. Churchill Livingstone Elsevier. PA USA.

Yukutake Y, Tsuji S, Hirano Y, Adachi T, Takahashi T, Fujihara K, Agre P, Yasui M and Suematsu M 2008 Mercury chloride decreases the water permeability of aquaporin-4-reconstituted proteoliposomes. *Biol Cell.* **100** 355-353.

Zachow RJ, Weitsman SR and Magoffin DA 1999 Leptin impairs the synergistic stimulation by transforming growth factor-β of follicle stimulating hormone-dependent aromatase activity and messenger ribonucleic acid expression in rat granulosa cells. *Biol Reprod.* **61** 1104-1109.

Zhang G, Garmey CJ and Veldhuis JD 2000 Interactive stimulation by luteinising hormone and insulin of StAR protein and 17α-hydroxylase/17, 20 Lyase (CYP17) genes inporcine theca cells. *Reprod Devel.* **141.** 2735-2742.

Zalányi S 2001 Progesterone and ovulation. *J Obst Gyn Reprod Biol.* **98** 152-159.

Zamorano PL, Mahesh VB and Brann DW 1996 Quantitative RT-PCR for neuroendocrine studies. A minireview. *Neuroendocrinology.* **63** 397-407.

Zampighi GA, Hall JE, Ehring GR and Simon SA 1989 The structural organization and protein composition of lens fiber junctions. *J Cell Biol.* **108** 2255-2275.

Zang T, Zhao C, Chen D and Zhou Z 2011 Overexpression of AQP5 in cervical cancer: correlation with clinicopathological features and prognosis. *Med Oncol* [Epub ahead of print].

Zeidel ML, Ambudkar SV, Smith BL and Agre P 1992 Reconstitution of functional water channels in liposomes containing purified red cell CHIP28 protein. *Biochemistry.* **31:** 7436-7440.

Zeuthen T 2010 Water-transporting proteins. *J Membr Biol.* **234** 57-73.

Zhao Y and Luck MR 1996 Bovine granulosa cells express extracellular matrix proteins and their regulators during luteinisation in culture. Reprod Fertil. Dev **8** 259-66.

Zhong H and Simons JW 1999 Direct comparison of GAPDH, β-Actin, Cyclophilin and 28s rRNA as internal standards for quantifying RNA levels under hypoxia. *Biochem Bioph Res Co.* **259** 523-526.

Zou H, Luo Q and Zhou D 2001 Affinity membrane chromatography for the analaysis and purification of proteins *J. Biochem. Biophys. Methods.* **49** 199-240.